



ISSCC 2021

SESSION 22

**Terahertz for Communication
and Sensing**

Paper 22.1

THz Prism: One-Shot Simultaneous Multi-Node Angular Localization Using Spectrum-to-Space Mapping with 360-to-400GHz Broadband Transceiver and Dual-Port Integrated Leaky-Wave Antennas

Hooman Saeidi*, Suresh Venkatesh*,
Xuyang Lu, Kaushik Sengupta

* Equally Credited Authors

Princeton University, Electrical Engineering, Princeton, NJ

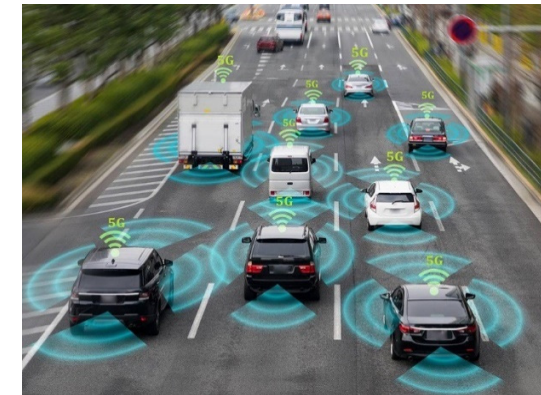
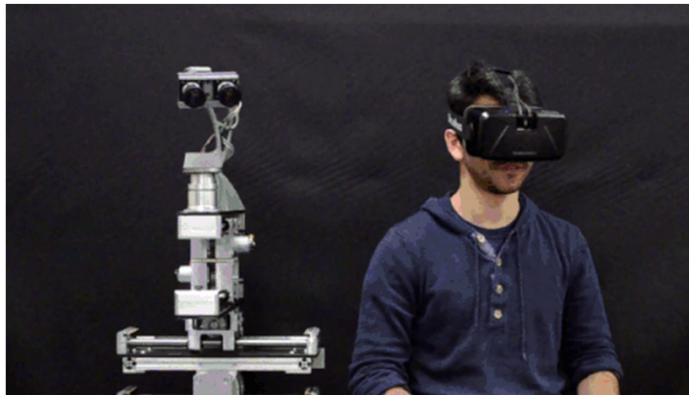


Speaker Intro

- 4th Year Ph.D. Student, Electrical Engineering, Princeton University
Advisor: Professor Kaushik Sengupta
- M.A, Electrical Engineering, Princeton University, June 2019
- B.Sc., Electrical Engineering, Sharif University of Technology,
June 2017



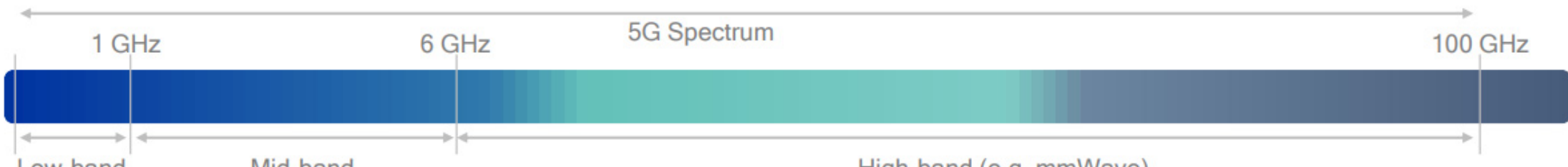
Communication and Sensing Co-existence at 100GHz and above



Connected Cities

AR/VR

Autonomous Vehicles

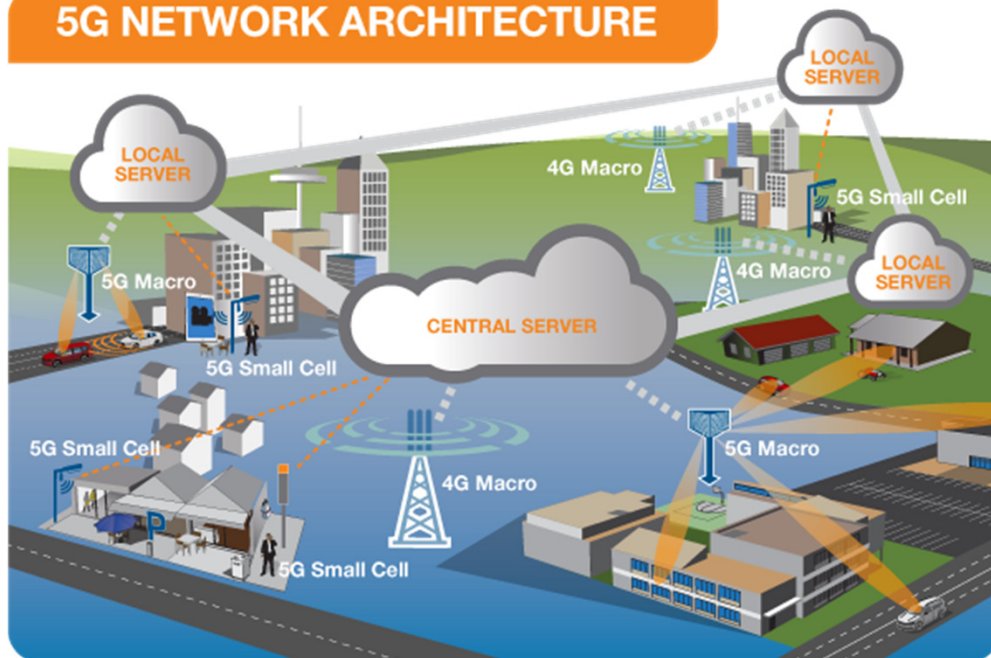


www.qualcomm.com/invention/5g/5g-unlicensed-shared-spectrum

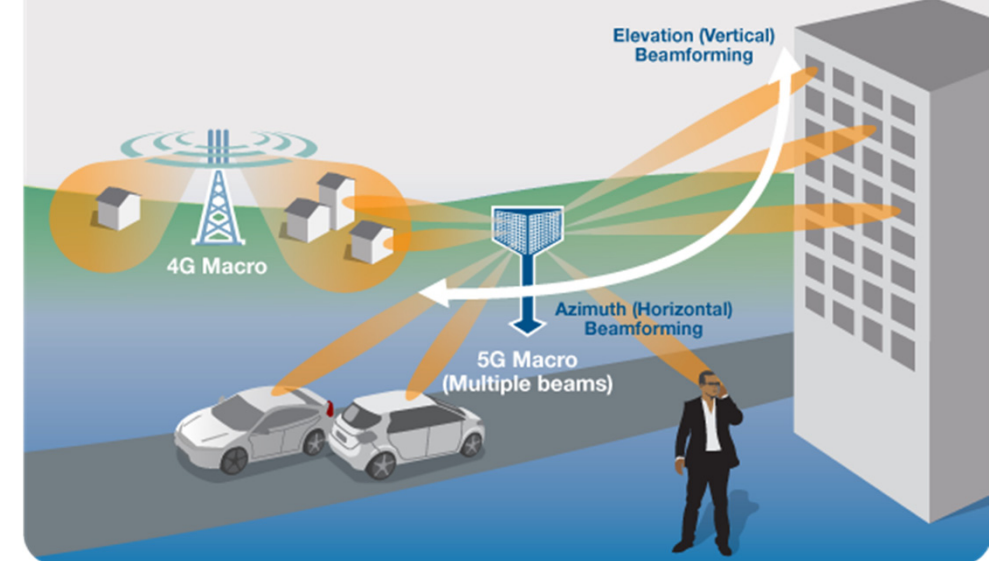
FCC is considering rules for 70/80/90GHz and has opened spectrum above 95GHz

5G and Beyond Network Architecture

5G NETWORK ARCHITECTURE

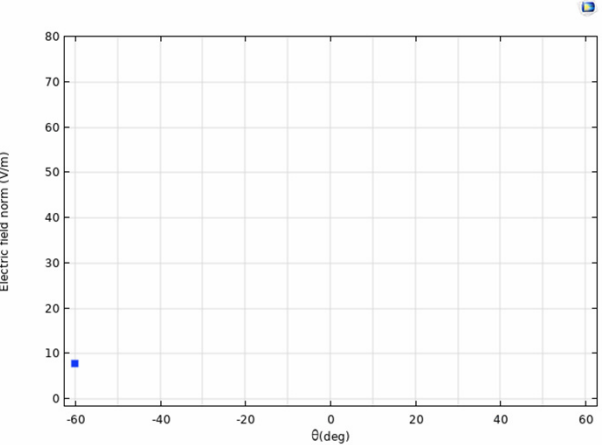


MIMO BEAMFORMING



- Significant growth in number of devices
- Links are established through sharp, highly directive beams
- Operate under stringent ultra-low latencies
- Therefore, requires novel approaches for link discovery and user terminal identification

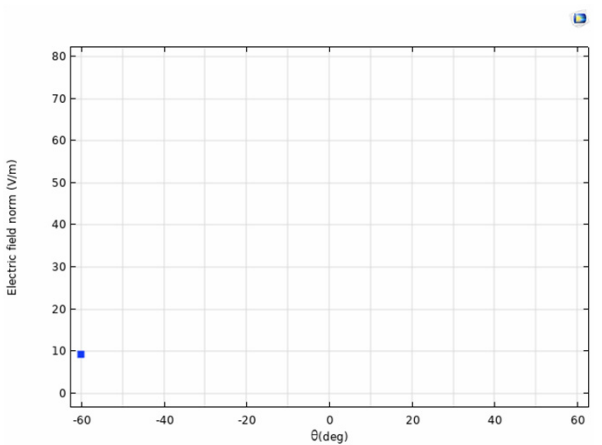
Directional Finding Concept



Received Power

Single-Broad Beam:

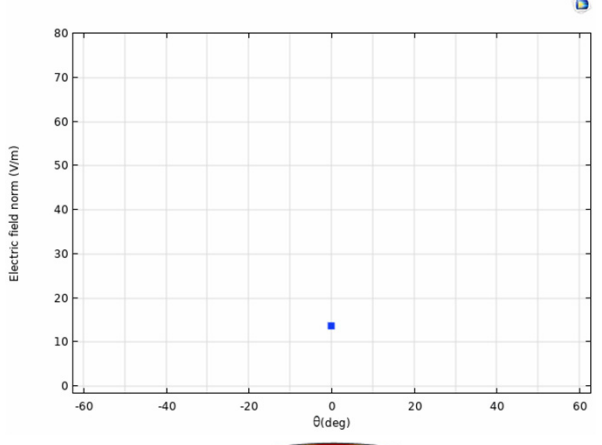
- Lower SNR
- Lower Accuracy
- Relatively Faster



Received Power

Single Narrow Beam:

- High SNR
- High Accuracy
- Slower

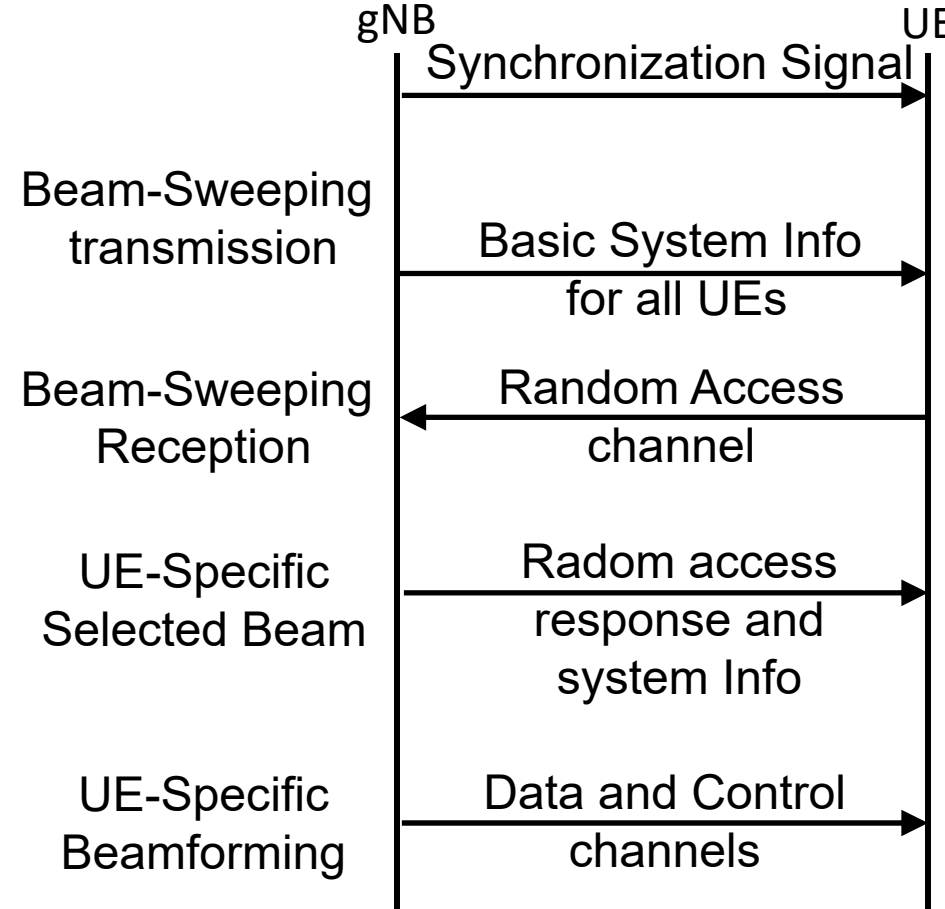
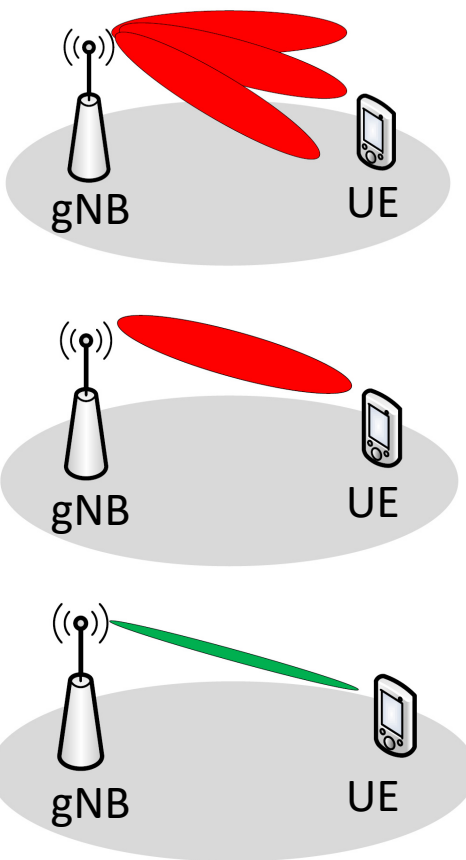


Received Power

Multi-Beam Mode:

- Medium SNR
- Medium Accuracy
- Relatively Faster

Directional Finding Concept in 5G NR



- Beam sweeping at lower frequency bands.
- Utilizing different frequency bands.

https://www.keysight.com/upload/cmc_upload/All/Understanding_the_5G_NR_Physical_Layer.pdf

Outline

- **Prior works in single-shot localization THz frequencies**
- **Enabling On-chip THz localization using frequency dispersive antennas**
- **On-chip 360-400GHz transceiver design and implementation**
- **Circuit implementation and characterization**
- **1D, chip-to-chip, and 2D angular measurement results**
- **Conclusions**

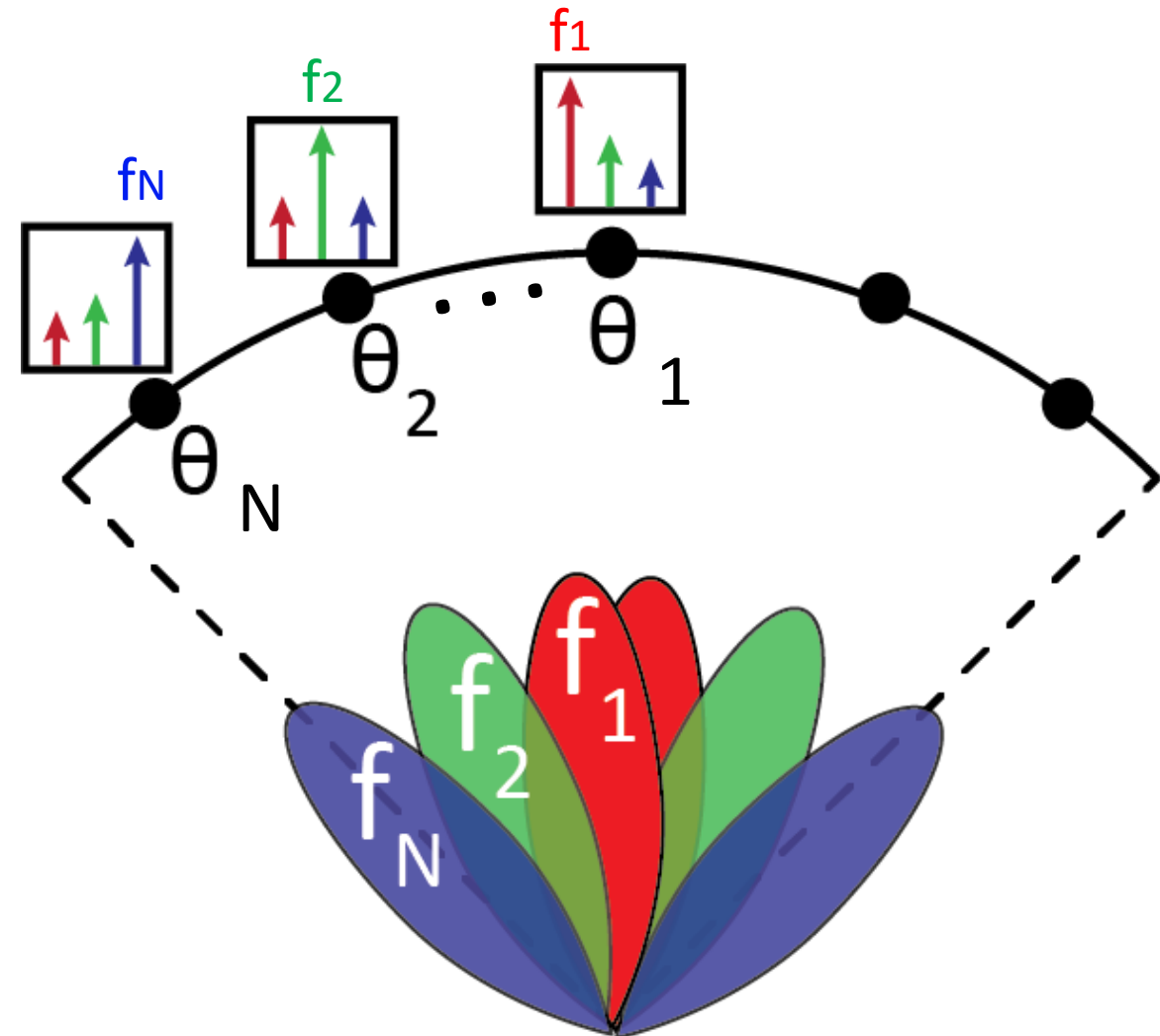
Outline

- **Prior works in single-shot localization THz frequencies**
- Enabling On-chip THz localization using frequency dispersive antennas
- On-chip 360-400GHz transceiver design and implementation
- Circuit implementation and characterization
- 1D, chip-to-chip, and 2D angular measurement results
- Conclusions

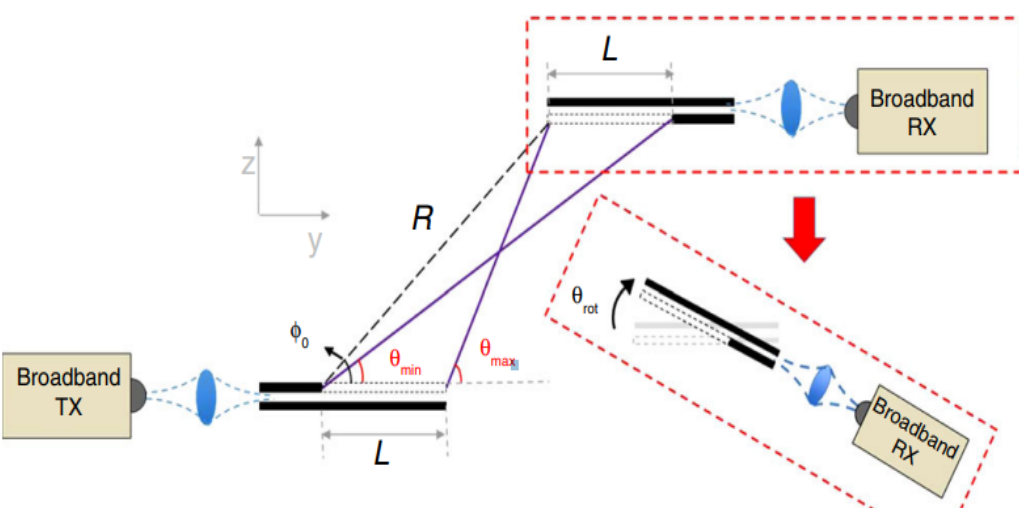
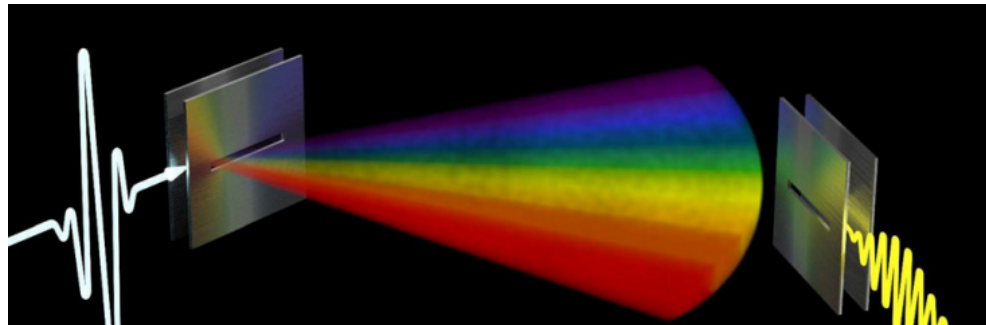
1D Single-Shot Localization Concept

Technique: Broadcasting chirped or broadband pulse from the unique 1D angle-to-spectrum mapped source.

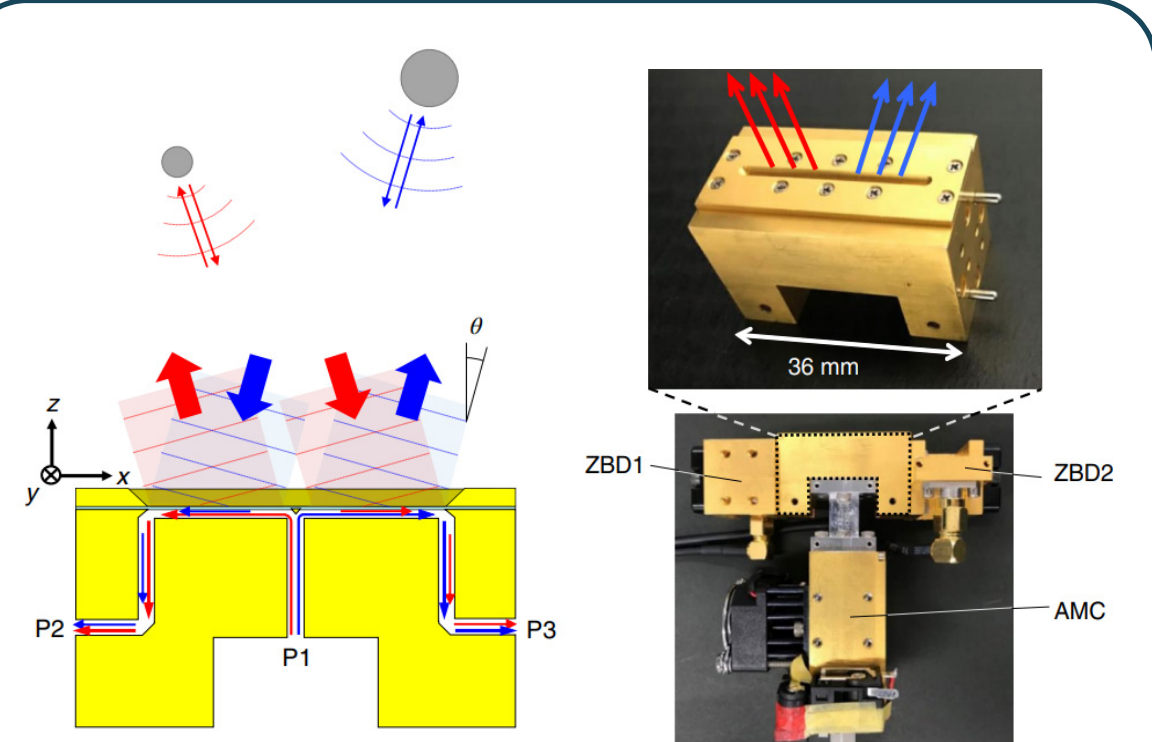
Goal: Simultaneous localization of multiple nodes at the 1D space



Prior 1D THz Localization Works

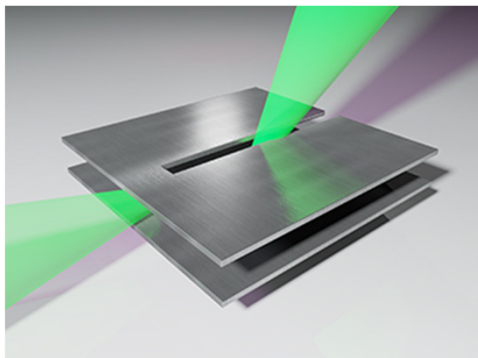
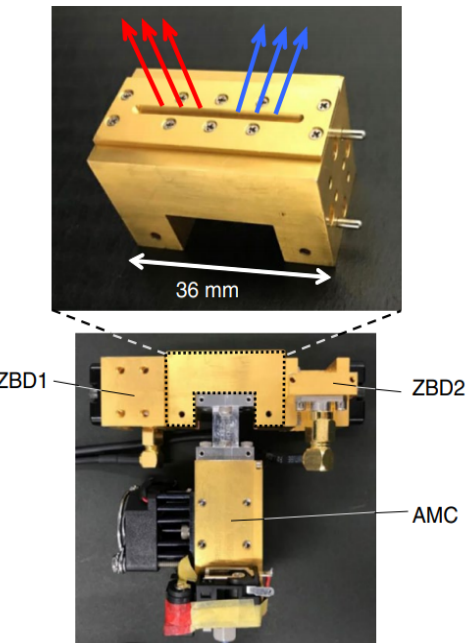


Yasaman Ghasempour et al., "Single-Shot Link Discovery for Terahertz Wireless Networks," Nature Comm. 11.1 (2020): 1-6.

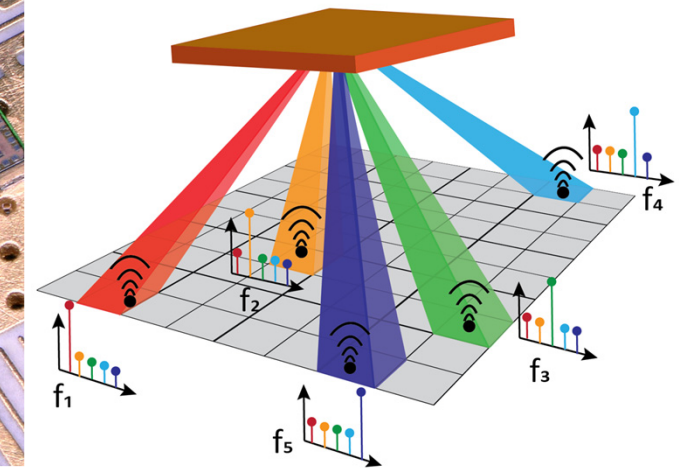
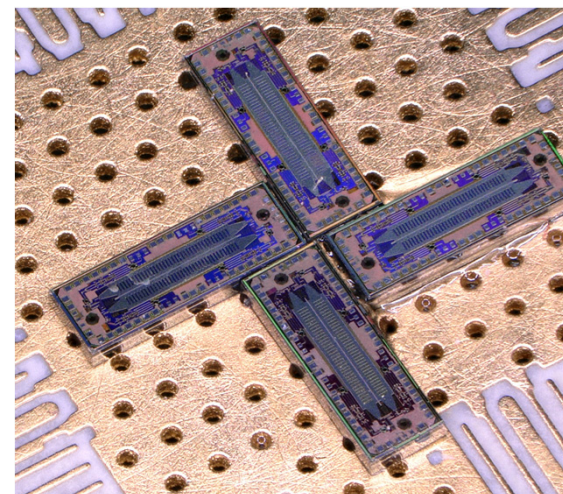


Hironori Matsumoto et al., "Integrated Terahertz Radar Based on Leaky-Wave Coherence Tomography," Nature Elect. 3.2 (2020): 122-129

2D Localization and Motivation



- External bulky THz sources
- Limited to 1D angular localization



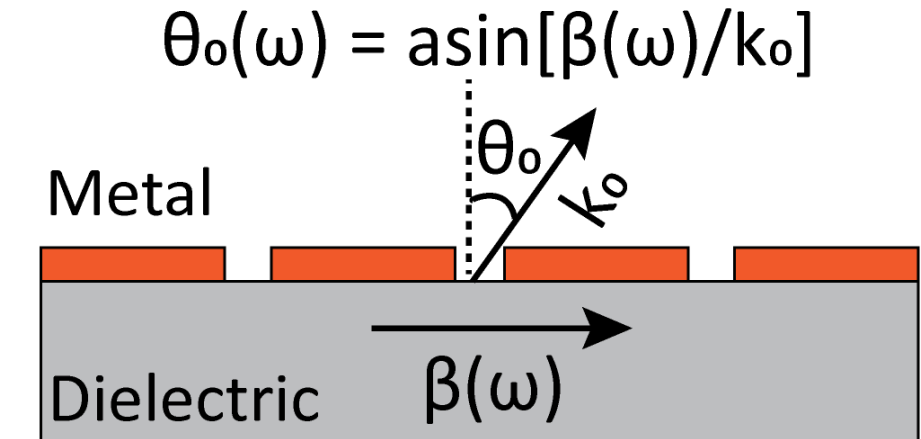
- Scalable and miniaturized
- On-chip reconfigurable back-end
- Low Power
- Enabling 2D localization

Outline

- Prior works in single-shot localization THz frequencies
- **Enabling On-chip THz localization using frequency dispersive antennas**
- On-chip 360-400GHz transceiver design and implementation
- Circuit implementation and characterization
- 1D, chip-to-chip, and 2D angular measurement results
- Conclusions

Dual-port LWAs for 1D Angular Coverage

- Periodic Leaky-wave antennas (PLWAs) due to frequency scanning capability, high directivity, and large radiation bandwidth.
- For a single mode, lower frequencies would result in emission towards broadside and the higher frequencies towards the end-fire.



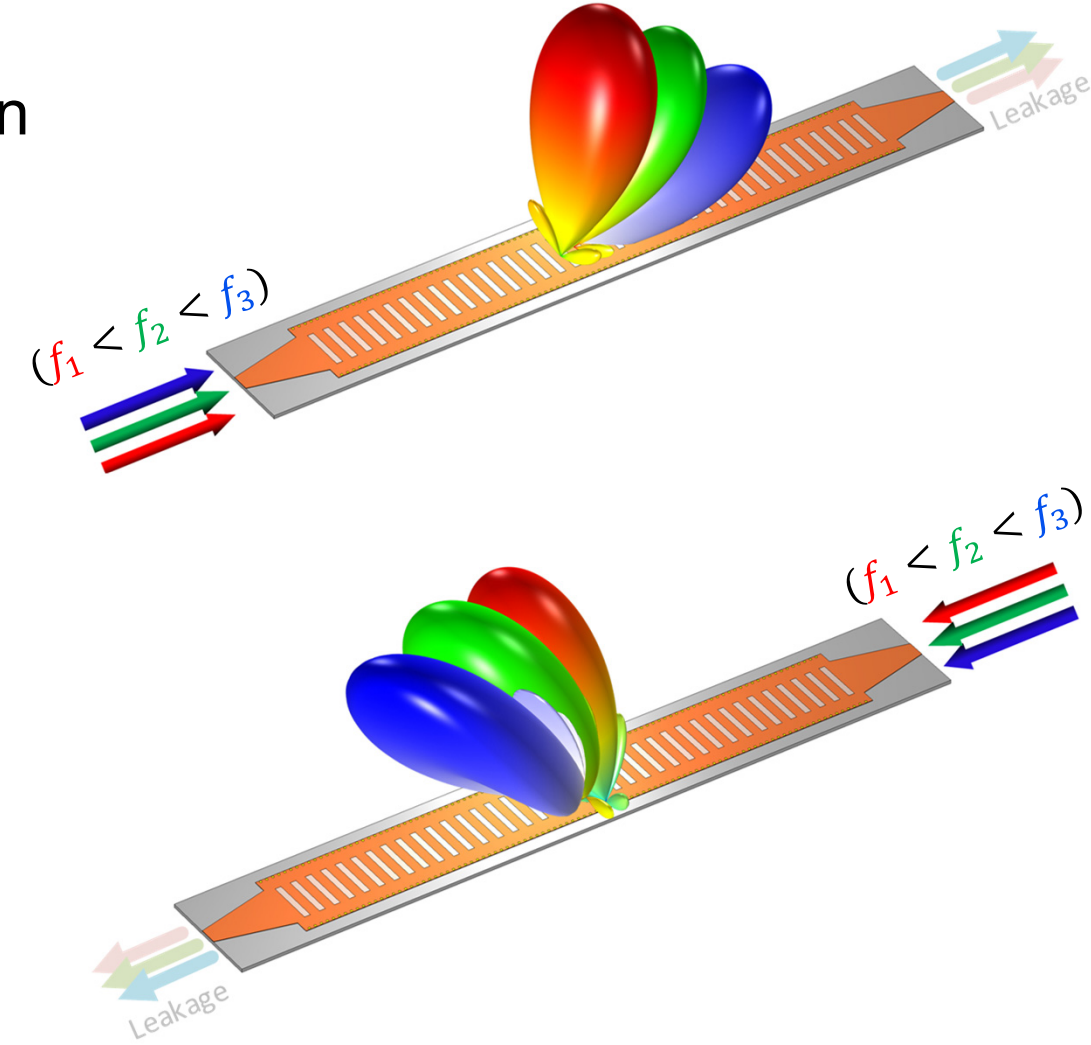
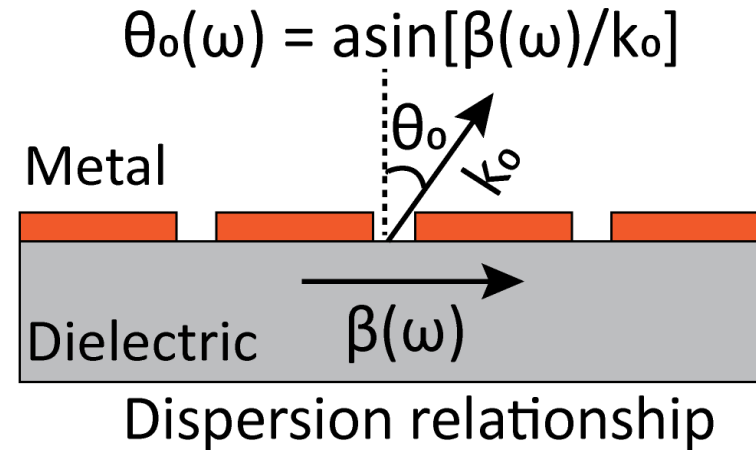
Dispersion relationship

Radiation Condition (fast wave):

$$\beta(\omega) < k_0$$

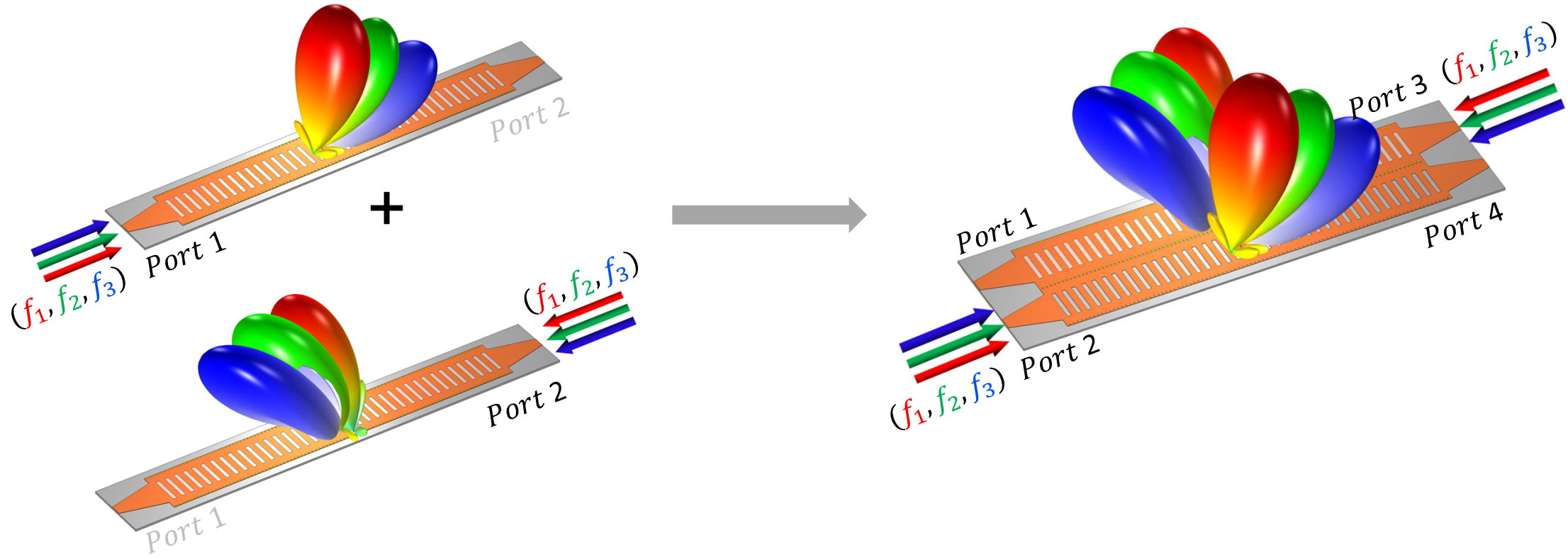
Dual-port LWAs for 1D Angular Coverage

- Injecting signal from the left hand would result in radiation within a single quadrant.
- Other ports can be excited to cover the full 1D hemisphere.



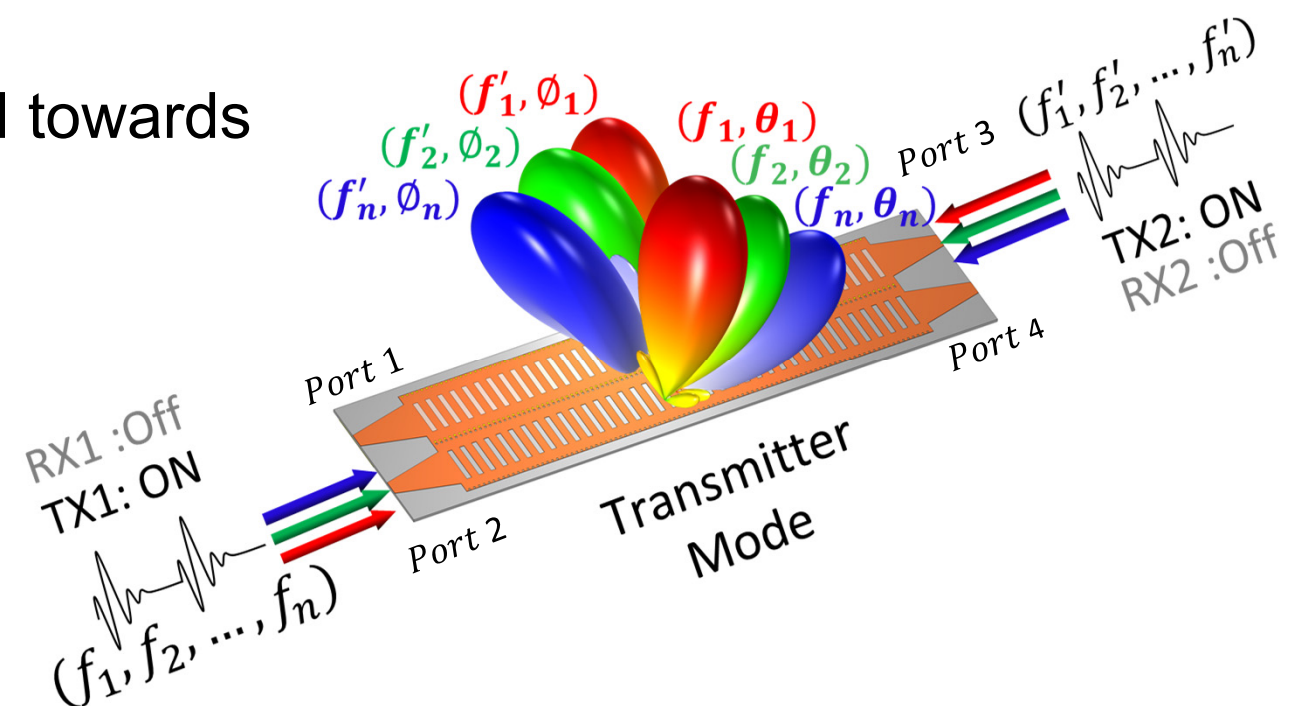
Dual-port LWAs for 1D Angular Coverage

- By Utilizing 2 LWAs excited from two opposite ports, full 1D hemisphere can be simultaneously covered.
- High isolation between 2 LWAs.
- Guided Mode separated by a via wall.



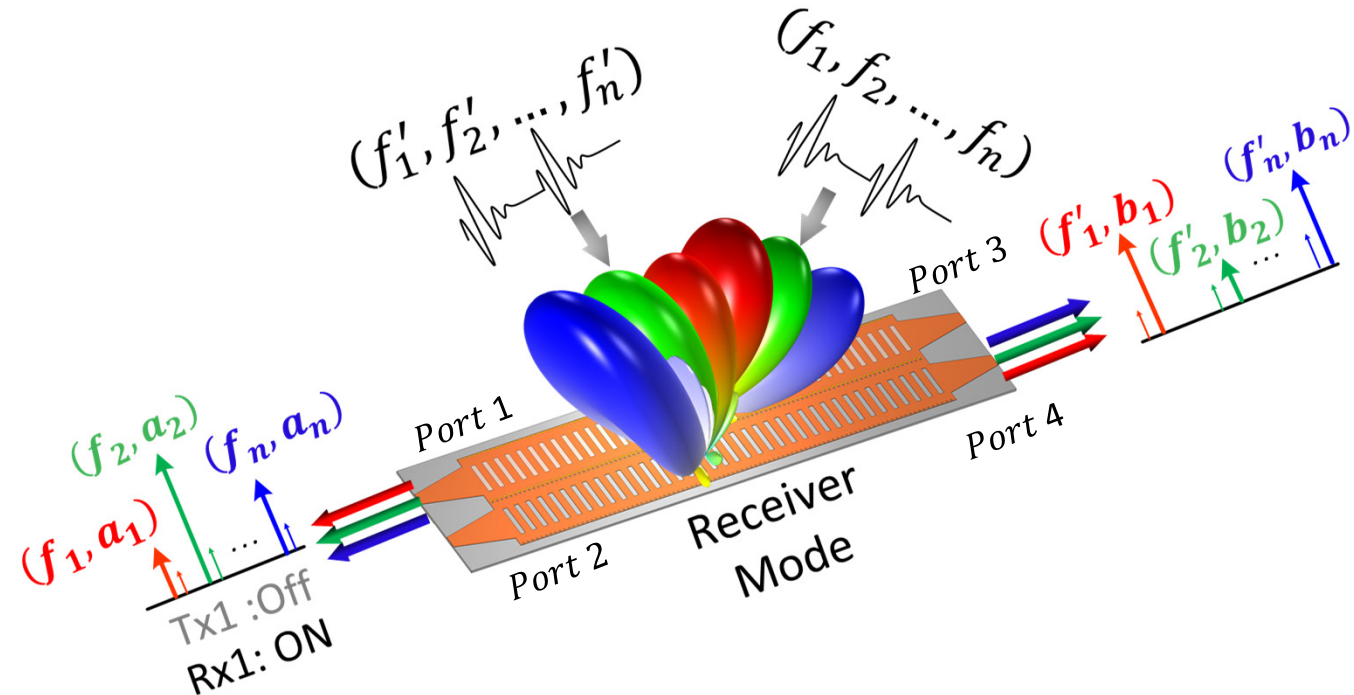
Two Dual-port LWAs at TX-mode

- Two Dual-port LWAs can be utilized in TX and/or RX modes .
- In TX mode, broadband signal from Port 2 and Port 3 are injected.
- Different frequencies will be directed towards different pointing angles
- Port 1 and Port 4 are turned off.



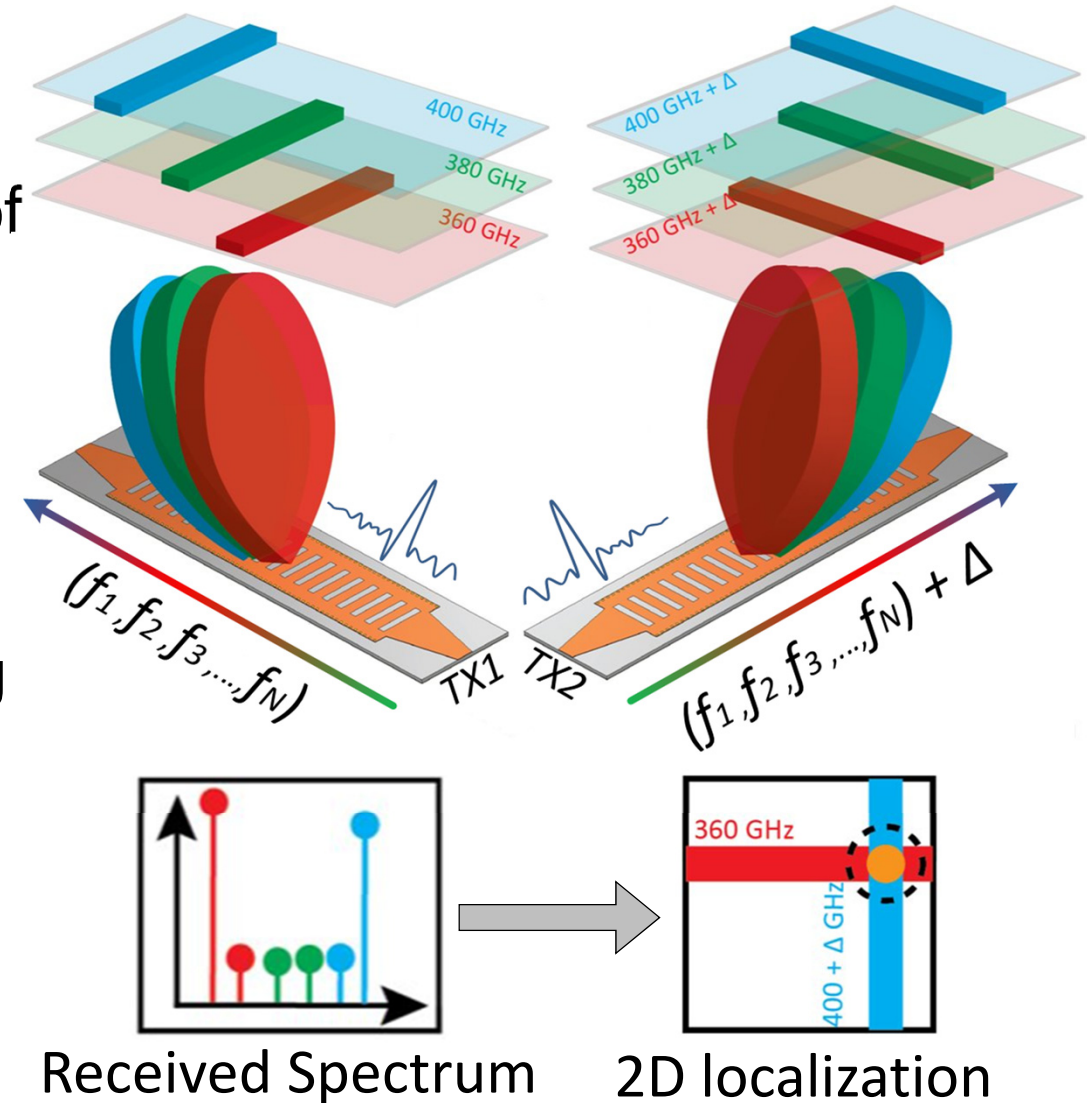
Two Dual-port LWAs at RX-mode

- In RX mode, broadband signal is received from unknown direction.
- Different frequencies are translated to different amplitudes across the broadband received spectrum based on the direction of transmitter
- Port 2 and Port 3 are turned off.



2D localization using orthogonal LWAs

- Enabling 2D frequency to space mapping and localization by orthogonal placements of two LWAs.
- Two broadband signals are injected into 2 LWAs.
- Slight frequency offset of Δ for differentiating between the received signal from the two transmitters.

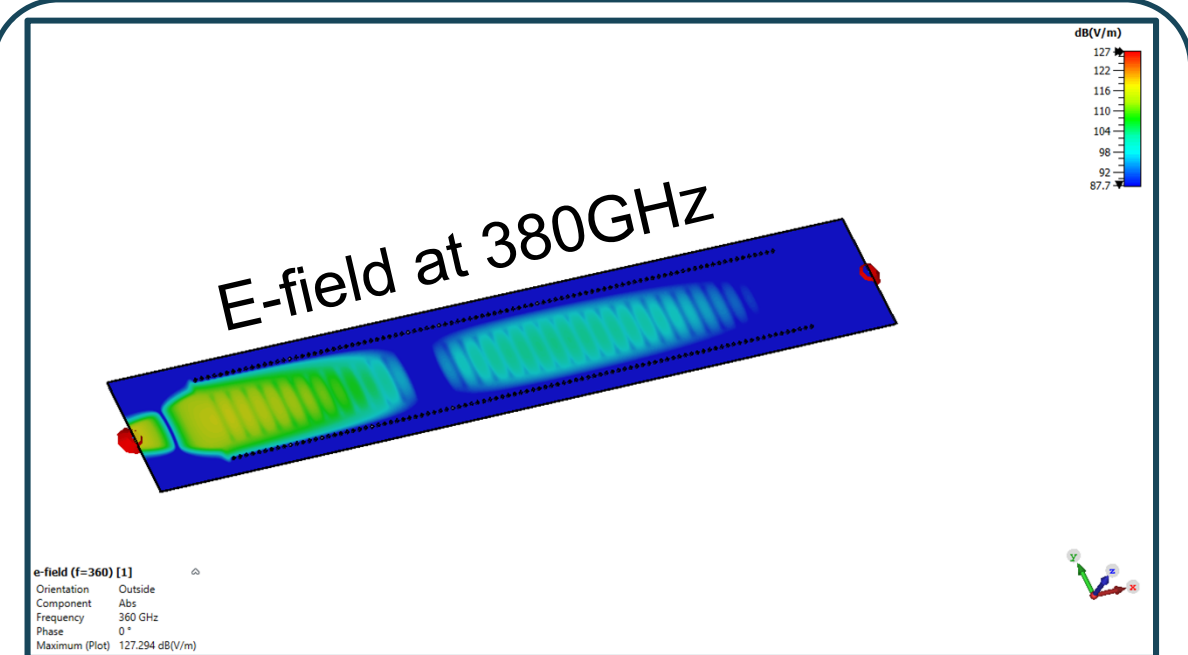
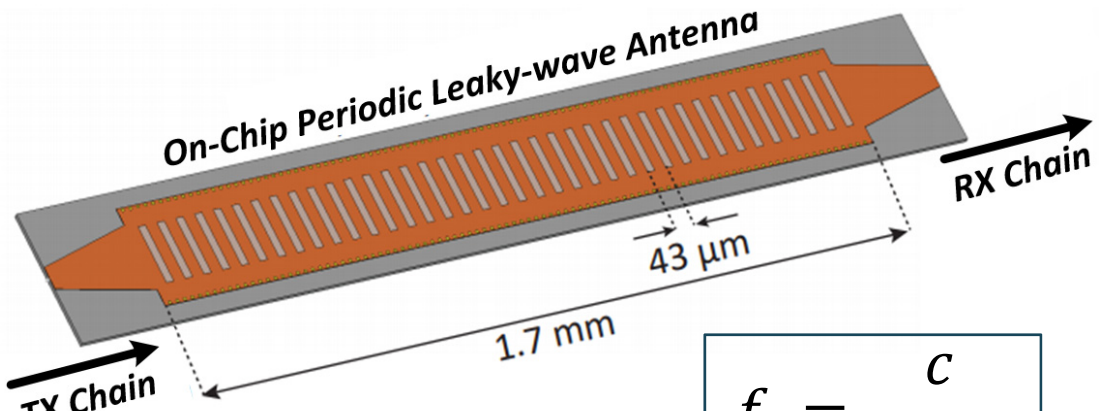
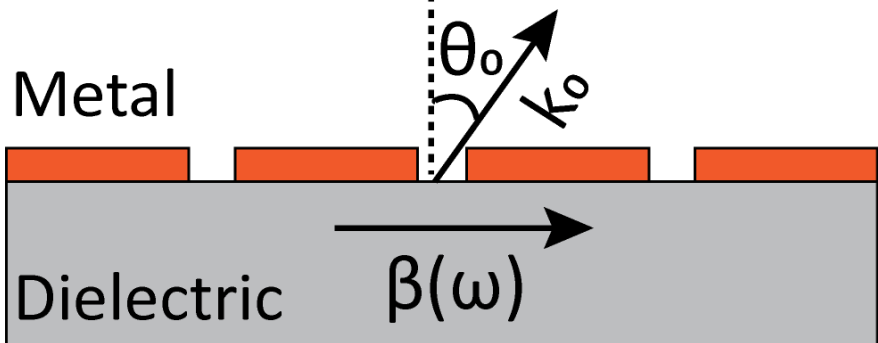


Outline

- Prior works in single-shot localization THz frequencies
- Enabling On-chip THz localization using frequency dispersive antennas
- **On-chip 360-400GHz transceiver design and implementation**
- Circuit implementation and characterization
- 1D, chip-to-chip, and 2D angular measurement results
- Conclusions

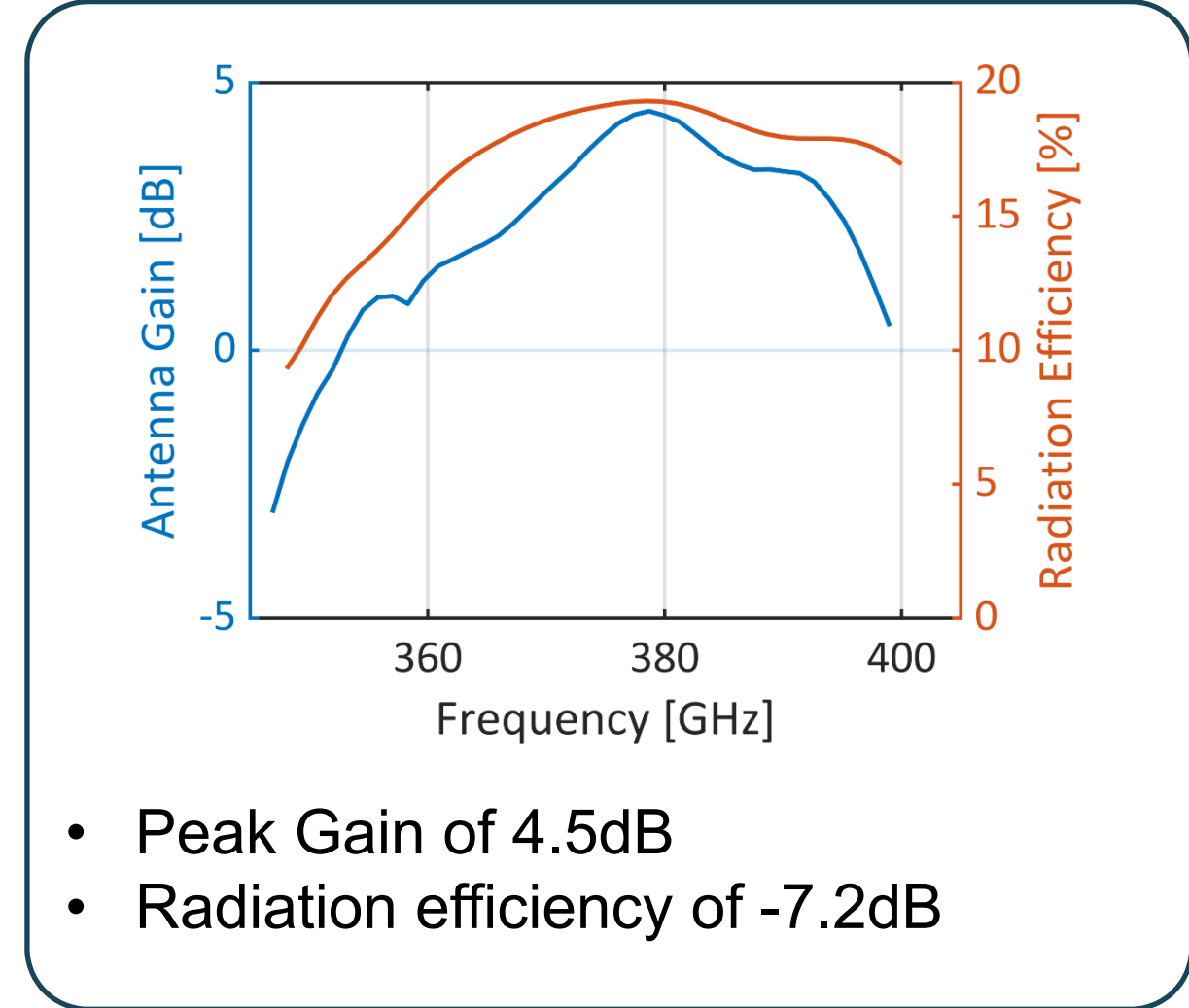
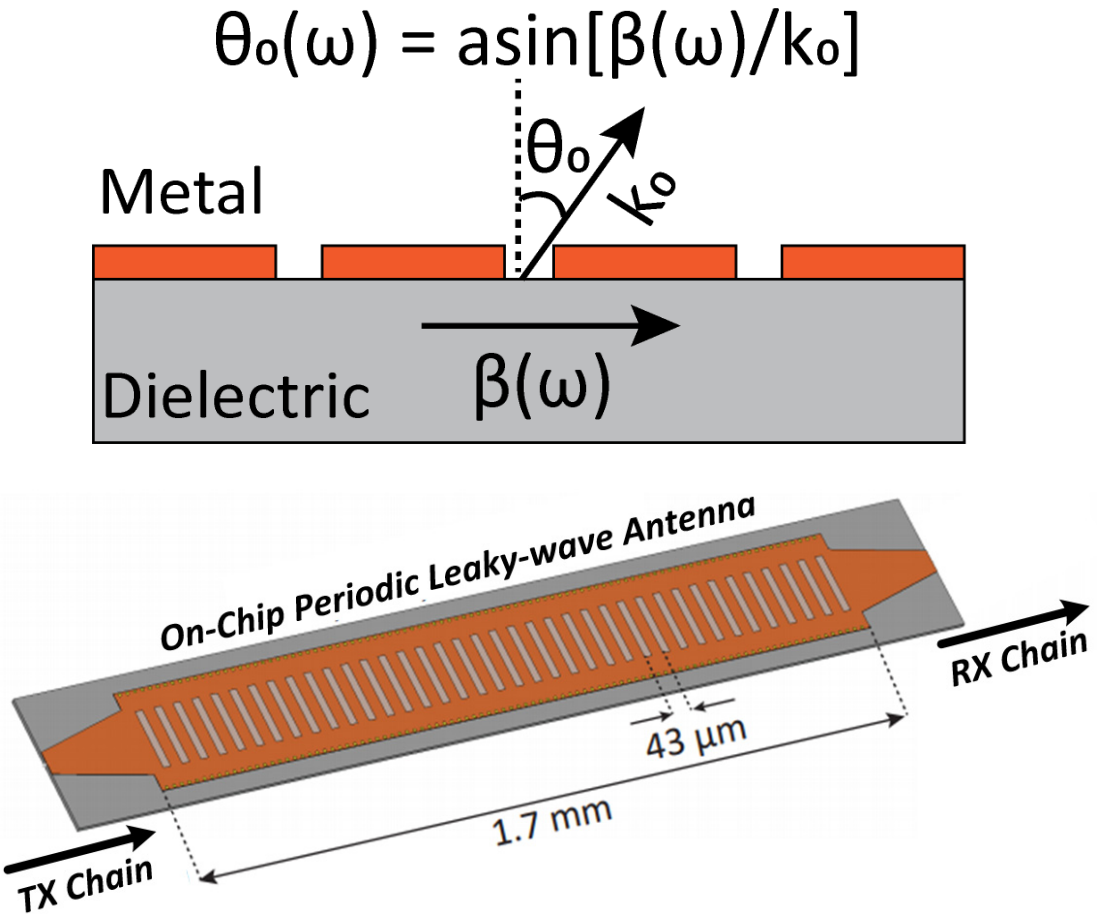
Periodic LWA design and Simulation

$$\theta_0(\omega) = \arcsin[\beta(\omega)/k_0]$$

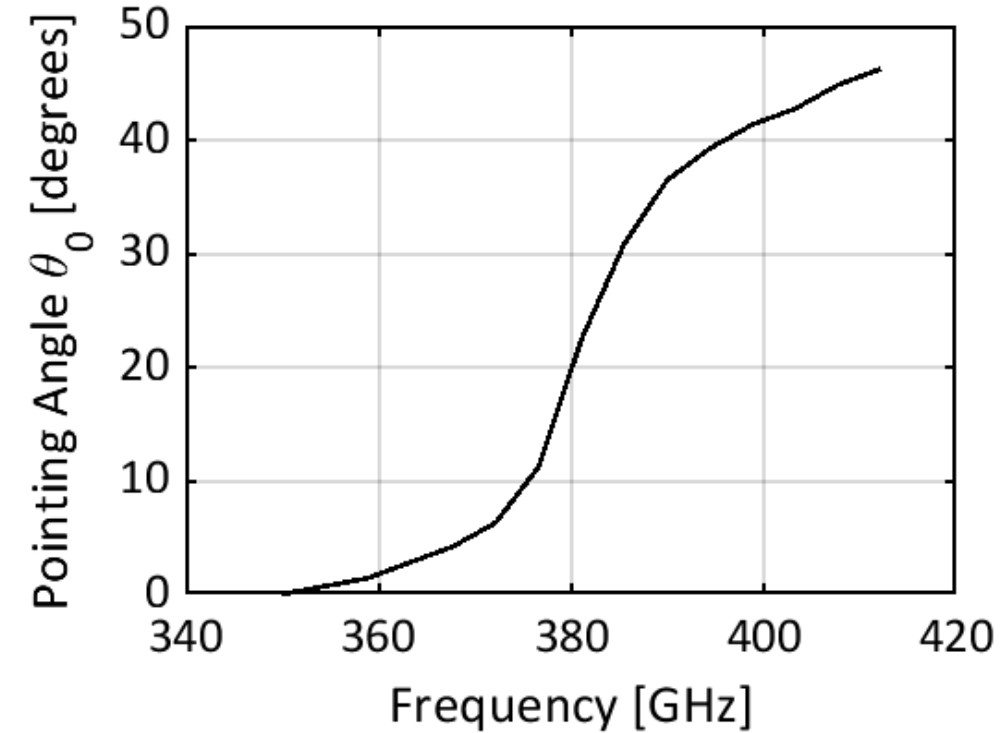
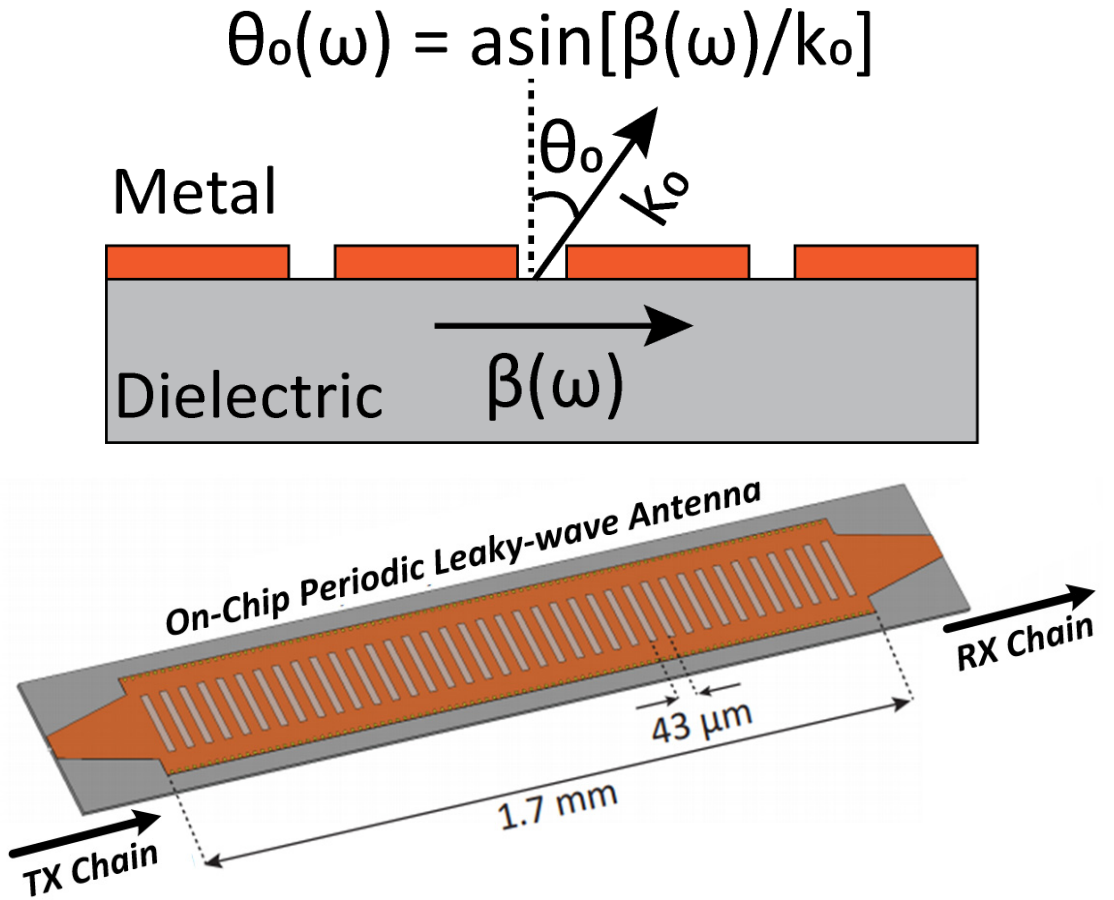


- Periodic Dual Port LWA is designed for 360-400GHz
- Length of 1.7mm, width of 225μm cutoff frequency of 320GHz and slot spacing of 43μm

Periodic LWA design and Simulation

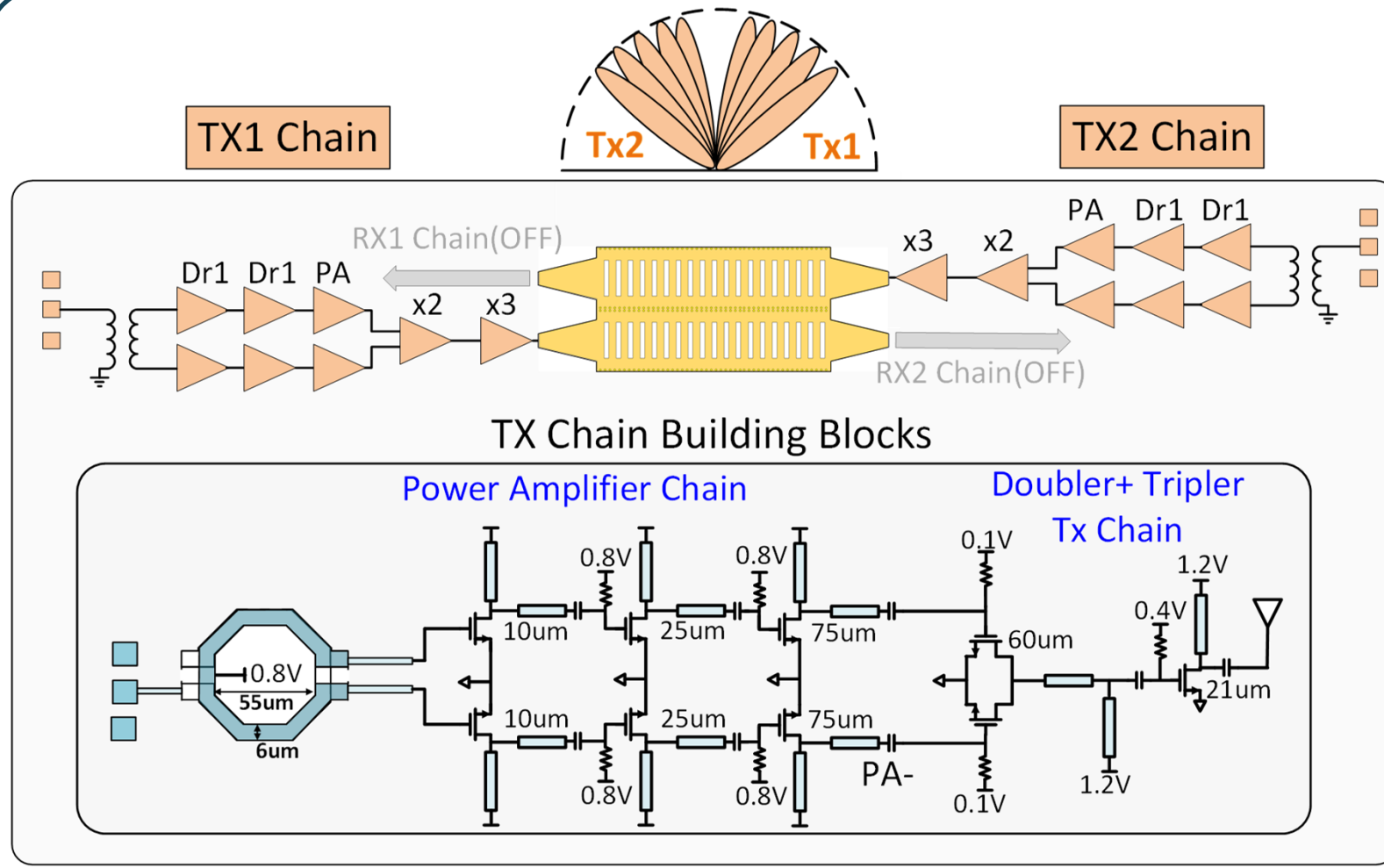


Periodic LWA design and Simulation



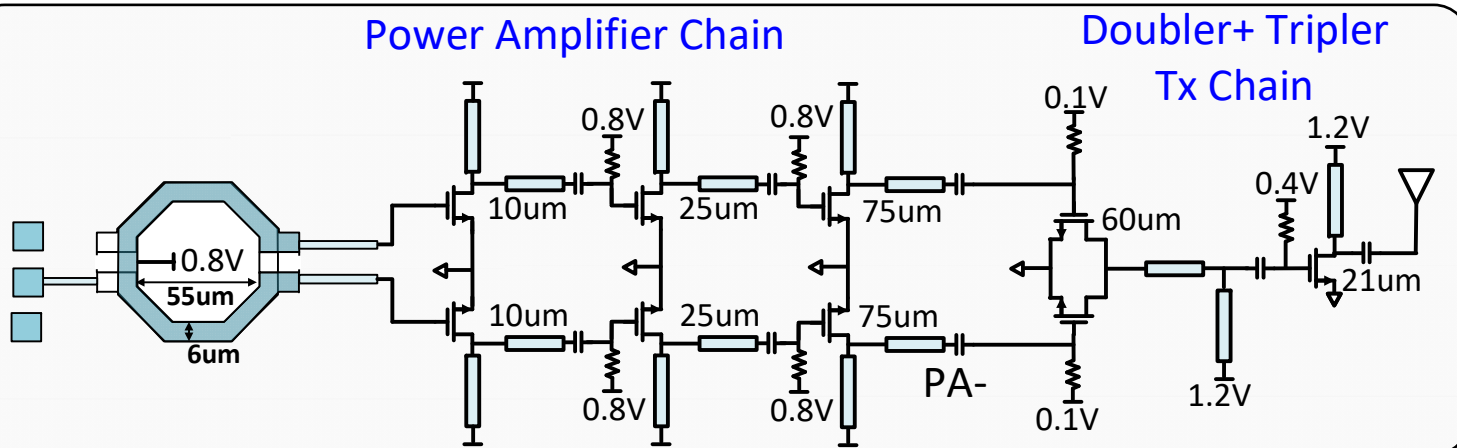
- Beams are pointing from Broadside to 41 degrees within 360 - 400GHz

TX-mode Schematic



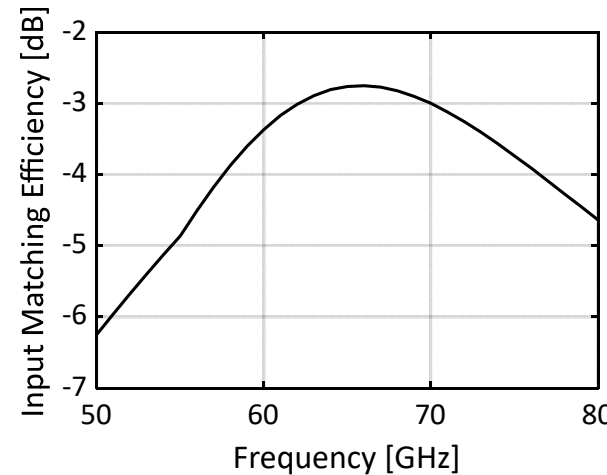
- Dual 360 – 400GHz TX Chain for full 1D hemispheric coverage.
- TX chain consists of 3-stage PA followed by wideband frequency Doubler and Tripler.

TX-mode Simulation Results

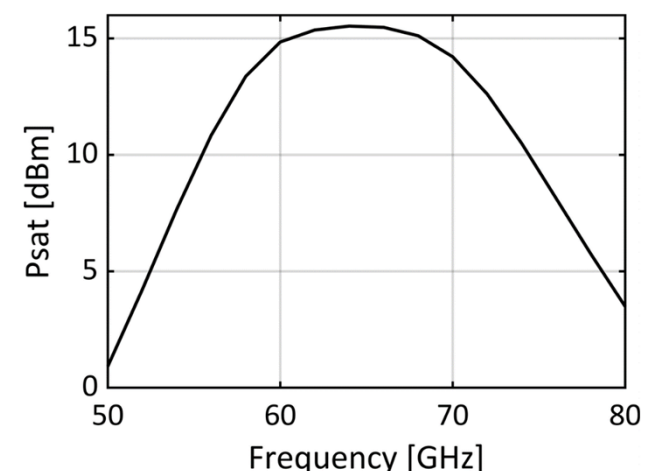


- 59-71 GHz PA with simulated Psat of 15.5dBm with PAE of 25.9%
- Frequency Doubler with peak Psat of 9.5dBm.

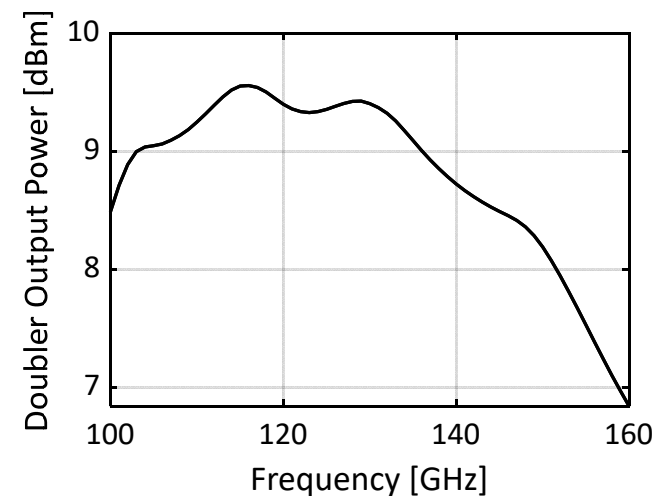
Input Matching Efficiency



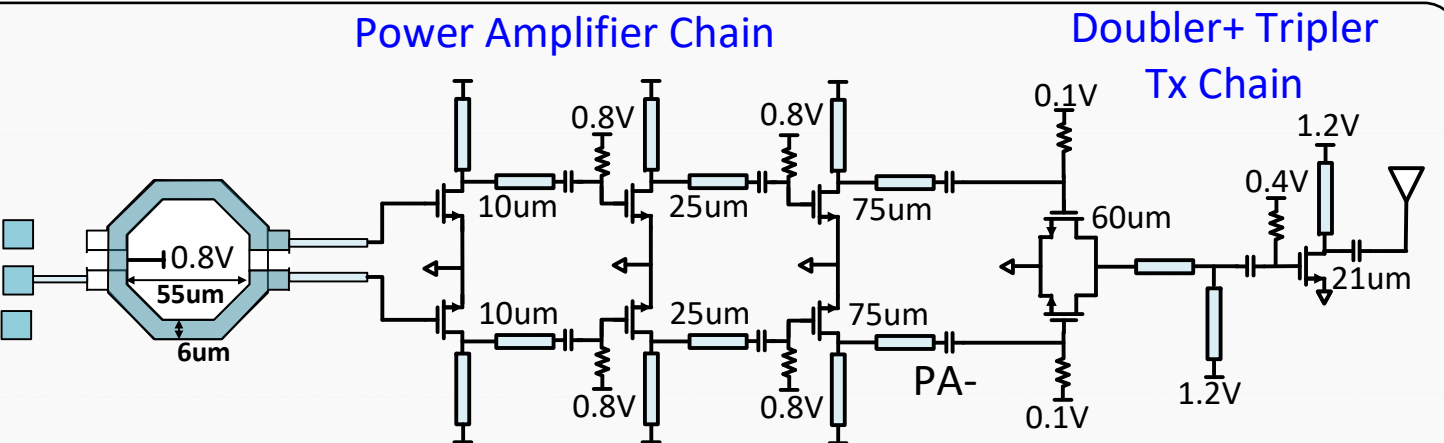
PA Psat vs. Frequency



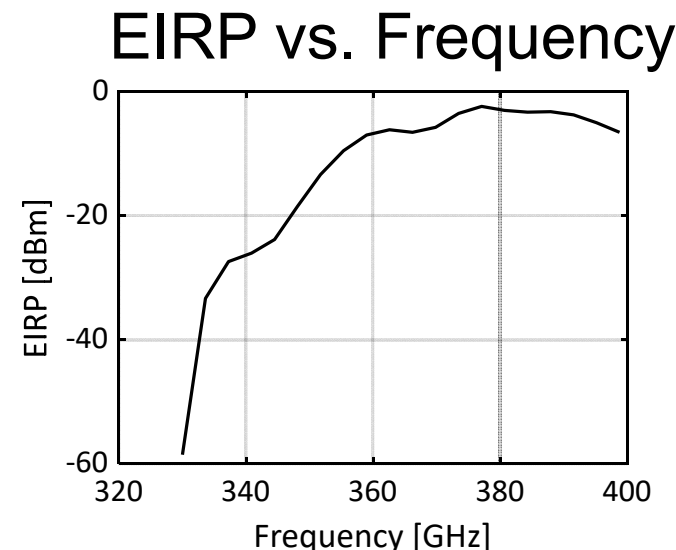
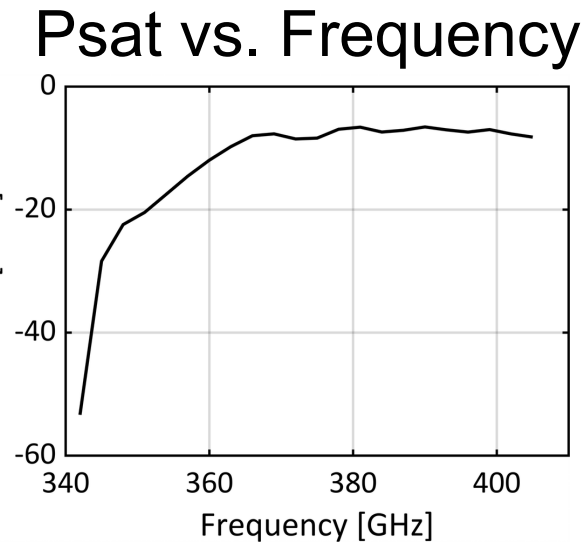
Doubler Psat



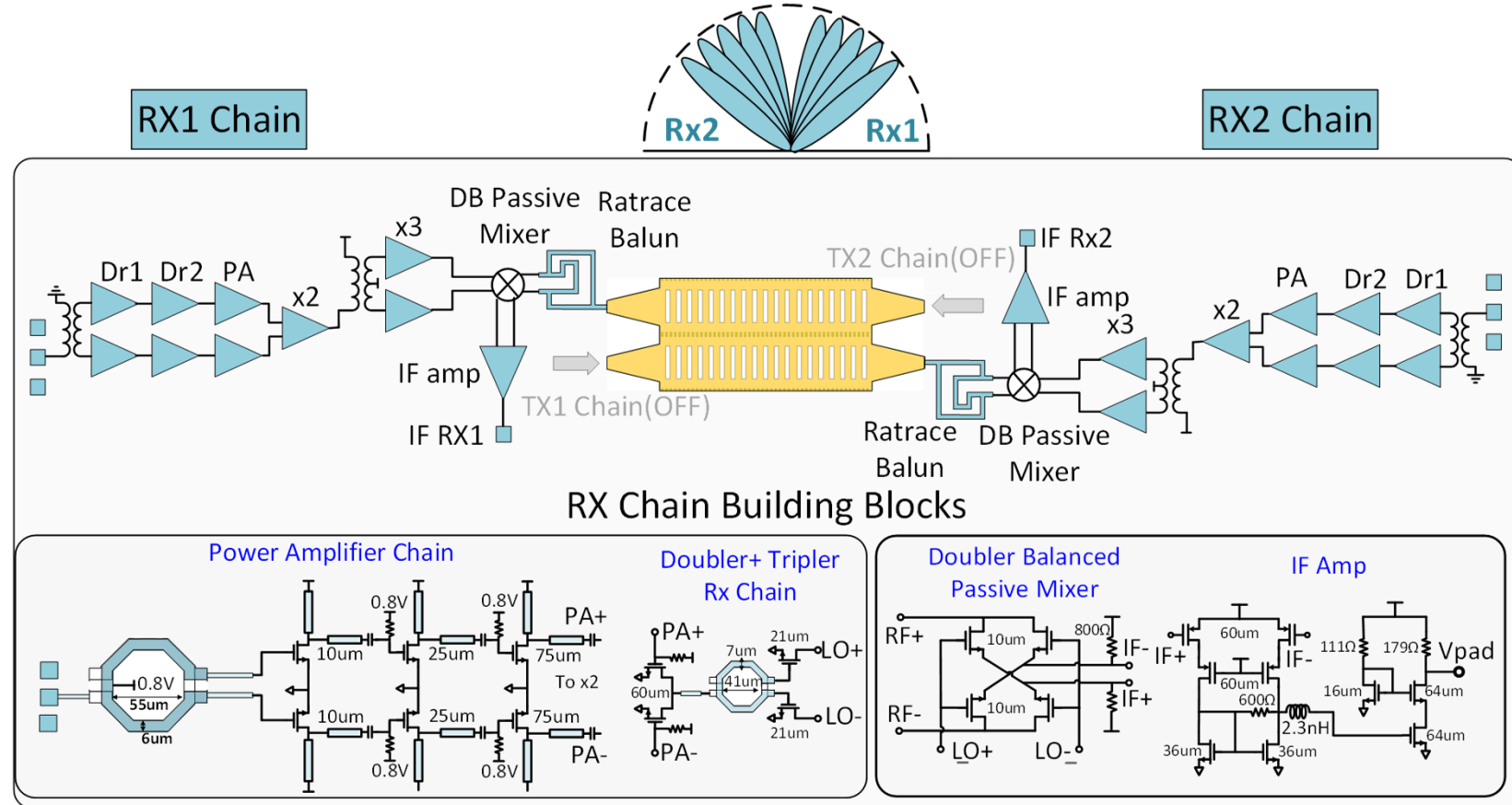
TX-mode Simulation Results



- Peak simulated Psat of -7.2dBm from 360-400GHz
- Peak Simulated EIRP of -2.7dBm at 378GHz



RX-mode Schematic

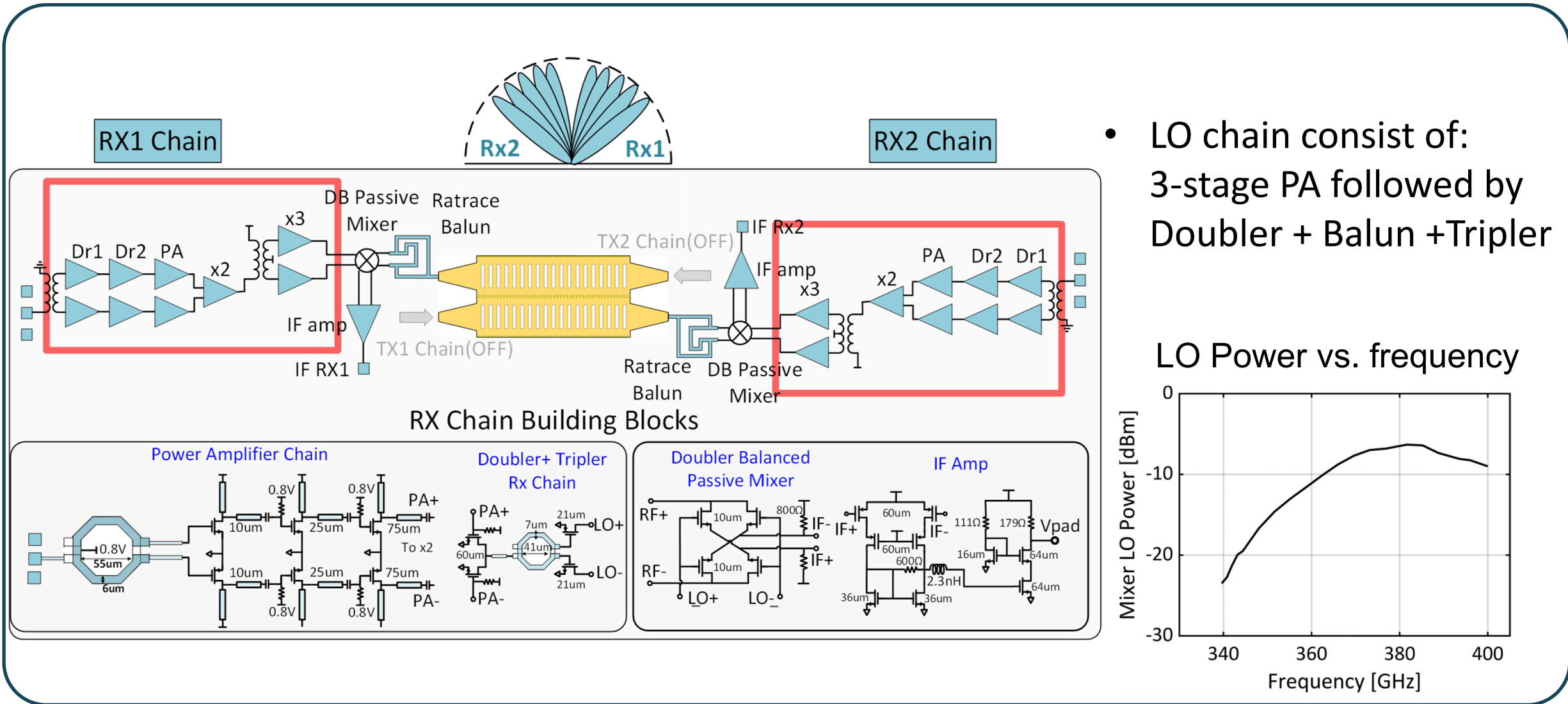


- Dual 360 – 400GHz RX Chain for full 1D hemispheric coverage

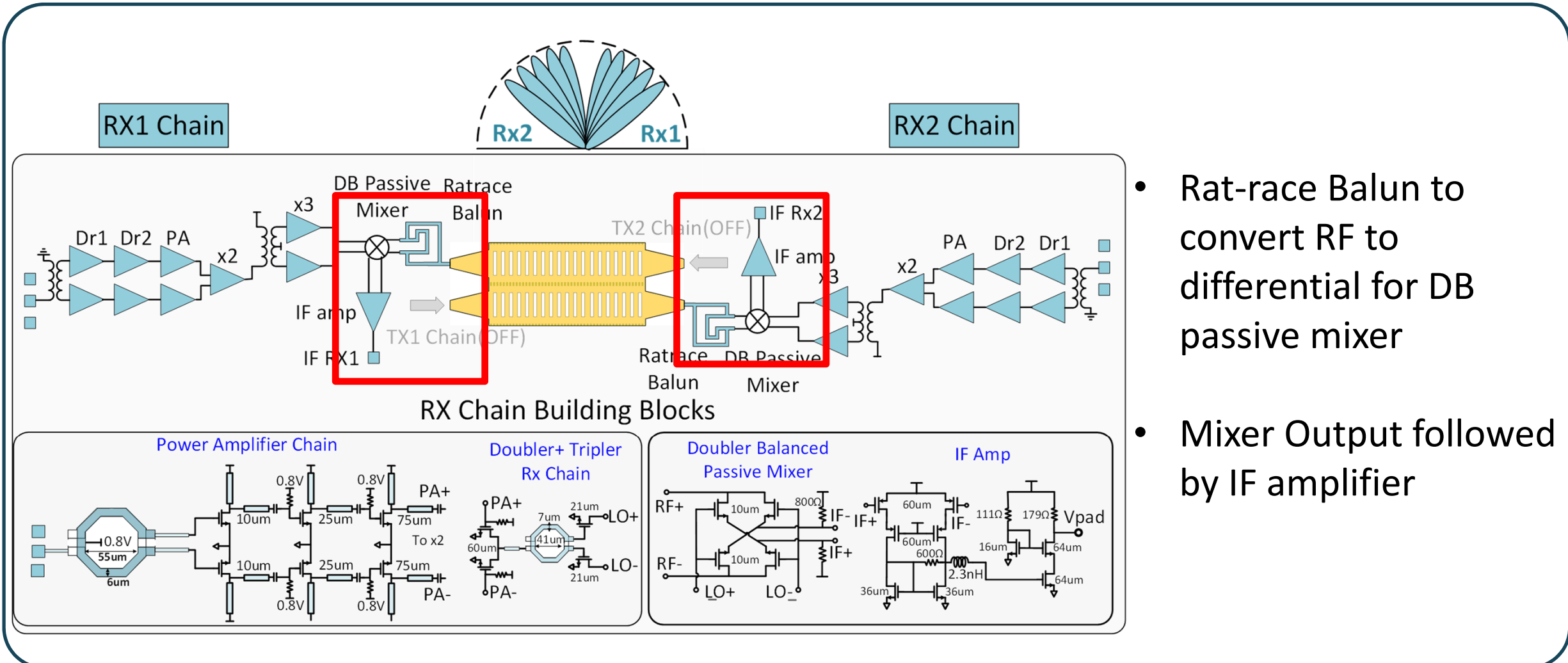
RX Chain:

- LO Generation
- DB passive Mixer
- Rat-race Balun
- IF amplifier

RX-mode Schematic

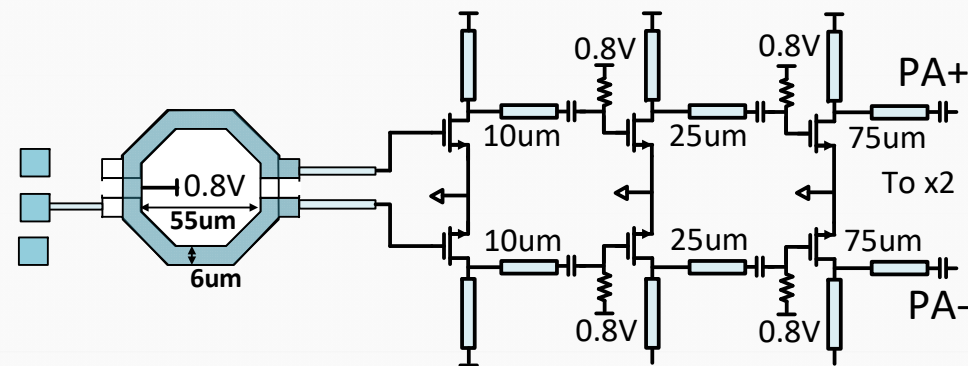


RX-mode Schematic

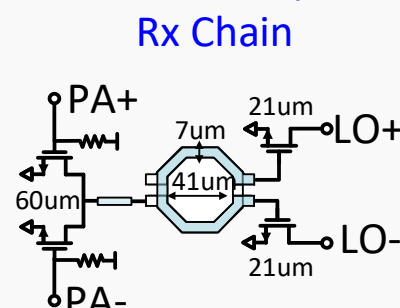


RX-mode Simulation Results

Power Amplifier Chain



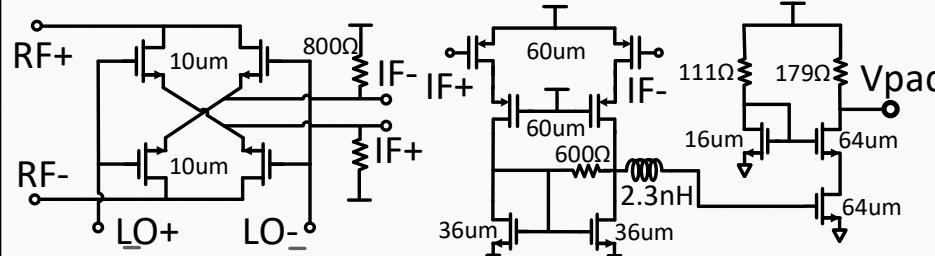
Doubler+ Tripler Rx Chain



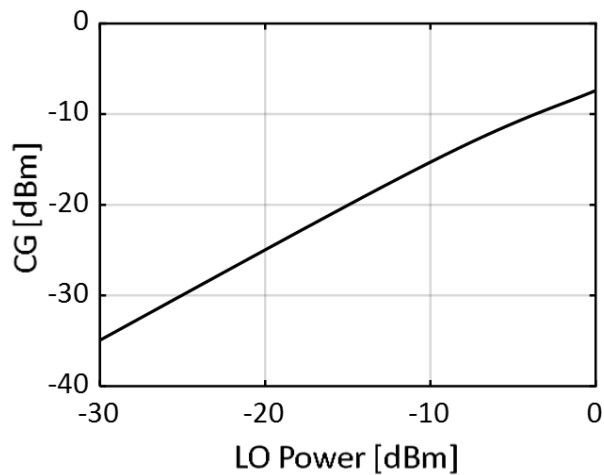
- Conversion Loss of 17.5dB at 375GHz
- IF amp gain of 16dB

Doubler Balanced Passive Mixer

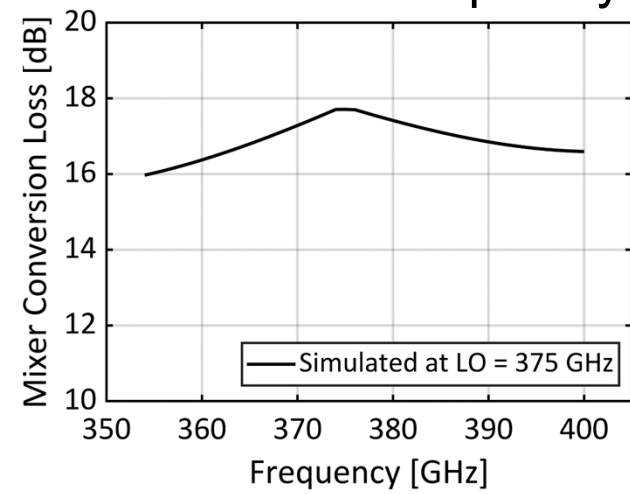
IF Amp



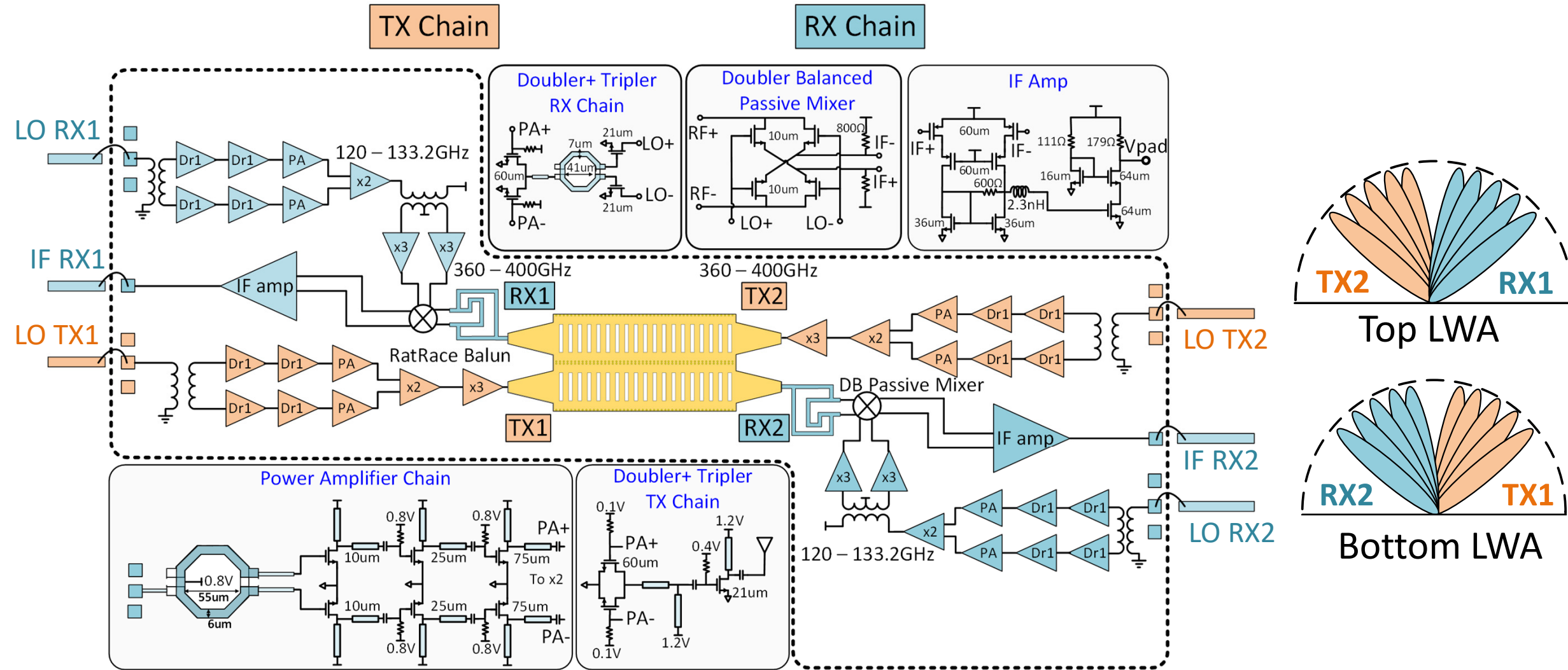
CG vs. LO Power



CG vs. RF frequency



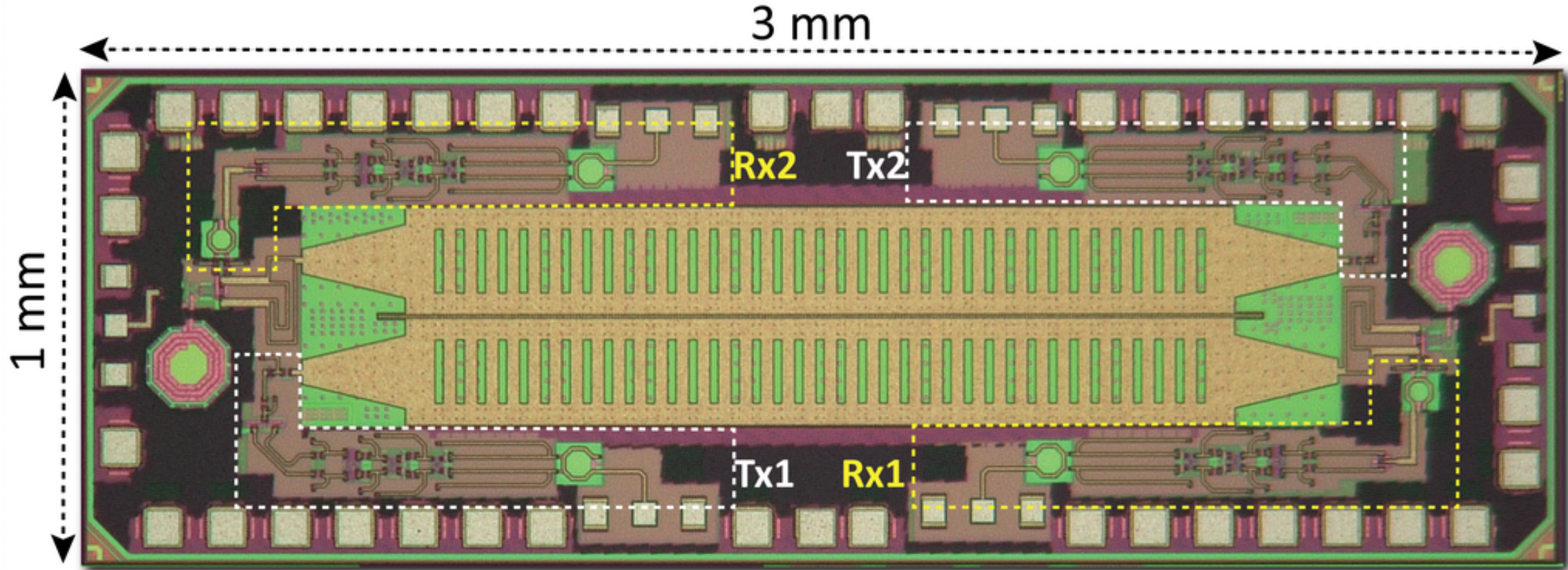
Overall TX/RX Circuit Architecture



Outline

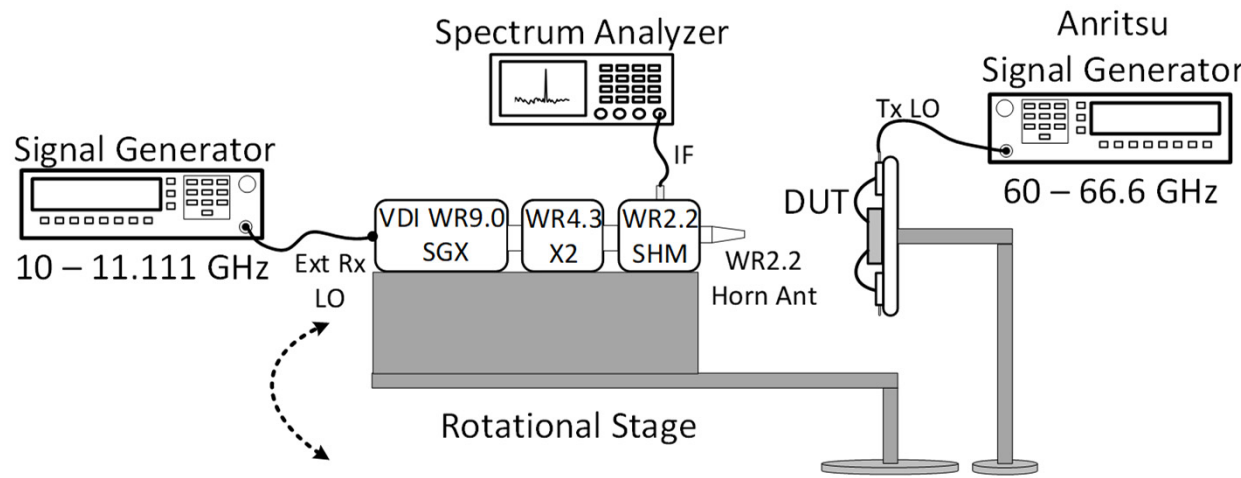
- Prior works in single-shot localization THz frequencies
- Enabling On-chip THz localization using frequency dispersive antennas
- On-chip 360-400GHz transceiver design and implementation
- **Circuit implementation and characterization**
- 1D, chip-to-chip, and 2D angular measurement results
- Conclusions

Chip Microphotograph

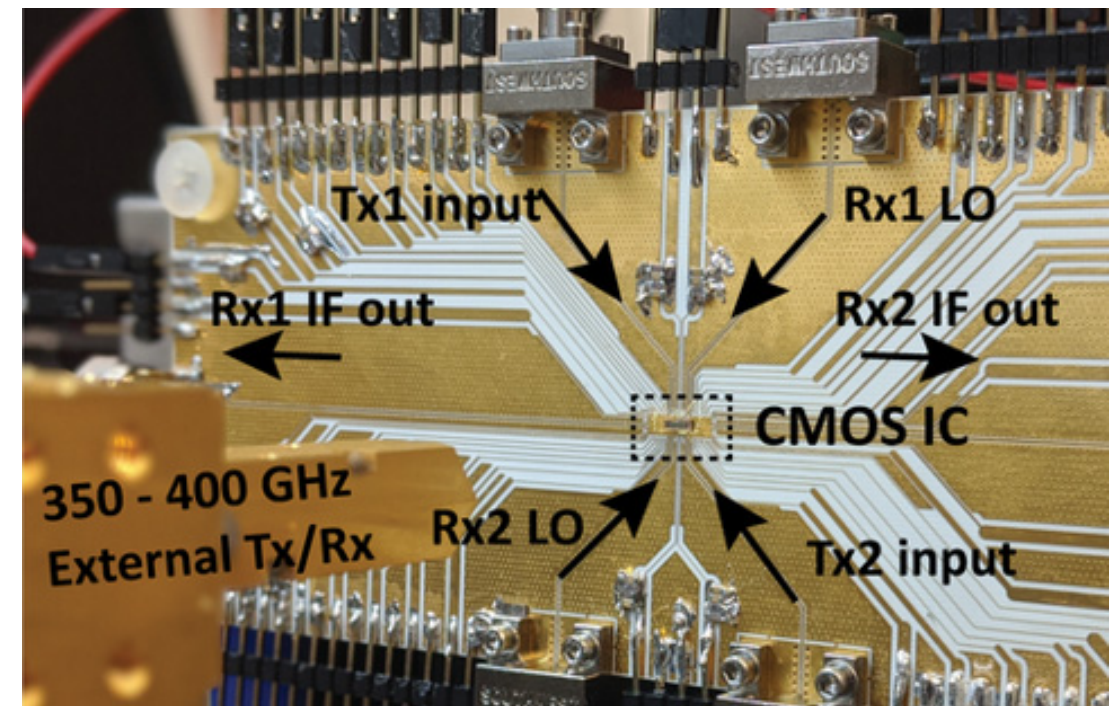


- TSMC 65nm CMOS Process
- Total area: 1mm x 3mm

Measurement Setup

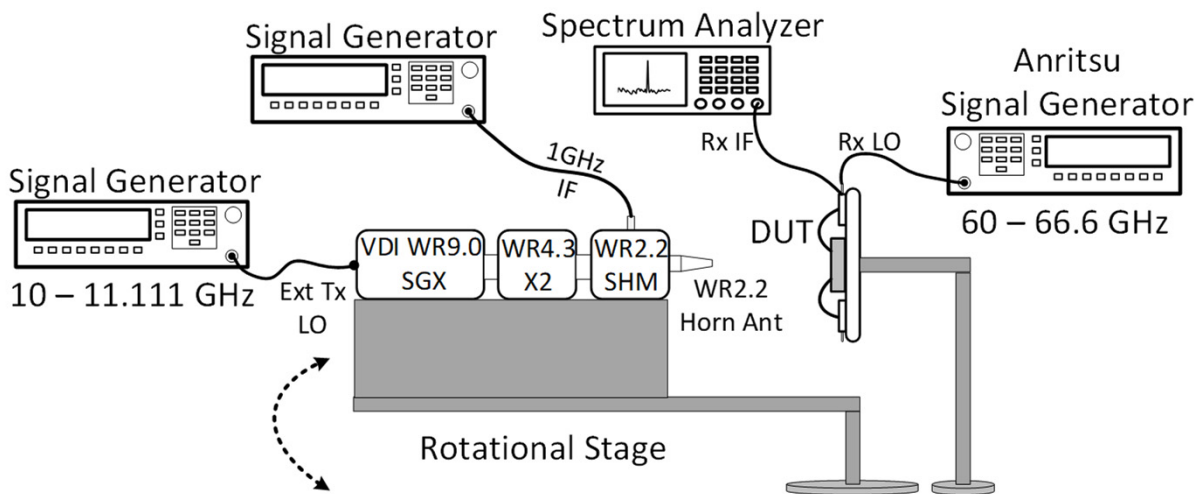


- TX-mode Measurement Setup
- External RX Chain:
VDI WR9.0 + WR4.3X2 + WR2.2 SHM

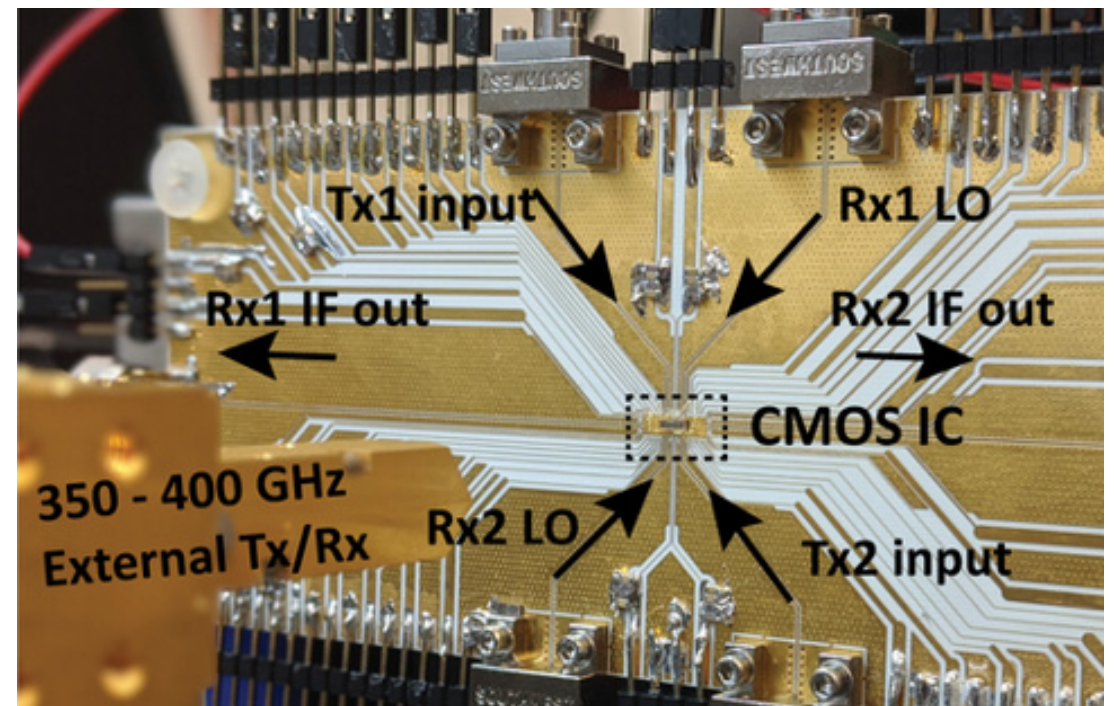


- Measurement Setup Photograph

Measurement Setup

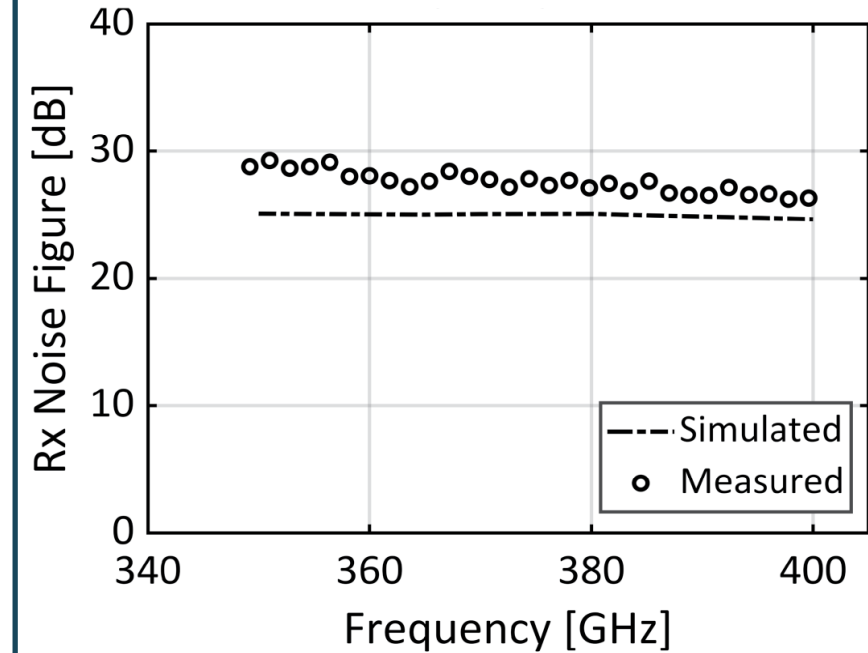
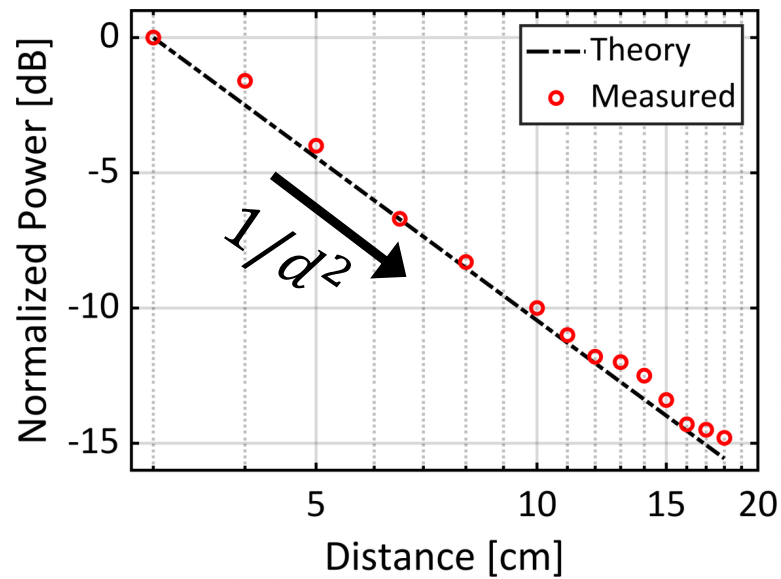
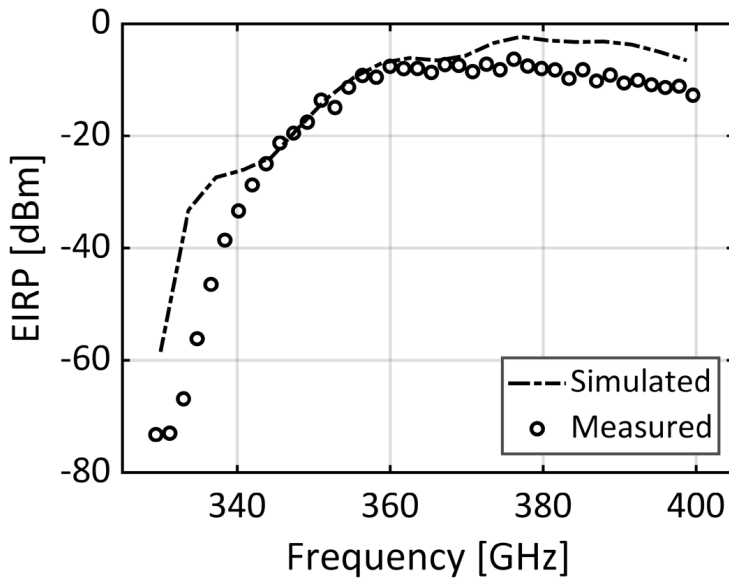


- RX-mode Measurement Setup
- External TX Chain:
VDI WR9.0 + WR4.3X2 + WR2.2 SHM



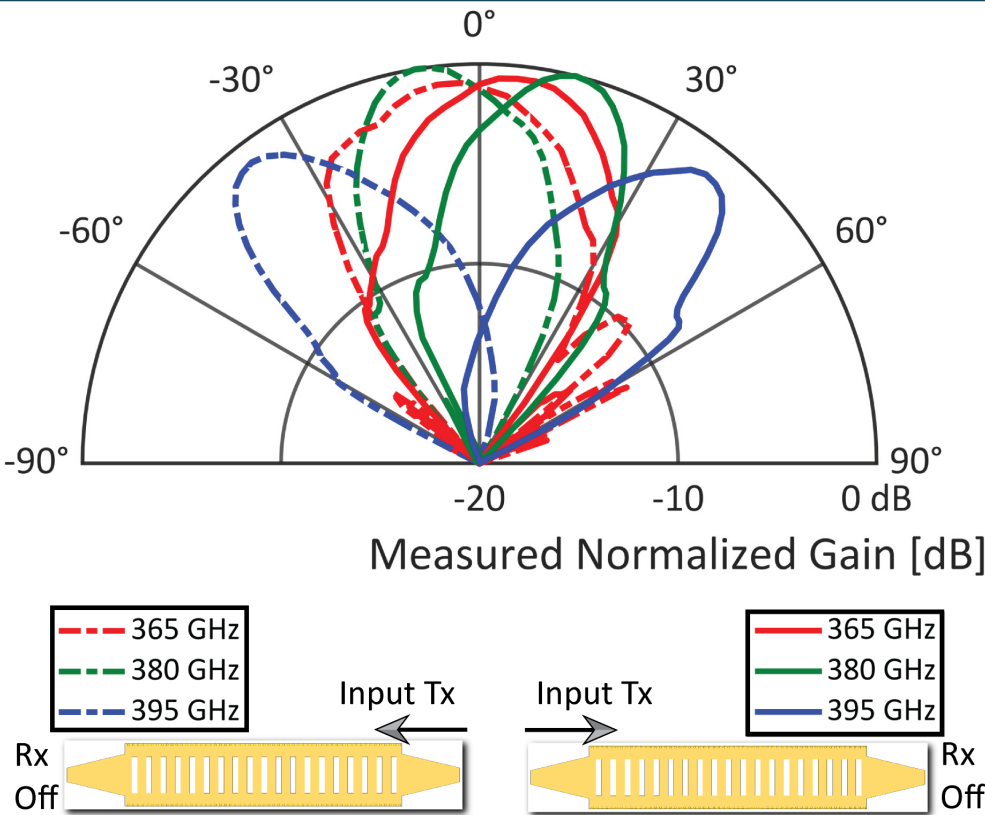
- Measurement Setup Photograph

EIRP and NF Measurement

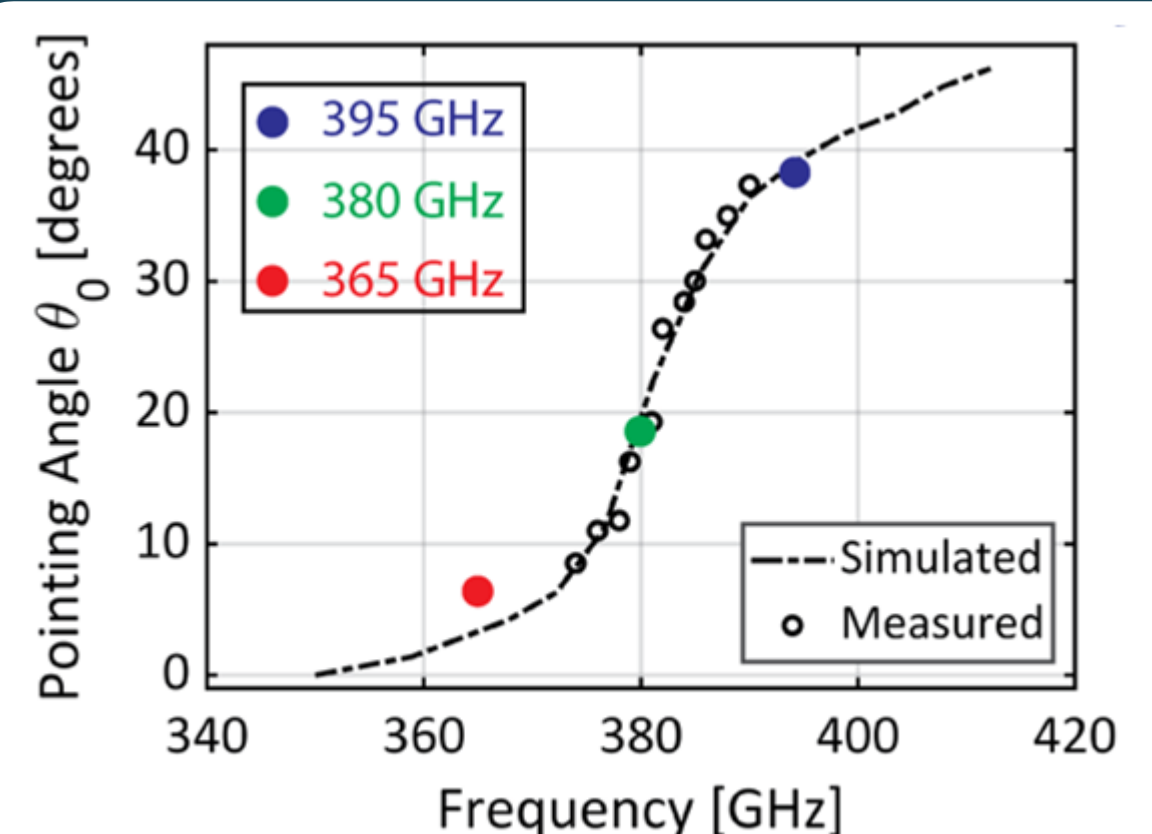


- Peak Measured EIRP of -6.4dBm across different distances.
- Average measured NF of 26.2dB.

Radiation Pattern Measurement



- Measured Radiation patterns by enabling both LWAs ports



- Pointing angles from broadside to $\pm 40^\circ$

Outline

- Prior works in single-shot localization THz frequencies
- Enabling On-chip THz localization using frequency dispersive antennas
- On-chip 360-400GHz transceiver design and implementation
- Circuit implementation and characterization
- **1D, chip-to-chip, and 2D angular measurement results**
- Conclusions

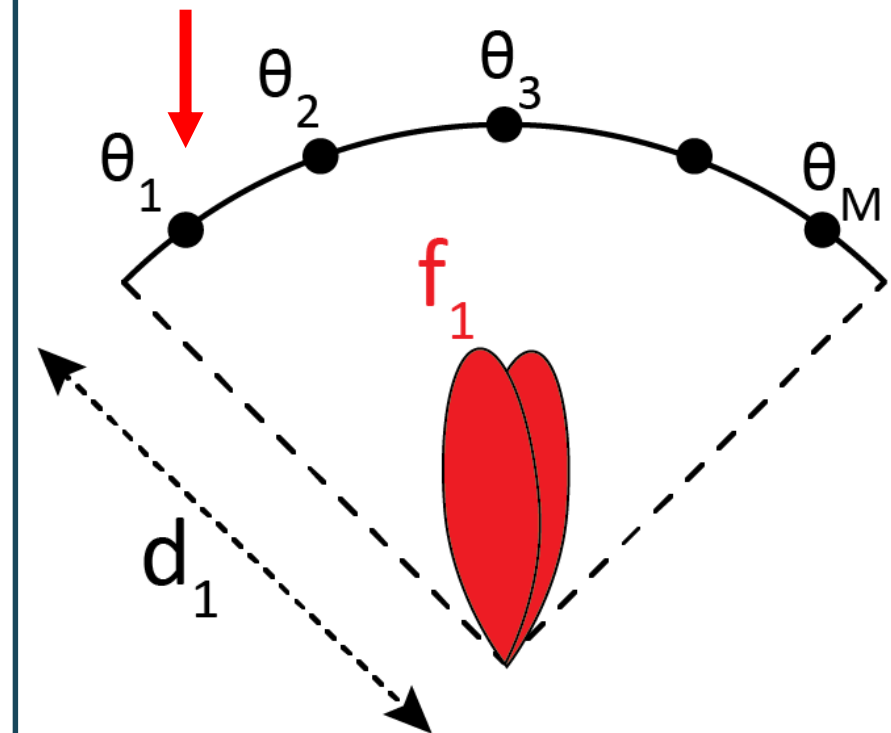
1D Localization Measurement Calibration

$$\mathbf{S}_{M \times N} = \begin{bmatrix} s(f_1, \theta_1) & s(f_2, \theta_1) & s(f_3, \theta_1) & \dots & s(f_N, \theta_1) \\ s(f_1, \theta_2) & s(f_2, \theta_2) & \dots & \dots & s(f_N, \theta_2) \\ \vdots & \ddots & \ddots & \dots & \vdots \\ s(f_1, \theta_M) & s(f_2, \theta_M) & \dots & \dots & s(f_N, \theta_M) \end{bmatrix}$$

f is the frequency set from $[f_1, f_2, f_3 \dots f_N]$

θ is the angle set from $[\theta_1, \theta_2, \theta_3 \dots \theta_M]$

- Based on the leaky-wave antenna radiation patterns, Frequency- Angle calibration map can be formed.

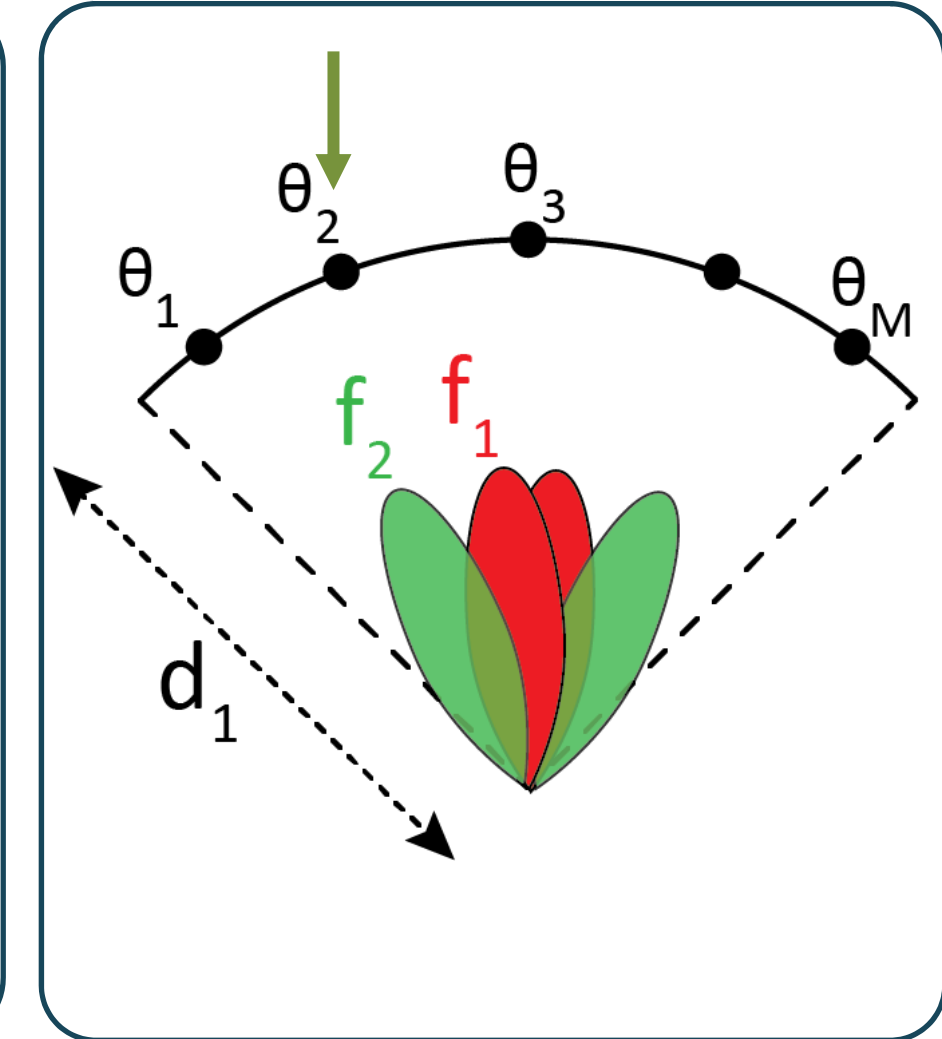


1D Localization Measurement Calibration

$$\mathbf{S}_{M \times N} = \begin{bmatrix} s(f_1, \theta_1) & s(f_2, \theta_1) & s(f_3, \theta_1) & \dots & s(f_N, \theta_1) \\ s(f_1, \theta_2) & s(f_2, \theta_2) & \dots & \dots & s(f_N, \theta_2) \\ \vdots & \ddots & \ddots & \dots & \vdots \\ s(f_1, \theta_M) & s(f_2, \theta_M) & \dots & \dots & s(f_N, \theta_M) \end{bmatrix}$$

f is the frequency set from $[f_1, f_2, f_3 \dots f_N]$
 θ is the angle set from $[\theta_1, \theta_2, \theta_3 \dots \theta_M]$

- Based on the leaky-wave antenna radiation patterns, Frequency- Angle calibration map can be formed.

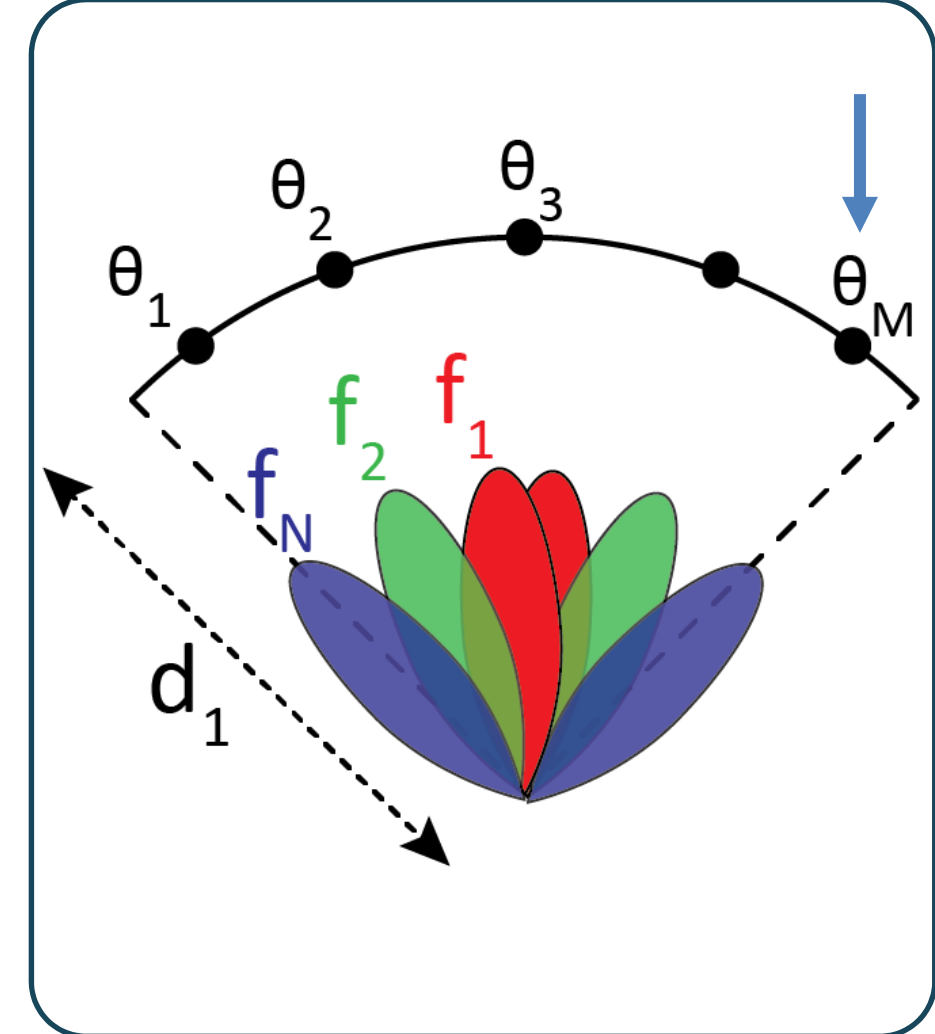


1D Localization Measurement Calibration

$$\mathbf{S}_{M \times N} = \begin{bmatrix} s(f_1, \theta_1) & s(f_2, \theta_1) & s(f_3, \theta_1) & \dots & s(f_N, \theta_1) \\ s(f_1, \theta_2) & s(f_2, \theta_2) & \dots & \dots & s(f_N, \theta_2) \\ \vdots & \ddots & \ddots & \dots & \vdots \\ s(f_1, \theta_M) & s(f_2, \theta_M) & \dots & \dots & s(f_N, \theta_M) \end{bmatrix}$$

f is the frequency set from $[f_1, f_2, f_3 \dots f_N]$
 θ is the angle set from $[\theta_1, \theta_2, \theta_3 \dots \theta_M]$

- Based on the leaky-wave antenna radiation patterns, Frequency- Angle calibration map can be formed.



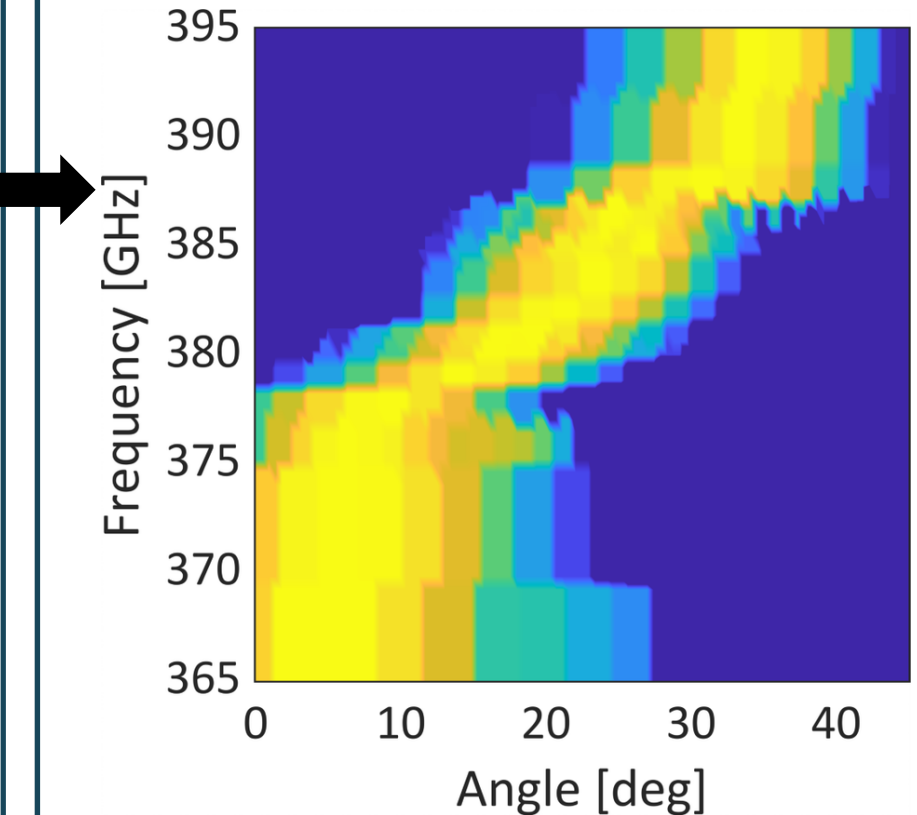
1D Localization Measurement Calibration

$$\mathbf{S}_{M \times N} = \begin{bmatrix} s(f_1, \theta_1) & s(f_2, \theta_1) & s(f_3, \theta_1) & \dots & s(f_N, \theta_1) \\ s(f_1, \theta_2) & s(f_2, \theta_2) & \dots & \dots & s(f_N, \theta_2) \\ \vdots & \ddots & \ddots & \dots & \vdots \\ s(f_1, \theta_M) & s(f_2, \theta_M) & \dots & \dots & s(f_N, \theta_M) \end{bmatrix}$$

f is the frequency set from $[f_1, f_2, f_3 \dots f_N]$

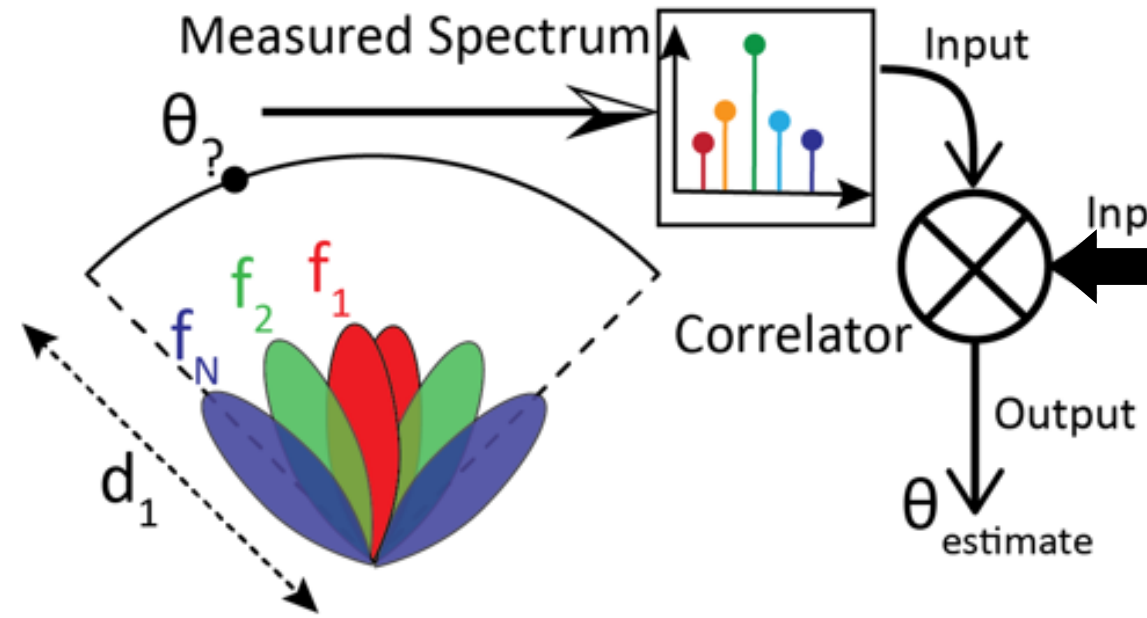
θ is the angle set from $[\theta_1, \theta_2, \theta_3 \dots \theta_M]$

- Based on the leaky-wave antenna radiation patterns, Frequency- Angle calibration map can be formed.

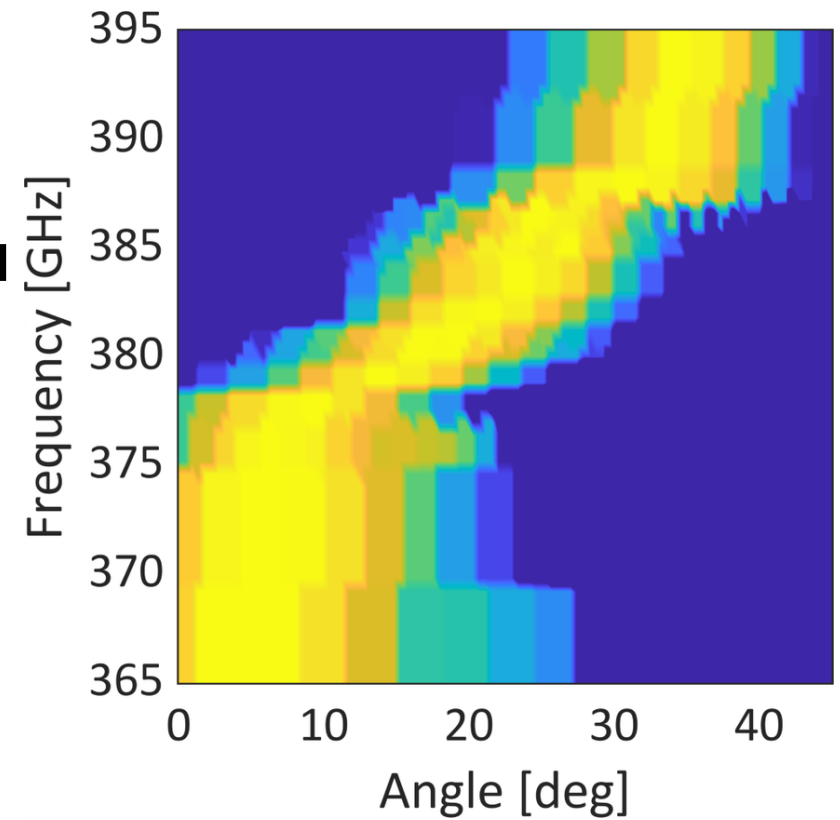


S = Calibration Matrix

1D Localization Measurement Calibration

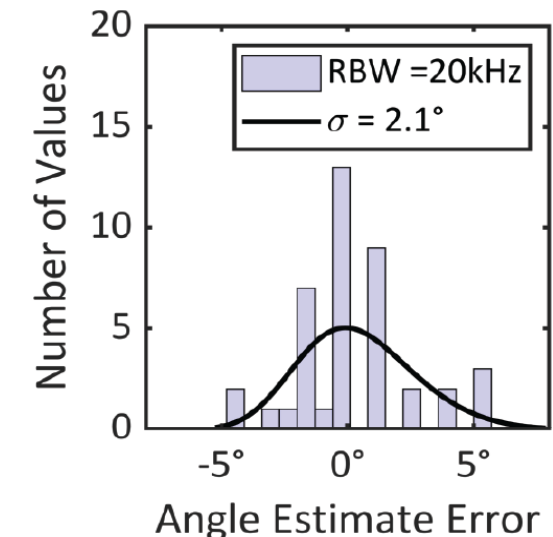
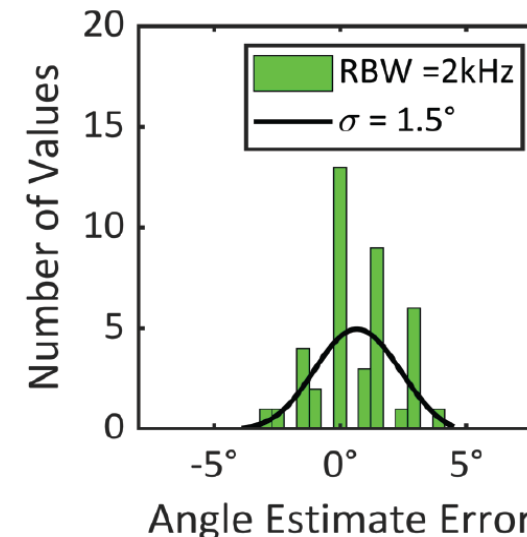
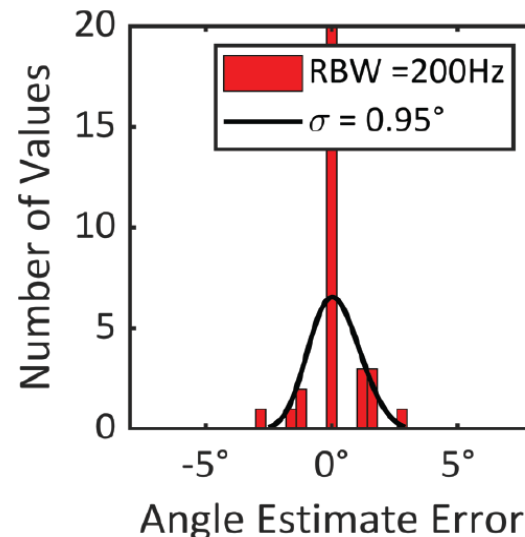
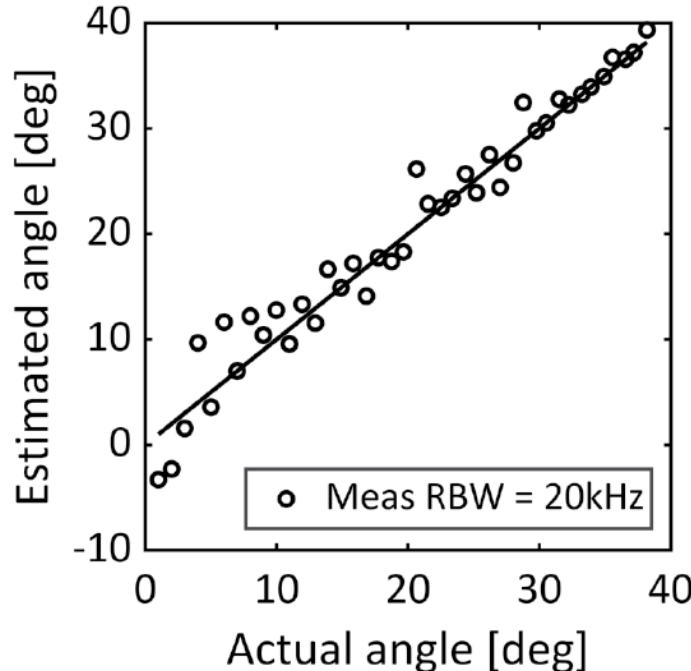


- The object(TX/Rx) is located at unknown angle $\theta_?$
- Based on the cross correlation between received powers and the calibration map, θ would be estimated.



S = Calibration Matrix

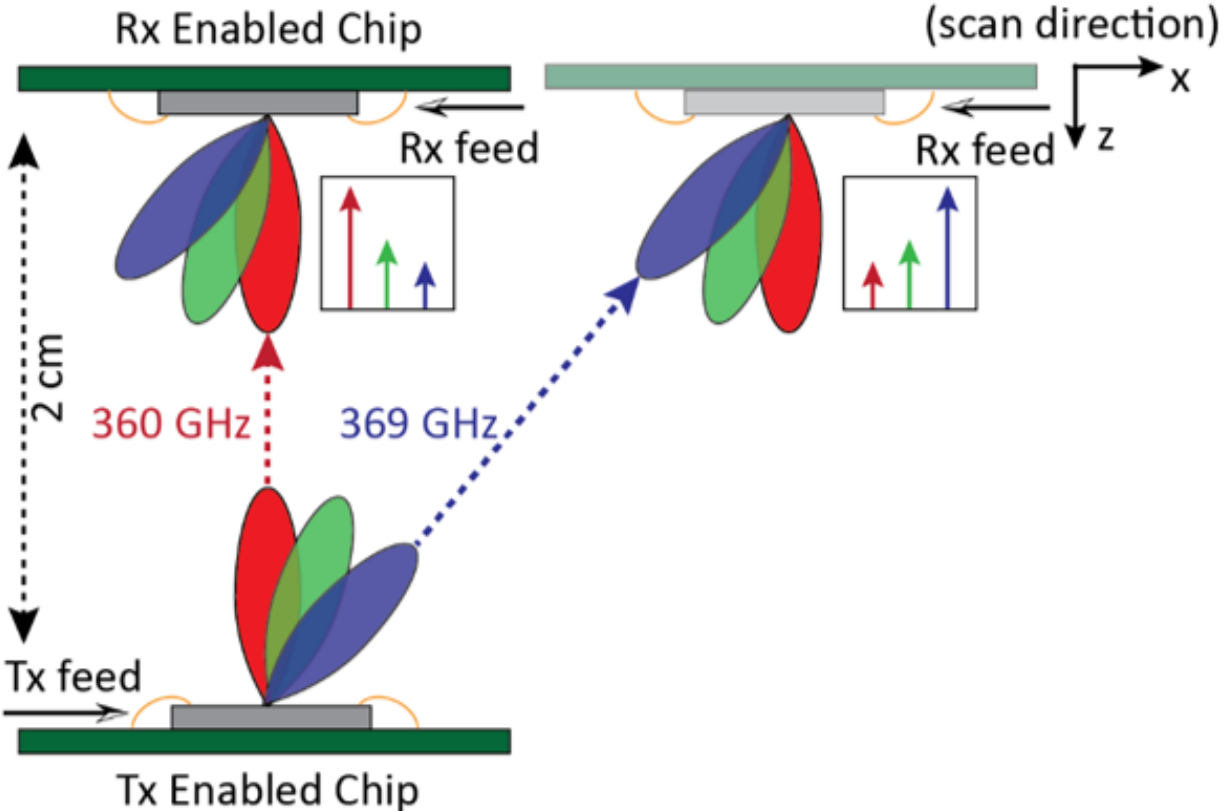
1D Localization Measurement results



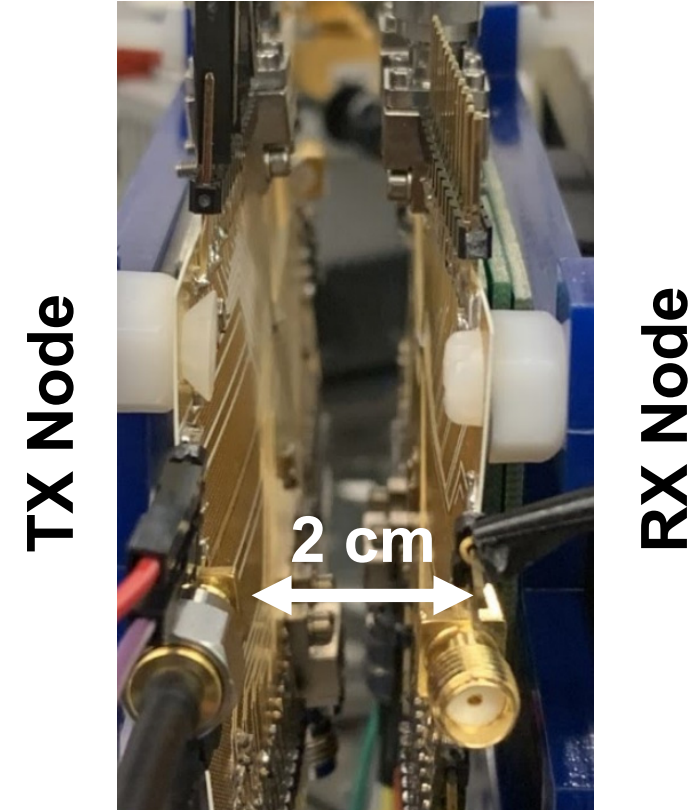
$$RBW \downarrow \equiv \sigma \downarrow$$

- Exploiting the cross-correlation method, 1D angular locations across 0 to 40 degrees at unknown directions are estimated.
- Increasing the measurement time(reducing RBW), error variance is getting reduced.

Chip-to-Chip (TX-to-RX) 1D Localization

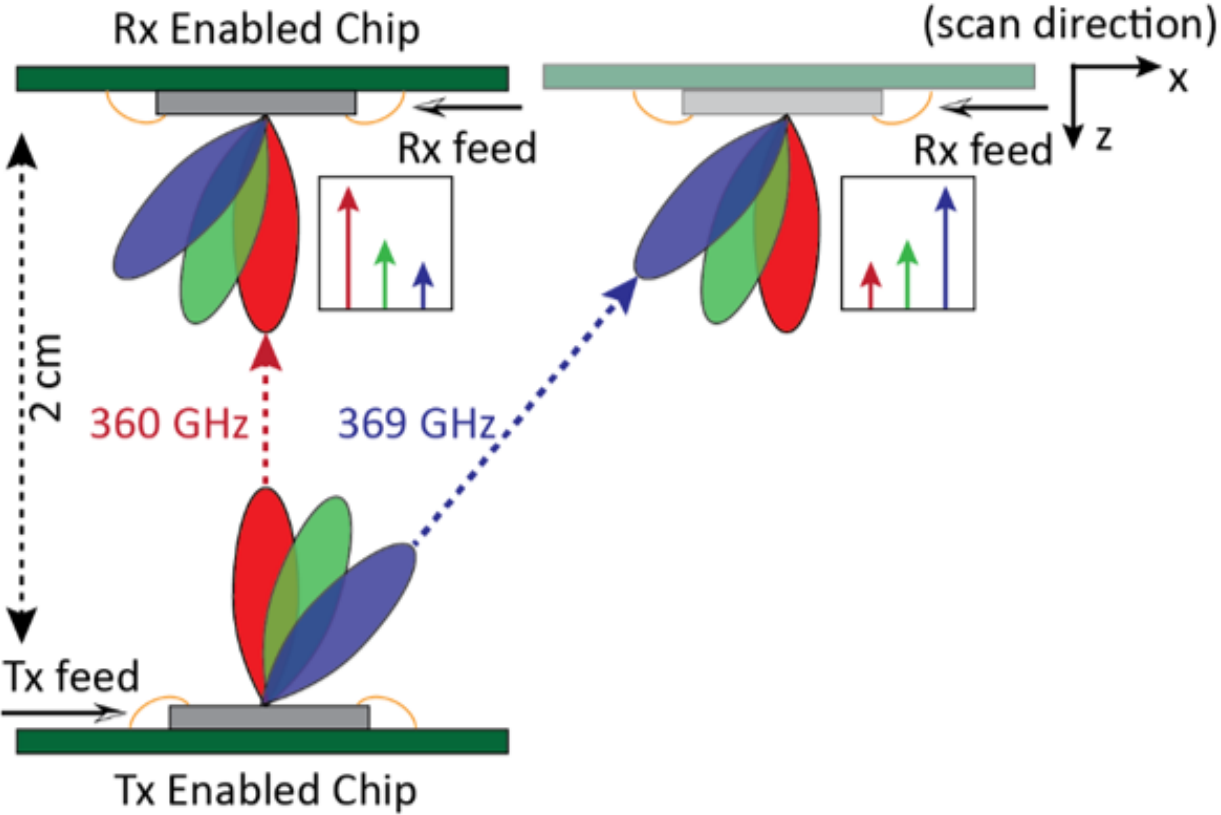


- Placing two TX and RX enabled chips for 1D angular localization

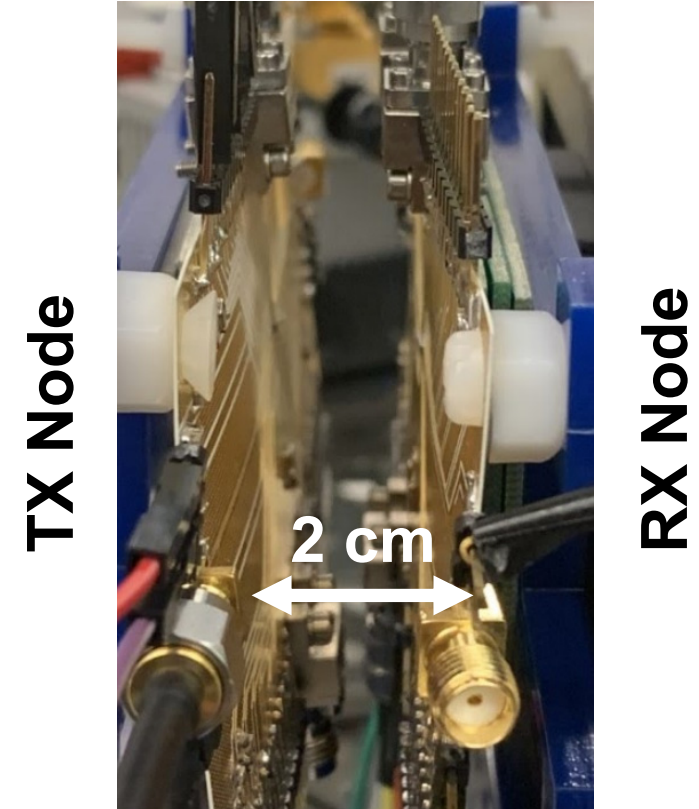


- Two TX and RX enabled chips with 2cm separation

Chip-to-Chip (TX-to-RX) 1D Localization

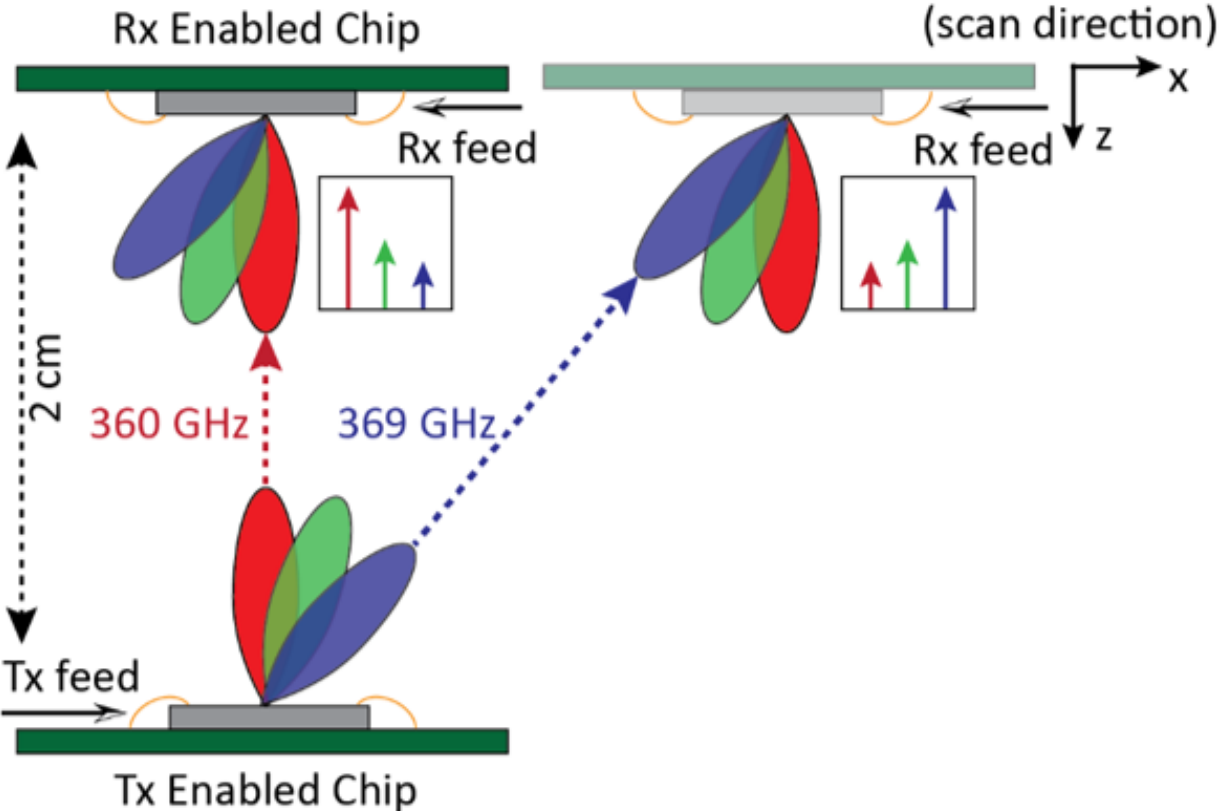


- The RX enabled chip is 1D scanned and the received power at the RX chip is monitored.

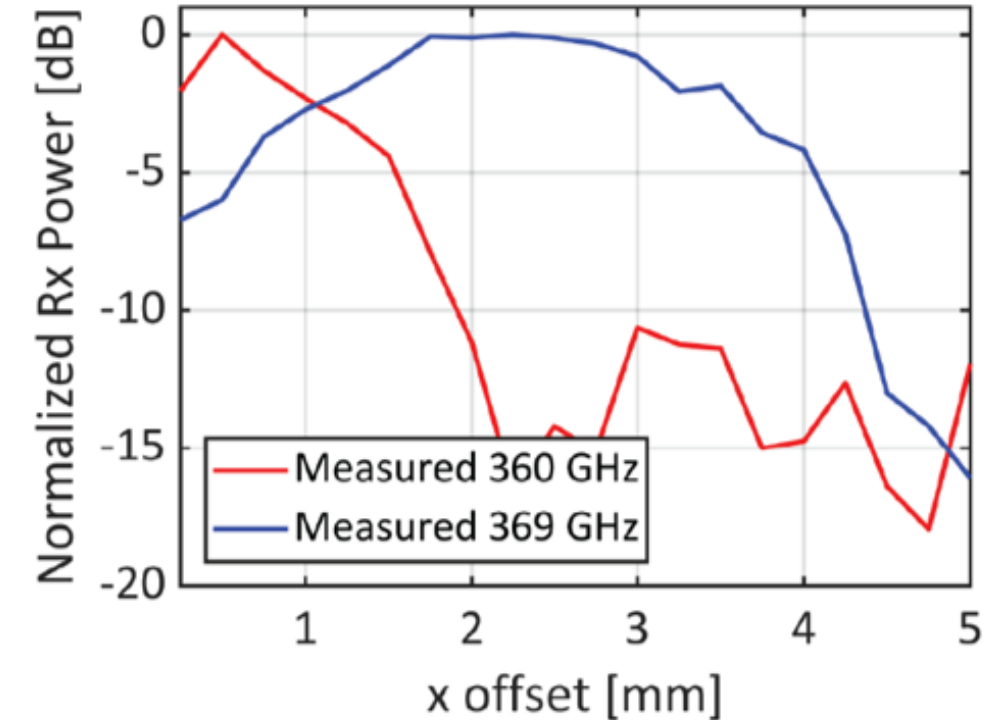


- Two TX and RX enabled chips with 2cm separation

Chip-to-Chip (TX-to-RX) 1D Localization

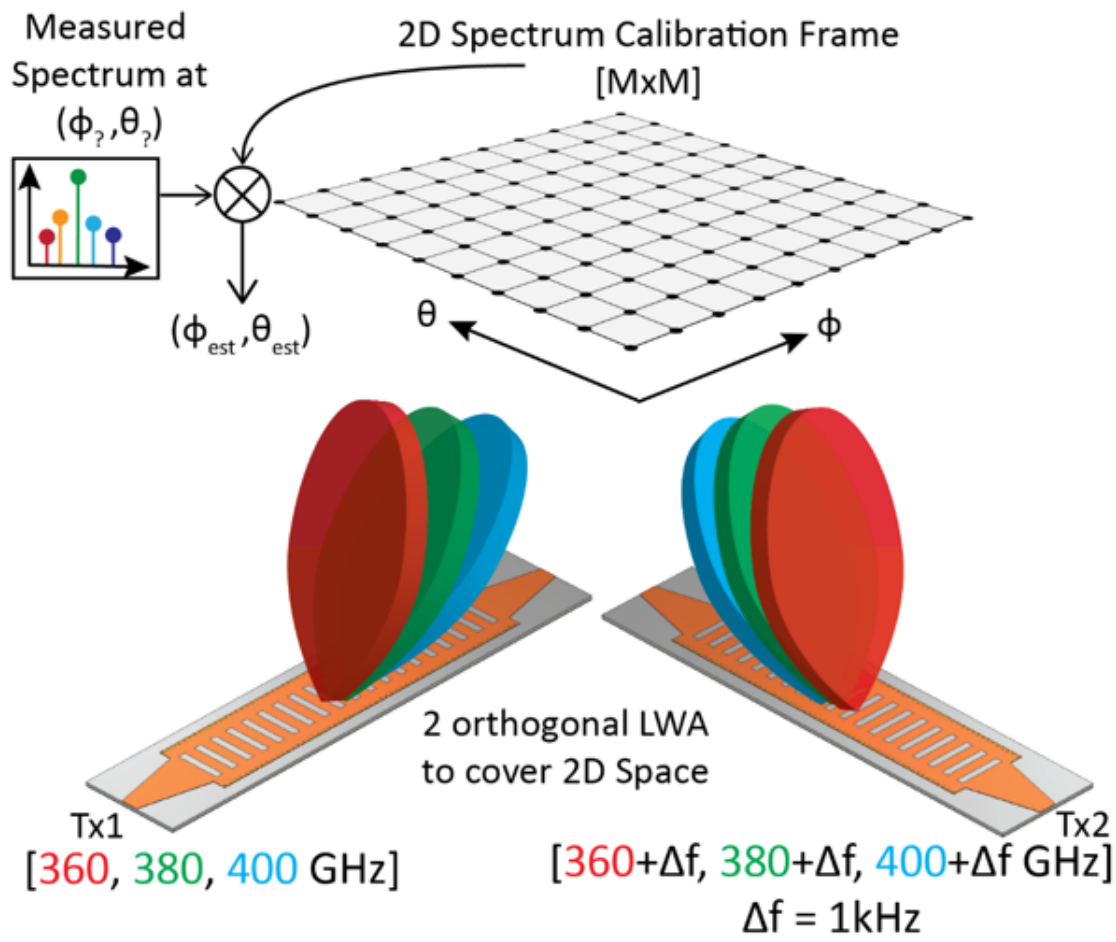


- The RX enabled chip is 1D scanned and the received power at the RX chip is monitored.



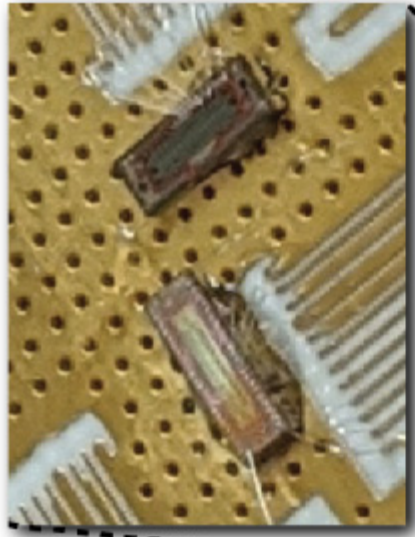
- Different frequencies will result in different angular peak locations.

2D Localization Calibration

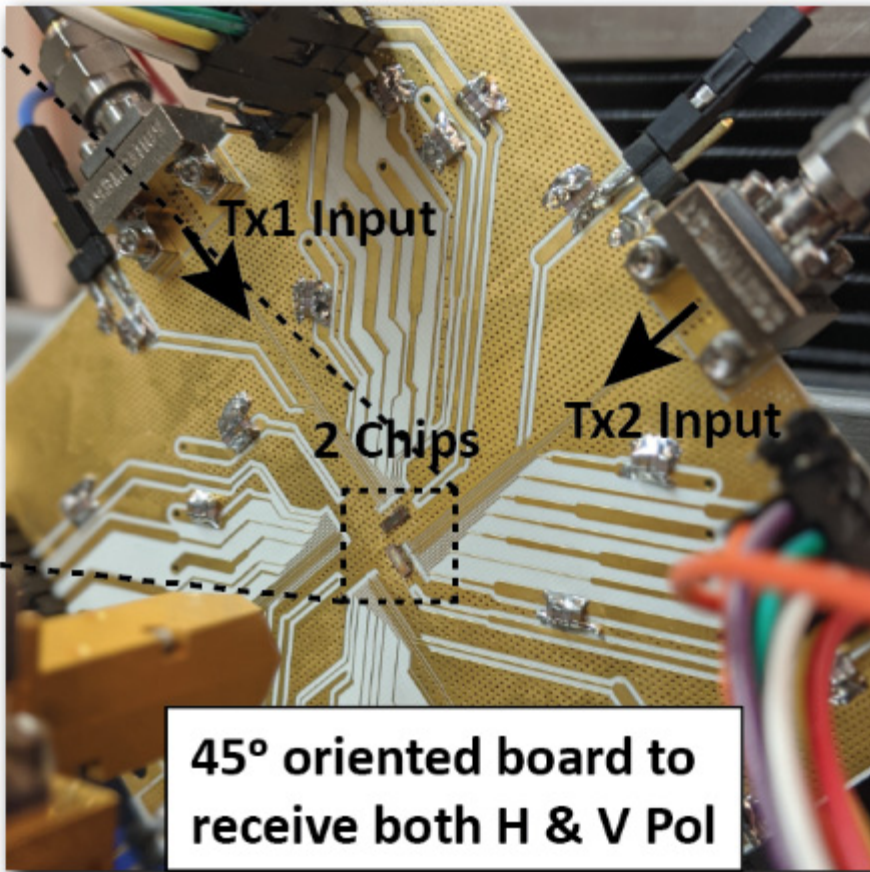


- 2D angular Calibration map is formed.
- The object (TX/RX) is located at unknown 2D angular location $(\phi_?, \theta_?)$
- In these measurements , 2 orthogonal TX enabled chips are casting frequencies across 360 – 400GHz with 1kHz frequency offset between TXs.
- Exploiting the cross-correlation method, 2D angular locations at unknown directions are estimated.

2D Localization Setup

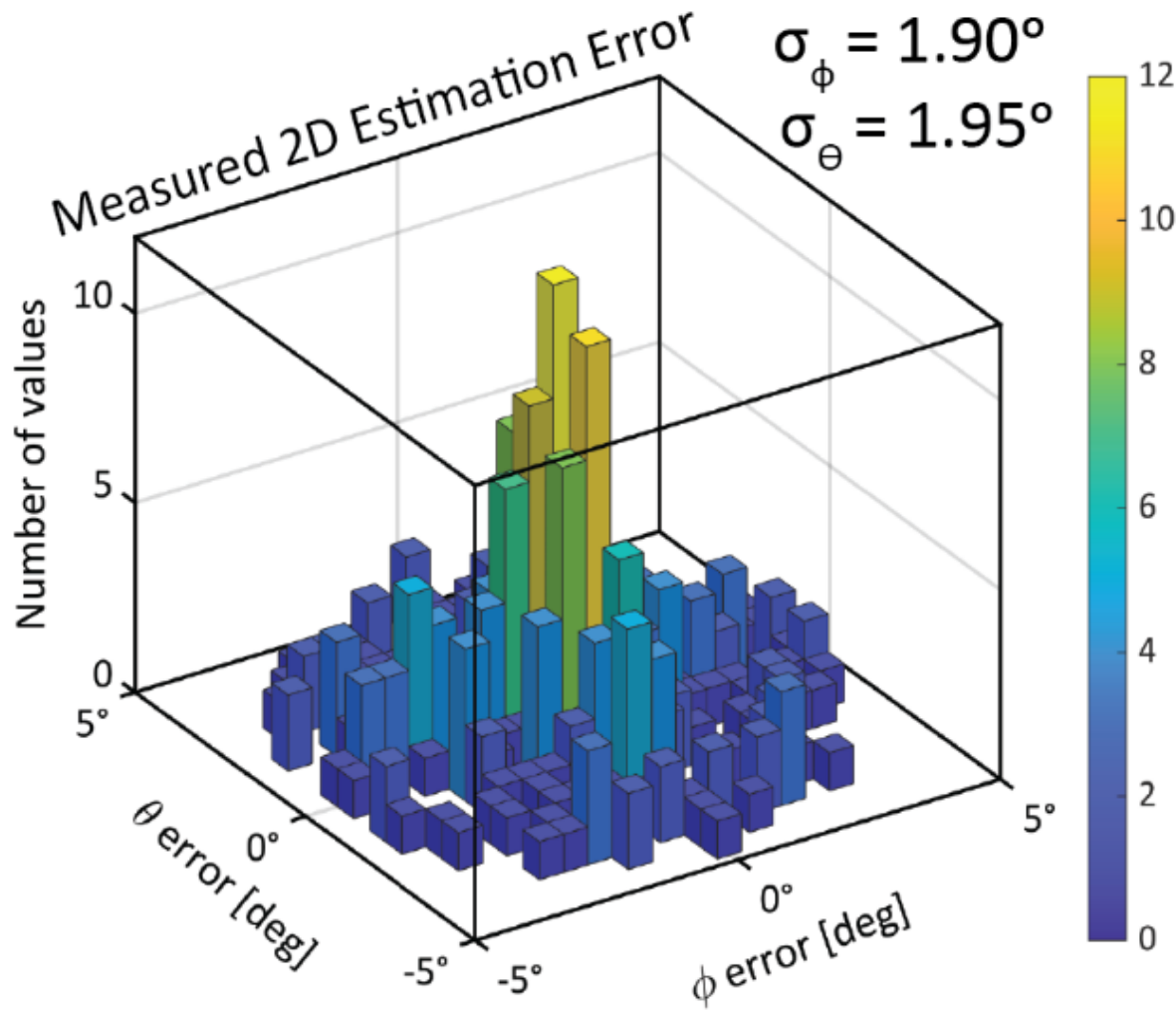


Two orthogonally placed ICs



- At each chip, single TX chain is enabled
- 2 orthogonally placed chips are 45° oriented to receive both H and V polarizations.

2D Localization Measurements

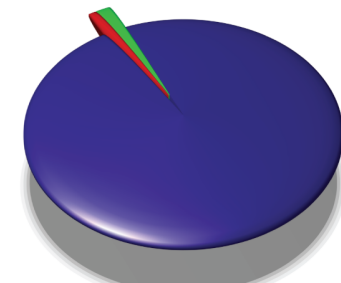


- The 2D angular estimation measurement is performed with RBW of 20Hz
- RX locations are at different random 2D angular locations.
- 2D estimation error of $\sigma_\theta = 1.95^\circ$ and $\sigma_\phi = 1.9^\circ$ is achieved.

Comparison with Prior Arts

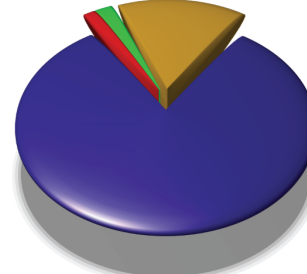
Metrics	This work	Nature Elect, '20 [2]	Nature Comm, '20 [1]	ISSCC '20 [4]	TTST '18 [5]
Architecture	TxRx + OnchipAnt	TxRx Dual off Chip Zero Bias detector + Dual off Chip LWA +Ext AMC	THz-TDS with fiber-coupled photoconductive antennas as source	TxRx FMCW comb radar with 5 on chip multimode SIW antenna	TxRx with On-Chip Patch antenna
Antenna Type	Periodic Leaky Wave	Uniform Leaky Wave waveguide	Uniform LWA (parallel plate waveguide)	multimode SIW antenna	Differential Patch Antenna
Frequency Range [GHz]	360 – 400	330 – 490	150 – 750	220 – 320	300 – 375
Prad per unit [dBm]	-10.9	-5 (off chip active x chain)	NA	0.6	3
Rx Noise Figure [dB]	26.2 (DSB avg)	NA	NA	22.2 DSB (min)	31.5 DSB avg (19.75 min)
Beam Coverage [deg]	-40 to +40	-51 to +51	+10 to +80	NA	NA
DoA Accuracy [deg]	+/- 0.95 (1D RBW= 200Hz) +/- 1.9 (2D RBW = 20Hz)	+/- 5	+/- 5	NA	NA
Full Duplex operation	Yes	No	No	No	No
Power DC per Tx/Rx	Tx 138mW Rx 163mW	NA (off chip components)	NA (off chip components)	840mW Total	Tx 568mW Rx 751mW
Area [mm ²]	3	NA	NA	5	2.85
Technology	65nm CMOS	GaAs Schottky barrier ZBD with waveguide components	Off-the-shelf THz spectrometer components	65nm CMOS	130nm SiGe

Tx Chain Total DC Power Consumption



PA = 136.8 mW
 Tripler = 1.85 mW
 Doubler = 0.12 mW
 Total = 138.77 mW

Rx Chain Total DC Power Consumption



PA = 136.8 mW
 IF Amp = 22.85 mW
 Doubler+Tripler = 2.0 mW
 DB Mixer = 1.7 mW
 Total = 163.35 mW

Outline

- Prior works in single-shot localization THz frequencies
- Enabling On-chip THz localization using frequency dispersive antennas
- On-chip 360-400GHz transceiver design and implementation
- Circuit implementation and characterization
- 1D, chip-to-chip, and 2D angular measurement results
- Conclusions

Conclusions

- **Realization of scalable 360-400GHz TX/RX architecture in 65nm CMOS with two integrated dual-port LWAs.**
- **1D spatial coverage of $\pm 40^\circ$ using Single IC.**
- **2 Dual-port LWAs for 1D and 2D angular localization.**
- **Demonstration of 1D DOA with angular accuracy of $\sigma_\theta = 2.1^\circ$ at $RBW = 20\text{kHz}$.**
- **Demonstration of 2D angular localization with angular accuracy $\sigma_\theta = 1.95^\circ$ and $\sigma_\phi = 1.9^\circ$ at $RBW = 20\text{Hz}$.**

Acknowledgments

- **Office of Naval Research (Young Investigator Program)**
- **Air Force Office of Scientific Research (MURI).**
- **Defense University Research Instrumentation Program (DURIP)**
- **Dr. John Suarez, U.S. Army CCDC C5ISR for technical discussions**
- **All members of the IMRL**



A 300GHz-Band Phased-Array Transceiver Using Bi-Directional Outphasing and Hartley Architecture in 65nm CMOS

Ibrahim Abdo¹, Carrel da Gomez¹, Chun Wang¹, Kota Hatano¹, Qi Li¹,
Chenxin Liu¹, Kiyoshi Yanagisawa¹, Ashbir Aviat Fadila¹, Jian Pang¹,
Hiroshi Hamada², Hideyuki Nosaka², Atsushi Shirane¹, Kenichi Okada¹

¹Tokyo Institute of Technology, Tokyo, Japan

²NTT, Kanagawa, Japan



Tokyo Institute of Technology



Self Introduction

- Ibrahim Abdo
- B.Sc. degree from Princess Sumaya University for Technology (PSUT), Amman, Jordan, in 2014
- M.Eng. degree from Tokyo Institute of Technology, Tokyo, Japan, in 2017
- Currently pursuing Ph.D. degree at Tokyo Institute of Technology
- My interests are in high data rate CMOS mm-wave and sub-THz wireless transceiver circuit design

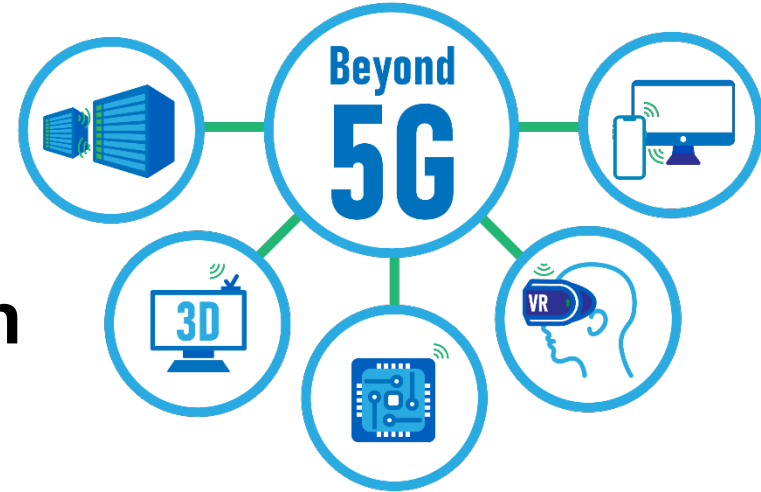


Outline

- Motivation & Background
- Proposed Bi-Directional Phased-Array TRX
 - Subharmonic Mixer
 - IF Distributed Amplifier
 - Phase Generation Circuit
- Phased-Array Implementation
- Measurement Results
- Conclusion

300GHz-band for Wireless Communications

- 300GHz-band link
 - Beyond 5G, IEEE802.15.3d (252~324GHz)
- CMOS $f_{max} \approx 300\text{GHz}$ → No amplification
 - Mixer-last(TX) / mixer-first(RX)
- High path loss
 - Short-distance link

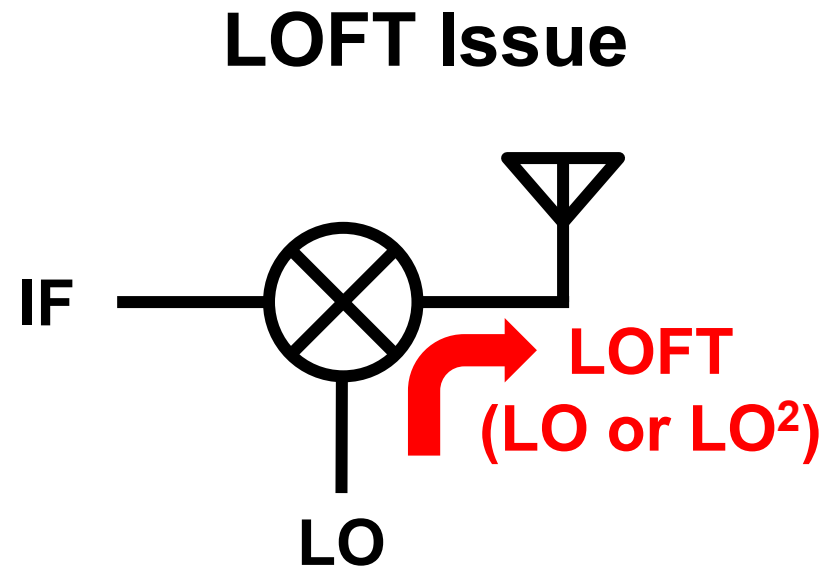


Solutions for the 300GHz link

- Phased-array → High $G_{antenna}$ and P_{OUT}
- Higher CMOS P_{OUT} → Improved SNR
- LOFT cancellation → Suppressed LO emission

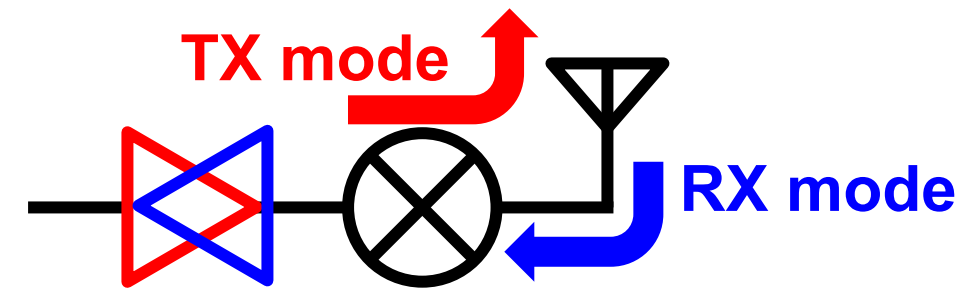
LOFT and Bi-Directional Operation

■ Mixer-last(TX) / mixer-first(RX) architecture



- ⌚ LOFT radiates from the antenna
- ⌚ Not suppressed by matching

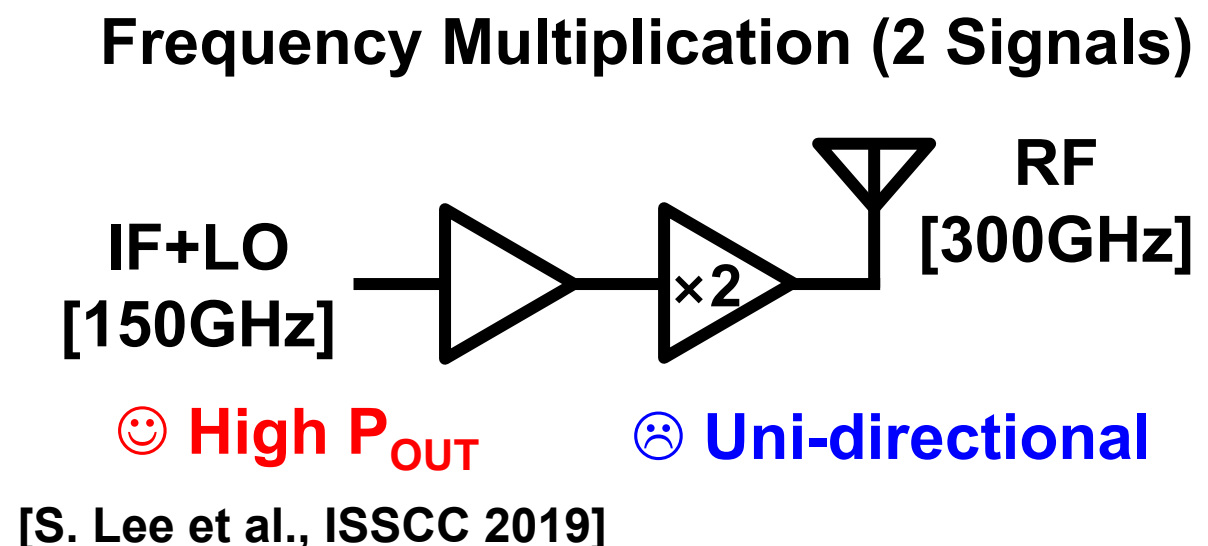
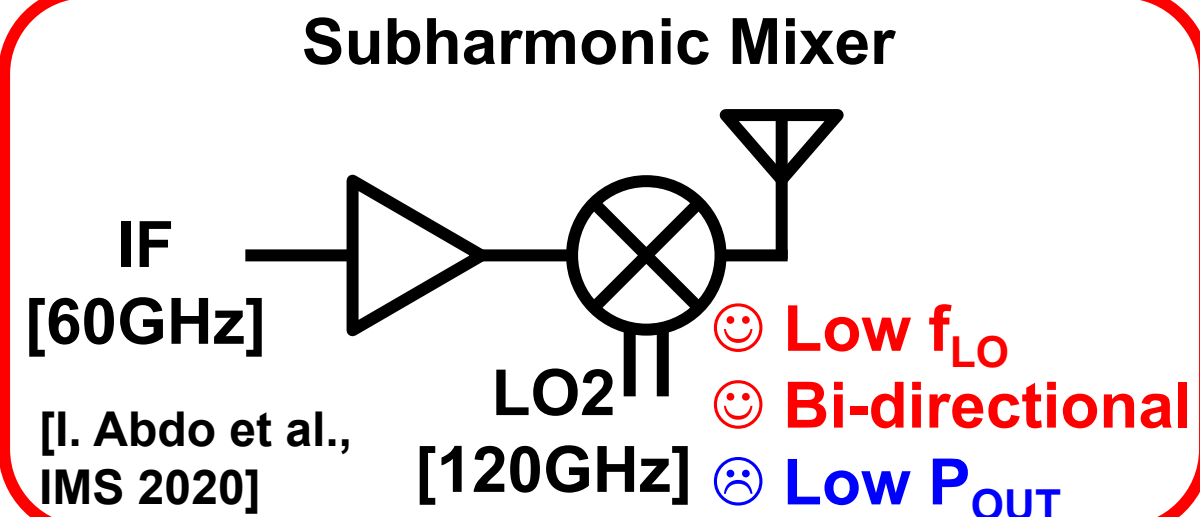
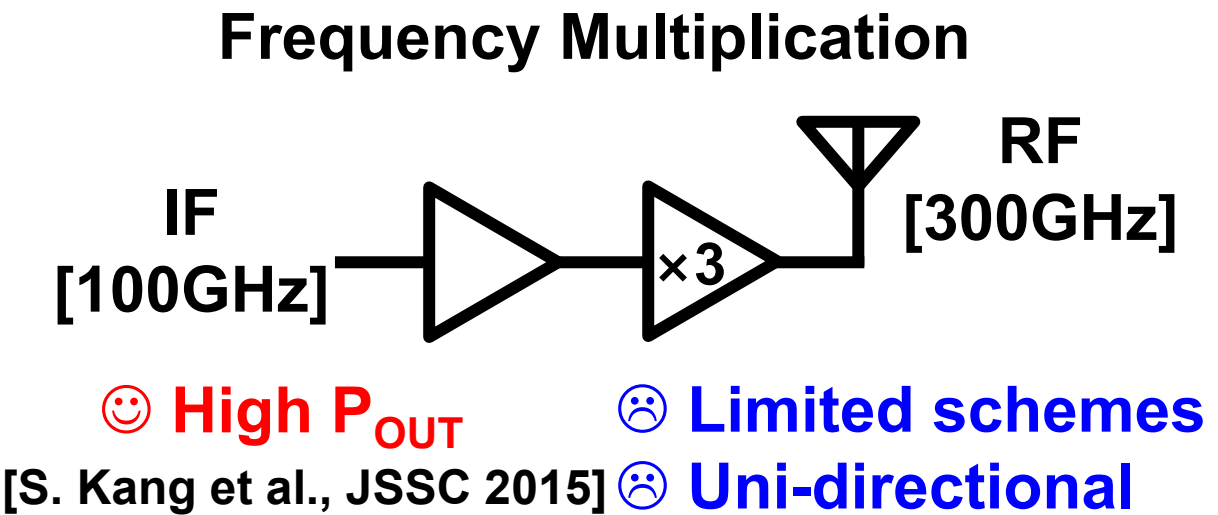
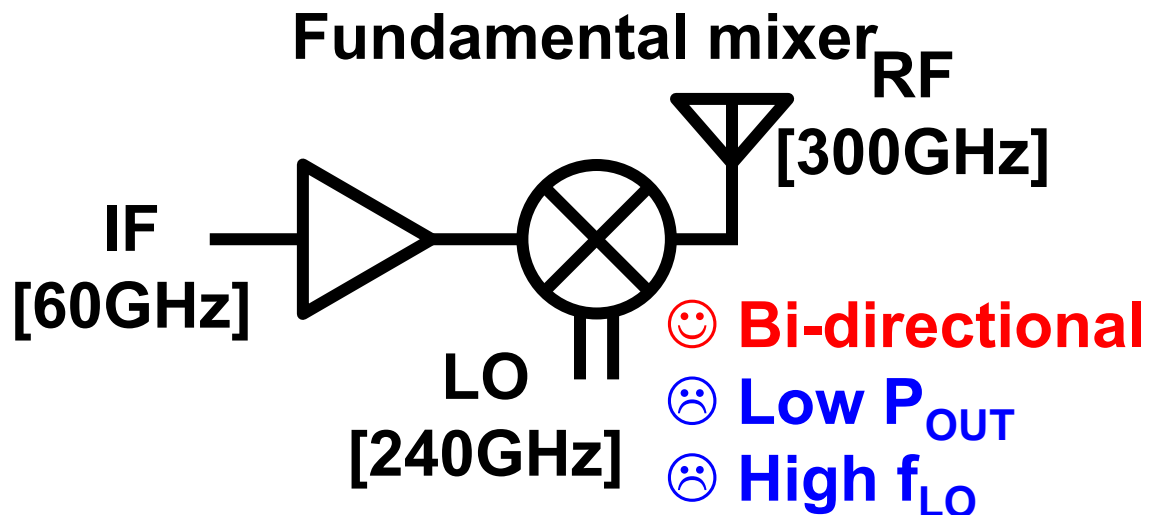
Bi-Directional Operation



- TX and RX sharing the same mixer

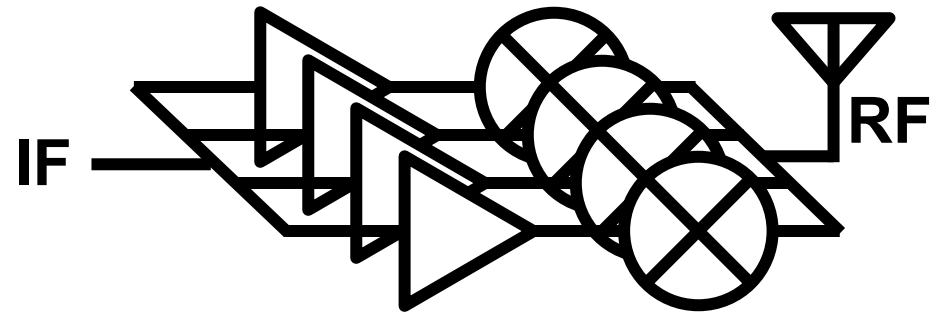
- 😊 Reduced area and P_{DC}
- 😊 Shared antenna
- 😊 Reduced complexity

Possible 300GHz-Band TX Architectures



Output Power Boosting Techniques

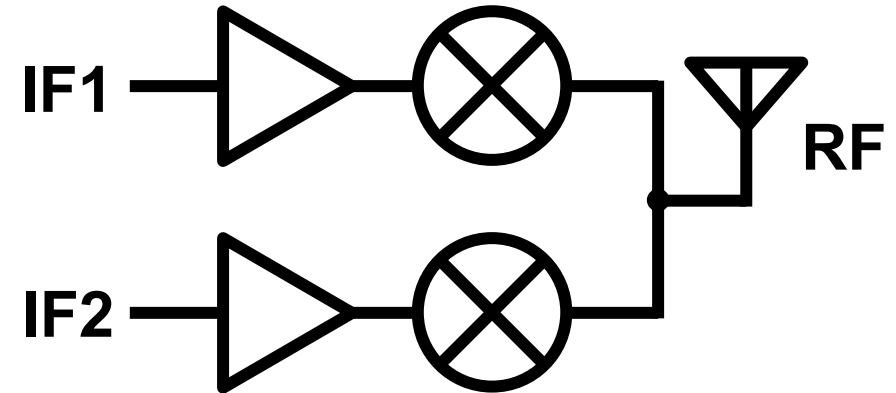
Power combining



- 😊 High P_{out}
- 😢 Large chip area
- 😢 Power back-off needed

[S. Lee et al., ISSCC 2019]

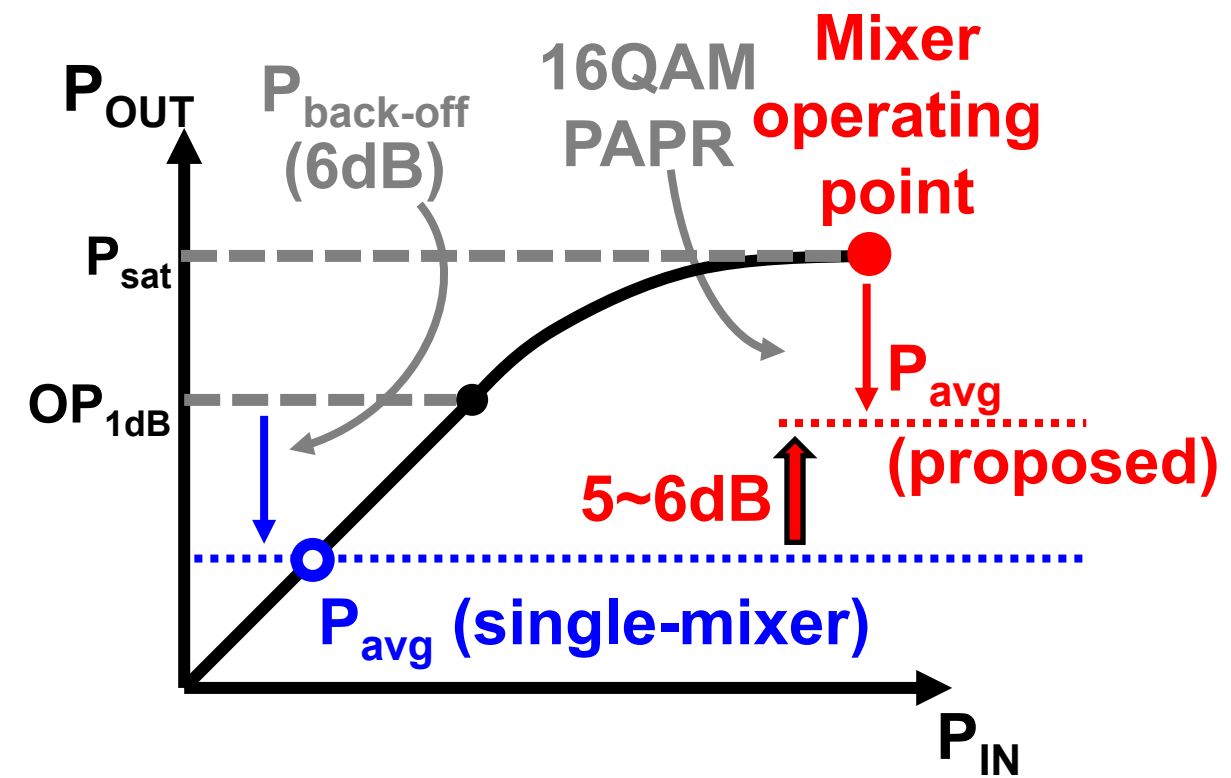
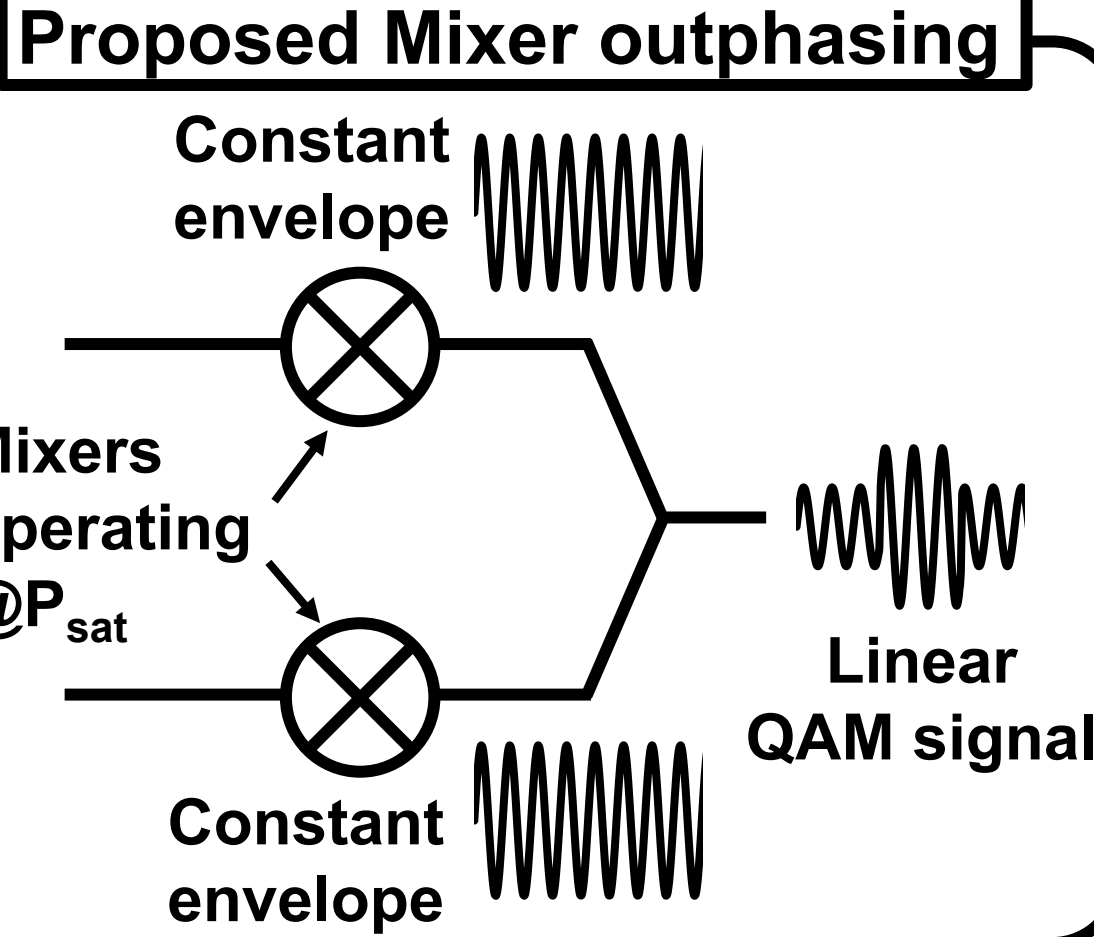
Outphasing



- 😊 High P_{avg}
- 😊 Mixer operates at P_{sat}

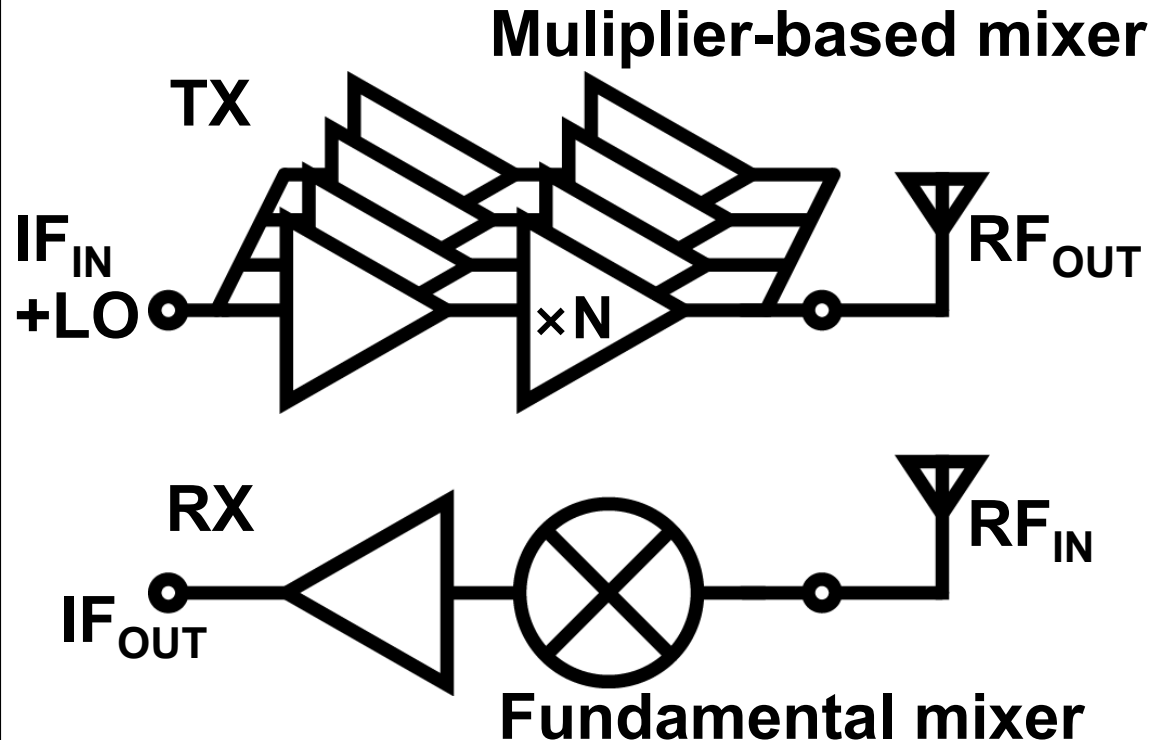
Mixer Outphasing as a Solution

- Higher P_{avg} to leverage the mixer P_{sat}



System Architecture

Conventional TRX

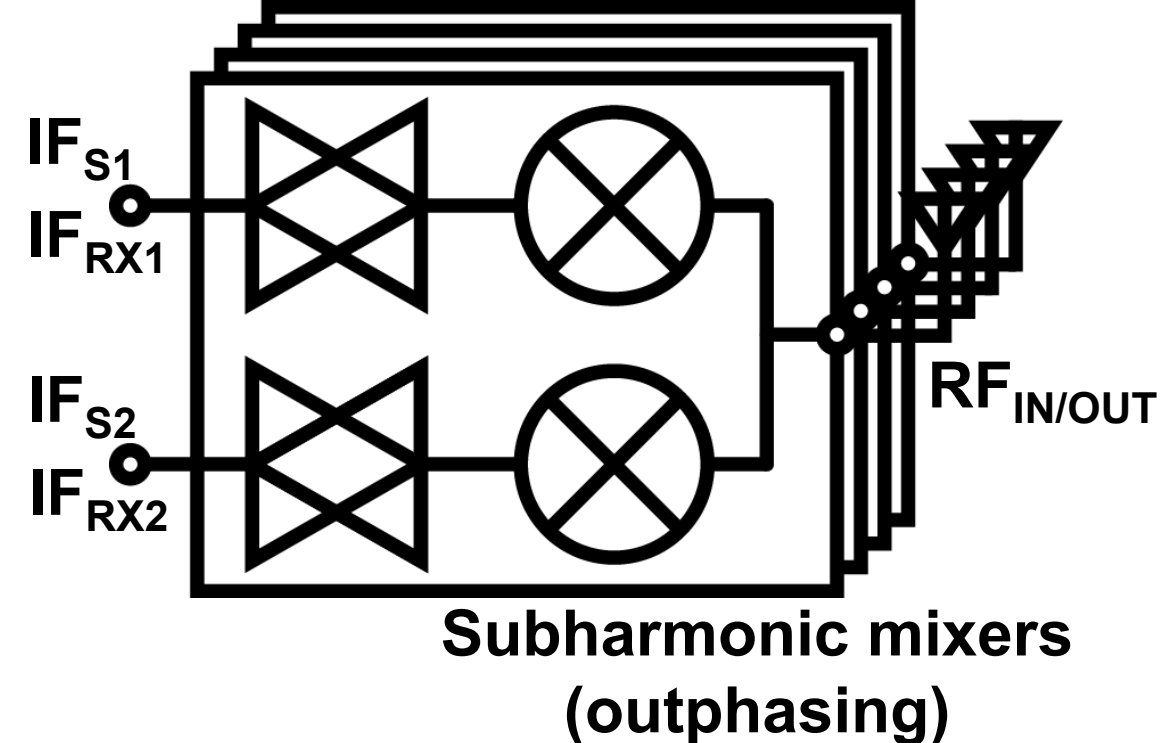


⌚ Separate circuitry / antennas(TX/RX)

[S. Lee et al., ISSCC 2019]

This Work

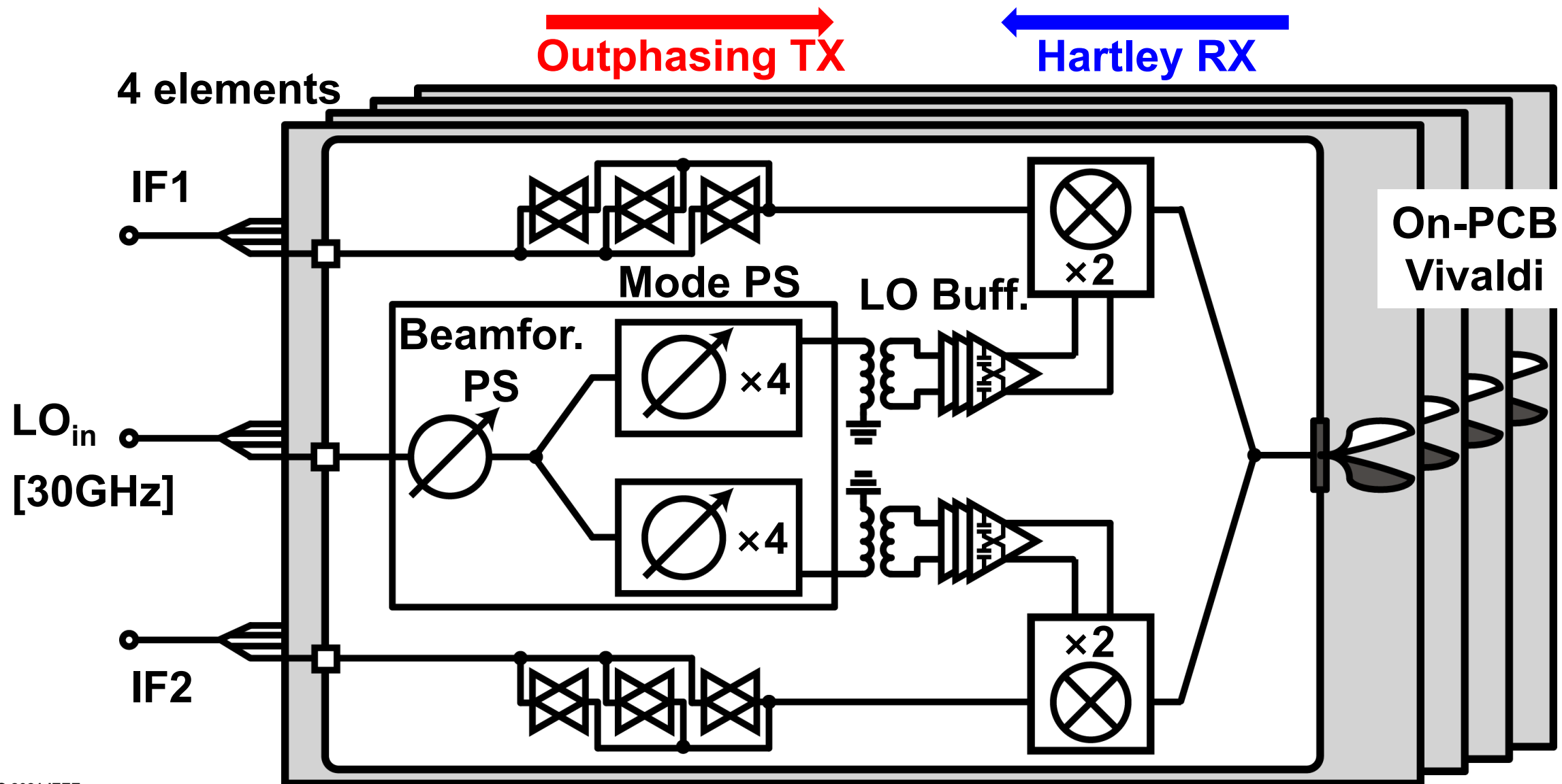
Bi-directional phased-array



⌚ Shared circuitry / antennas

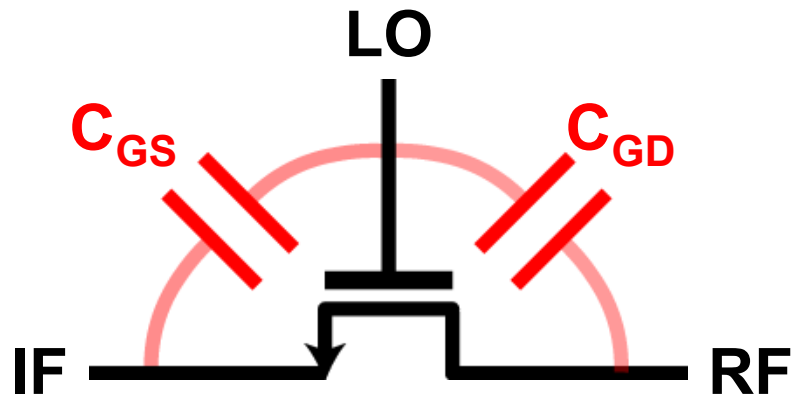
⌚ Beamforming / good P_{avg}

Proposed Bi-directional Phased-Array



300GHz-Band CMOS Mixers

■ Can the conventional mixers work at >200GHz?



- LO frequency > 200GHz
 - (:(Low P_{LO}
 - (:(Effect of gate parasitics

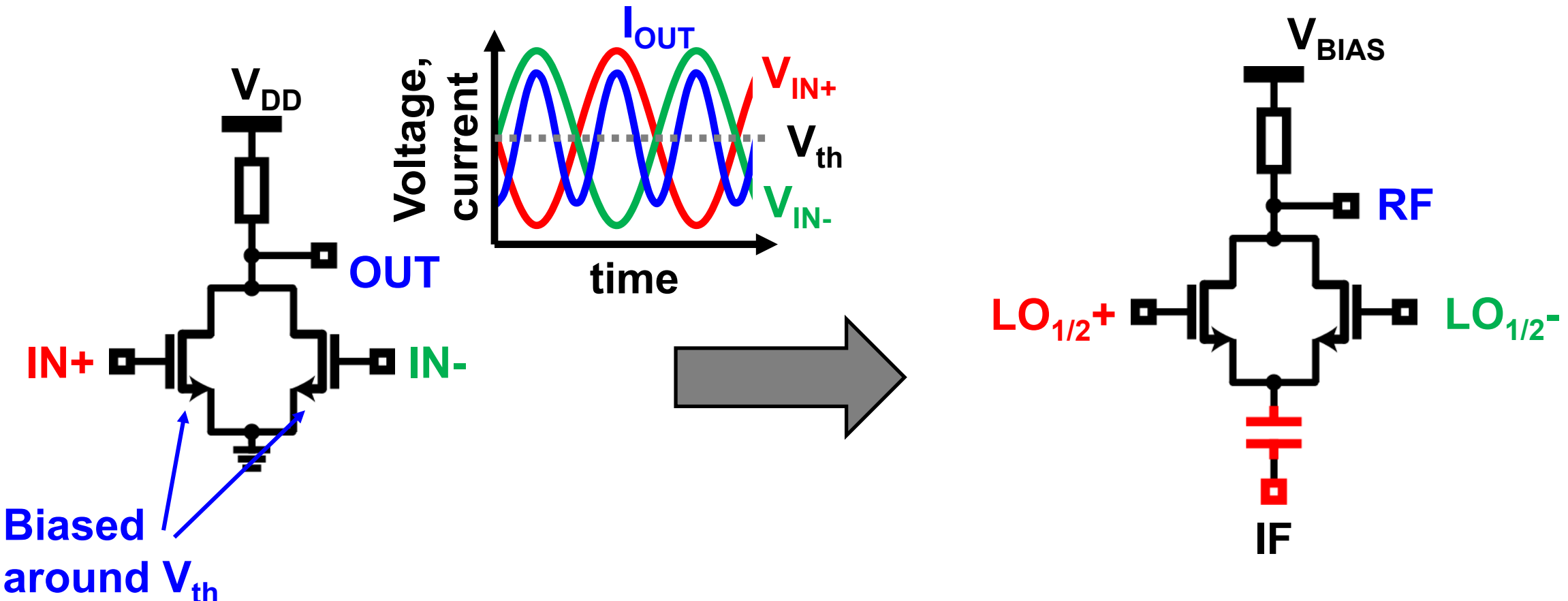
Very low conversion gain and output power

New mixer circuitry is required:

- Subharmonic operation
- High power and conversion gain

Proposed 300GHz-Band Mixer

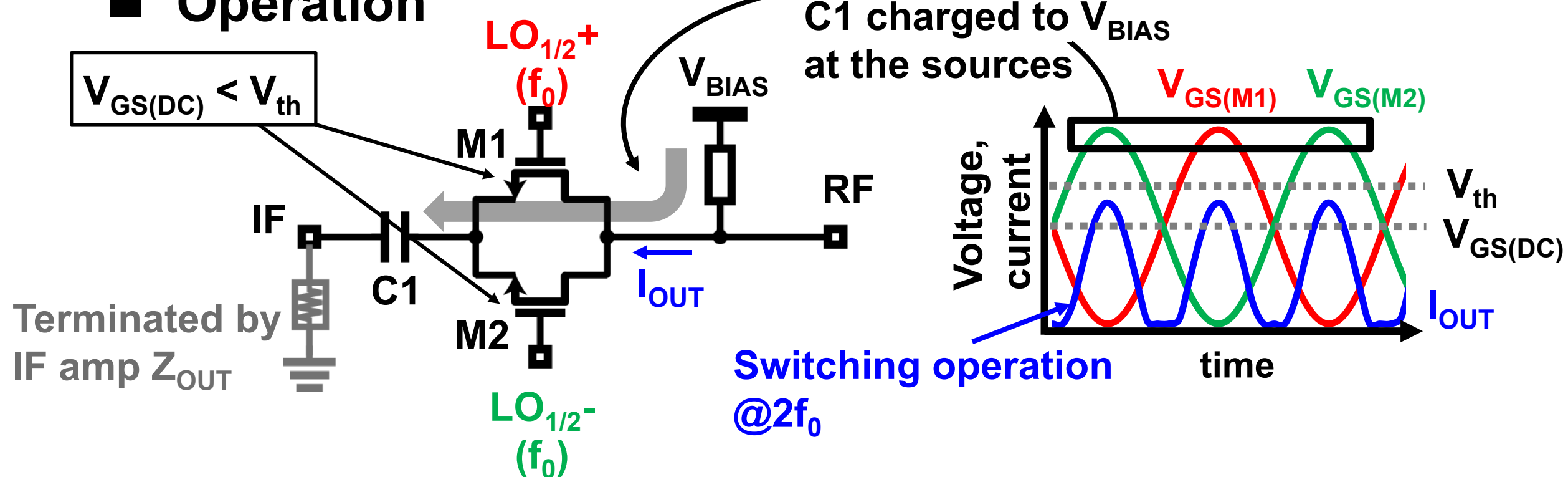
- Push-push topology with DC blocking cap.



[I. Abdo et al., IMS 2020]

Proposed 300GHz-Band Mixer

■ Operation

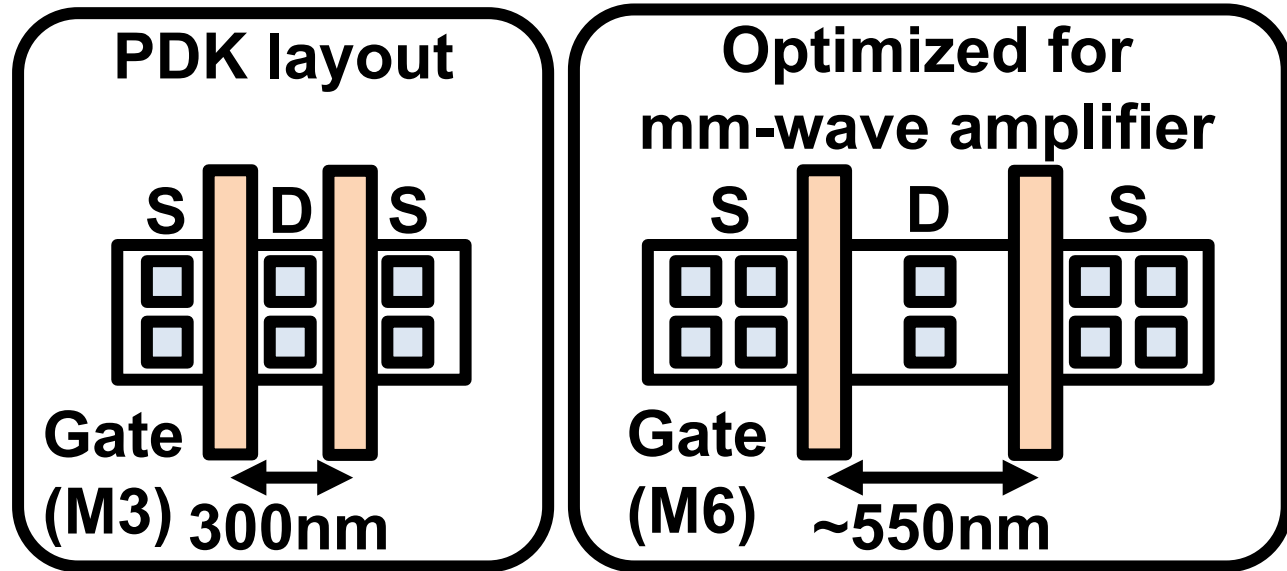


- ☺ Subharmonic, but fundamental-like
- ☺ Completely passive
- ☺ Separated IF and LO ports

Transistor Sizing and Layout Optimization

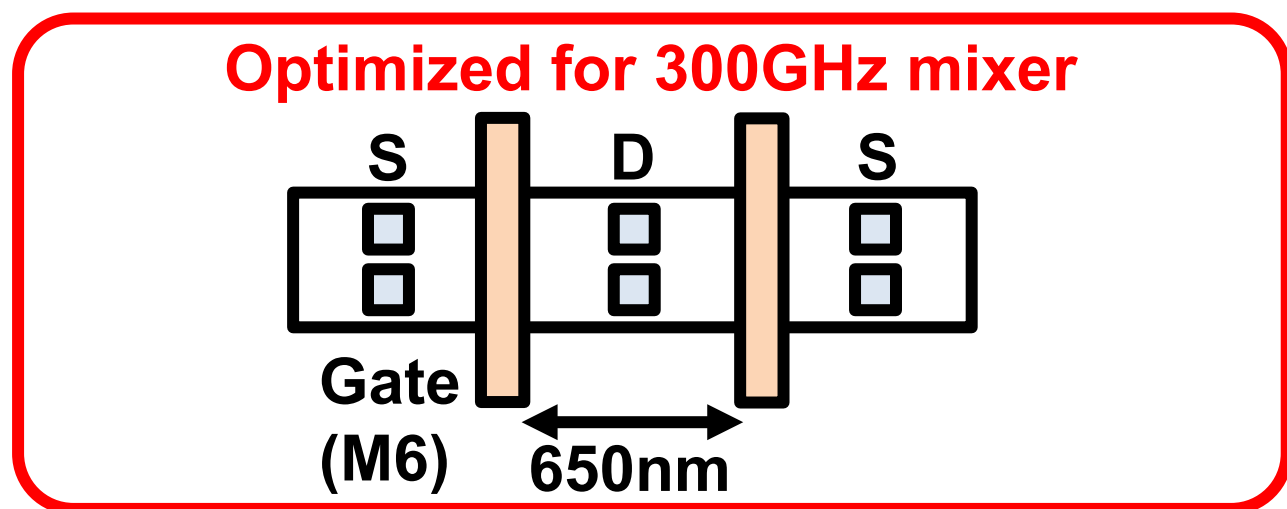
■ Transistor size:

- Optimal size:
 - $14\mu\text{m}$ for 65nm CMOS
- Acceptable P_{OUT}
- Small parasitics

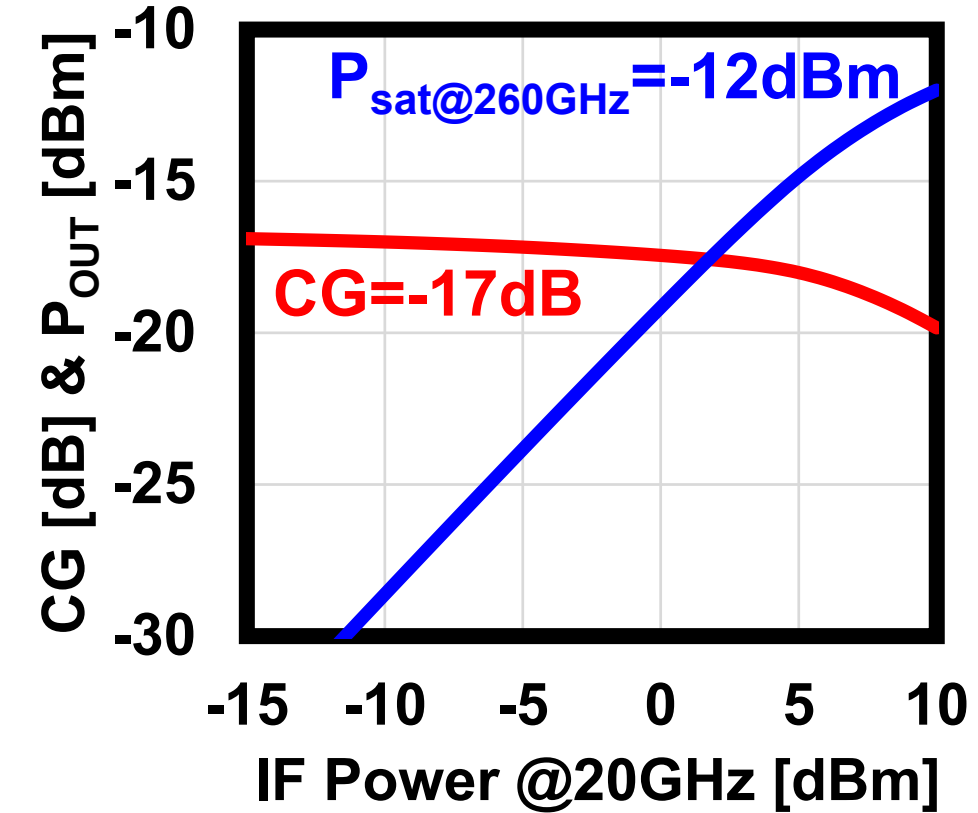
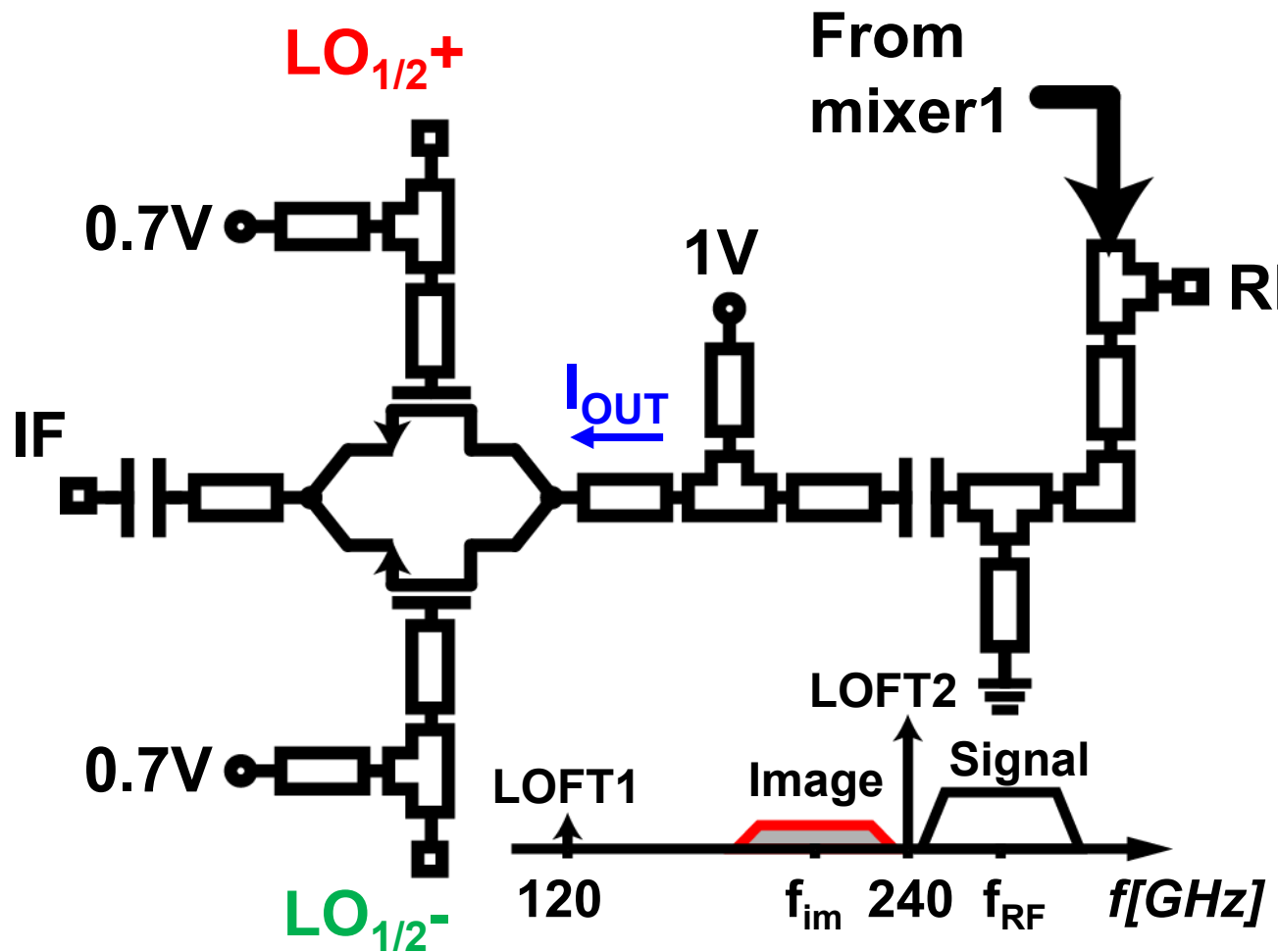


■ Layout Optimization

- Finger spacing
- Higher metal layers ($>\text{M4}$) for S and G
- 1-column contact

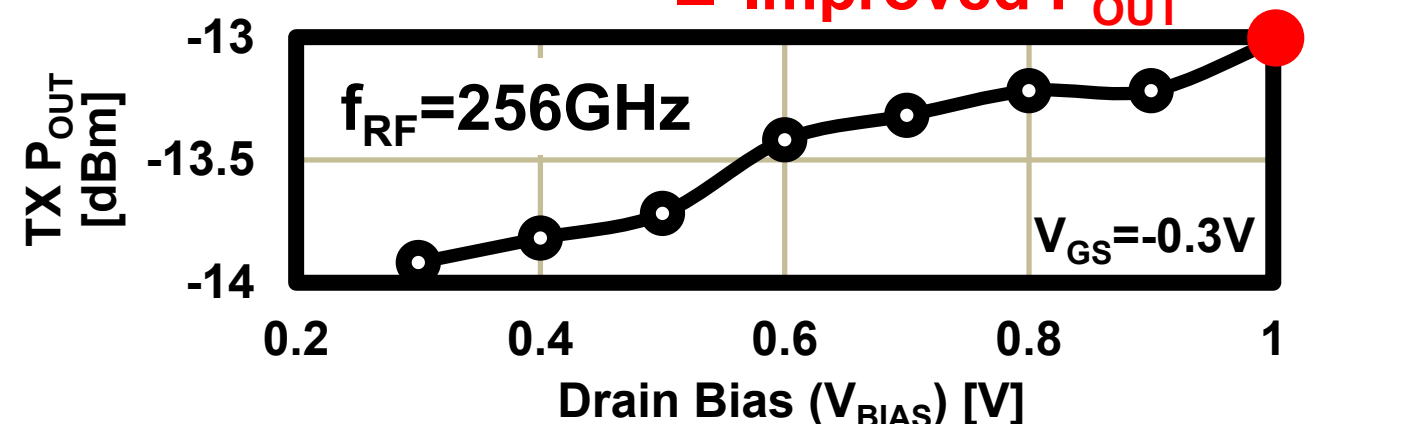
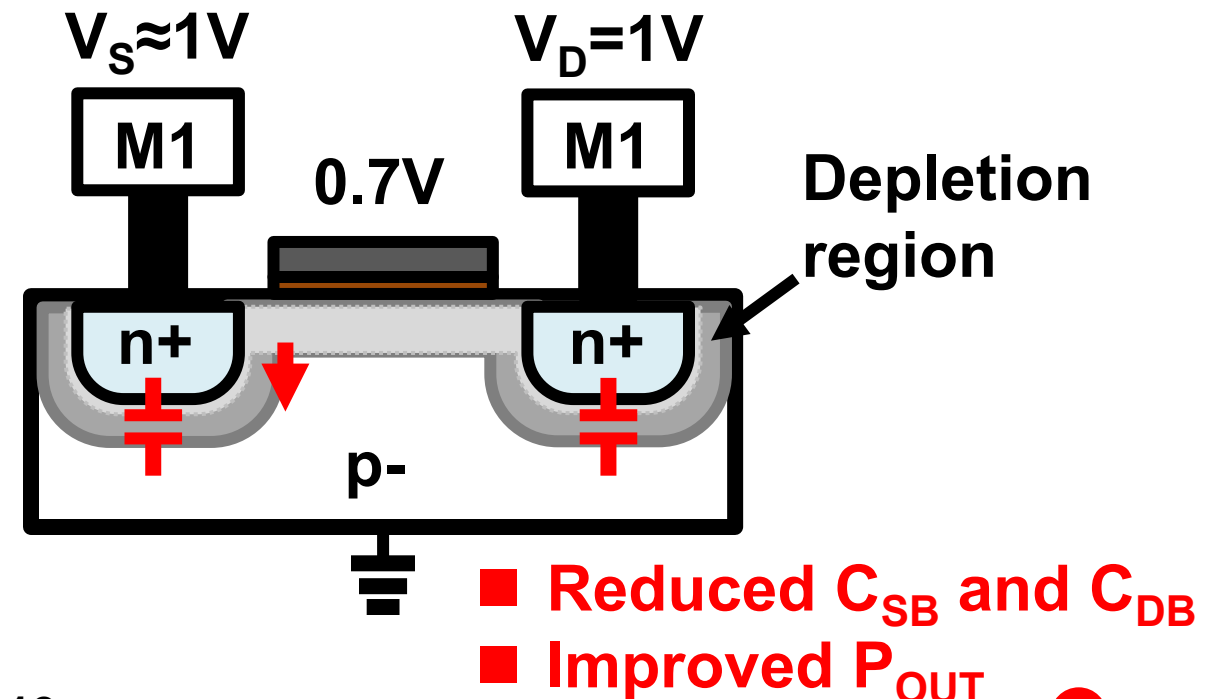
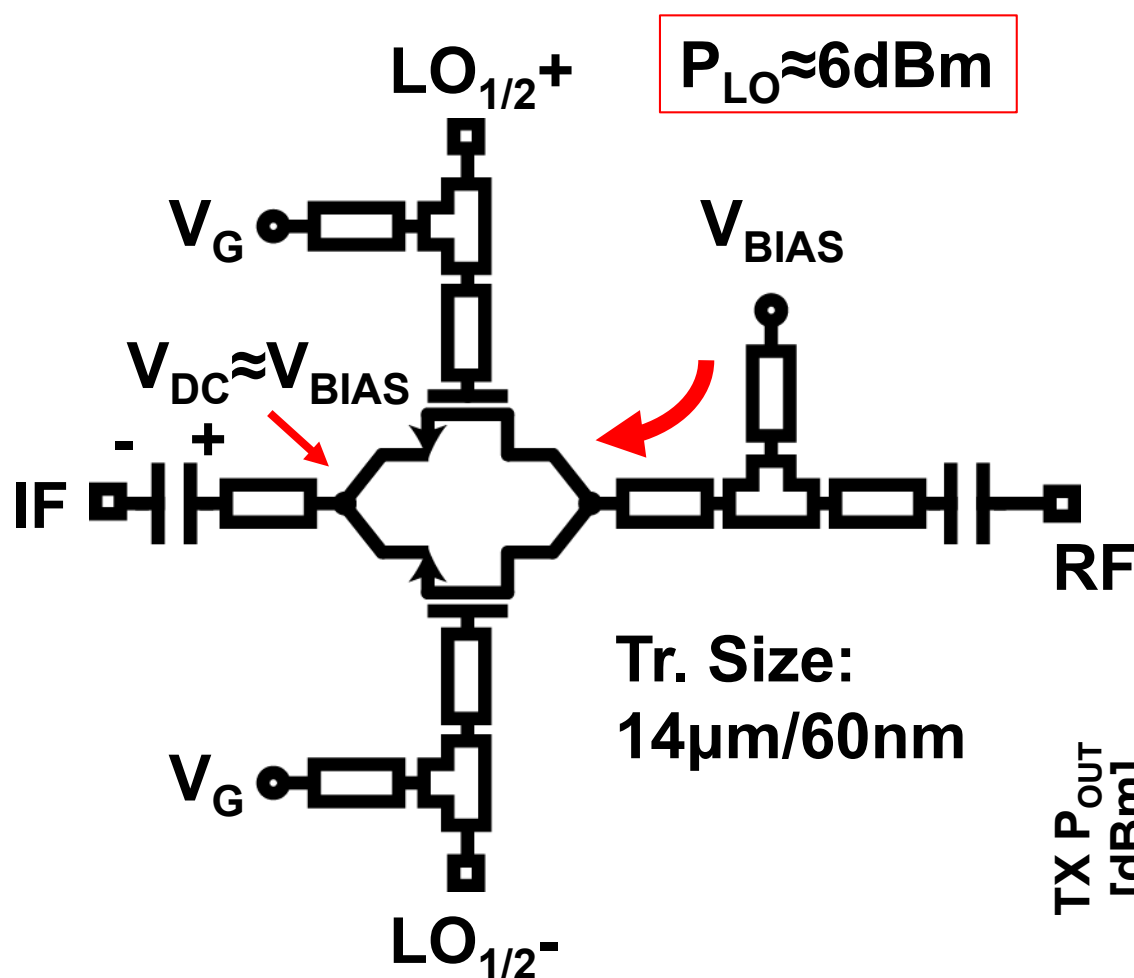


Mixer Circuit and Simulation

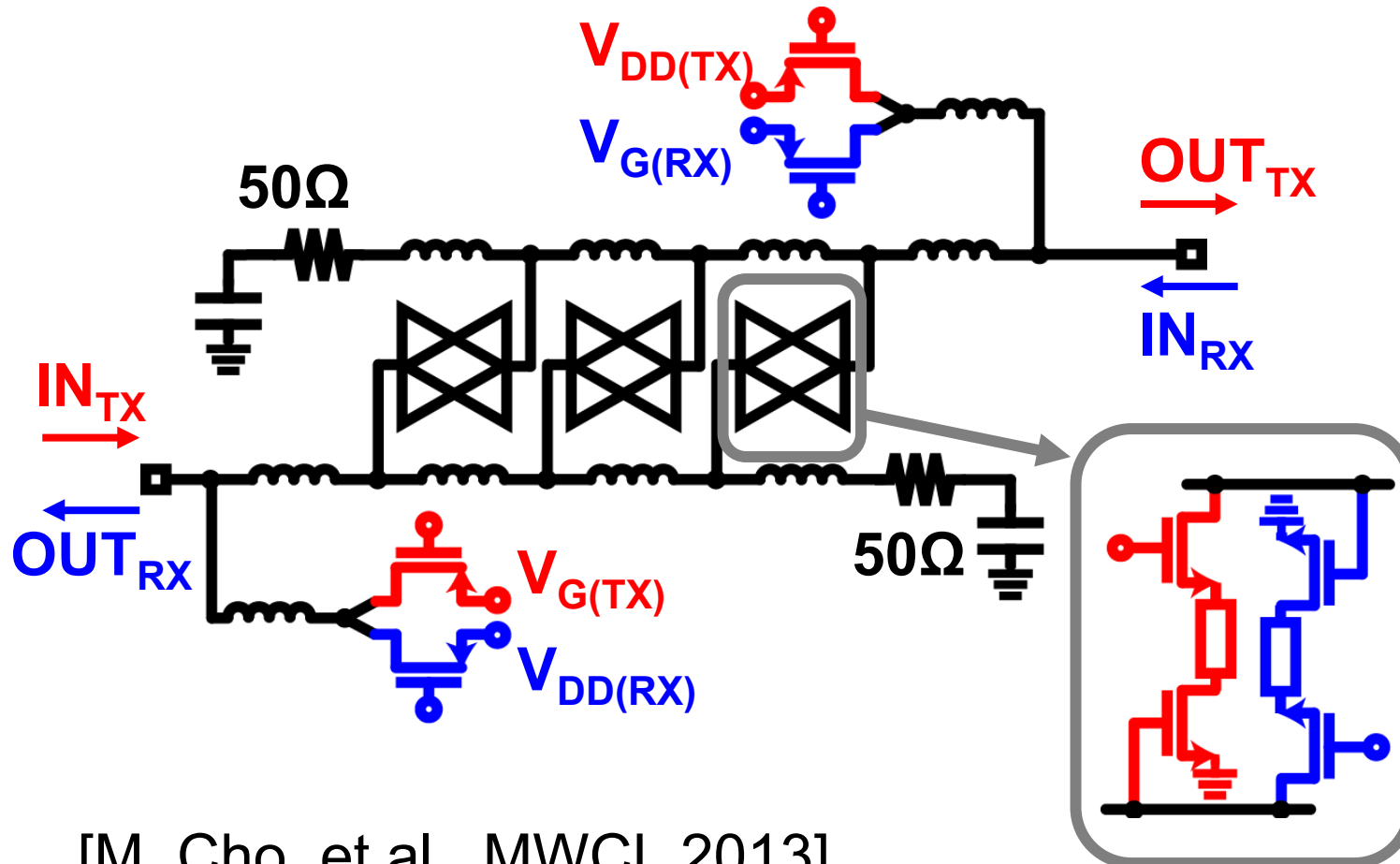


:(Large LOFT2
:(Large image

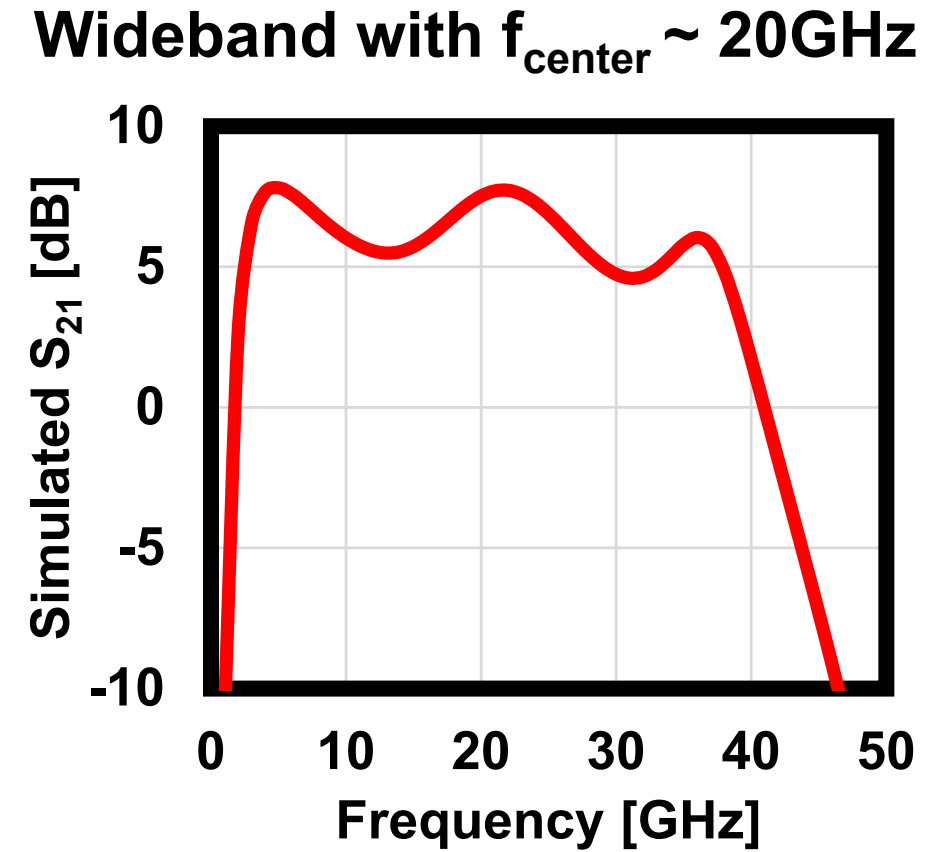
Mixer Biasing Technique



IF Distributed Amplifier

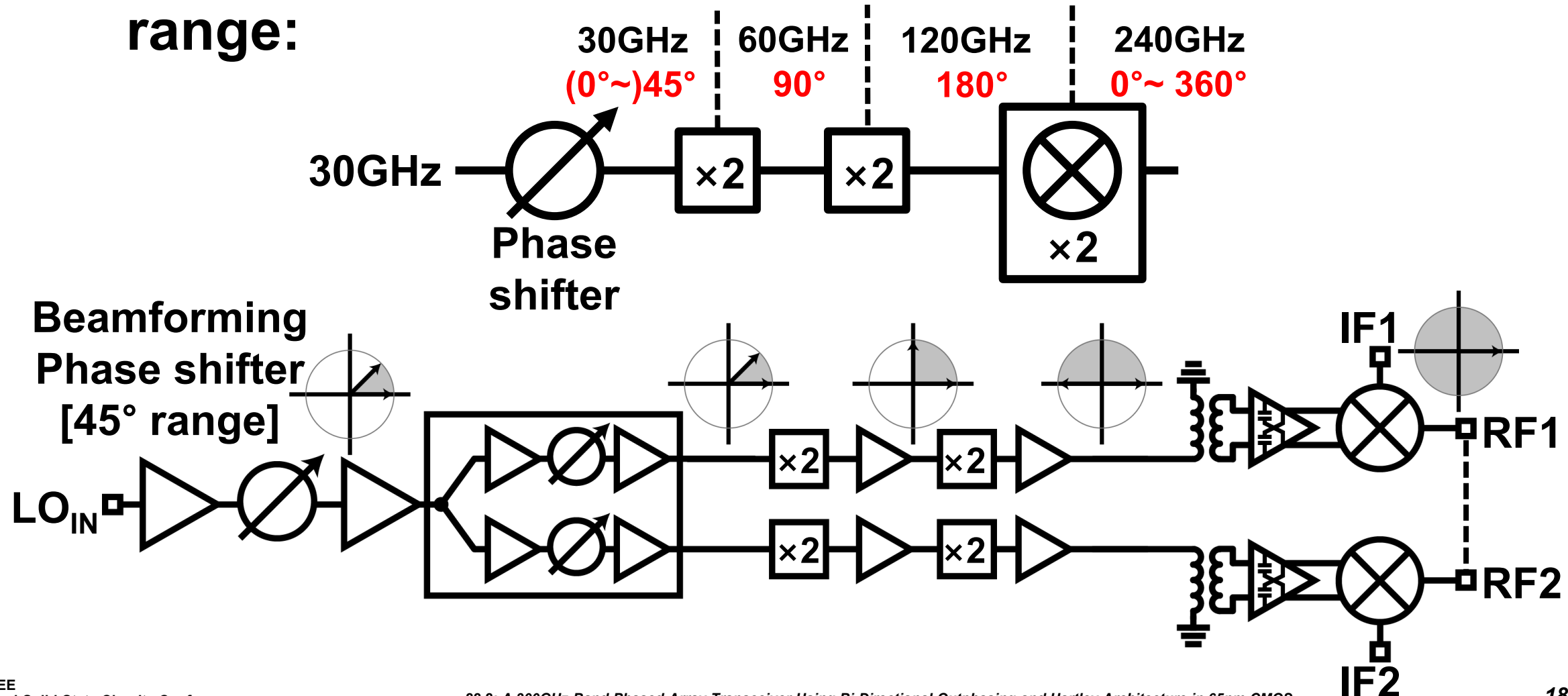


[M. Cho, et al., MWCL 2013]



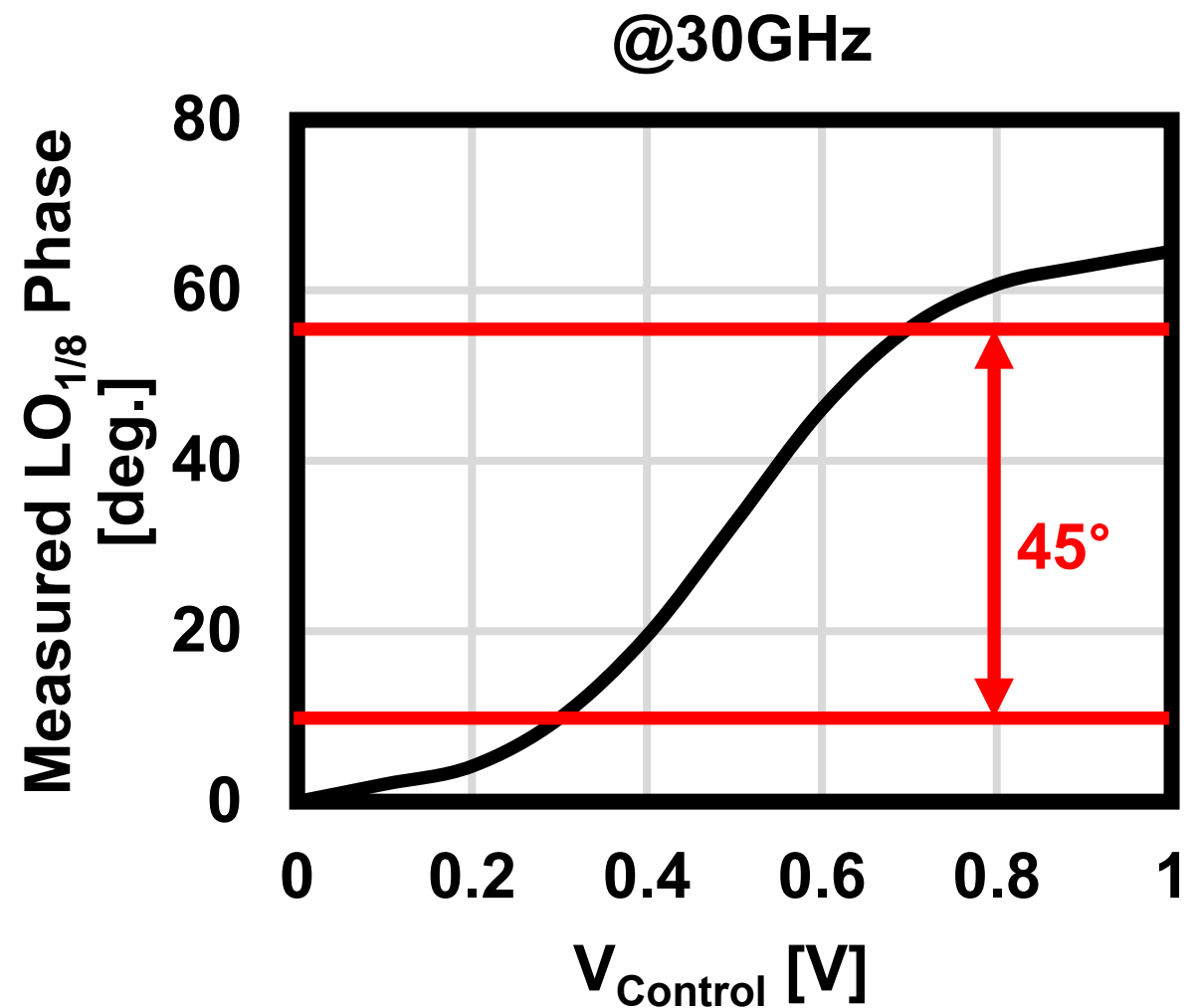
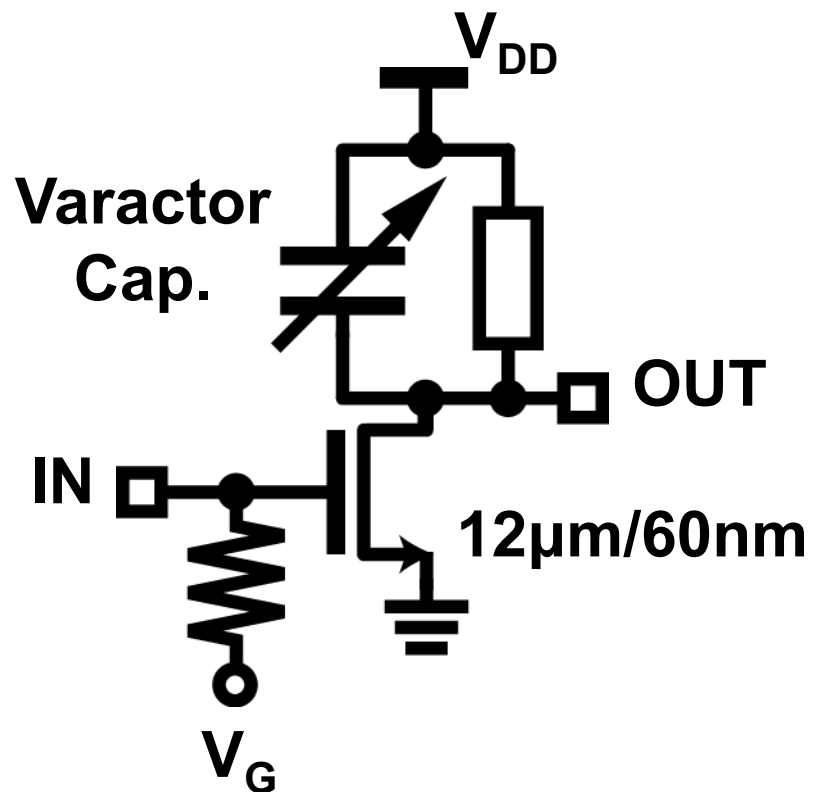
LO Chain and Phase Generation

- Utilizing the frequency multipliers to extend the range:

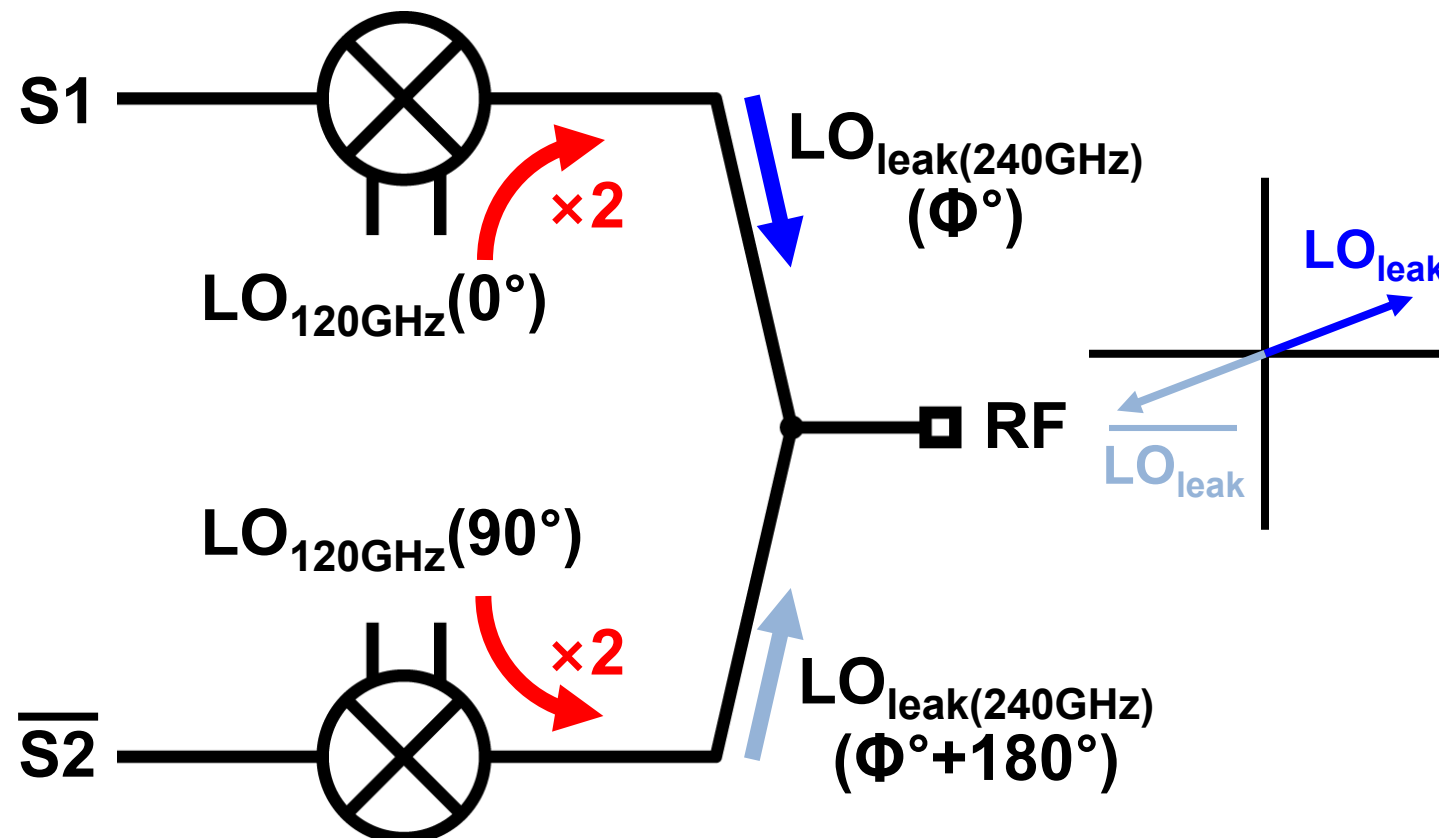


45° Phase Shifter

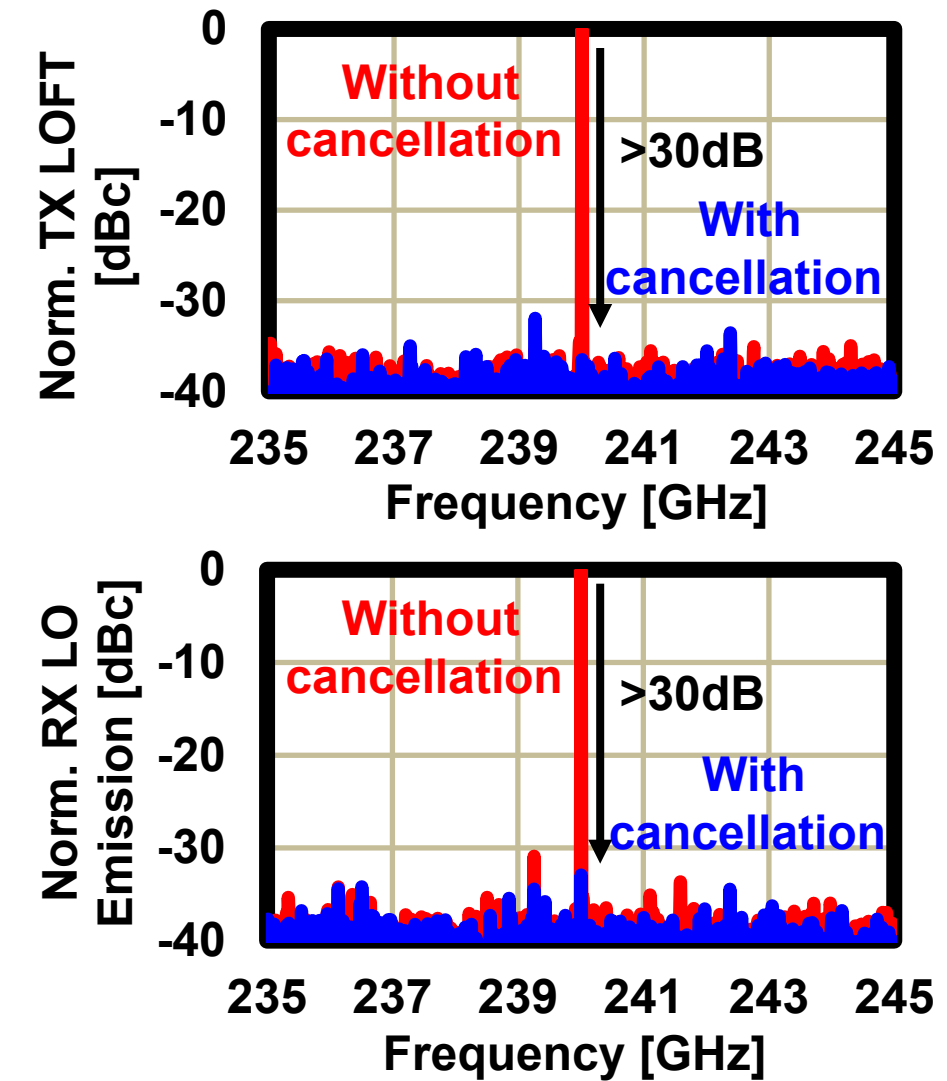
■ Simple LC circuit



LOFT Cancellation

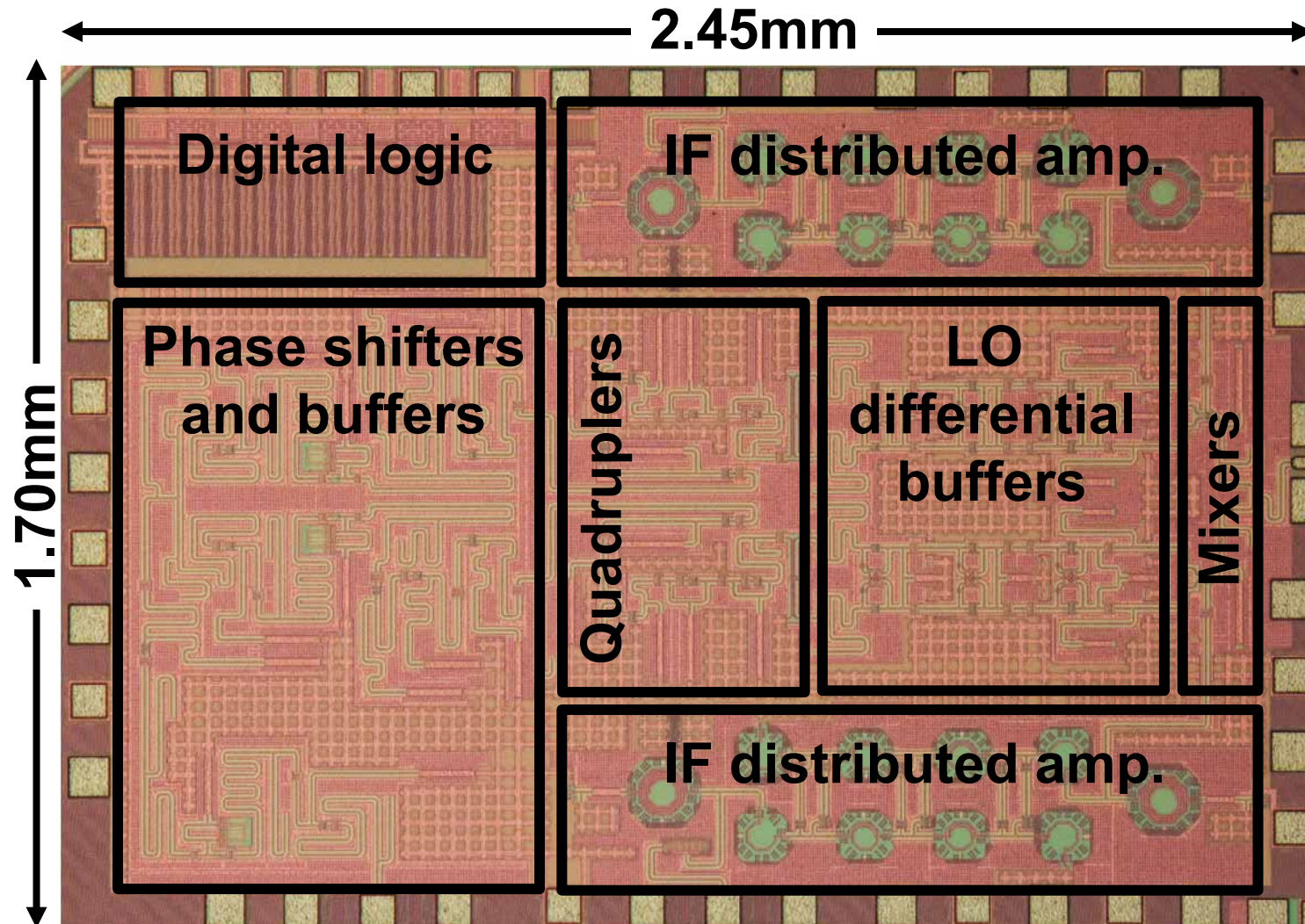


Measured results



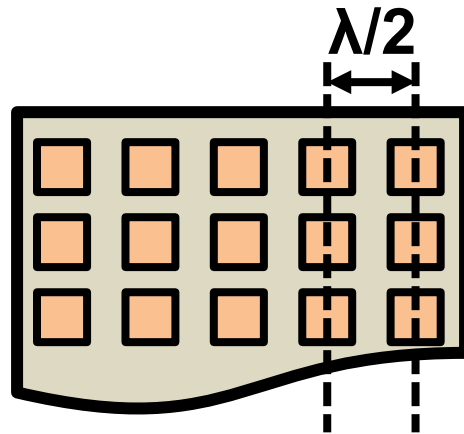
Die Micrograph

1.70mm × 2.45mm
in 65nm CMOS



mm-Wave Phased-Array

Two-dimensional array



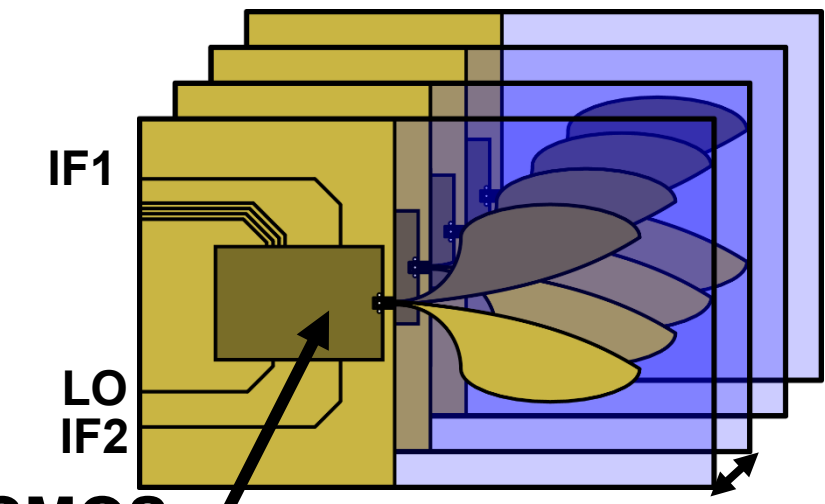
5.4mm @28GHz
0.5mm @300GHz

On-chip antenna array

- ⌚ Huge chip size
- ⌚ Large Si substrate loss

[H. Saeidi et al., ISSCC 2020]

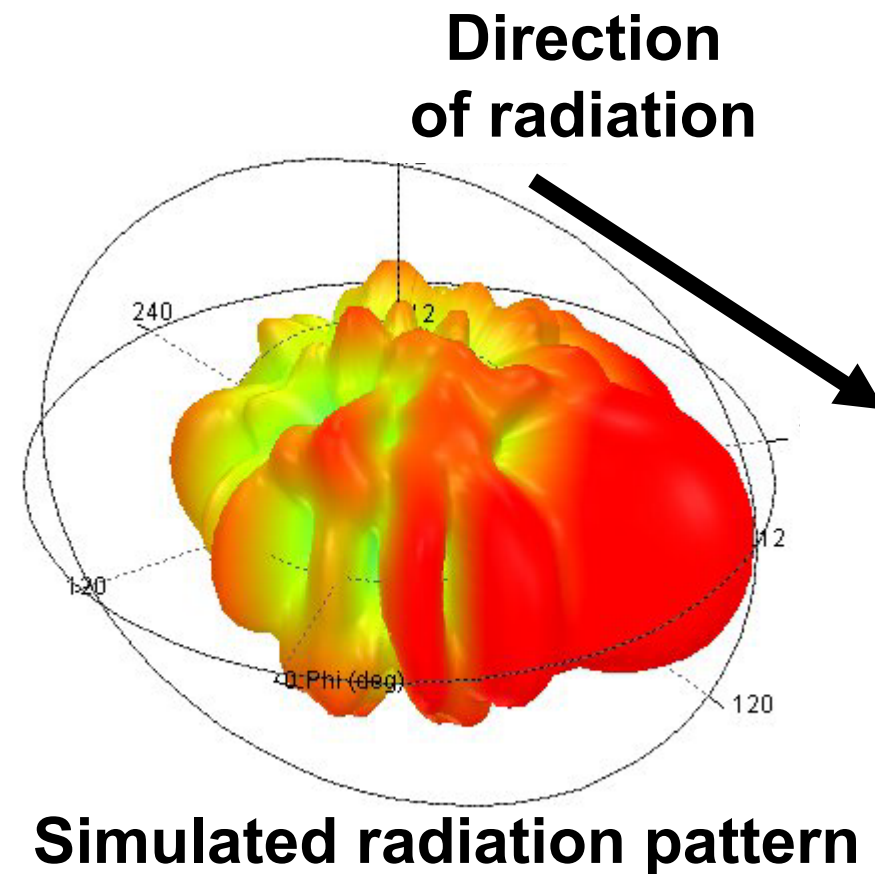
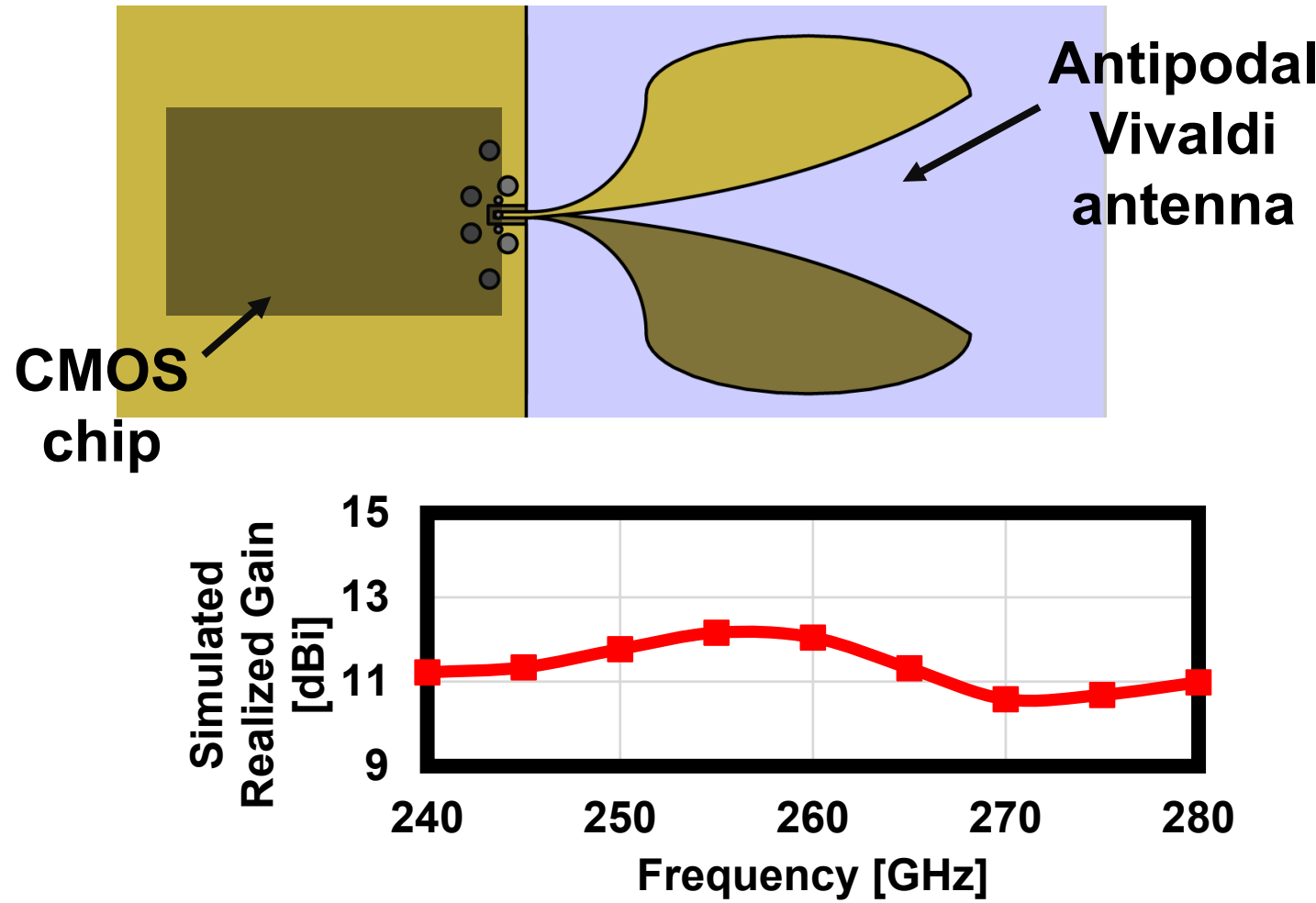
End-fire antennas stacked vertically



0.7mm
0.6 λ @260GHz

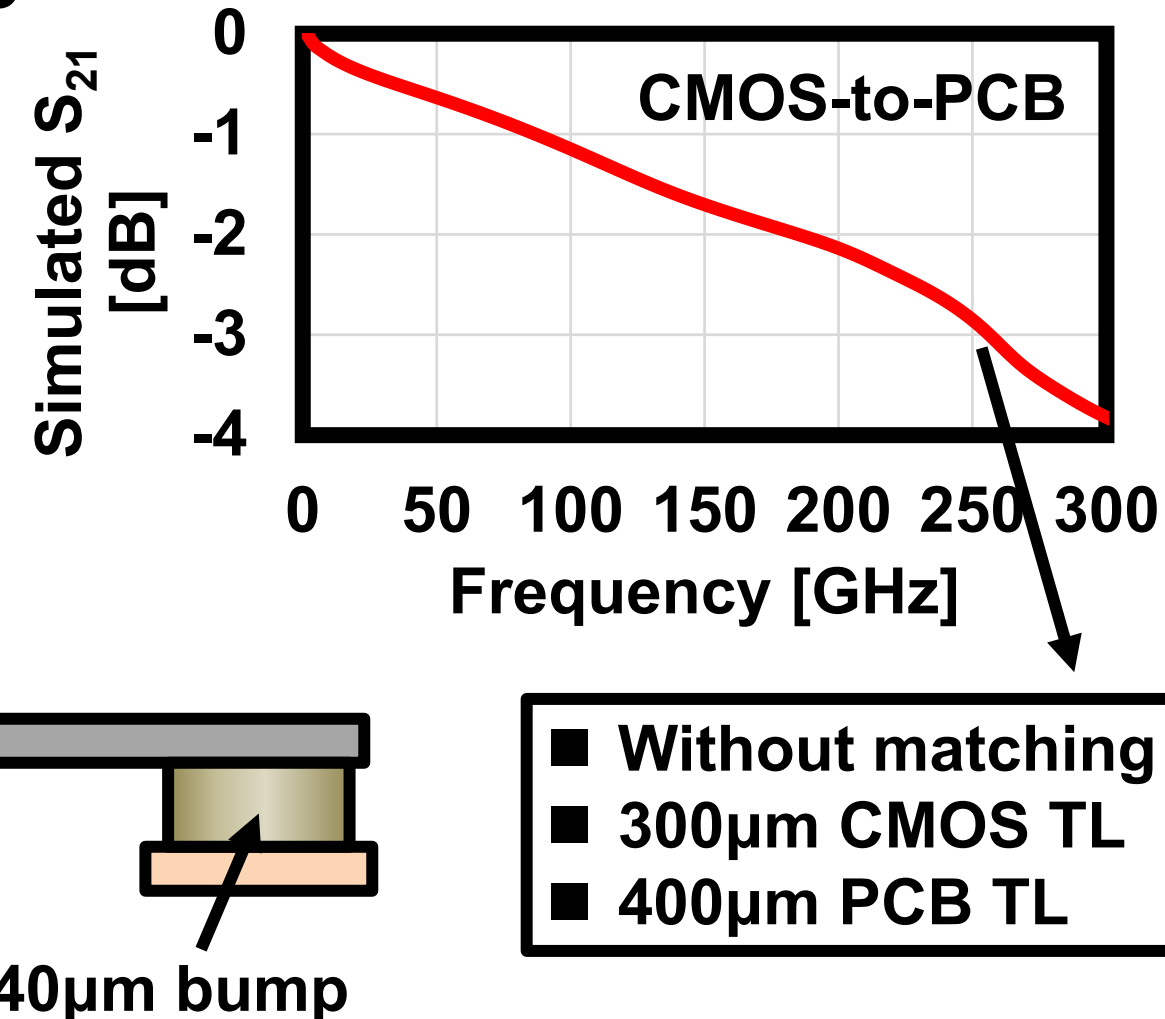
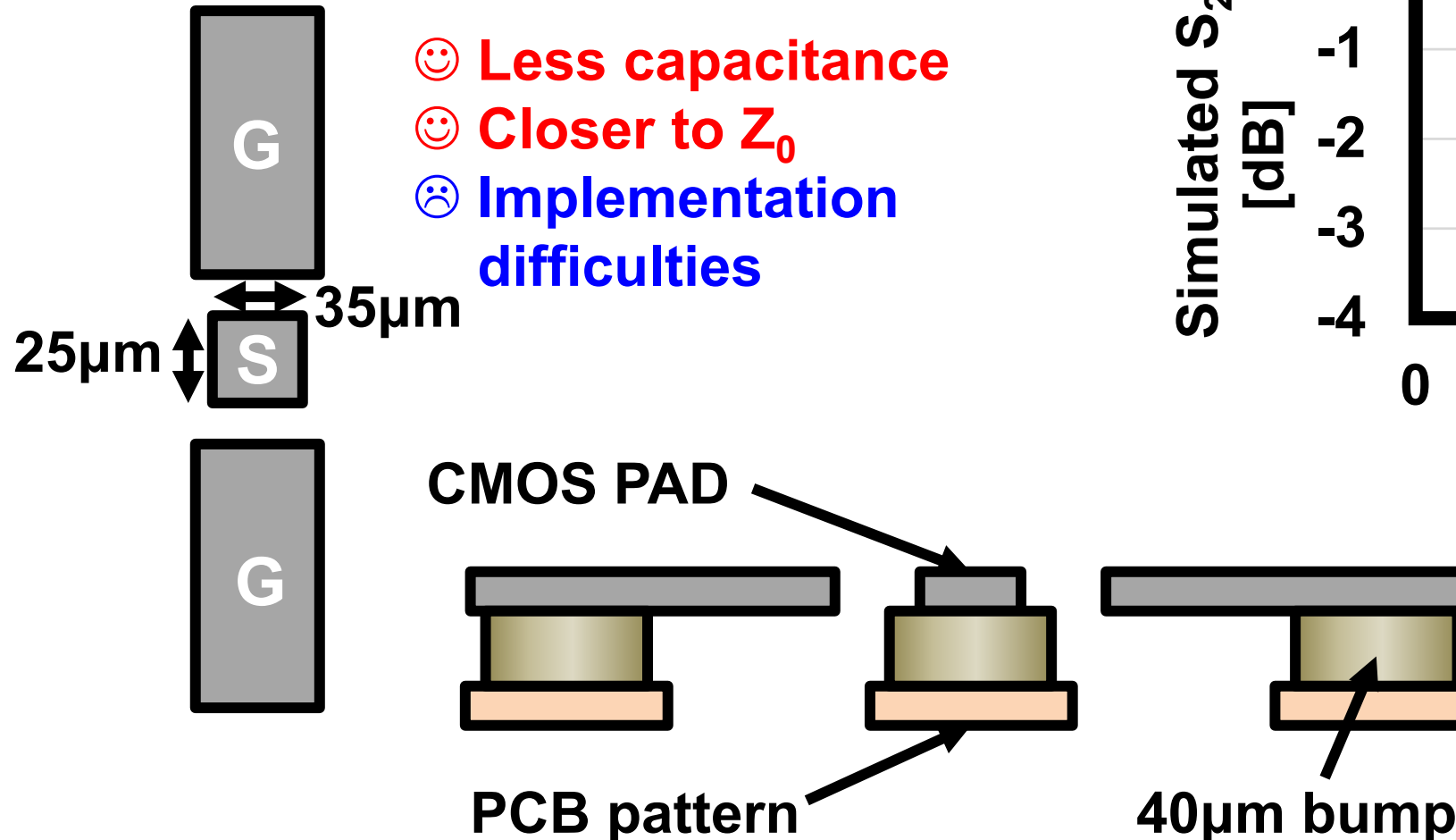
Vivaldi antenna:
End-fire / High gain / Wideband

On-PCB Vivaldi Antenna

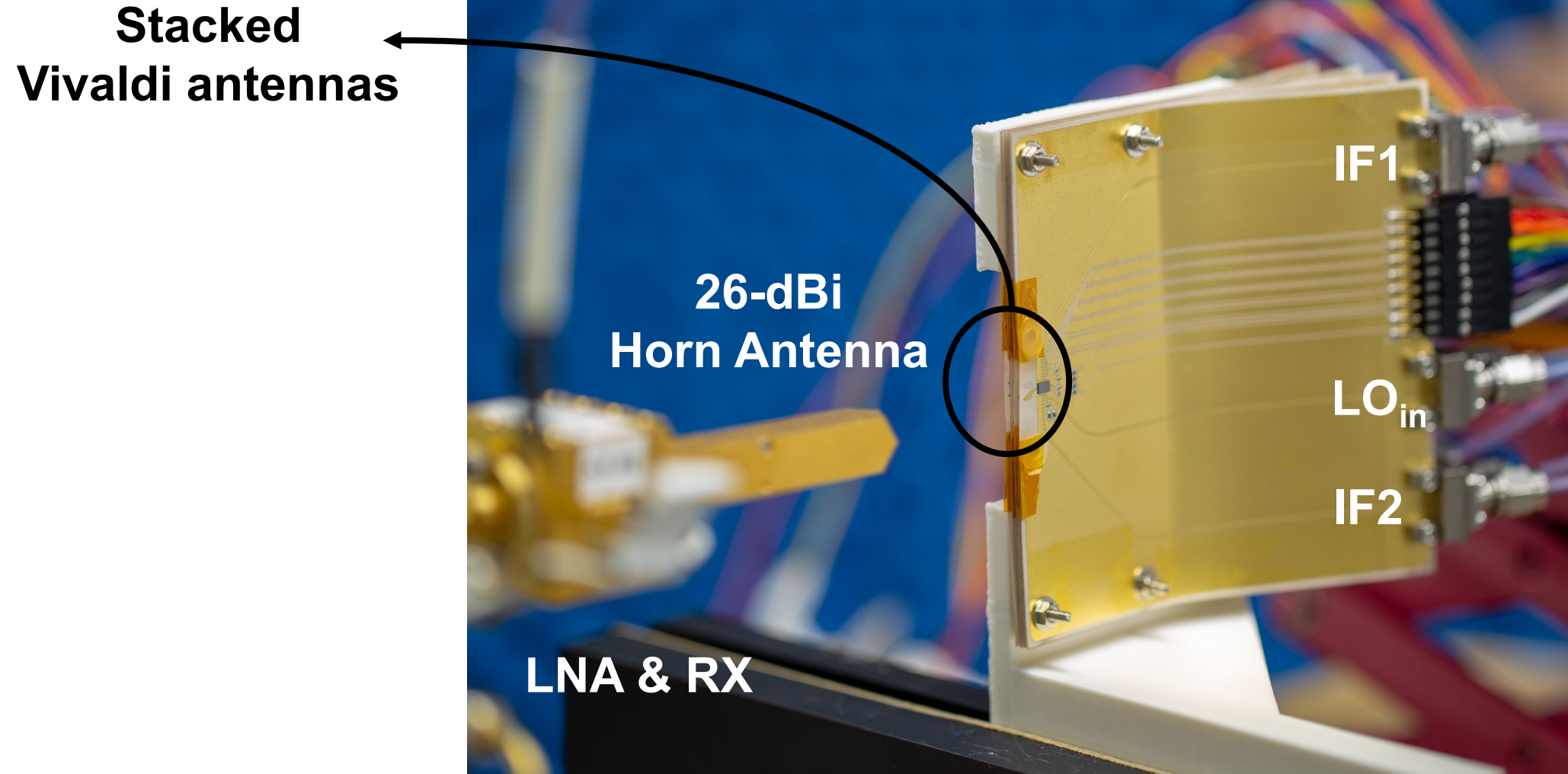


PCB-CMOS Connection

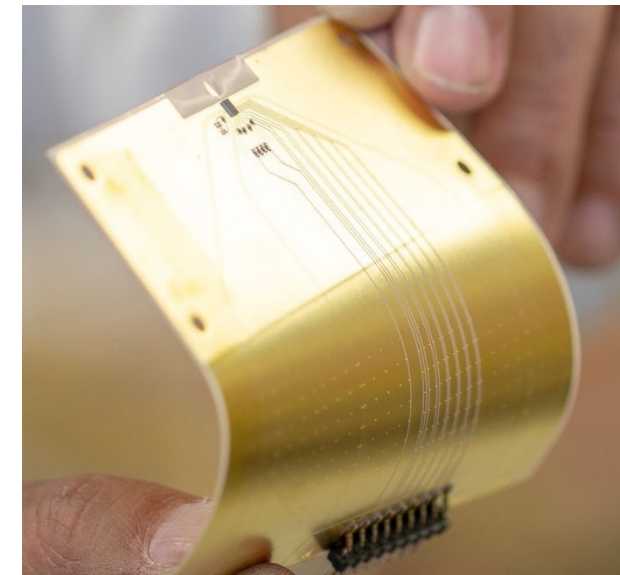
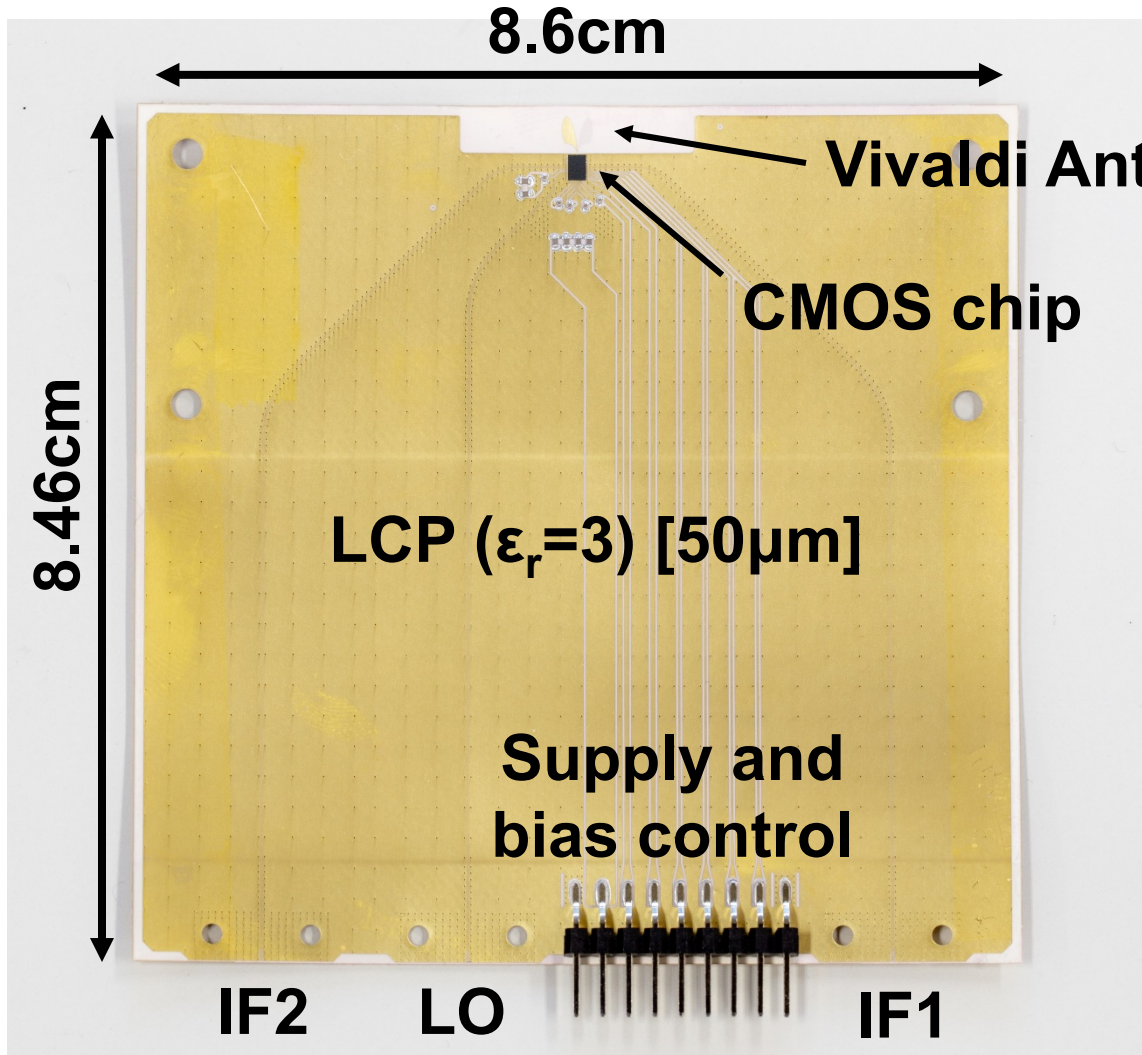
■ Minimized signal PAD size



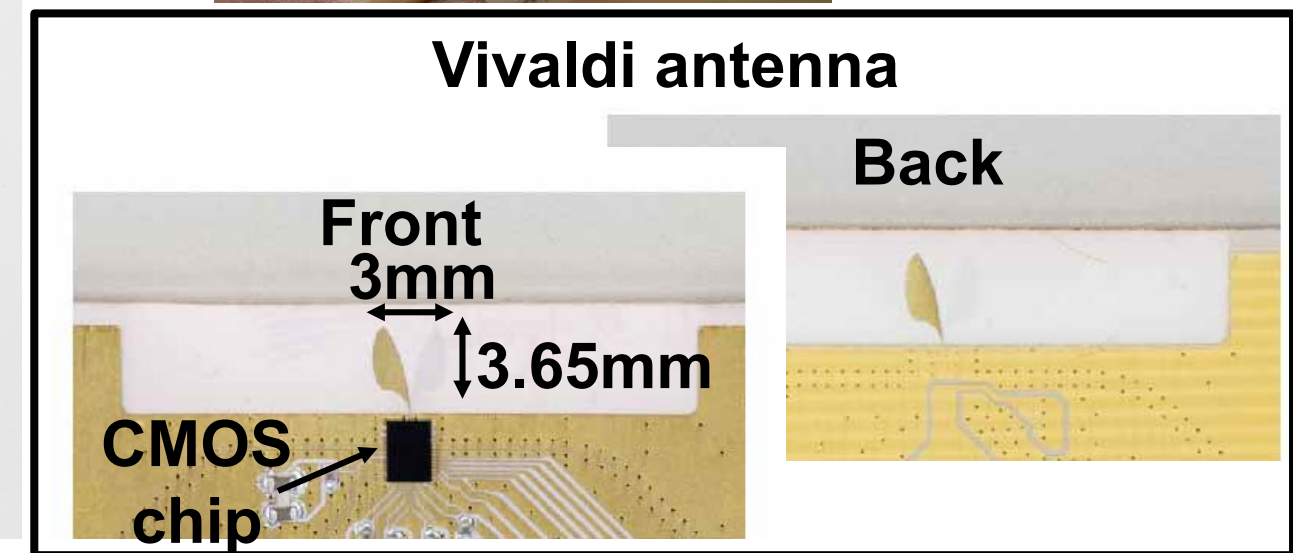
Phased-Array Implementation



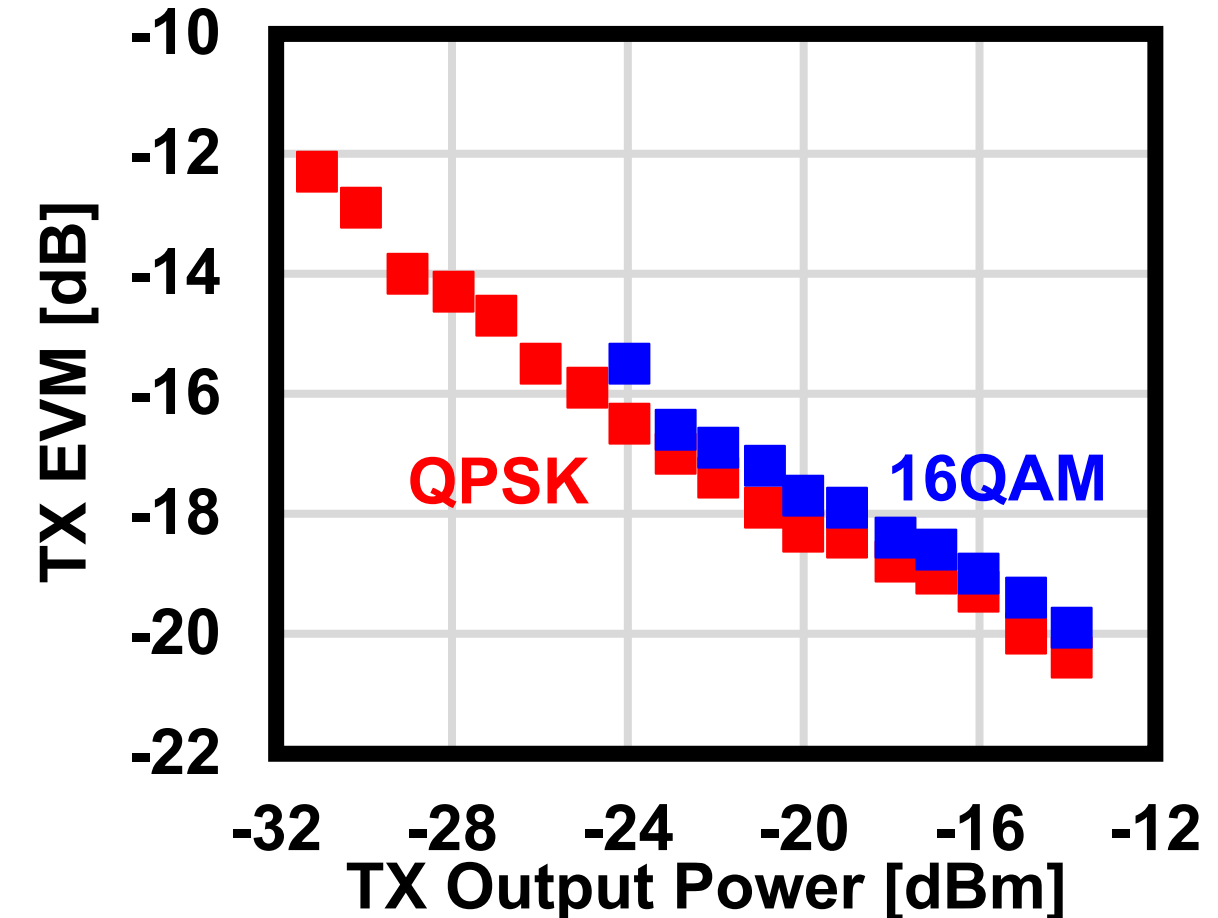
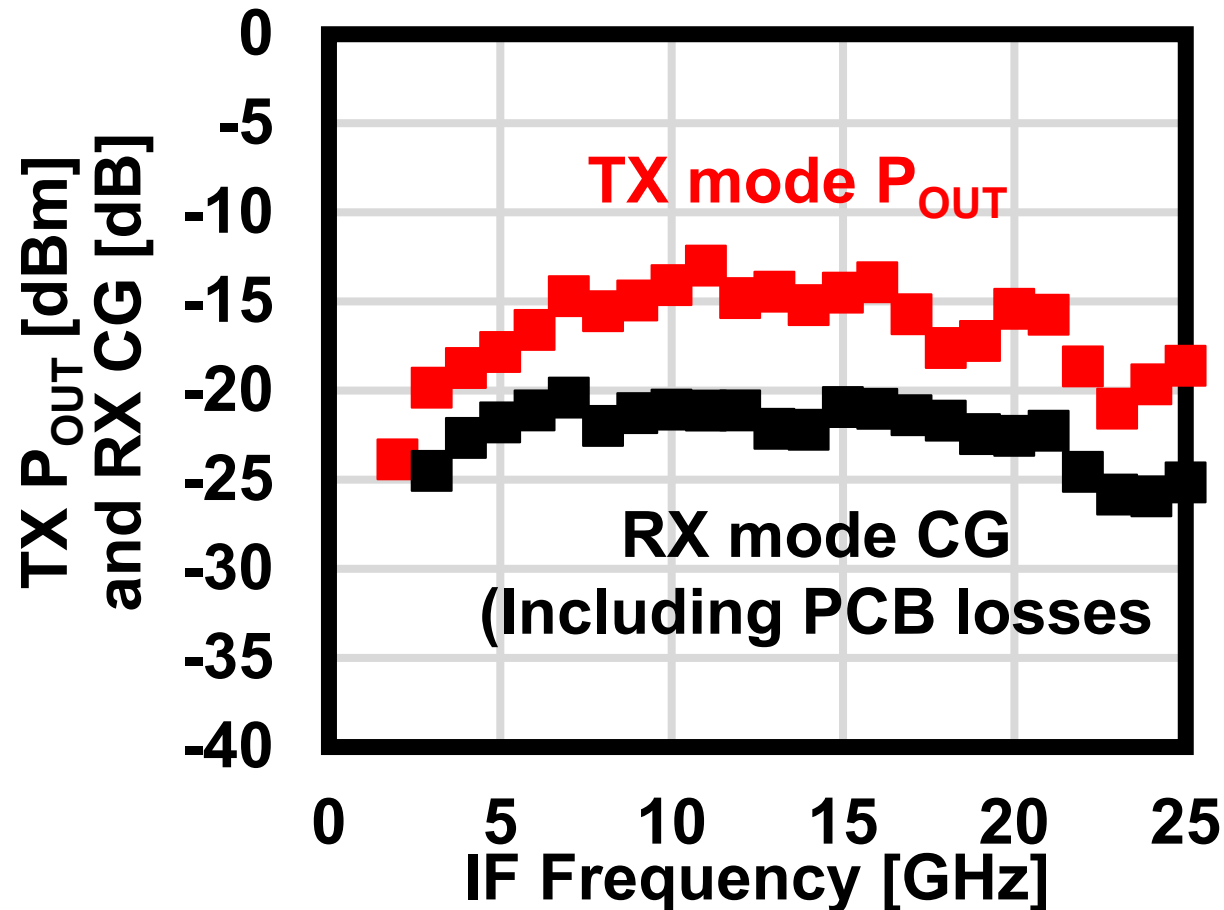
Phased-Array Implementation



Flexible to fit
the connectors



Measured Characteristics



*Results are de-embedded using probe and external mixer loss

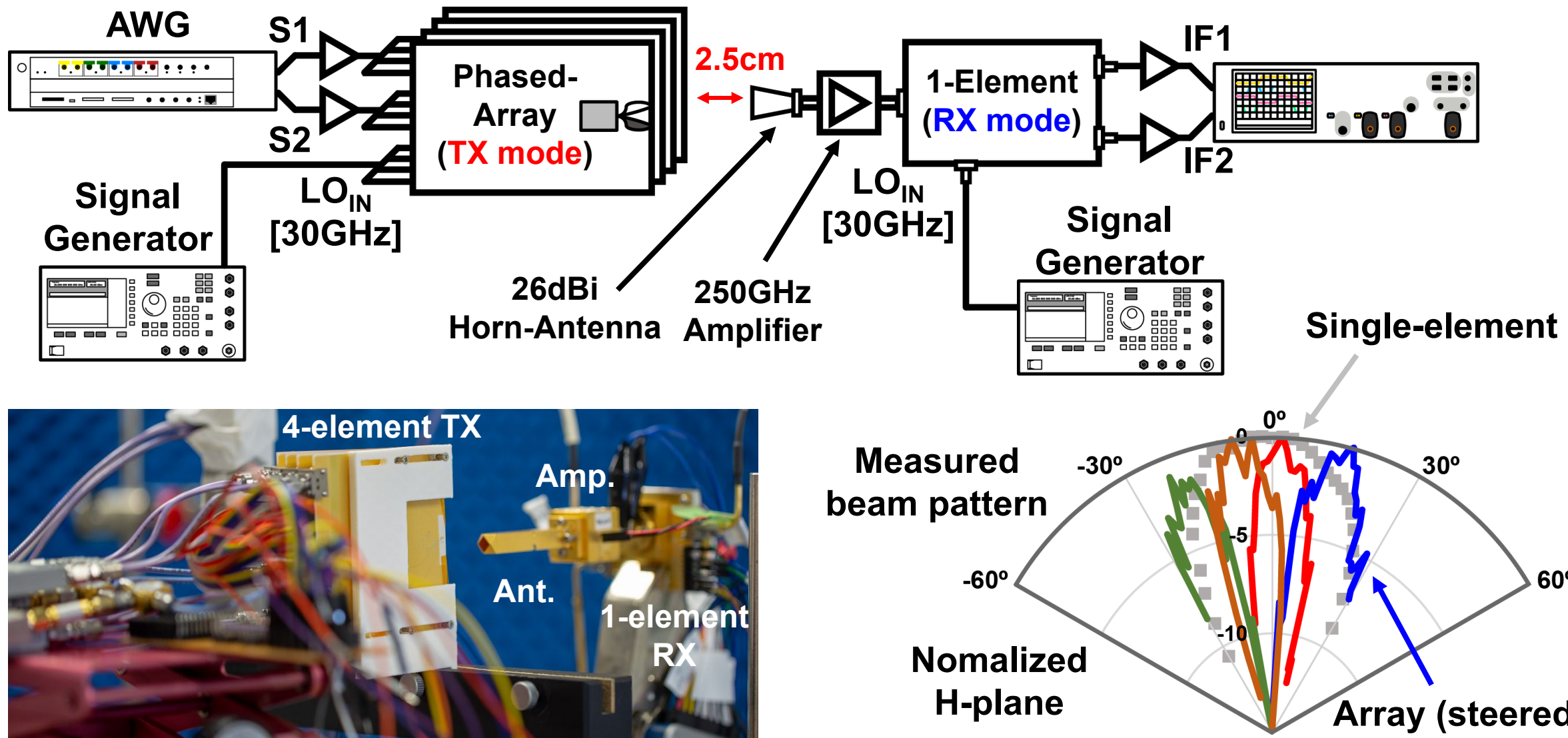
Measured TX Mode

	Max. data rate conditions		IEEE802.15.3d channels	
Channel ID	N/A	N/A	Ch. 66	Ch. 57
Modulation	QPSK	16QAM	QPSK	16QAM
f_{center} [GHz]	256	256	265.68	259.2
Sym. rate [Gbaud]	26	12	21.12	10.56
Data rate [Gb/s]	52	48	42.24	42.24
TX down converted constellation				
TX EVM [dB]	-9.8	-16.6	-11.5	-16.8

Measured RX Mode

	Max. data rate conditions		IEEE802.15.3d channels	
Channel ID	N/A	N/A	Ch. 57	Ch. 2
Modulation	QPSK	16QAM	QPSK	16QAM
f_{center} [GHz]	256	256	259.2	255.96
Sym. rate [Gbaud]	18	3	10.56	1.76
Data rate [Gb/s]	36	12	21.12	7.04
RX down converted constellation				
RX EVM [dB]	-10.1	-16.8	-10.8	-17.1

Phased-Array Beam Pattern Measurement



Comparison Table

	[1],[6] UCB	[3],[4] Hiroshima&NICT	[5] Hiroshima	[2] Tokyo Tech	This work
Tech. [nm]	65 CMOS	40 CMOS	40 CMOS	65 CMOS	65 CMOS
RF freq. [GHz]	240*	290*	252-279	278-304	242-280
Structure	Single-element	Single-element	Single-element	Single-element	Phased array
Architecture	Uni-directional	Uni-directional	Uni-directional	Uni-directional	Bi-directional
TX Topology	Single stream tripler-last	Power combining	Power combining	Single stream mixer-last	Outphasing +Hartley
Max. Baud rate [Gbaud]	TX: 8 RX: 8	TX: 21 RX: 14	TX: 28 RX: N/A	17	TX: 26 RX: 18
P _{DC} [W]	TX: 0.22 RX: 0.26	TX: 1.4 RX: 0.65	TX: 0.89 RX: 0.9	TX: 0.27 RX: 0.14	TX: 0.75 RX: 0.75
Area [mm ²]	TX: 2 RX: 2	TX: 5.19 RX: 3.15	TRX: 11	TX: 1.9 RX: 1.9	TRX: 4.17

*Center frequency

Conclusion

- A 300GHz-band CMOS bi-directional phased-array transceiver is introduced.
 - Outphasing TX mode and Hartley RX mode are utilized
 - The circuit is completely shared between TX and RX
 - Stacked Vivaldi antennas form the narrow-pitched array
- The 4-element array steers the beam from -18° to +18°
- A 26Gbaud QPSK baud rate is achieved in TX mode while a 18Gbaud baud rate is achieved in the RX mode.

Acknowledgement

This work is partially supported by STAR, and VDEC in collaboration with Cadence Design Systems, Inc., Synopsys Inc., Mentor Graphics, Inc., and Keysight Technologies Japan, Ltd.

References

- [1] S. Kang et al., "A 240 GHz Fully Integrated Wideband QPSK Transmitter in 65 nm CMOS," *IEEE J. Solid-State Circuits*, vol. 50, no. 10, pp. 2256-2267, Oct. 2015.
- [2] I. Abdo et al., "A 300GHz Wireless Transceiver in 65nm CMOS for IEEE802.15.3d Using Push-Push Subharmonic Mixer," *IEEE MTT-S Int. Microw. Symp. Dig.*, pp. 623-626, June 2020.
- [3] K. Takano et al., "A 105Gb/s 300GHz CMOS transmitter," *ISSCC Dig. Tech. Papers*, pp.308-309, Feb. 2017.
- [4] S. Hara et al., "A 32Gbit/s 16QAM CMOS Receiver in 300GHz Band," *IEEE MTT-S Int. Microw. Symp. Dig.*, pp. 1703-1706, June 2017.
- [5] S. Lee et al., "An 80-Gb/s 300-GHz-Band Single-Chip CMOS Transceiver," *IEEE J. Solid-State Circuits*, vol. 54, no. 12, pp. 3577-3588, Dec. 2019.
- [6] S. V. Thyagarajan et al., "A 240 GHz fully integrated wideband QPSK receiver in 65 nm CMOS," *IEEE J. Solid-State Circuits*, vol. 50, no. 10, pp. 2268–2280, Oct. 2015.
- [7] M. Cho, J. Kim and D. Baek, "A Switchless CMOS Bi-Directional Distributed Gain Amplifier With Multi-Octave Bandwidth," *IEEE Microwave and Wireless Components Letters*, vol. 23, no. 11, pp. 611-613, Nov. 2013.
- [8] A. Standaert and P. Reynaert, "A 390-GHz Outphasing Transmitter in 28-nm CMOS," *IEEE Journal of Solid-State Circuits*, vol. 55, no. 10, pp. 2703-2713, Oct. 2020.

Thank you

A 0.42THz Coherent TX-RX System Achieving 10dBm EIRP and 27dB NF in 40nm CMOS for Phase-Contrast Imaging

Dragan Simic, Kaizhe Guo and Patrick Reynaert
KU Leuven - MICAS, Belgium



Self Introduction

■ Education

- 2011 - 2015, B.Sc. Studies, Electronics, University of Belgrade, Serbia
- 2015 - 2016, M.Sc. Studies, Electronics, University of Belgrade, Serbia
- 2016 - present, Ph.D. Studies, THz Electronics, KU Leuven, Belgium

■ Internships

- March 2015 - May 2015, Mikroelektronika, Belgrade, Serbia, PCB design
- May 2015 – August 2016, NovellIC, Belgrade, Serbia, Analog and RF IC design

■ Research Interests

- Design of mm-wave and THz circuits
- 3D Imaging



Outline

- Motivation
- Proposed TX-RX System Architecture
- Measurement Results
- Imaging Demonstrations
- Conclusion

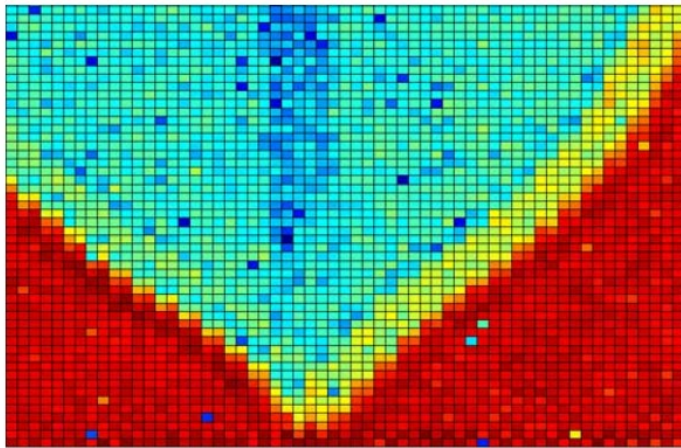
Outline

- Motivation
- Proposed TX-RX System Architecture
- Measurement Results
- Imaging Demonstrations
- Conclusion

THz Imaging, Advantages

- Small wavelength
 - High resolution
- Penetrates through dielectrics
 - Imaging through clothes, plastic, paper...
- Strong absorption by water
 - Easy water detection
- Non-Ionizing radiation
 - Safe for humans and animals

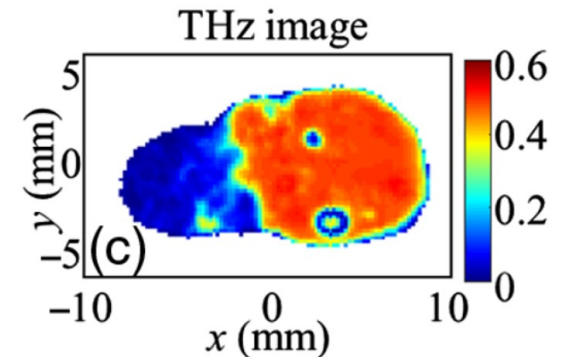
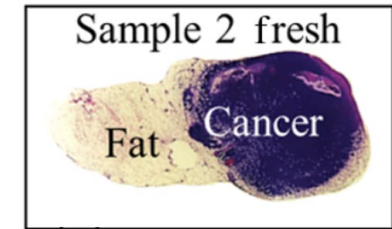
THz Imaging, Applications



[Steyaert W. et al., JSSC, 2014]



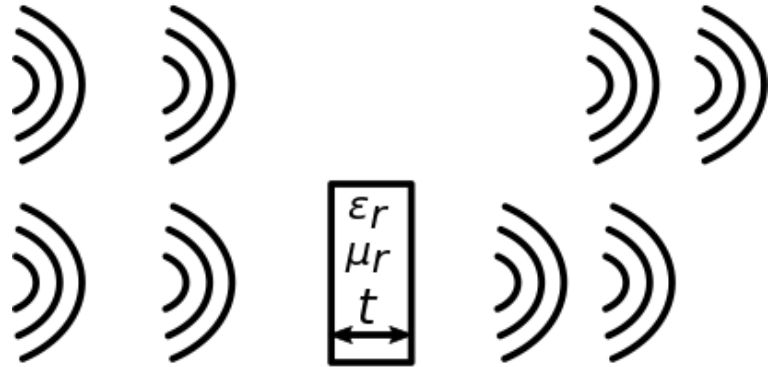
[Hillger P. et al., TTST, 2019]



[Bowman T. et al., JBO, 2018]

■ Biological, Security, Medical, Industrial...

Phase Detection Added Value



$$\Delta\varphi = 2\pi t f_{RF} \frac{(\sqrt{\varepsilon_r \mu_r} - 1)}{c_0}$$

- Detecting cross section of imaged object
 - Thickness measurement
 - Dielectric characterization
 - 3D Imaging
- Detecting weakly absorbing materials
 - Imaging of paper, plastic...

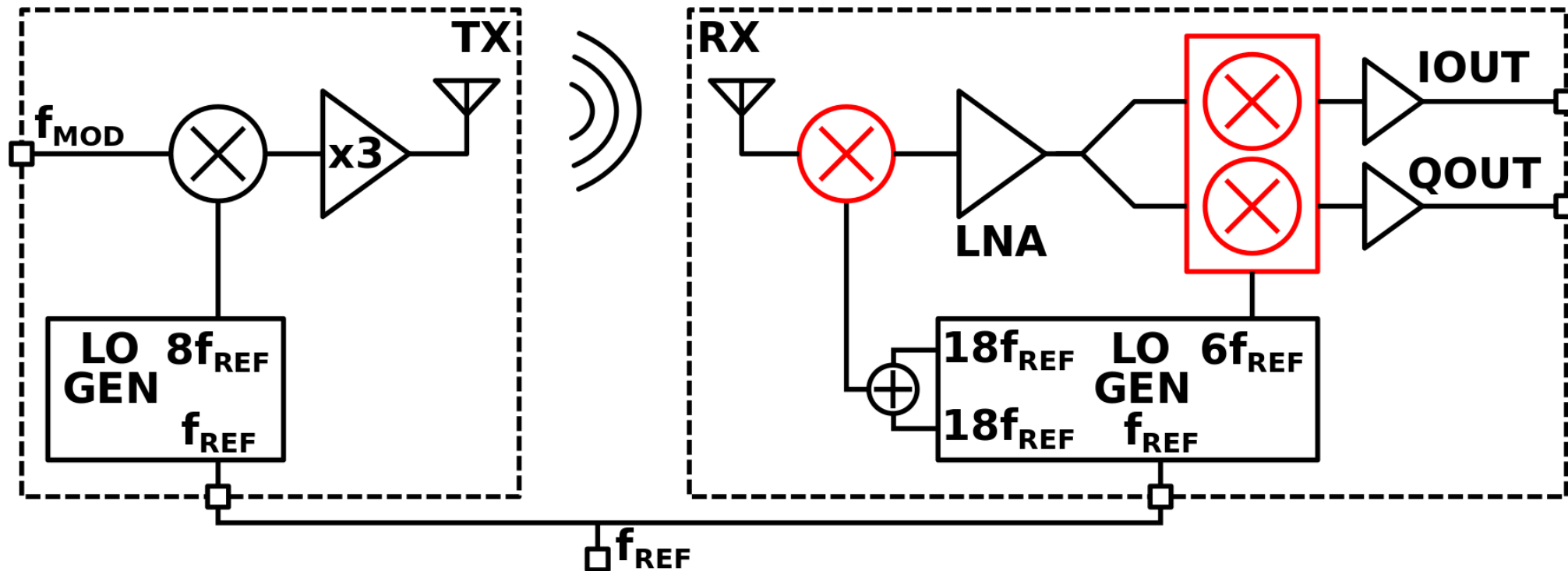
Outline

- Motivation
- **Proposed TX-RX System Architecture**
- Measurement Results
- Imaging Demonstrations
- Conclusion

Phase Detection Requirements

- Coherent RX
 - Phase information is not lost
- TX-RX frequency synchronization
 - Stable reconstructed phase
- High output SNR
 - Imaging time
 - Imaging distance
 - Imaging quality

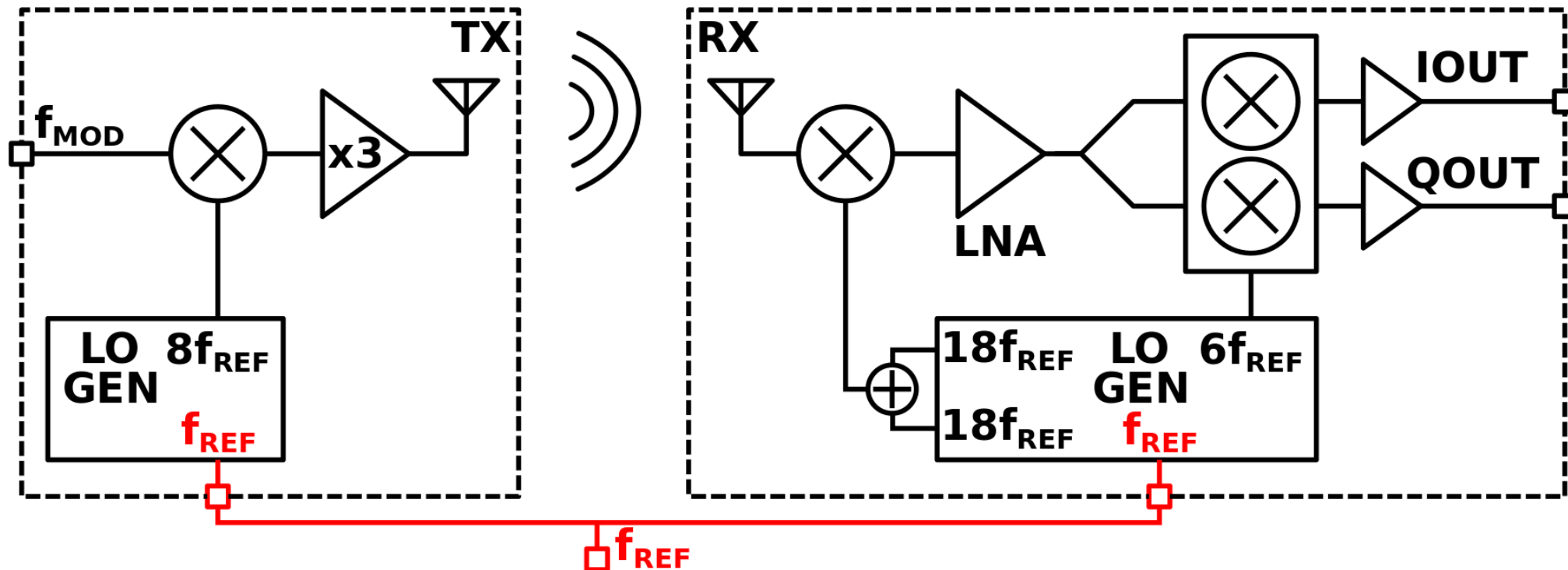
System Architecture, Coherent RX



■ Coherent RX

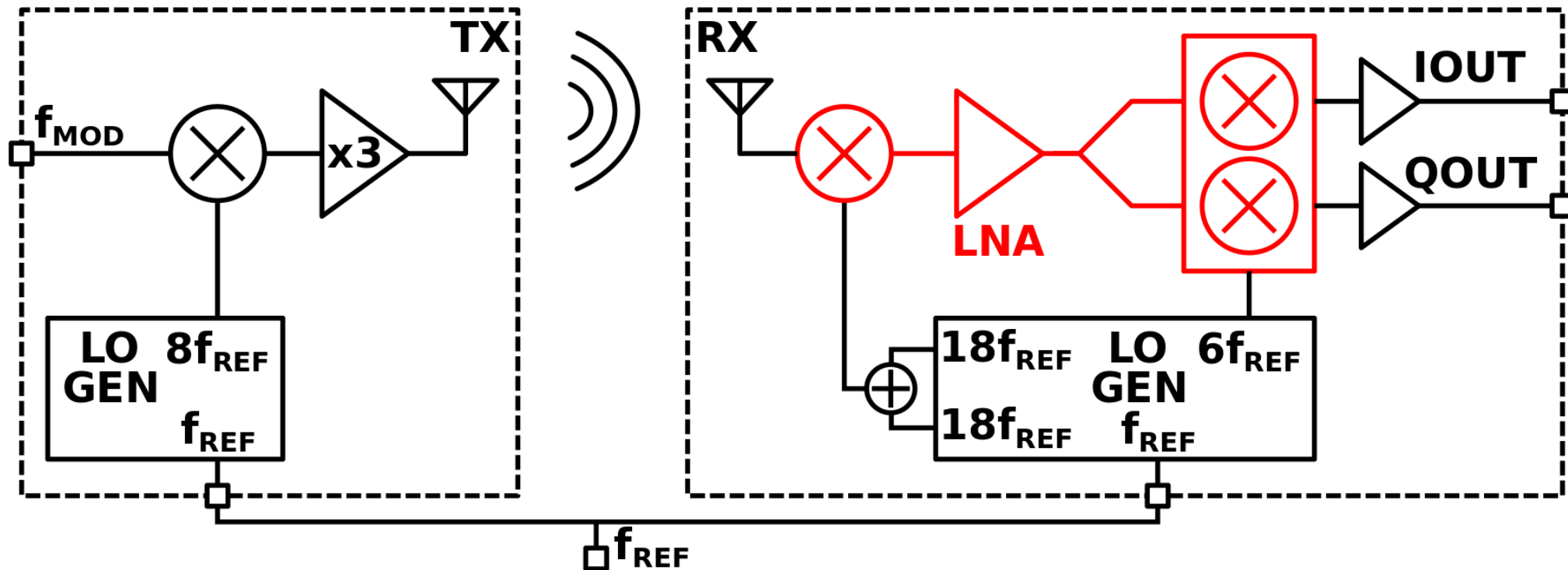
- Heterodyne IQ RX

System Architecture, Freq. Sync.



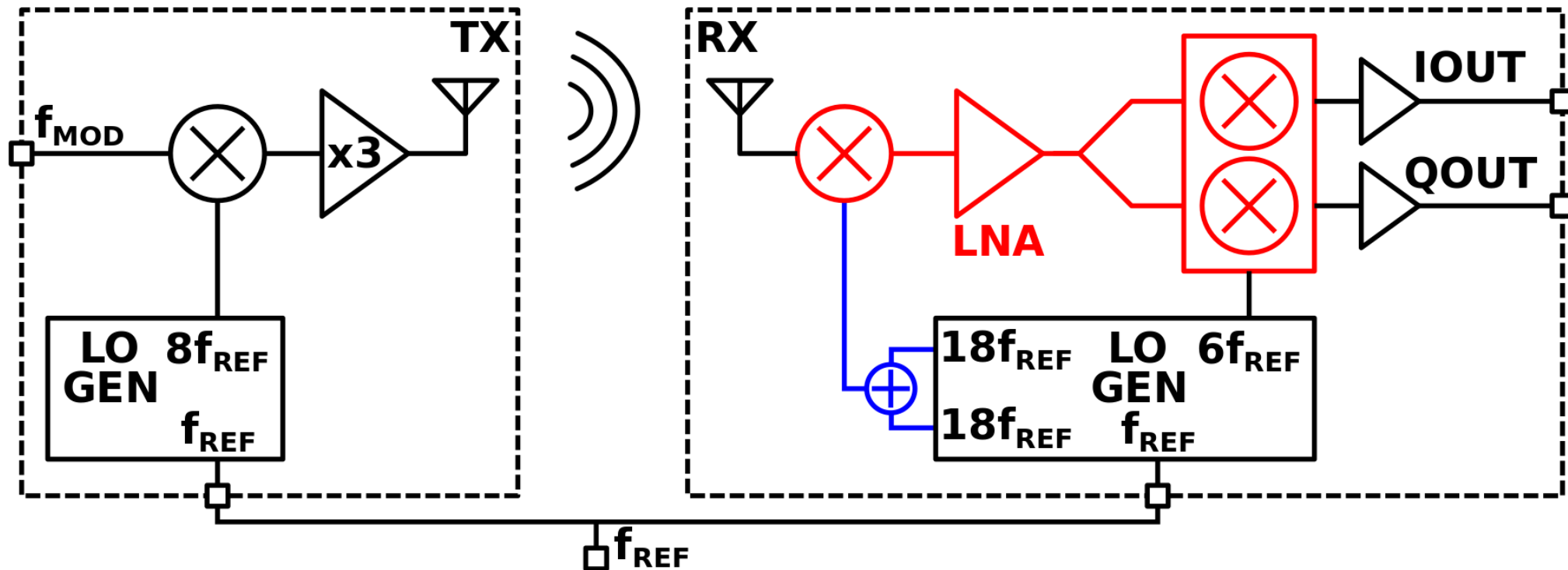
- TX-RX frequency synchronization
 - TX-RX frequency sharing

System Architecture, High SNR



- High output SNR
 - Two-step down-conversion RX with LNA in between

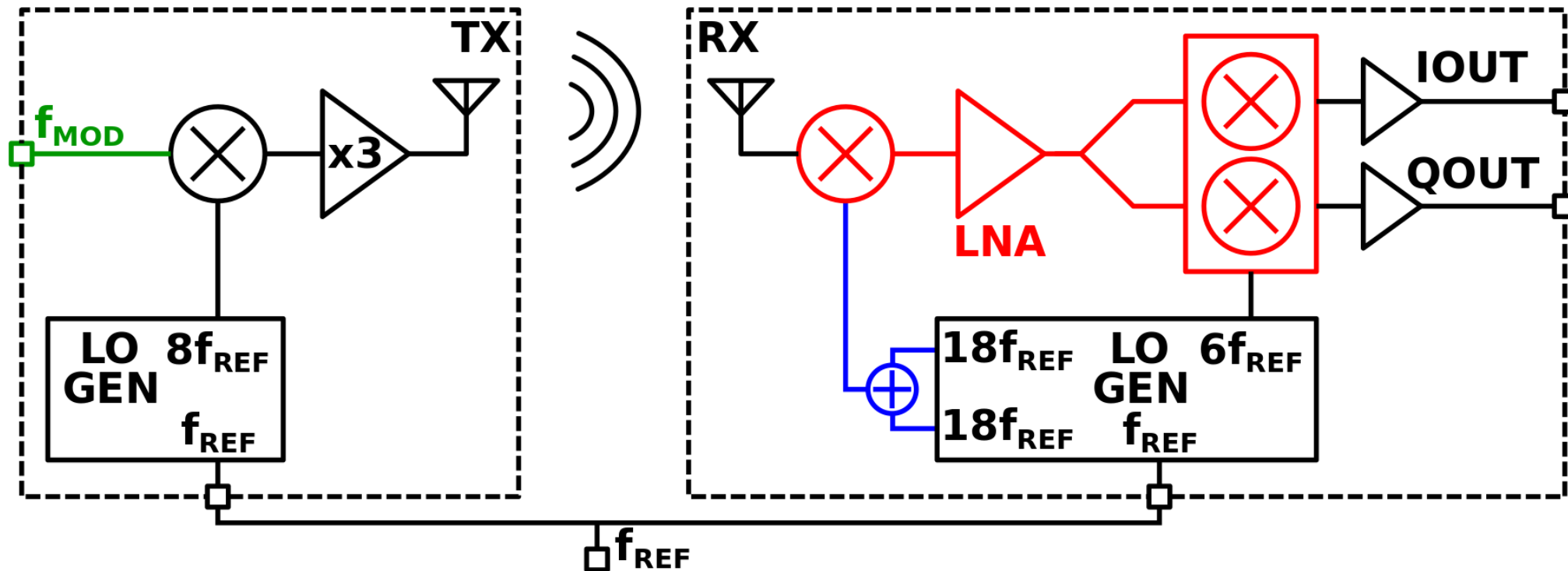
System Architecture, High SNR



■ High output SNR

- Two-step down-conversion RX with LNA in between
- LO two-way power combining

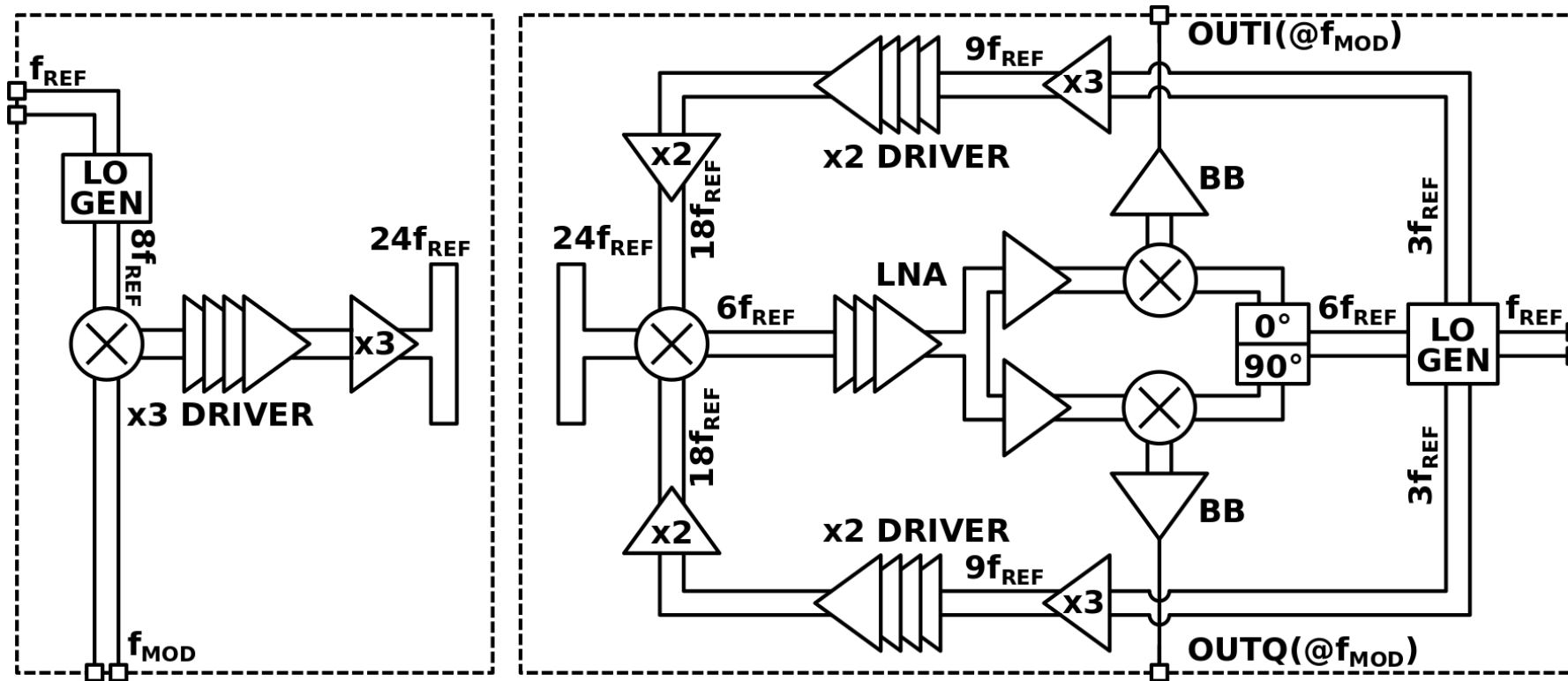
System Architecture, High SNR



■ High output SNR

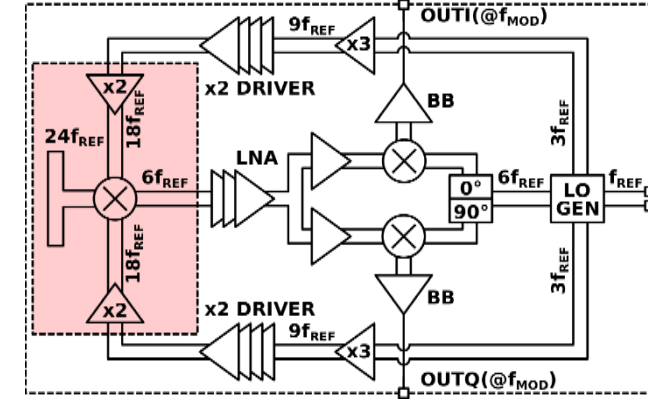
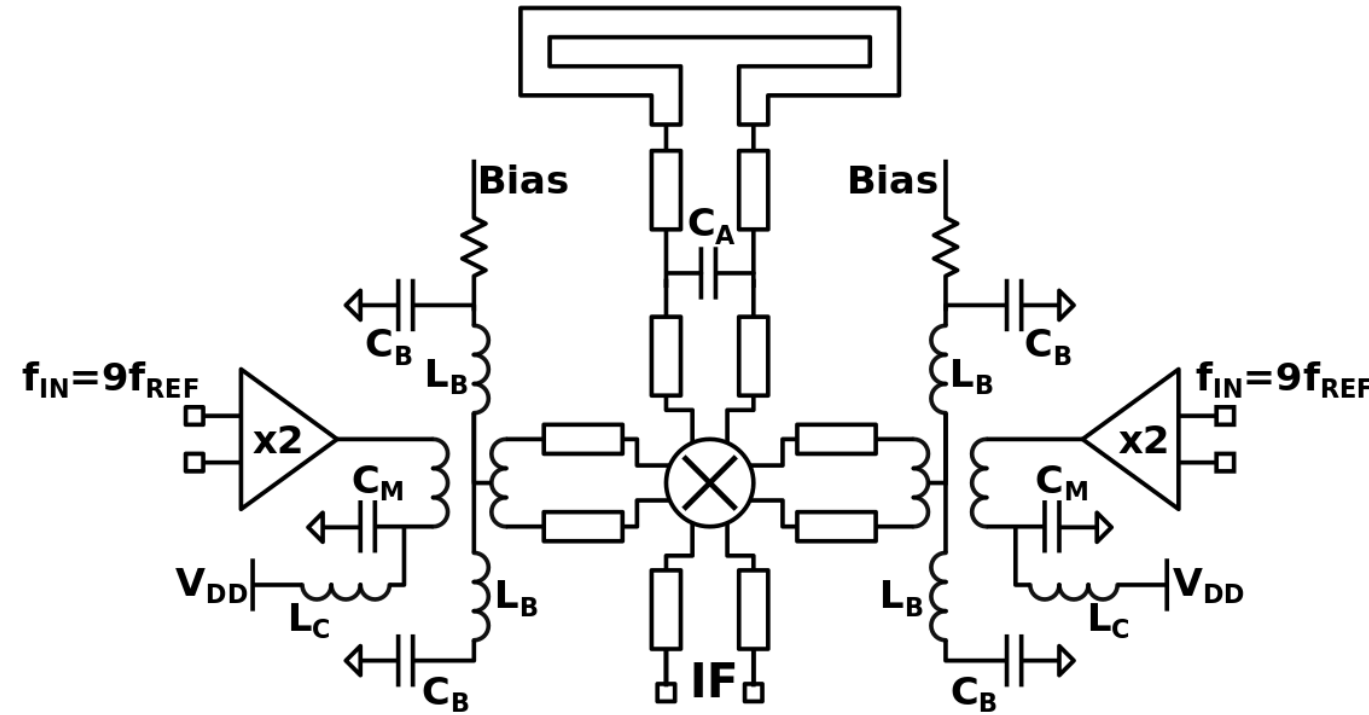
- Two-step down-conversion RX with LNA in between
- LO two-way power combining
- TX (-1,1) modulation to avoid RX 1/f noise

Full TX and RX Schematics



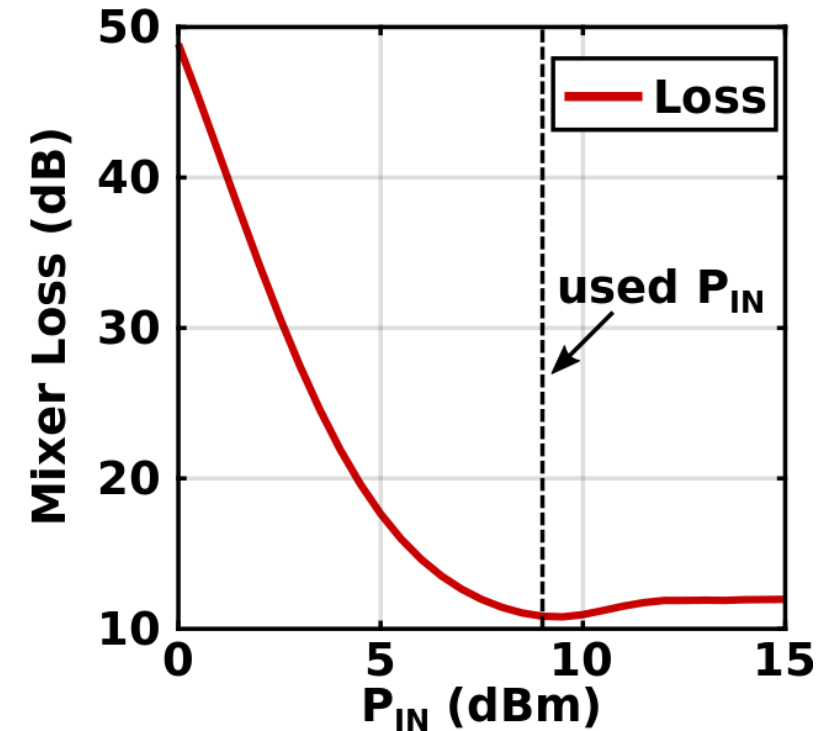
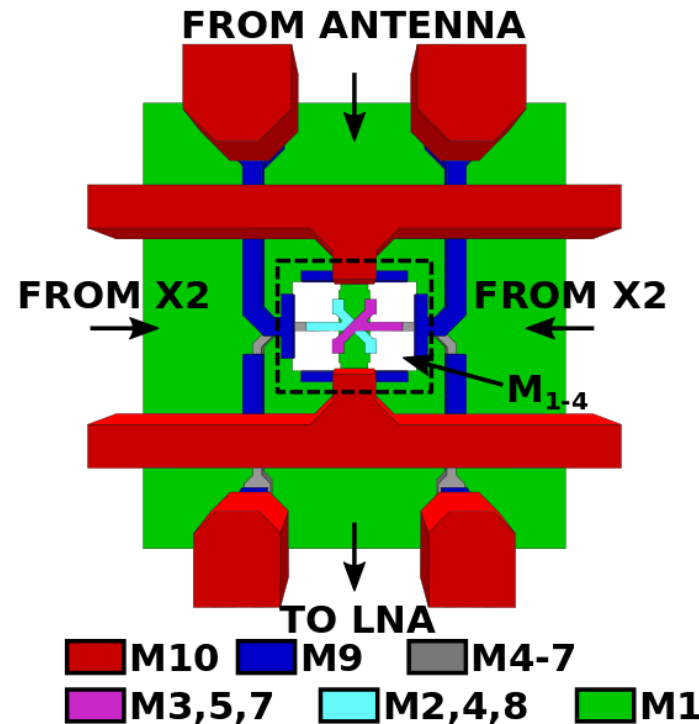
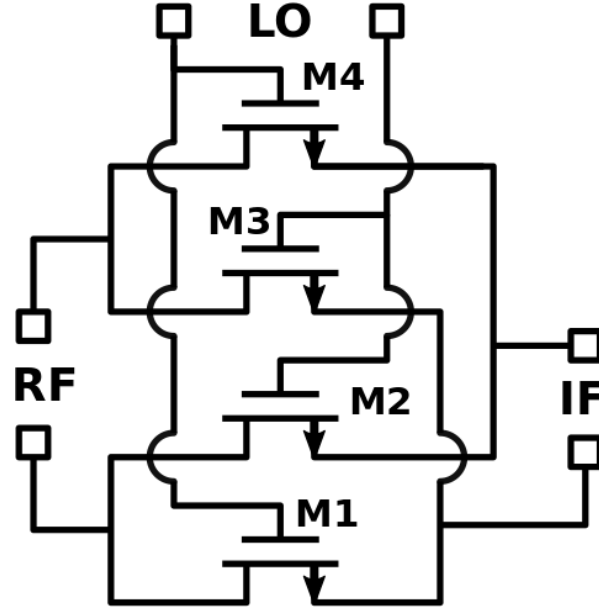
- Negligible parasitic radiation
 - Significant TX radiation at 420GHz and 140GHz
 - Significant RX radiation at 157.5GHz
 - Image and IF RX frequency equal to 210GHz and 105GHz

RX Design, Core



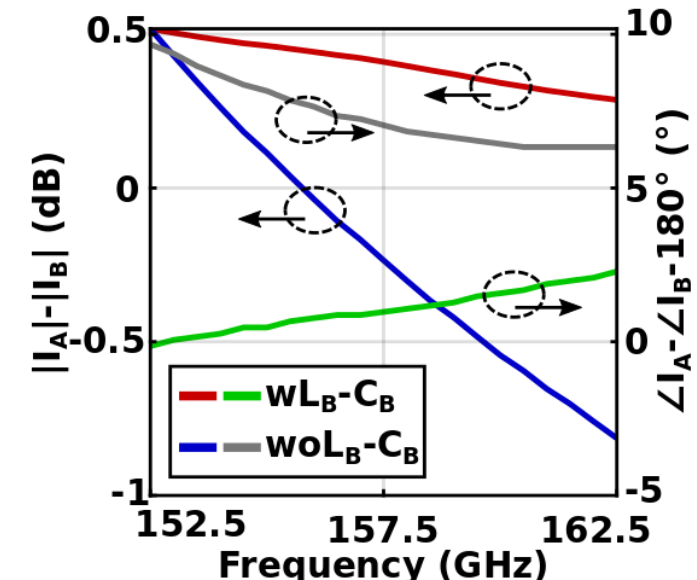
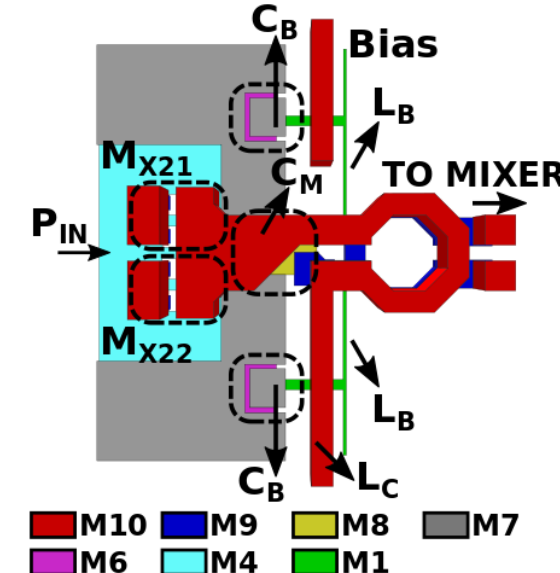
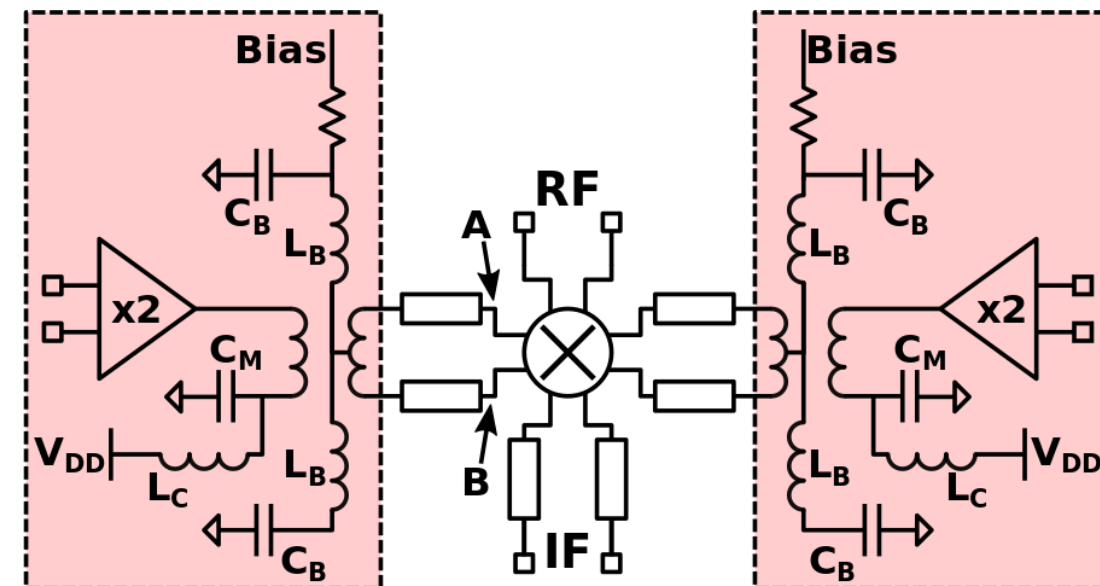
- Double-balanced mixer
- Two-way LO power combining
- Doubler based LO generation
- Folded dipole antenna

RX Design, Core - Mixer



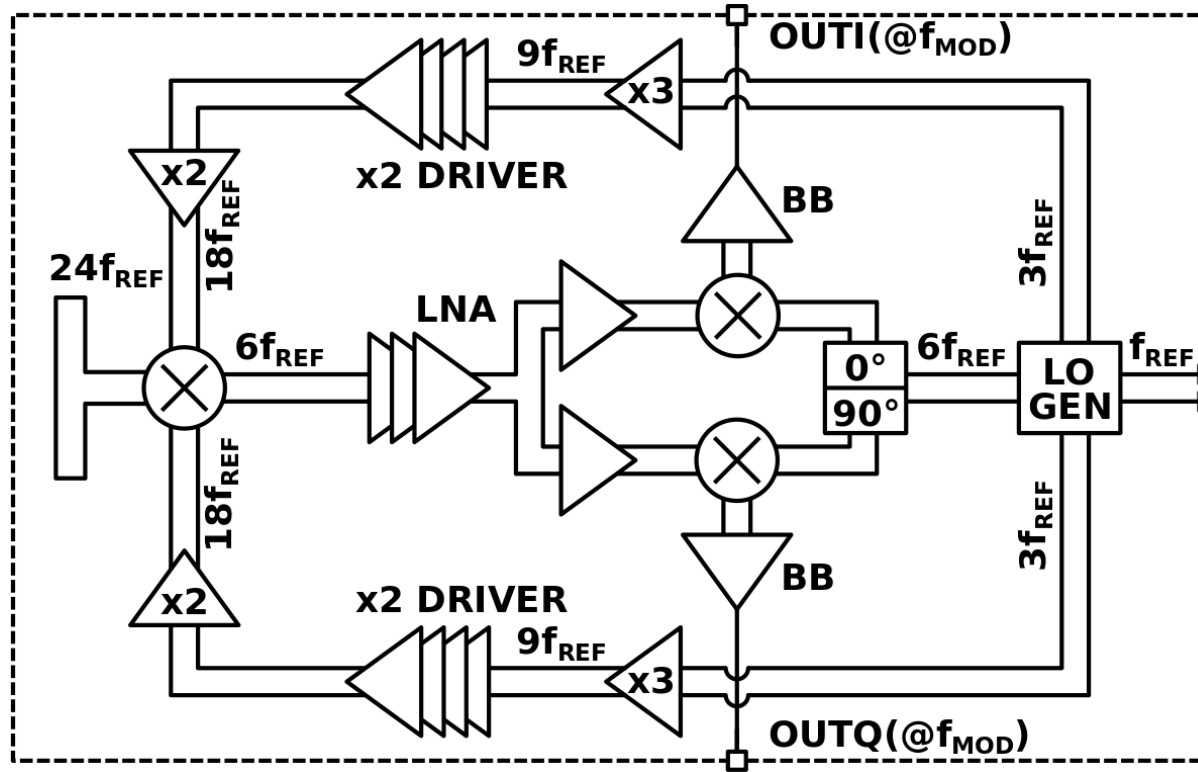
- LO combining paths from opposite sides
- Insertion loss of 10.8dB

RX Design, Core - Doubler



- Transformer based balun
- Balancing LC AC-short

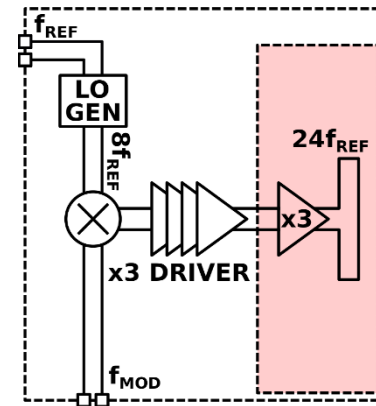
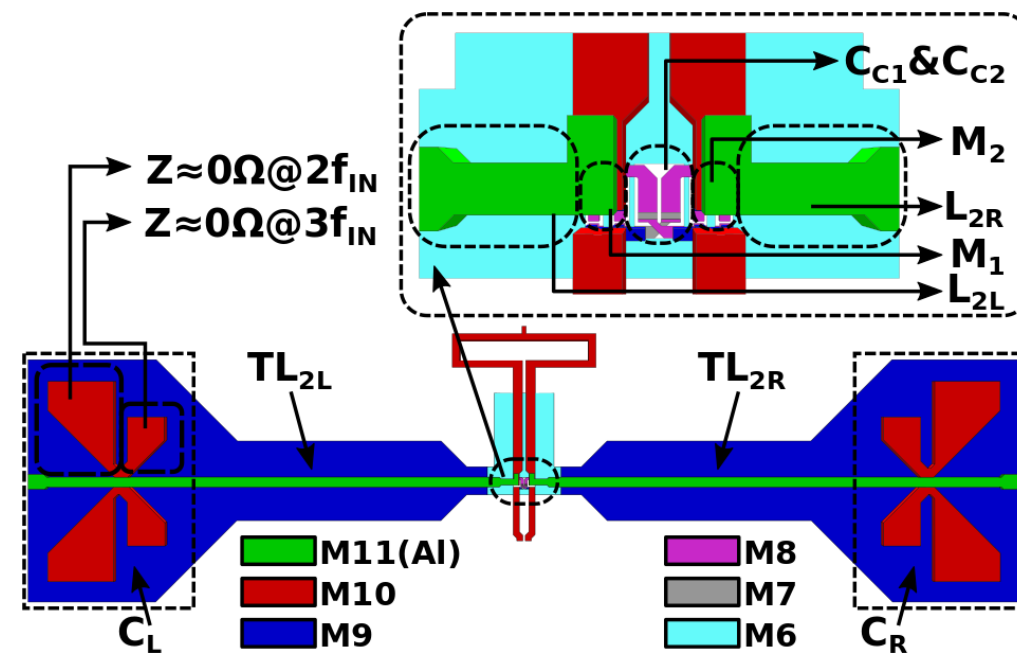
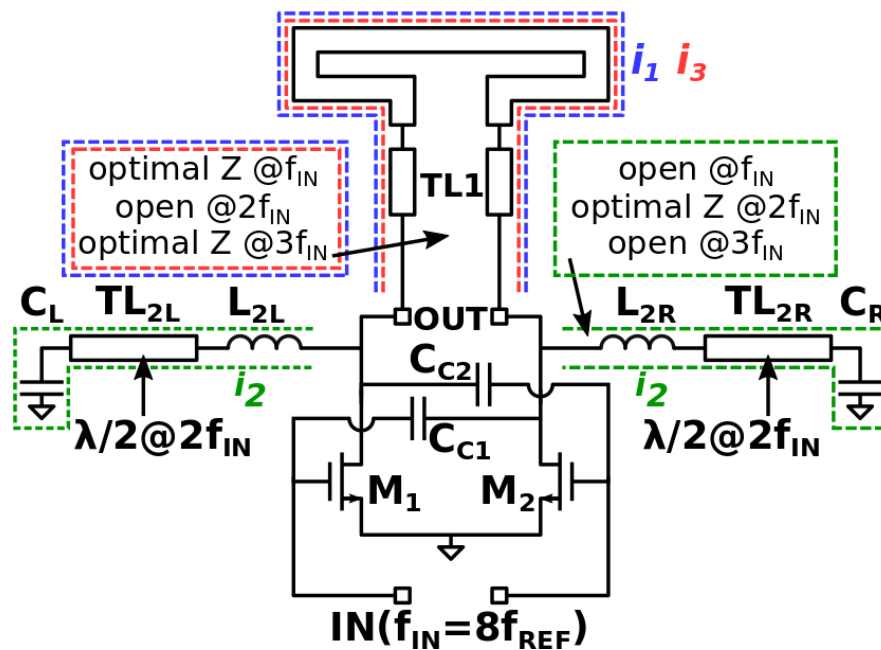
RX, Total Simulated Performance



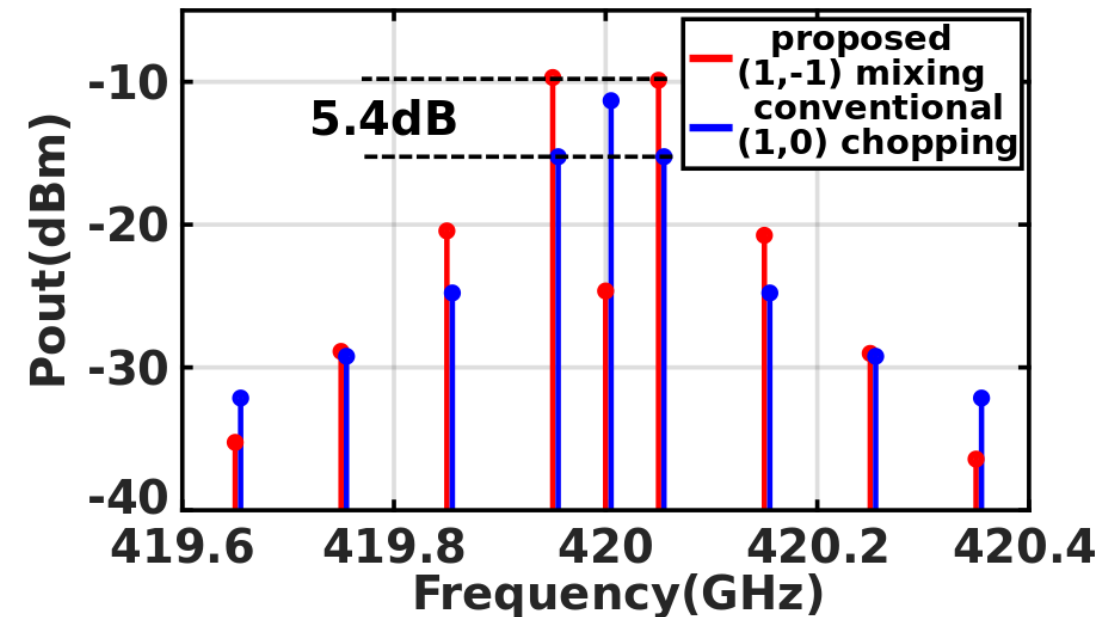
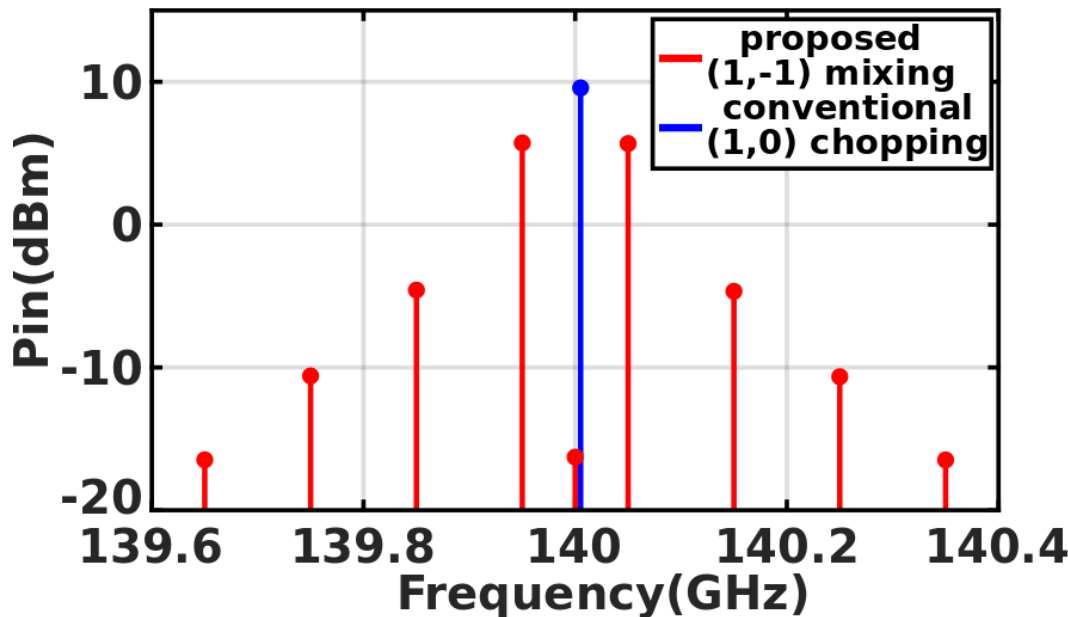
- Simulated LO driver output power (@157.5GHz) equal to 9dBm
- Simulated LNA plus 2nd mixer NF equal to 10.1dB
- Total simulated RX NF equal to 24dB

TX Design, Core

- X3 with optimized 1st, 2nd, 3rd harmonic load impedances
- Simulated radiated power of -8.9dBm



TX Design, Spectrum

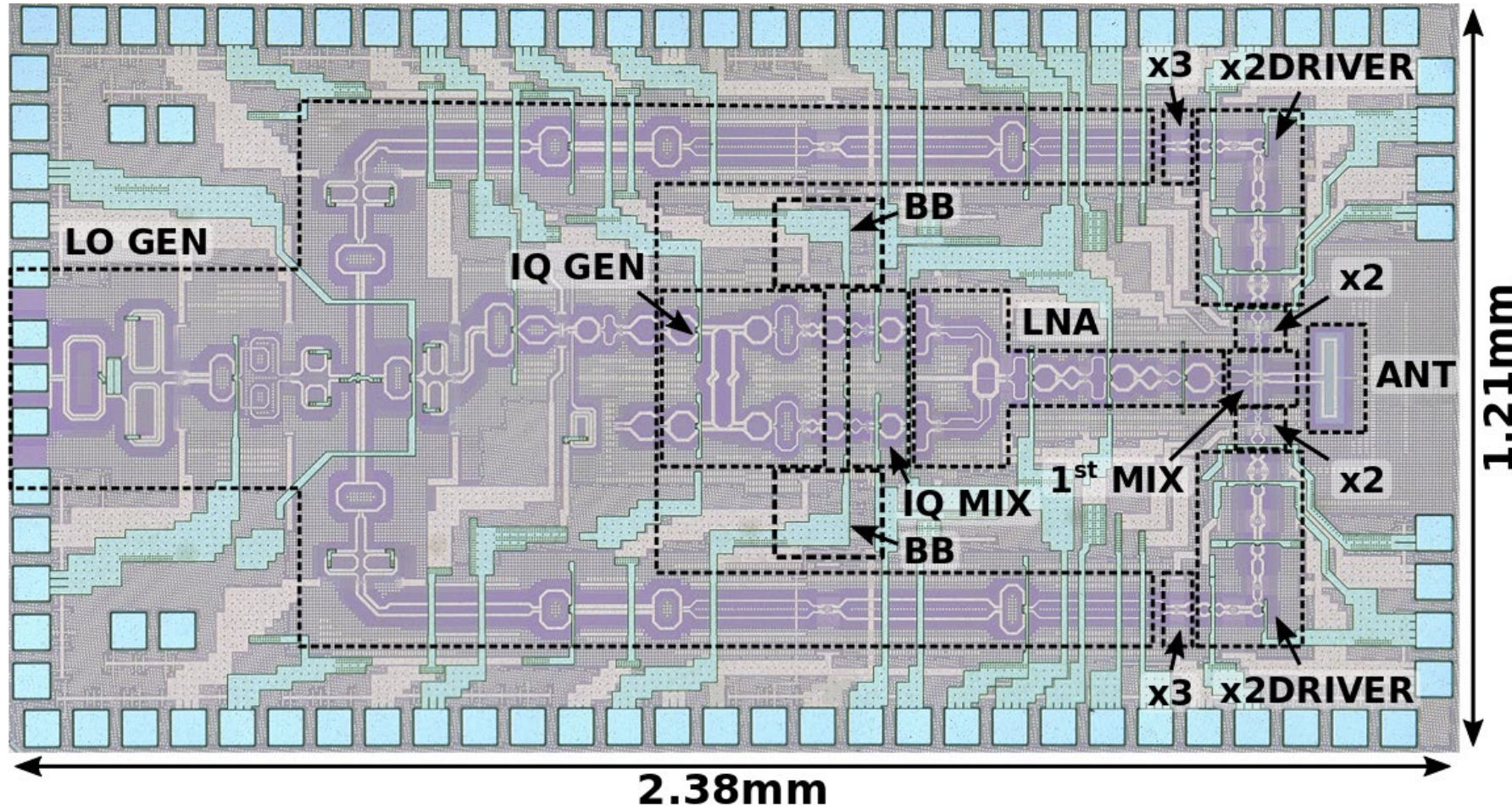


- (-1,1) TX modulation
- 5.4dBm more power in $24f_{REF} \pm f_{MOD}$ harmonics compared to (1,0) case

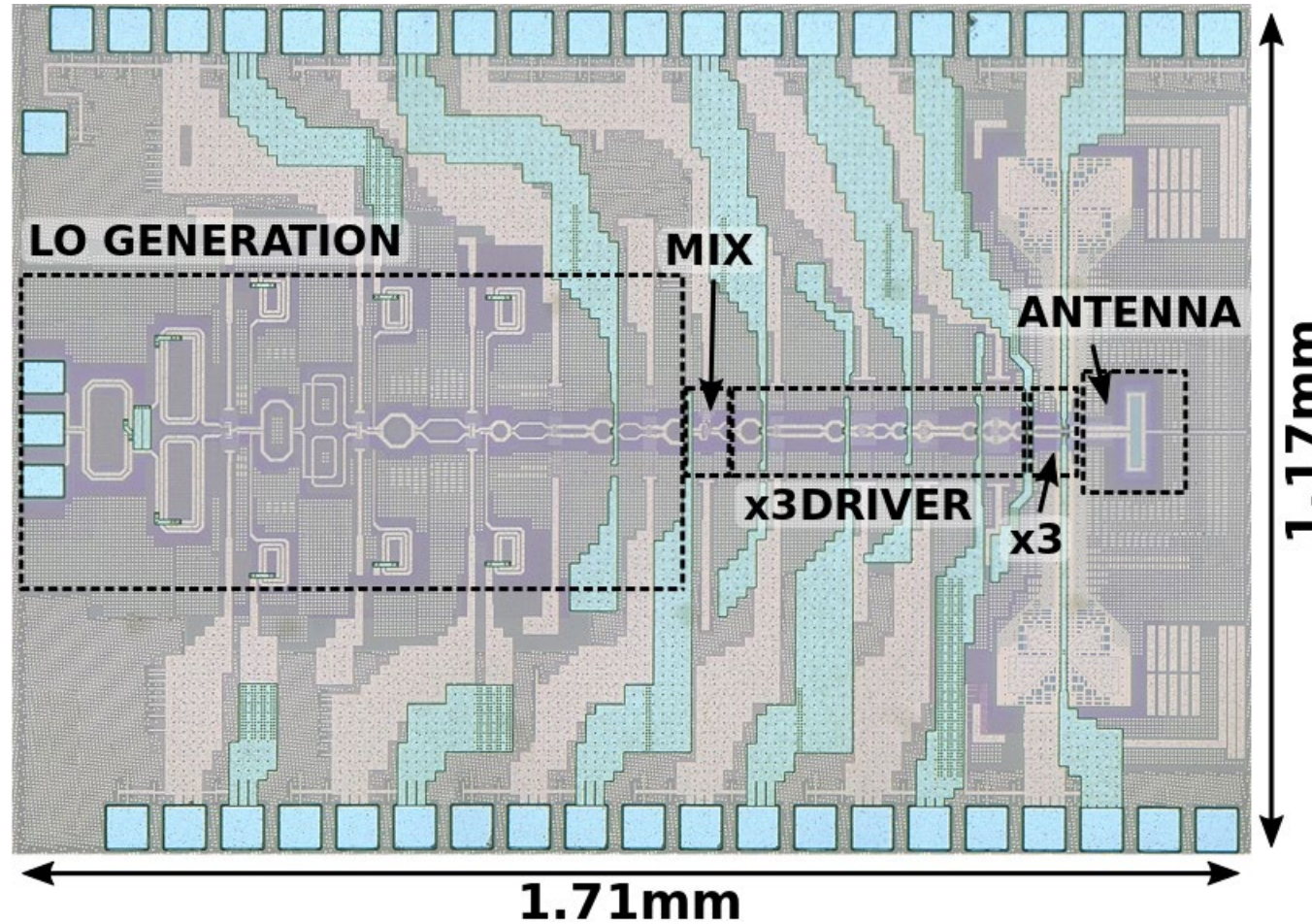
Outline

- Motivation
- Proposed TX-RX System Architecture
- Measurement Results
- Imaging Demonstrations
- Conclusion

RX Die Photograph



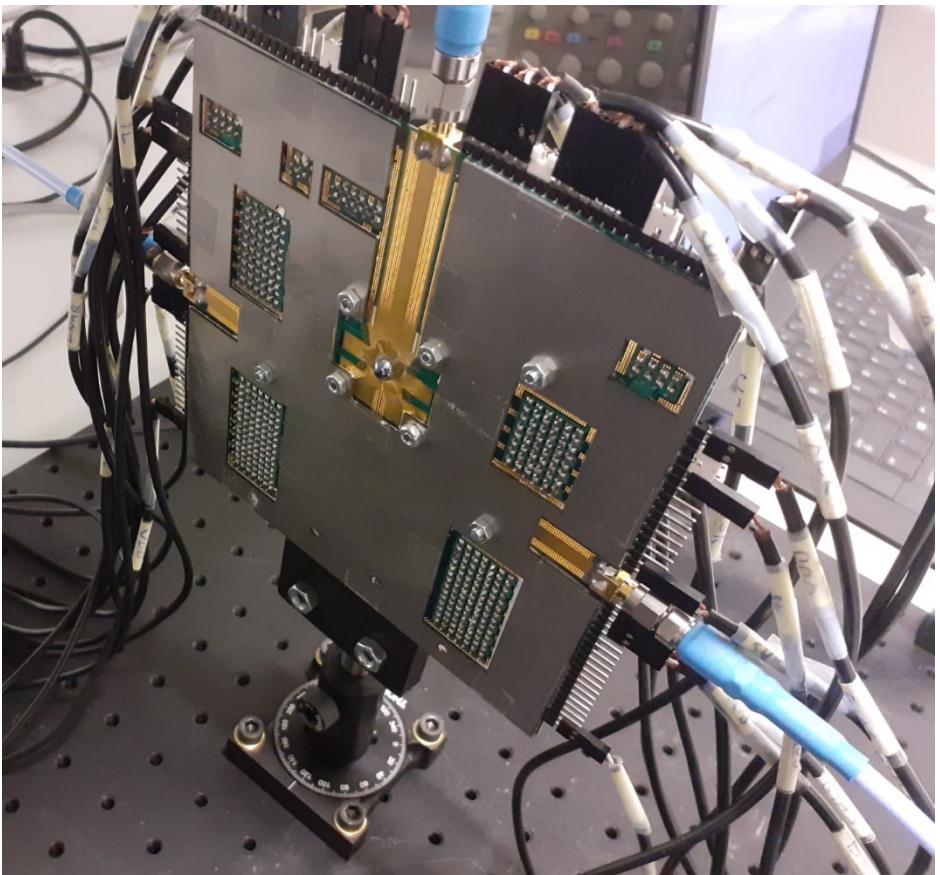
TX Die Photograph



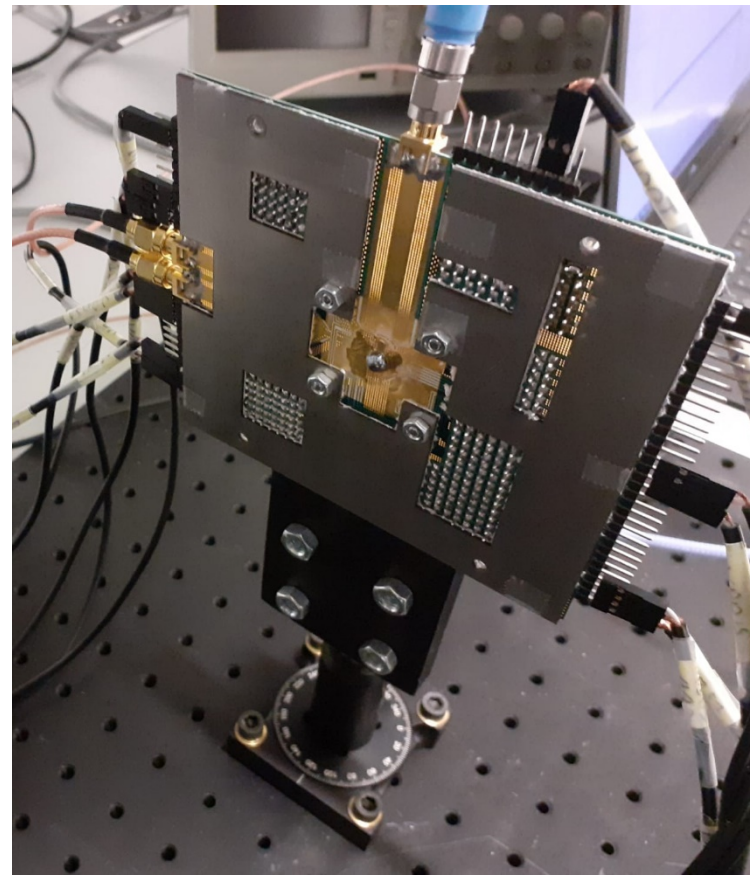
- 40nm CMOS
- 2mm²

Chips Packaging

RX

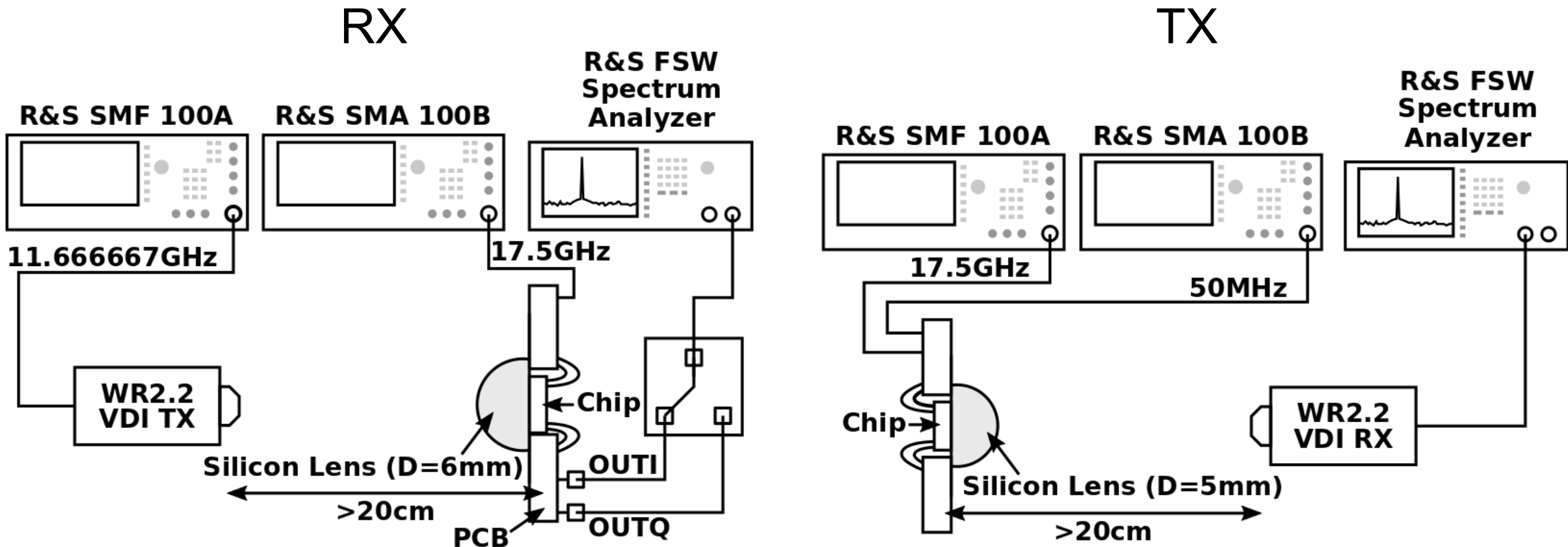


TX

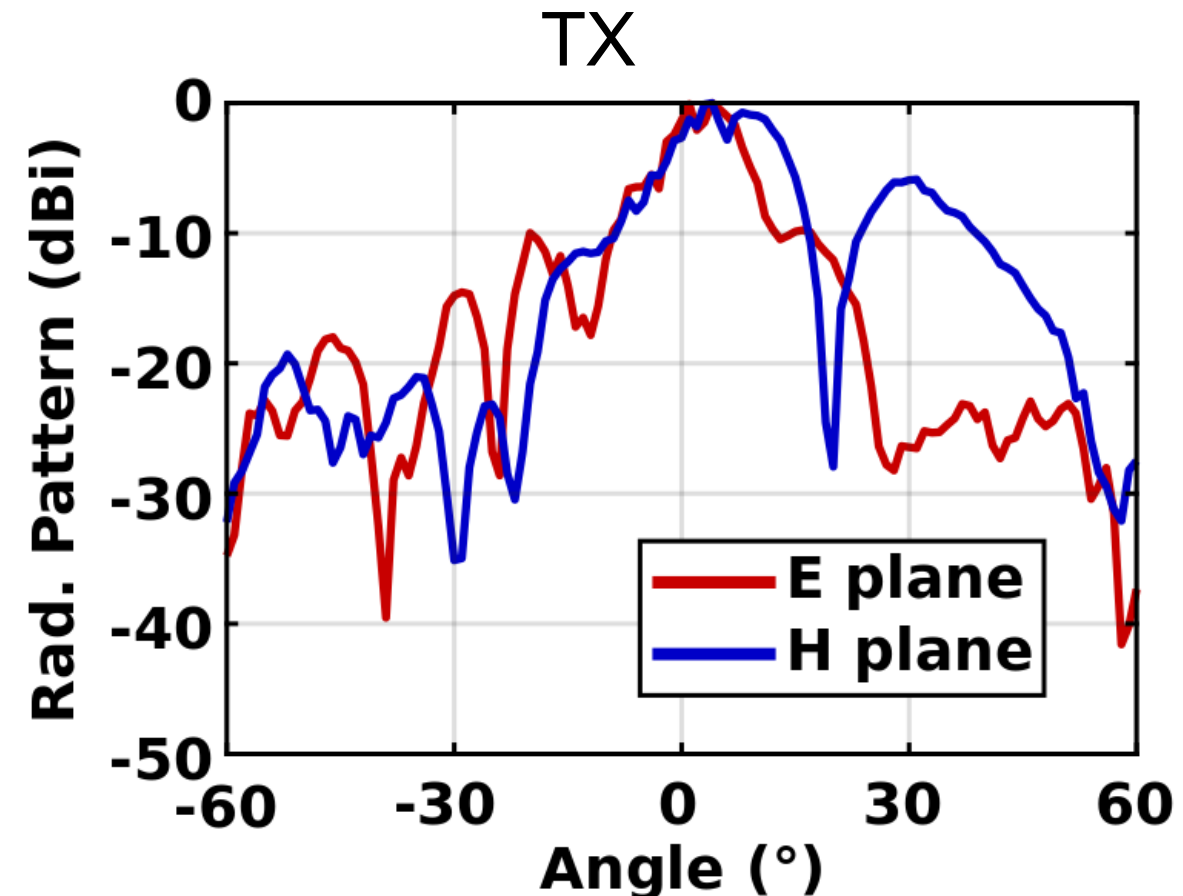
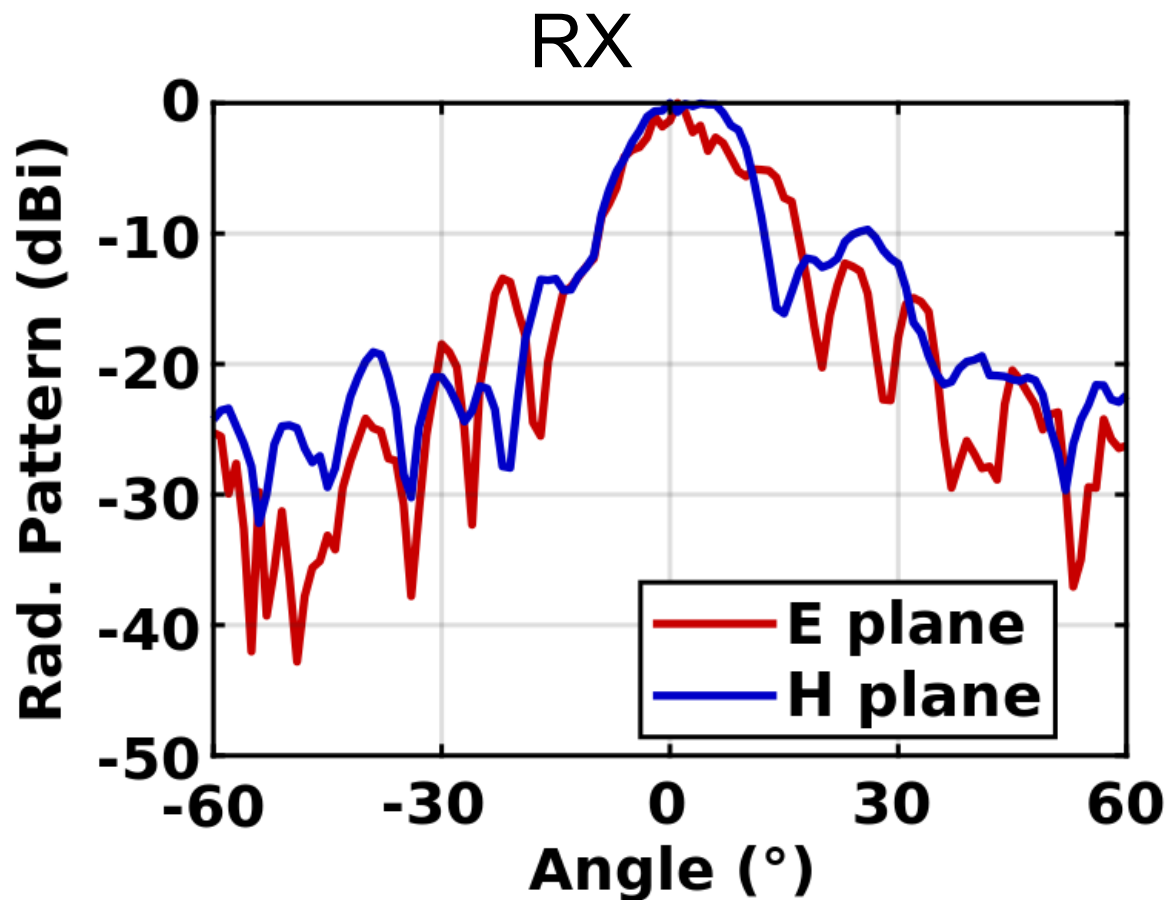


- Hemispherical Silicon lenses attached to the chips back sides
- $D_{RX}=6\text{mm}$, $D_{TX}=5\text{mm}$

Measurement Setup

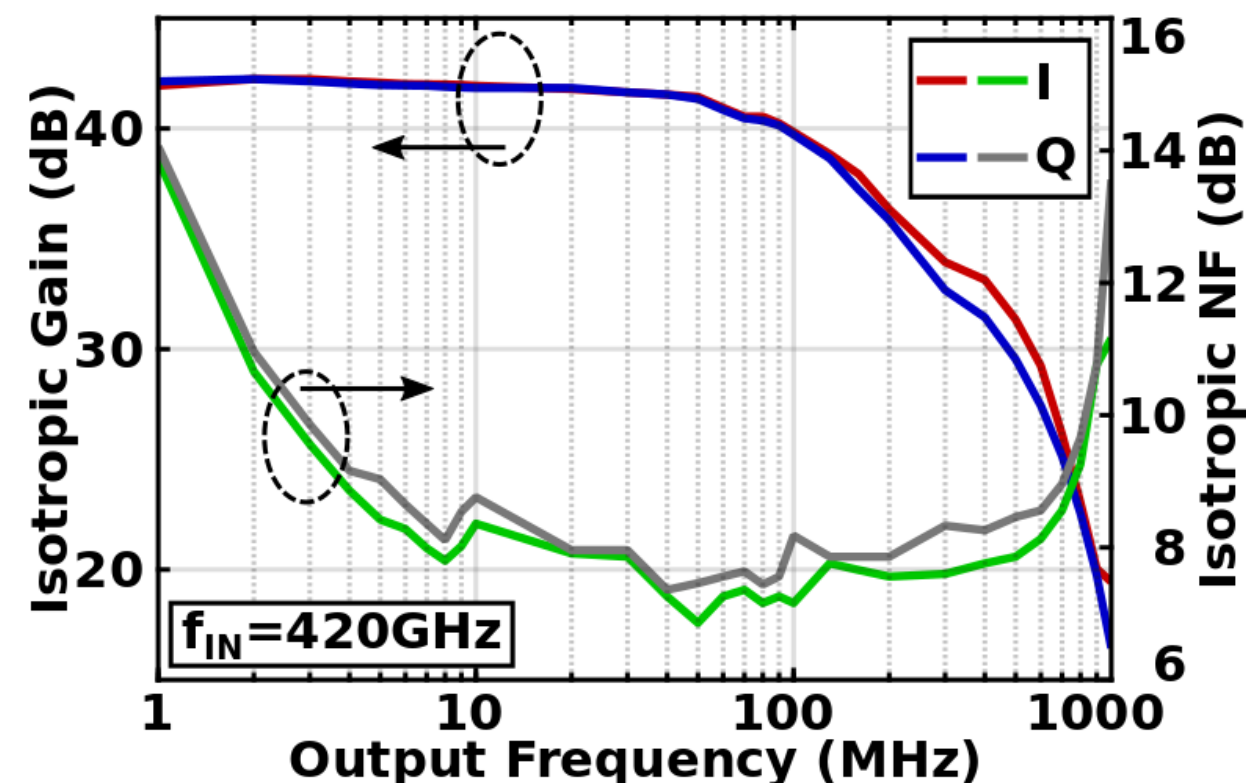
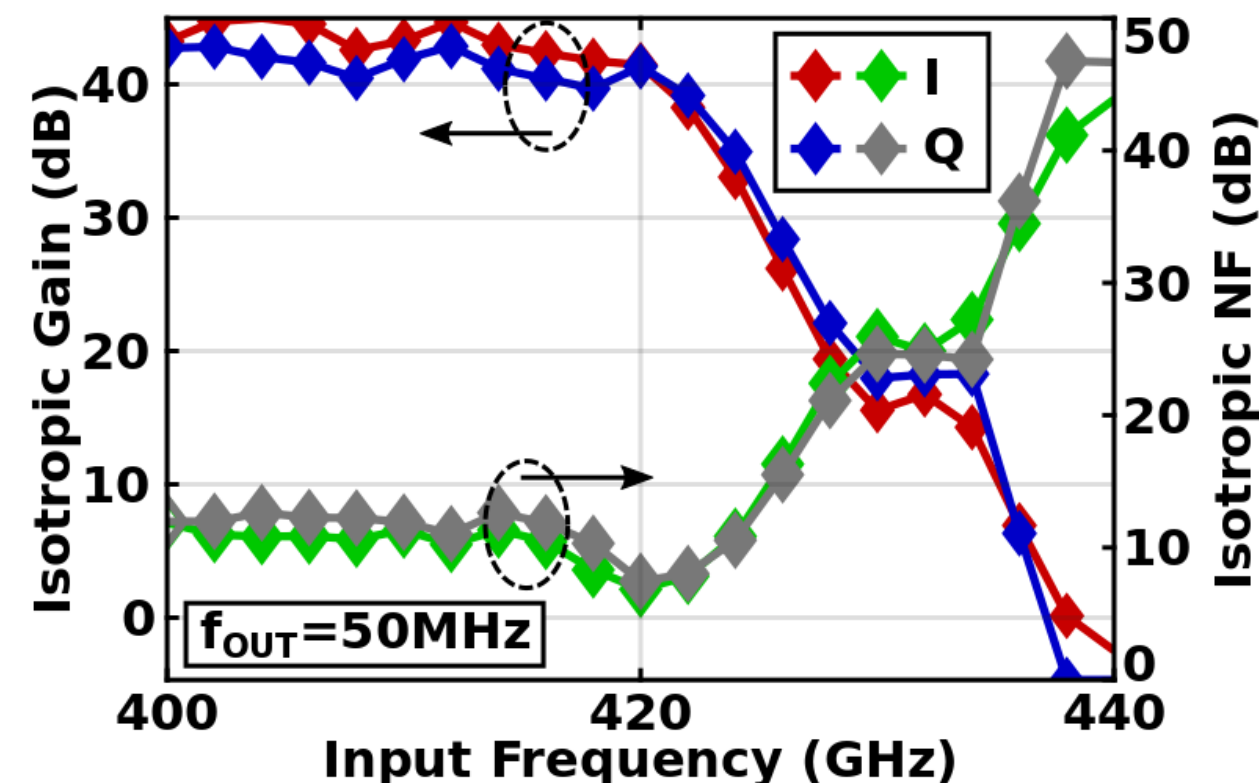


Antenna Performance



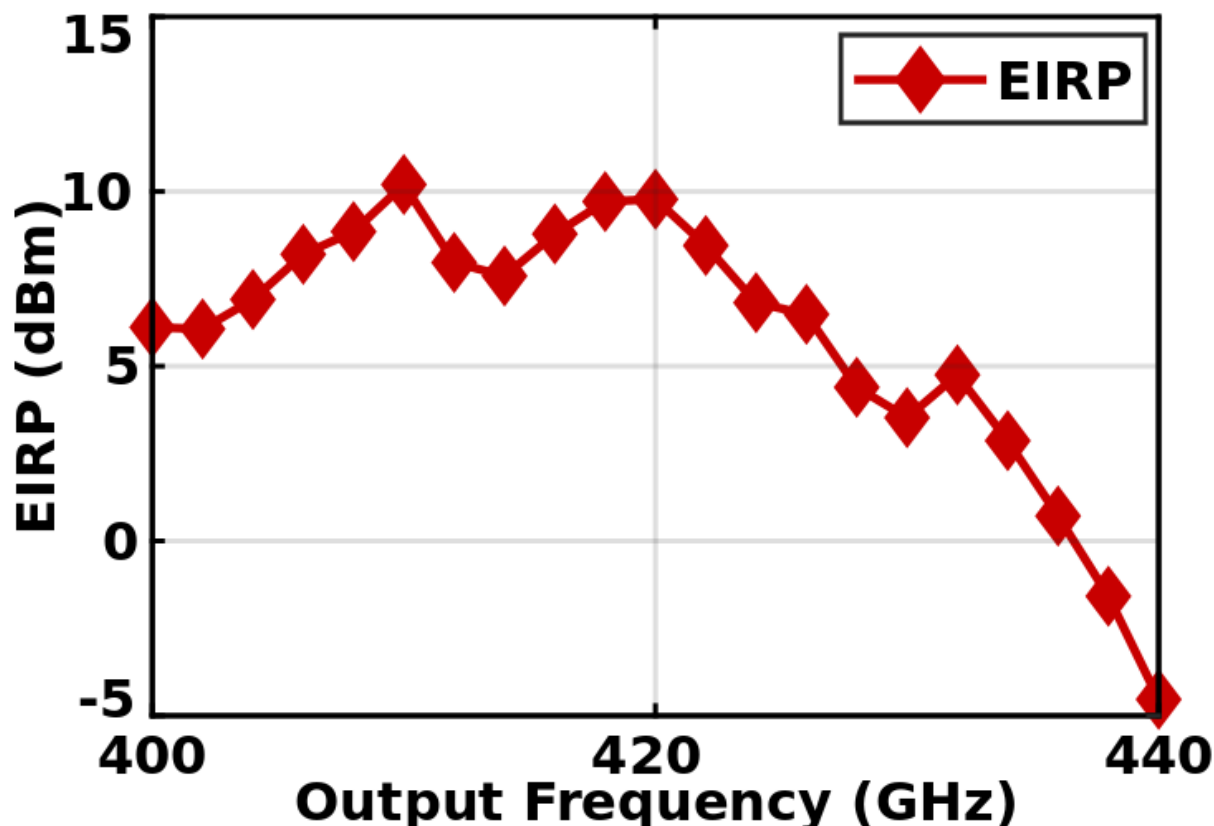
- $\text{DIR}_{\text{RX}}=20.5\text{dBi}$, $\text{DIR}_{\text{TX}}=19\text{dBi}$

RX Performance

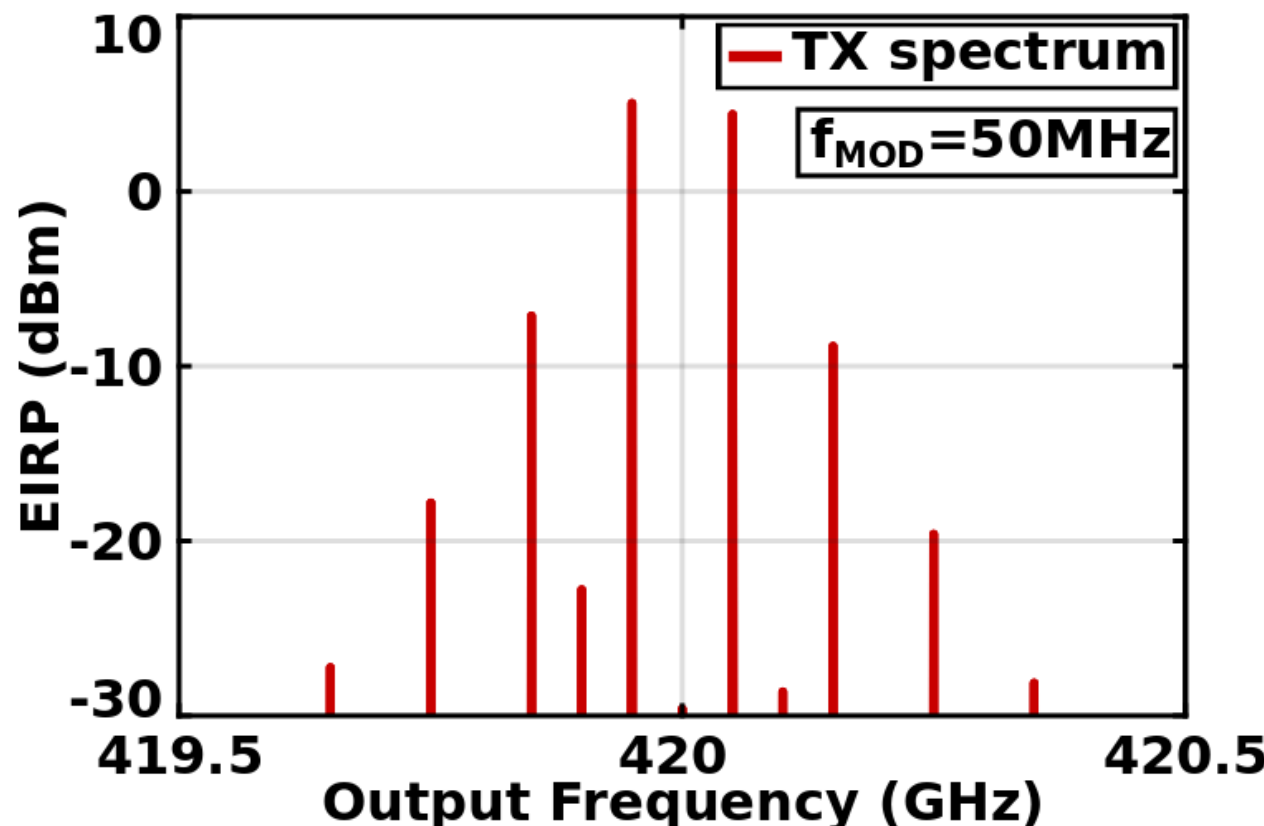


- Gain=21dB (@420GHz, 20.5dBi RX antenna directivity de-embedded)
- NF=27dB (@420GHz, 20.5dBi RX antenna directivity de-embedded)

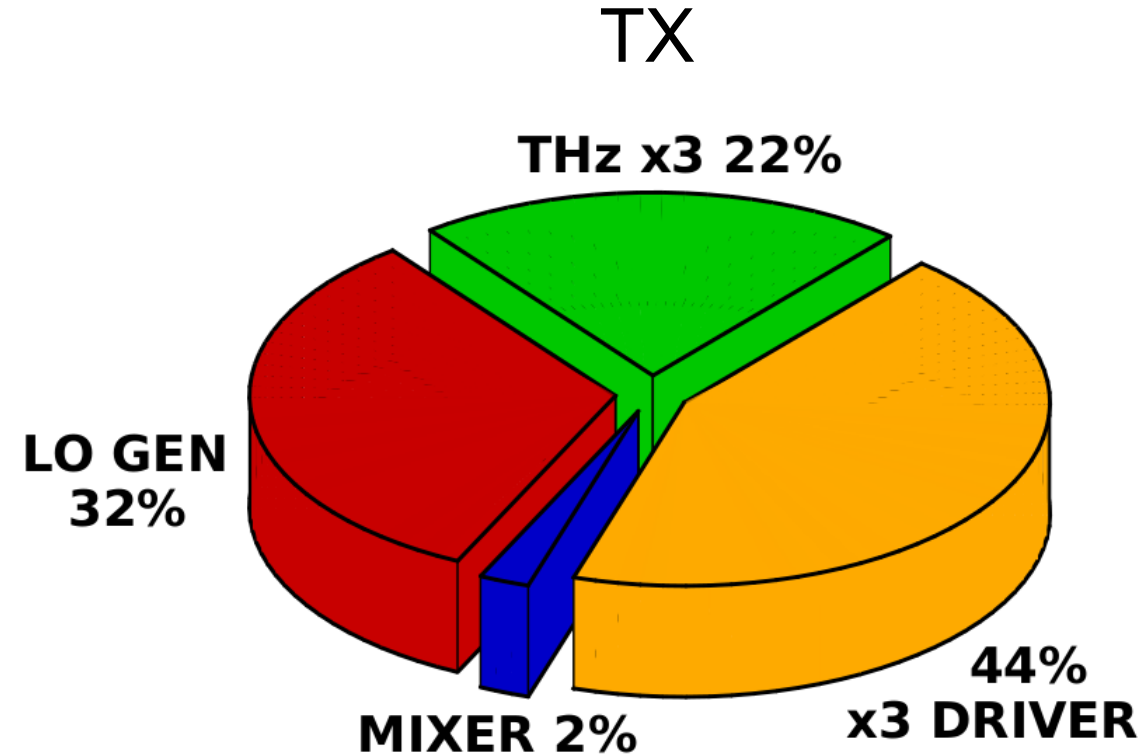
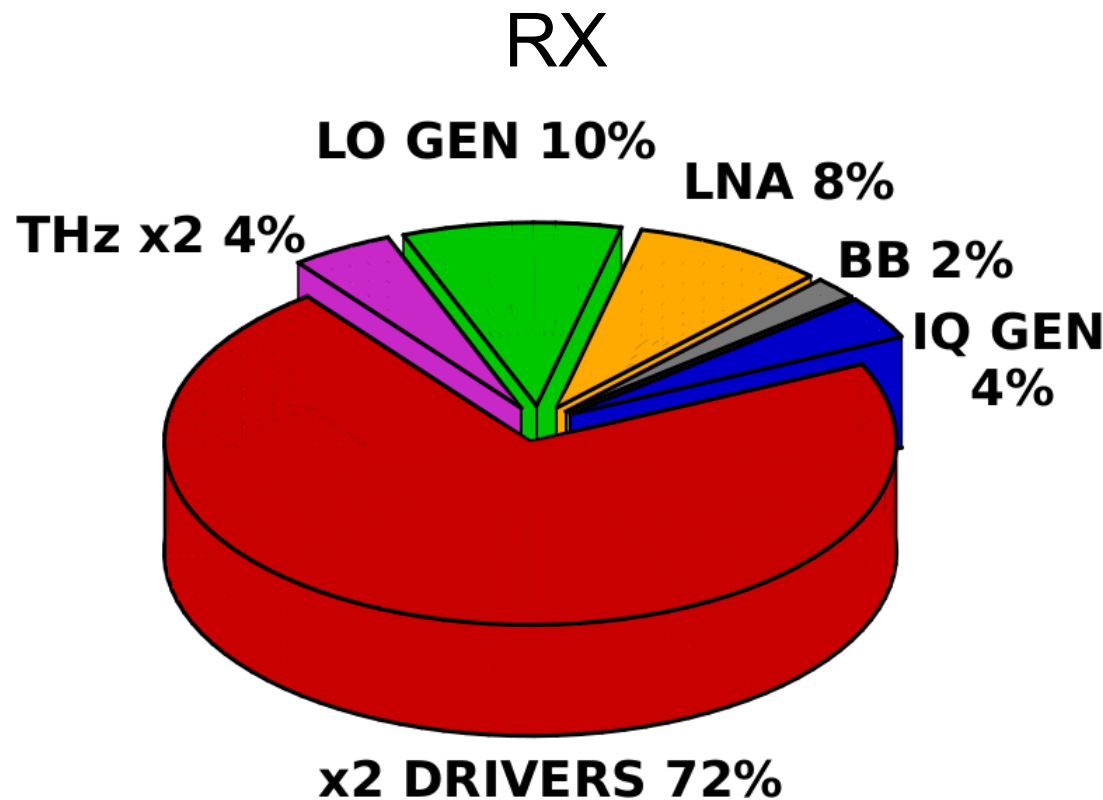
TX Performance



- EIRP=10dBm (@420GHz)
- $P_{RAD}=-9\text{dBm}$ (@420GHz)



DC Power Consumption



- $PDC_{RX} = 601\text{mW}$
- $PDC_{TX} = 304\text{mW}$

RX Comparison Table

	This work	VLSI18	ISSCC20	ISSCC17
Technology	40nm CMOS	65nm CMOS	65nm CMOS	45nm SOI CMOS
Mixing Topology	2 step Fund.	1 step 4 th SHM	1 step 2 nd SHM	1 step 4 th SHM
IQ Mixing	Yes	No	No	No
Frequency (GHz)	420	550	490	115-325
Gain (dB)	21	-13*	Not reported	1**
NF (dB)	27	35*	42.7****	29-37
DC Power (mW)	601	Not reported	32***	36

*Referred to an isotropic antenna

**Peak gain (around 210GHz)

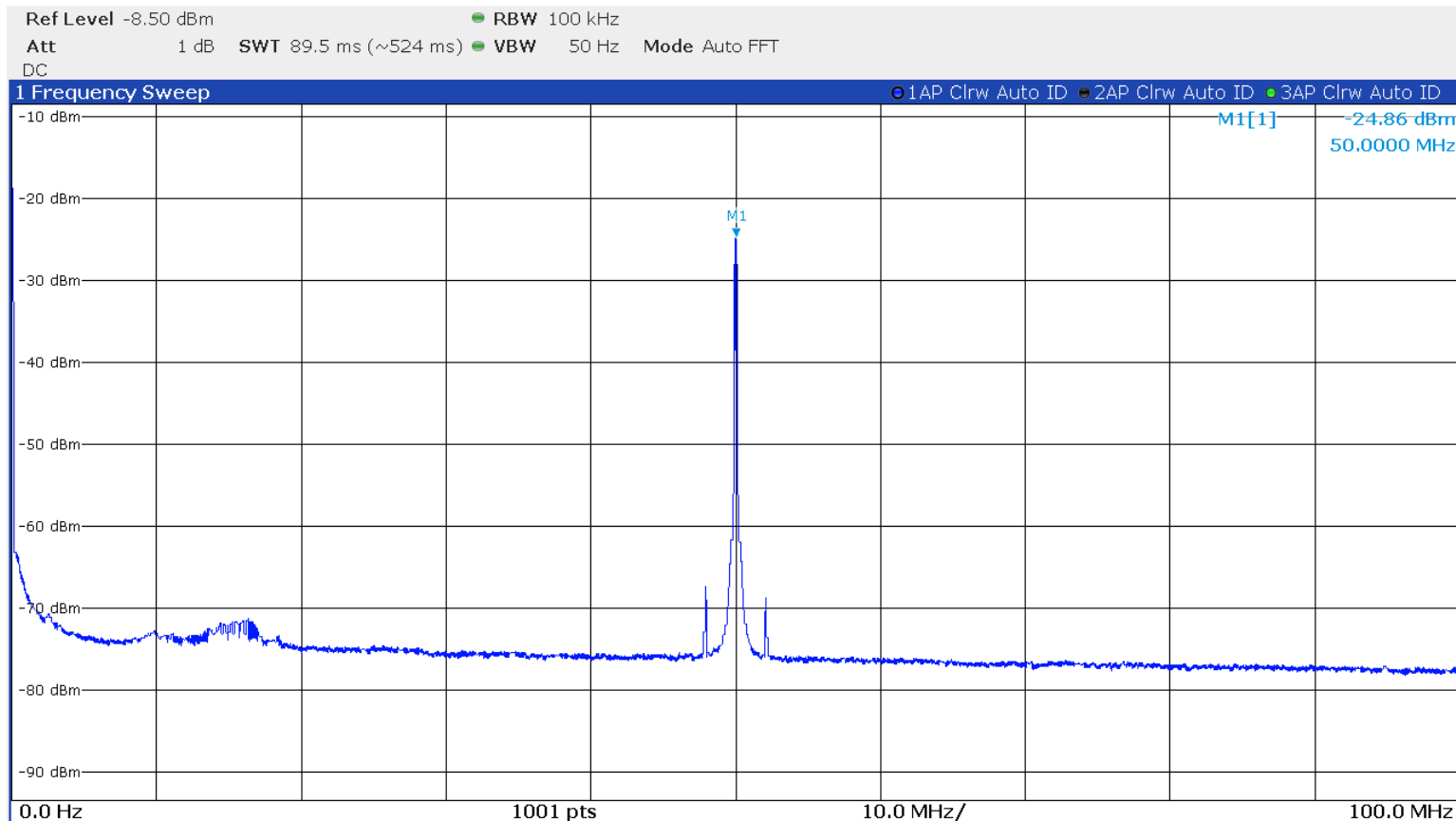
***Including FLL

****Calculated using MDS given in the paper

TX Comparison Table

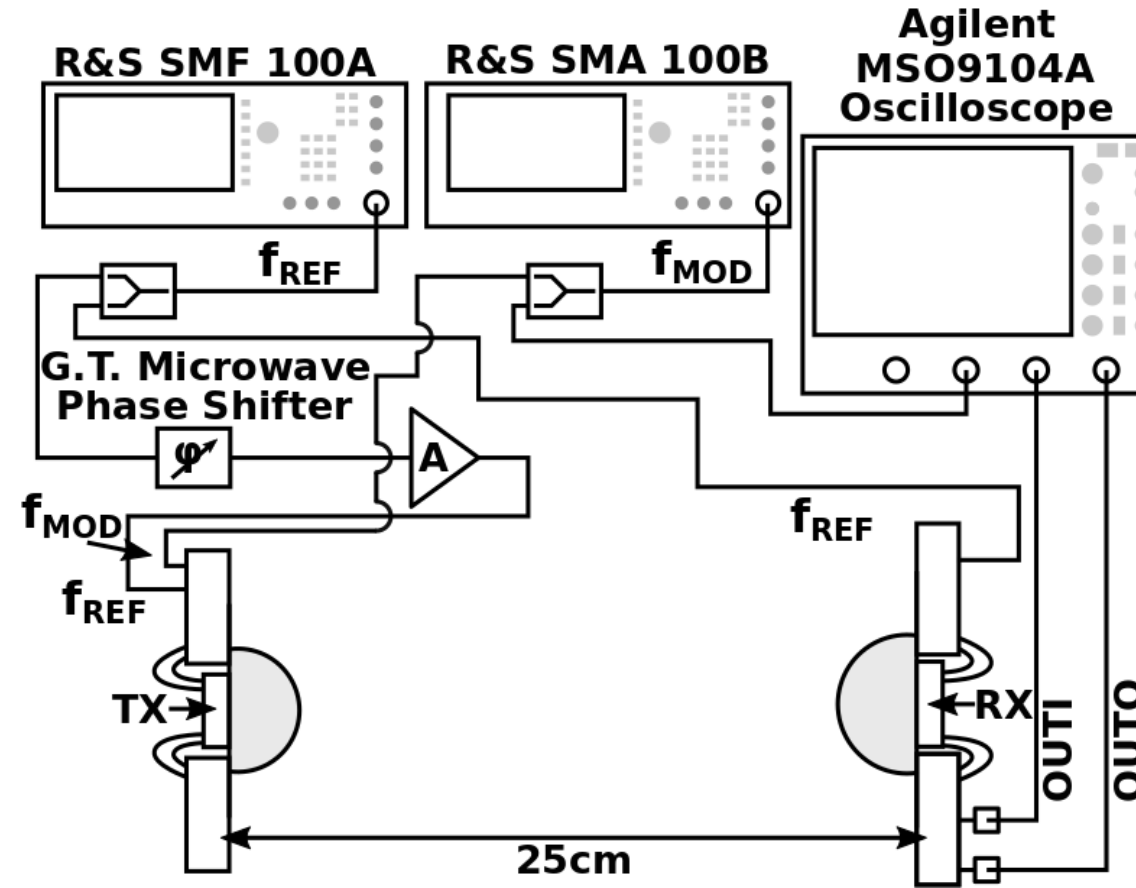
	This work	JSSC19	TM TT16	TM TT13
Technology	40nm CMOS	40nm CMOS	45nm SOI CMOS	45nm SOI CMOS
Source Topology	Mult. Chain	IL-Osc. Chain	Mult. Chain	Mult. Chain
No. of Rad. Elements	1	4	8	8
Frequency (GHz)	420	531.5	390	420
EIRP (dBm)	10	2.3	8	3
P_{RAD} (dBm)	-9	-12	-7	-10
DC Power (mW)	304	260	1500	700

TX-RX Performance



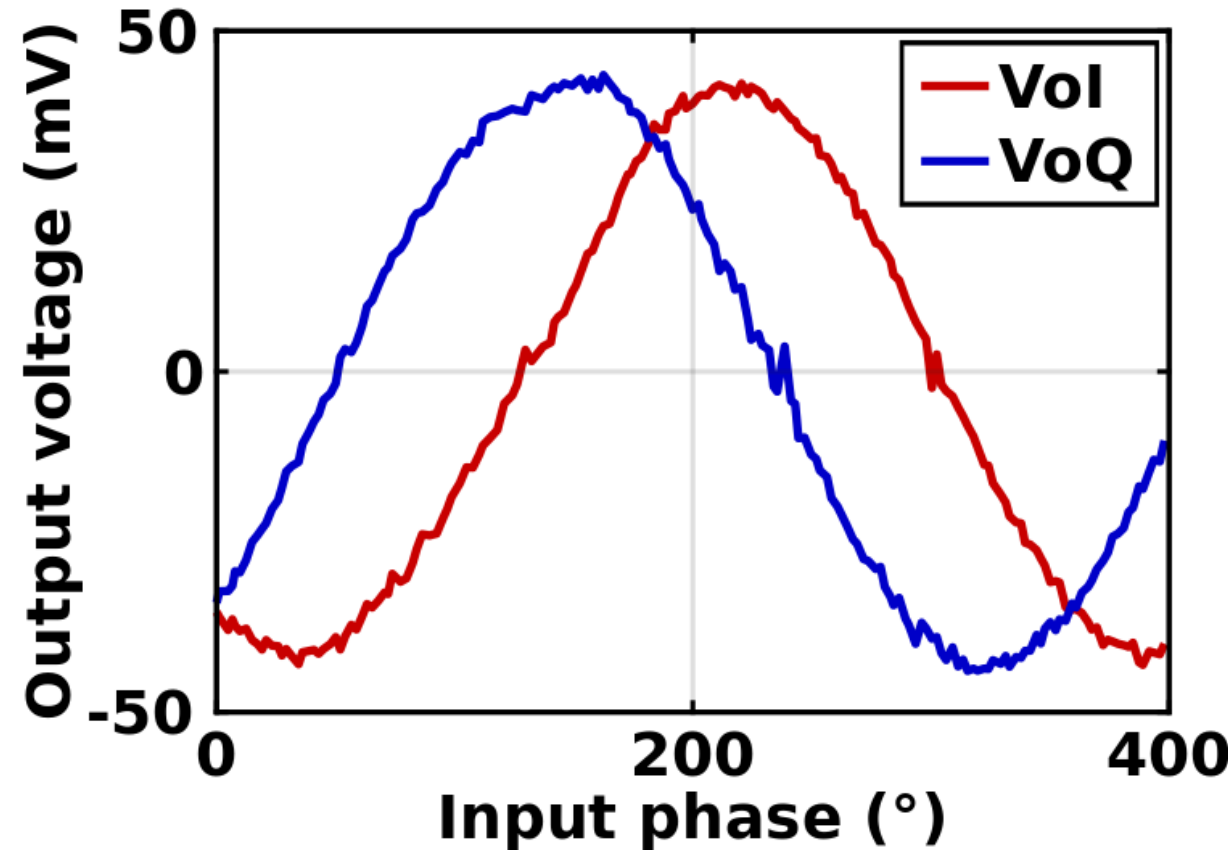
- Non-modulated TX, TX-RX frequency offset $\approx 50\text{MHz}$
- SNR=52dB (25cm, 100kHz RBW)

Phase Reconstruction Setup

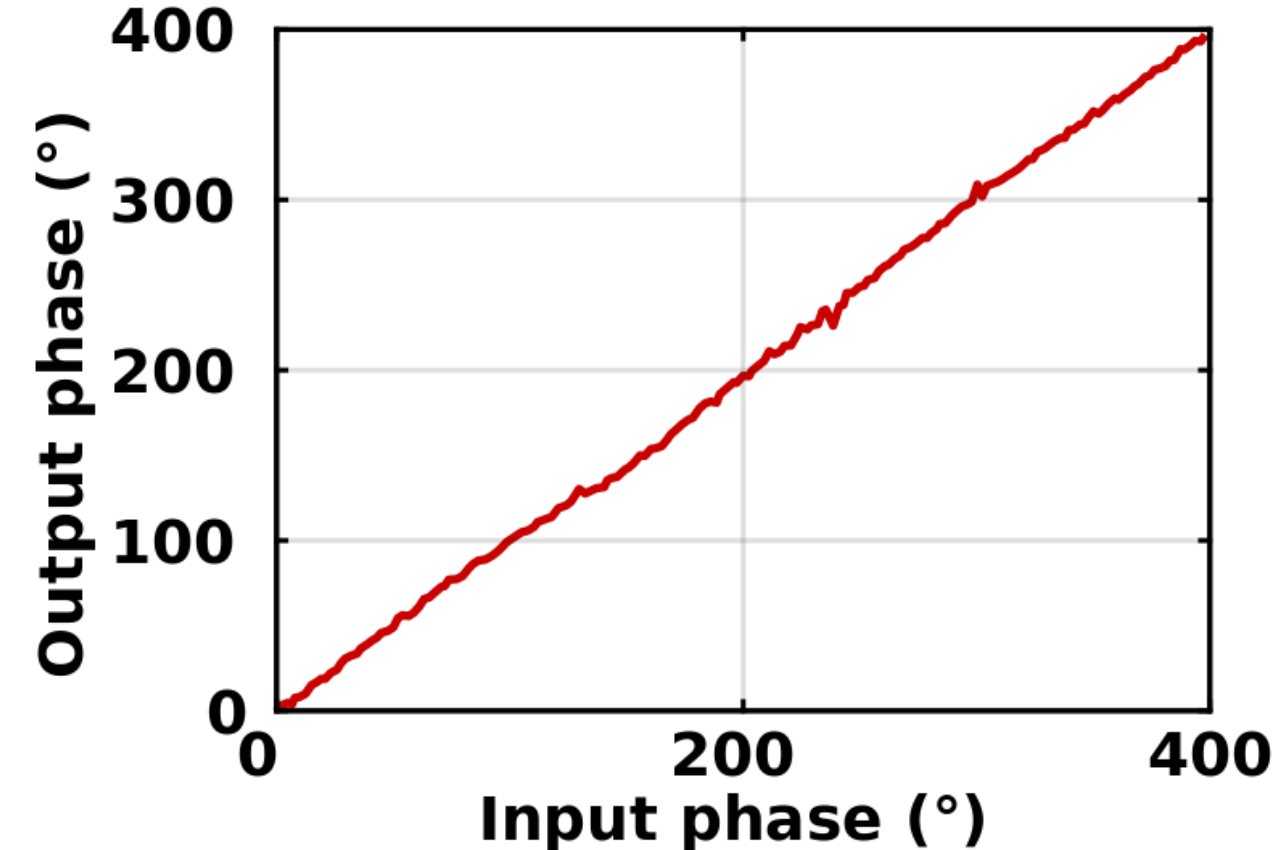


- Sharing 17.5GHz reference
- Inserting phase shift in the TX path (0.1° step @ 17.5GHz)

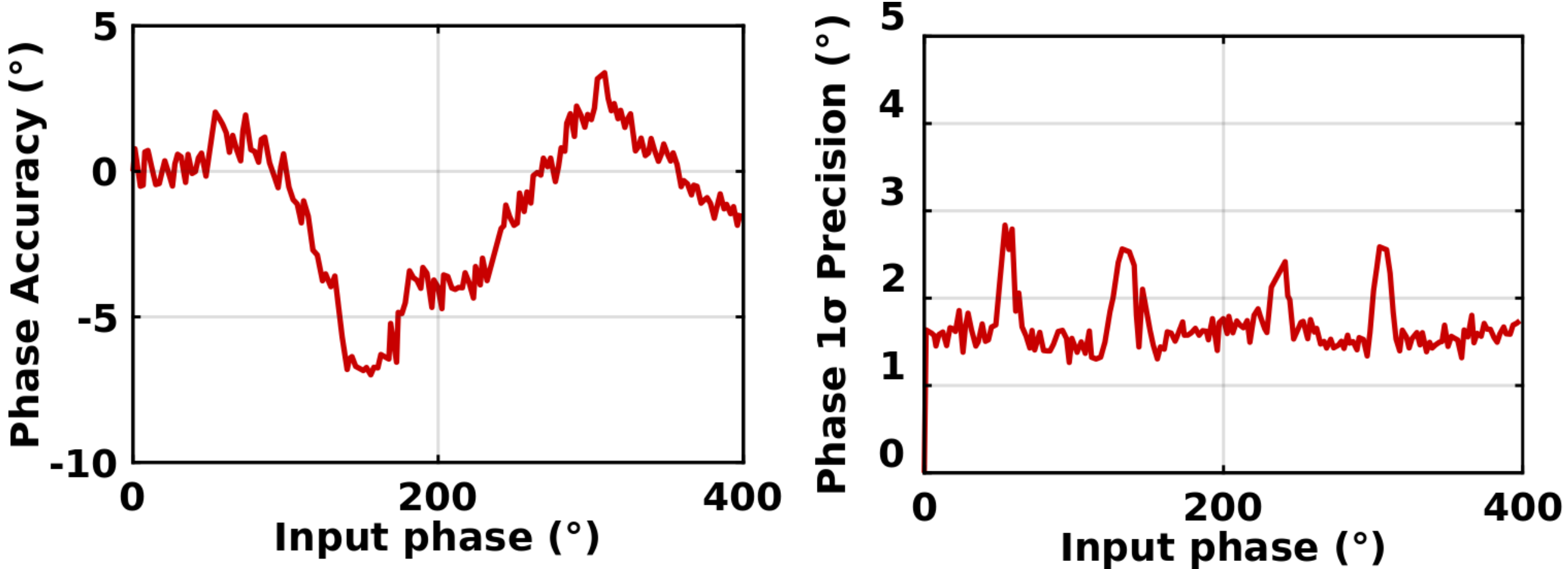
RX Output and Reconstructed Phase



- Range of 400° (@420GHz)
- $f_{MOD}=10\text{MHz}$, 500ns/point



Phase Detection Quality

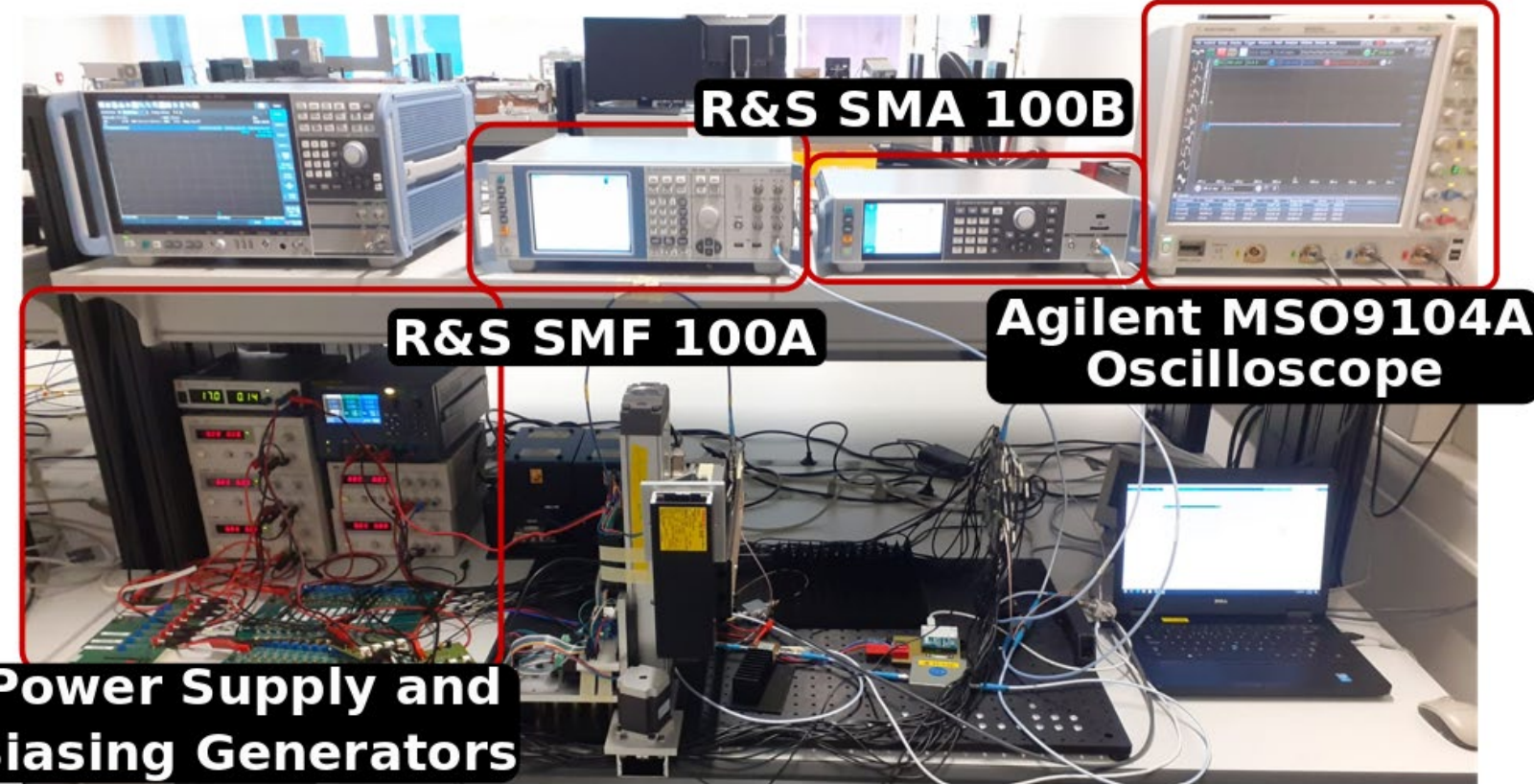


- RMS Accuracy of 2.8° (400° range, 100 measurements)
- RMS 1σ Precision of 1.7° (400° range, 100 measurements)

Outline

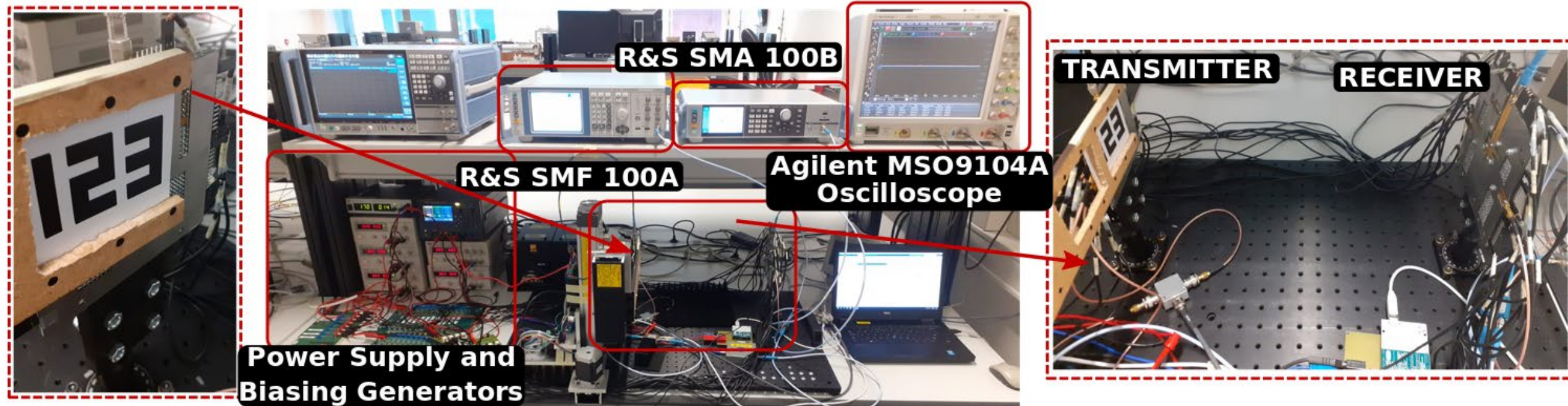
- Motivation
- Proposed TX-RX System Architecture
- Measurement Results
- Imaging Demonstrations
- Conclusion

Imaging Setup



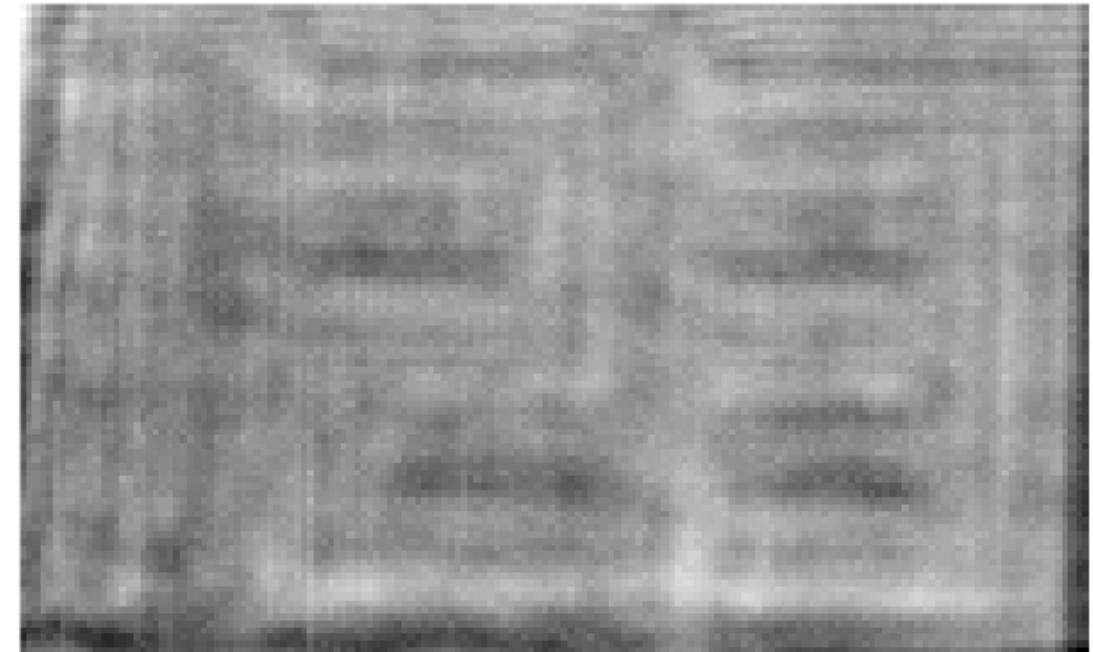
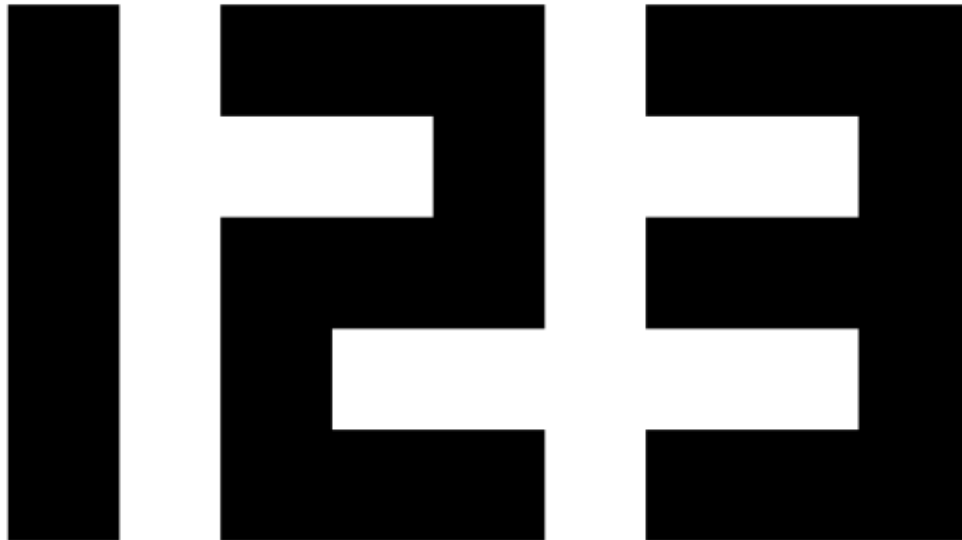
- Stepper motors for moving of the imaged object in 2 axes
- Capturing the reconstructed phase in every point

Printed Text Reconstruction



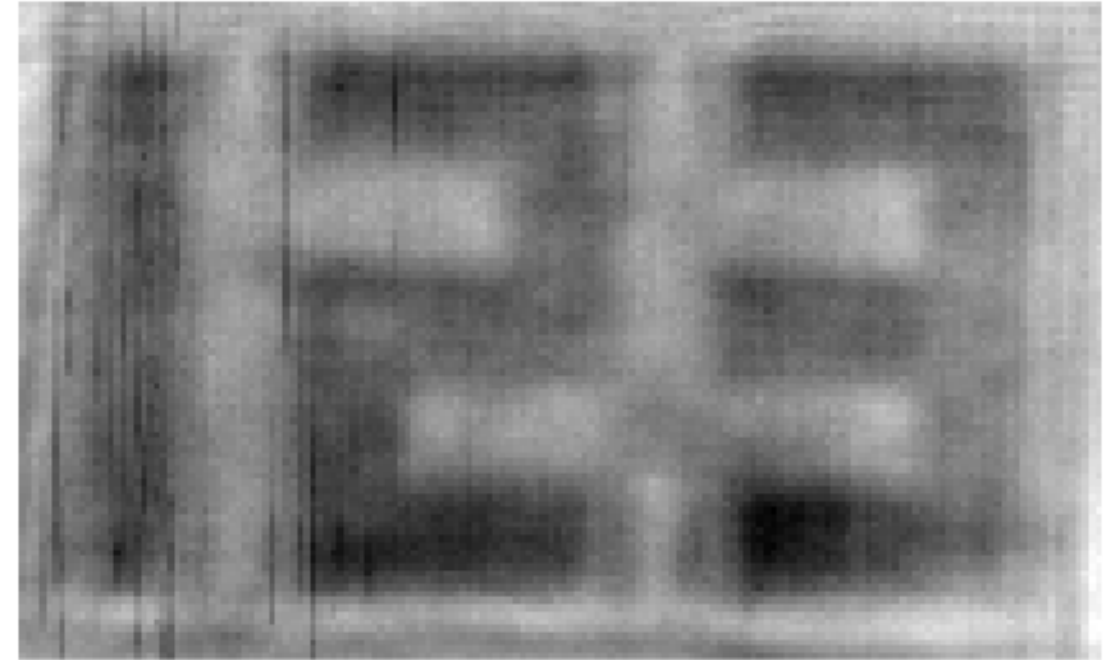
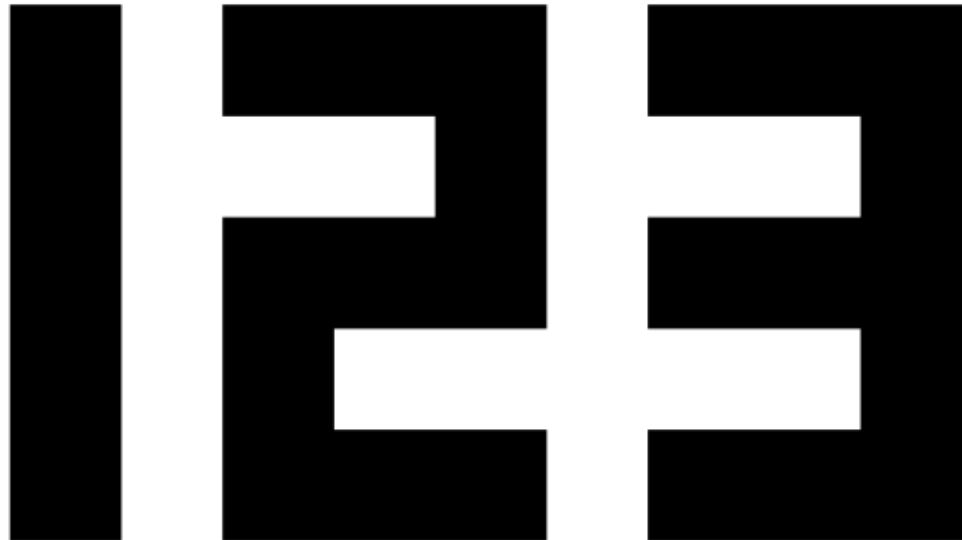
- Text Size: 5.7cm x 3.2cm
- Pixel Size: 0.4mm x 0.4mm

Printed Text, Amplitude Response



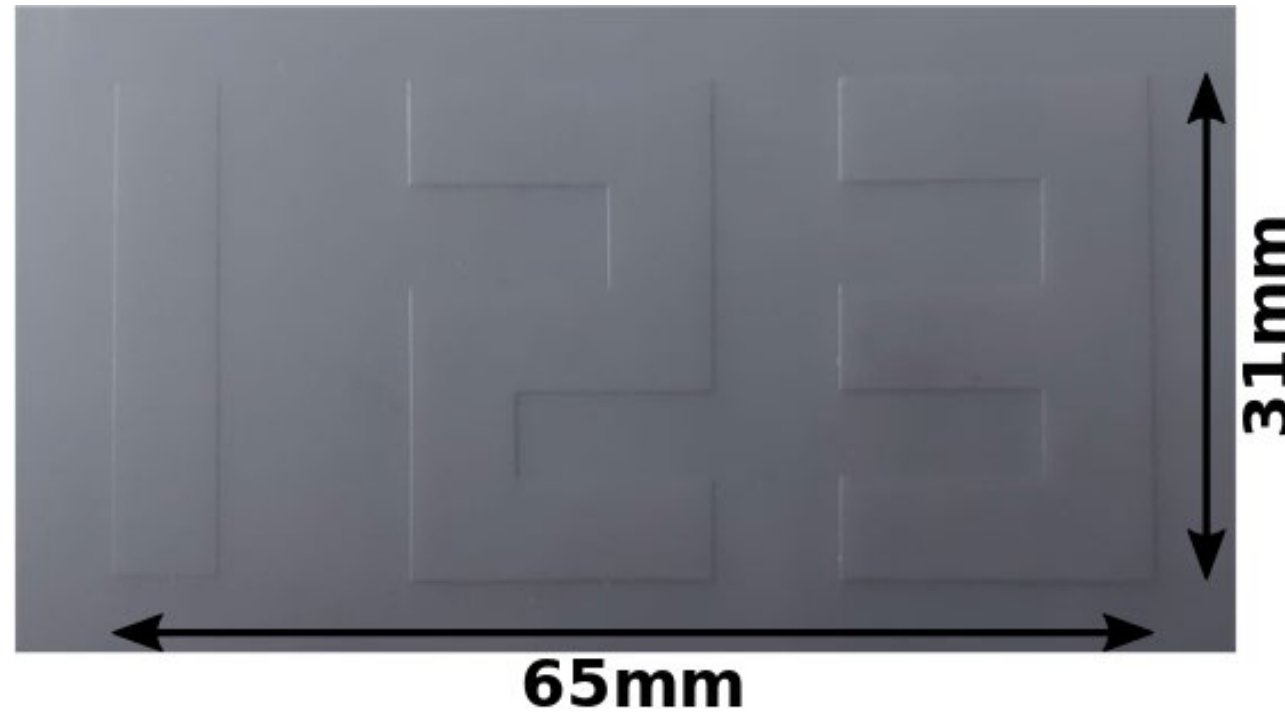
- Ink attenuation is difficult to be measured
- Text can not be reconstructed

Printed Text, Phase Response



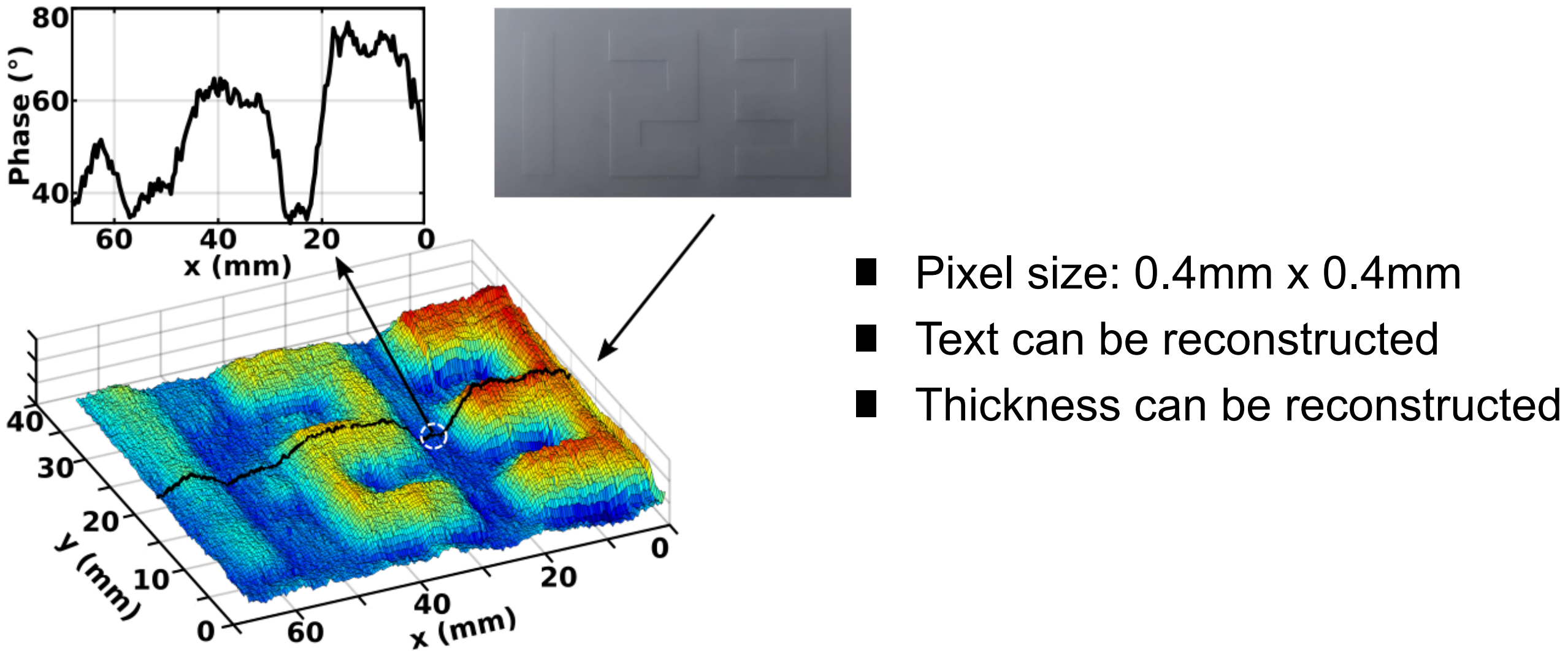
- Introduced phase change is easy to measure
- Text is clearly recognizable

Printed Text, Phase Response



- 3D Printed Text Served as the Imaging Object
- “1” Height – 50 μ m, “2” Height – 100 μ m, “3” Height – 150 μ m

Printed Text, Phase Response



Outline

- Motivation
- Proposed TX-RX System Architecture
- Measurement Results
- Imaging Demonstrations
- Conclusion

Conclusion

- THz Phase Detection is opening door for new imaging applications
- Two-step down-conversion and LO power combining to decrease RX NF
- 10dBm TX EIRP and 27dB RX NF, leading to 52dB SNR (25cm, 100kHz RBW)
- 2.8° RMS Accuracy and 1.7° RMS 1σ Precision (400° range, 25cm, 500ns/point)
- THz Phase Imaging was demonstrated, illustrating potential of presented work

22.4: A 250GHz Autodyne FMCW Radar in 55nm BiCMOS with Micrometer Range Resolution

S.M. Hossein Naghavi¹, Saghar Seyedabbaszadehesfahlani¹, Farzad Khoeini¹, Andreia Cathelin², and Ehsan Afshari¹



¹University of Michigan, Ann Arbor, MI, USA

²STMicroelectronics, Crolles, France

Self Introduction



- **S.M. Hossein Naghavi**
 - **B.Sc. from Amirkabir University of Technology, Tehran, Iran**
 - **M.Sc. from the University of Tehran, Tehran, Iran**
 - **Ph.D. candidate at the University of Michigan, Ann Arbor**
 - **My interests are in the field of THz electronics for imaging, sensing, spectroscopy, and communications.**

Outline

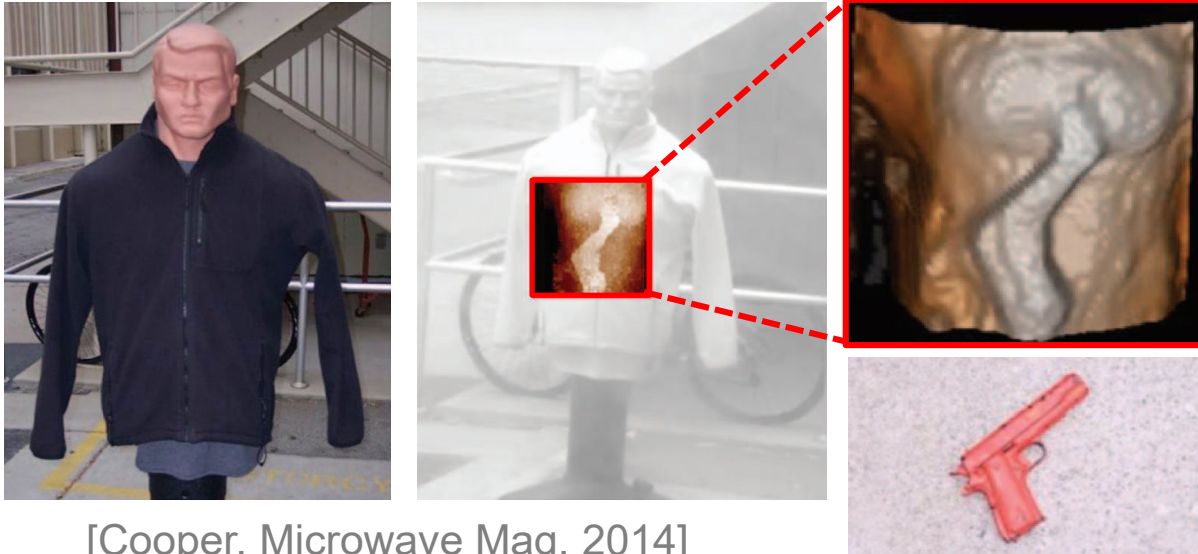
- Introduction
- Phase Processing Method
- Circuit Implementation for Autodyne FMCW Radar
- Measurement Results
- Conclusion

Outline

- Introduction
- Phase Processing Method
- Circuit Implementation for Autodyne FMCW Radar
- Measurement Results
- Conclusion

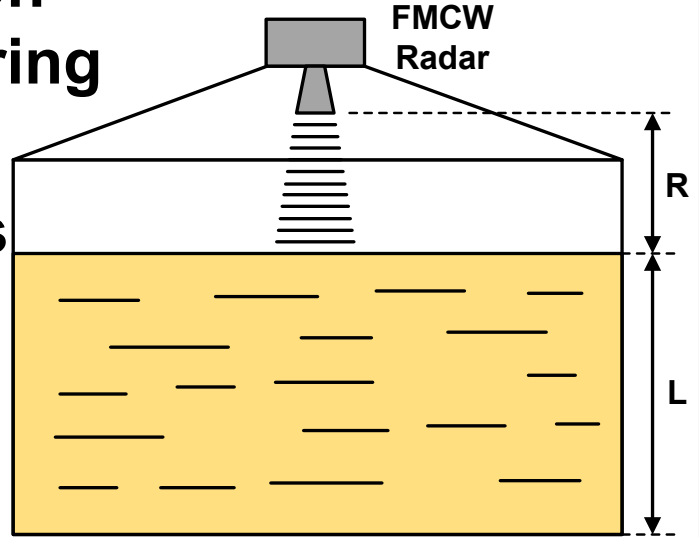
High-Resolution Radar Applications

Concealed Object Detection

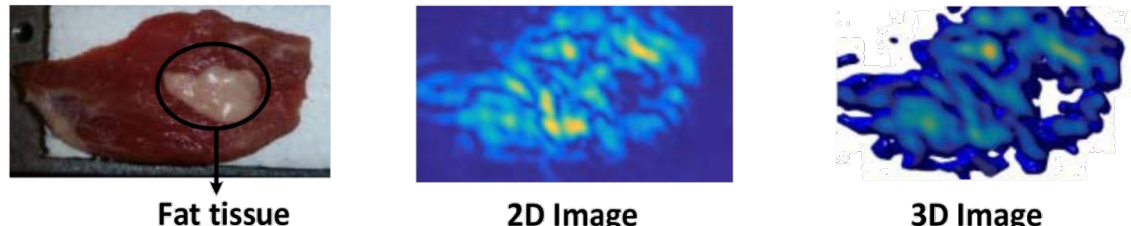


High-precision Level-Measuring Radar in Closed Tanks

[Komarov,
Artech House, 2003]

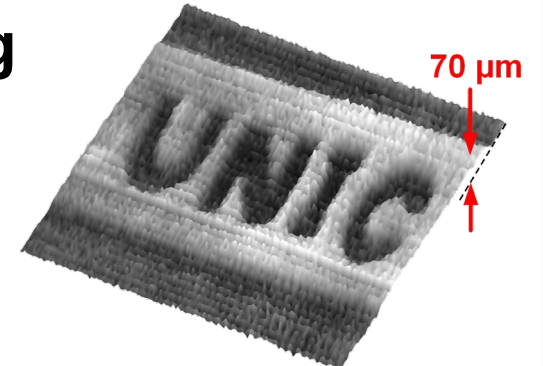


Biomedical Imaging (Hydration Sensing)



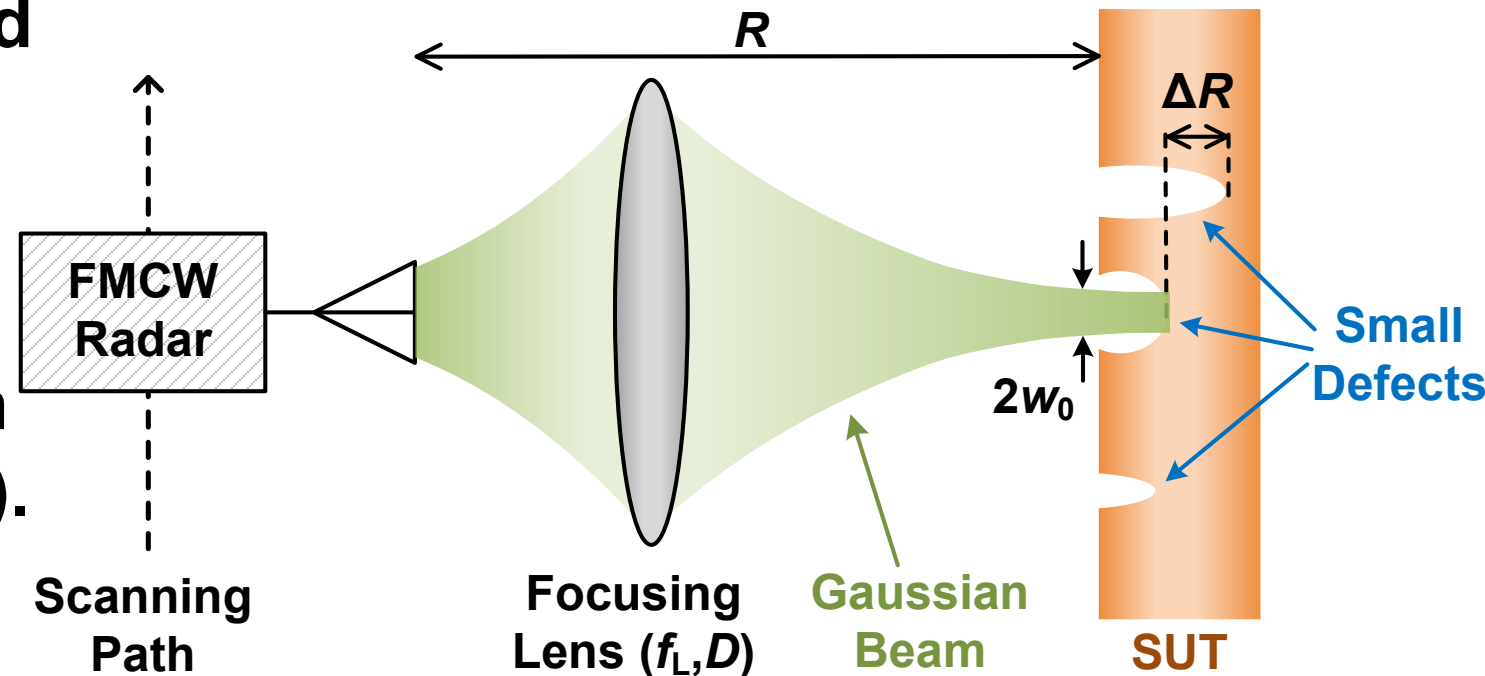
[Mostajeran, TMTT 2019]

Surface Screening



High-Resolution Radar for Defect Detection

- Focusing beam increases the interaction of E/M field with the small defect → Higher sensitivity
- Cross-range resolution depends on the Gaussian beam waist ($2w_0=4\lambda f_L/\pi D$).
- Micrometer range resolution (ΔR) using phase processing of the IF signal



High-precision THz radars for small defect detection on smooth surfaces

Outline

- Introduction
- Phase Processing Method
- Circuit Implementation for Autodyne FMCW Radar
- Measurement Results
- Conclusion

FMCW Signal Analysis

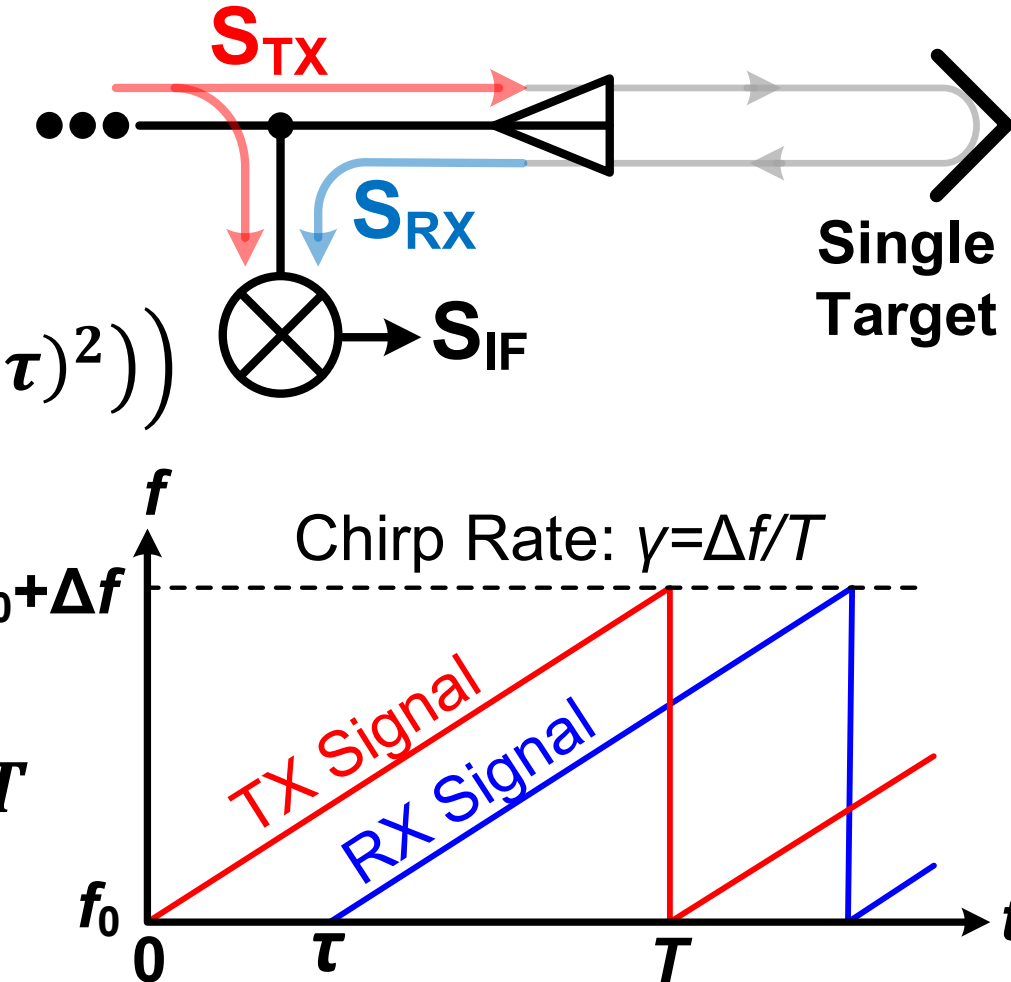
■ FMCW TX and RX Signals:

$$S_{TX}(t) = A_{TX} \exp(j(2\pi f_0 t + \pi\gamma t^2))$$

$$S_{RX}(t) = A_{RX} \exp(j(2\pi f_0(t - \tau) + \pi\gamma(t - \tau)^2))$$

■ Continuous-Time IF Signal:

$$S_{IF}(t) \approx A_{IF} \exp(j(2\pi f_0 \tau + 2\pi\gamma\tau t)), \tau \ll T$$



Integrated Methods of IF Signal Analysis

- Amplitude analysis(depend on target RCS) 

$$S_{\text{IF}}(t) \approx A_{\text{IF}} \exp(j(2\pi f_0 \tau + 2\pi \gamma \tau t))$$

- Frequency analysis (linear function of τ) 

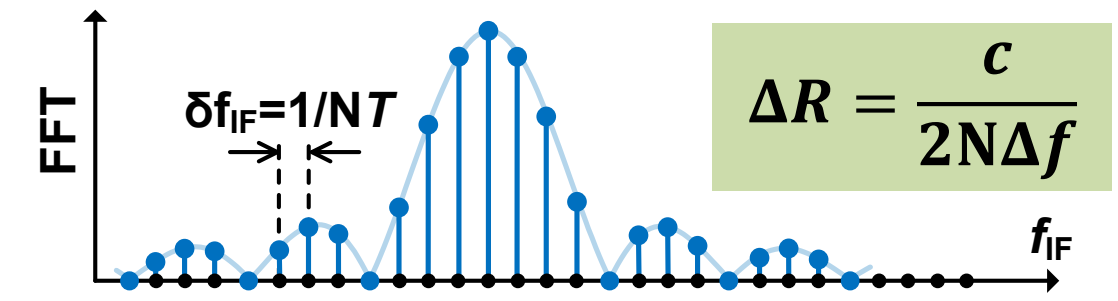
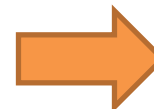
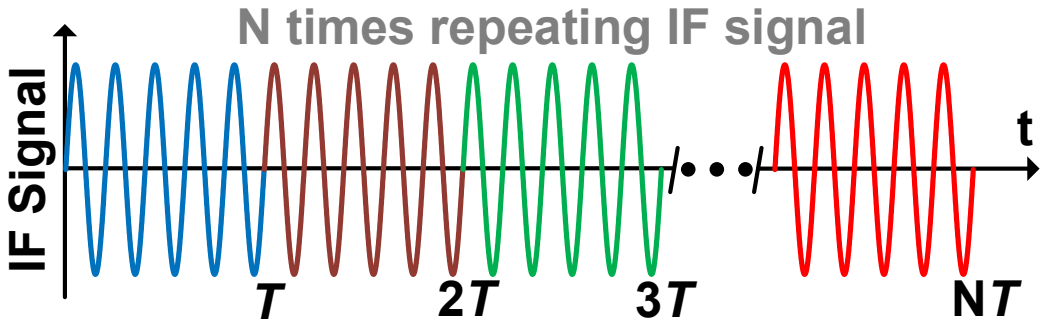
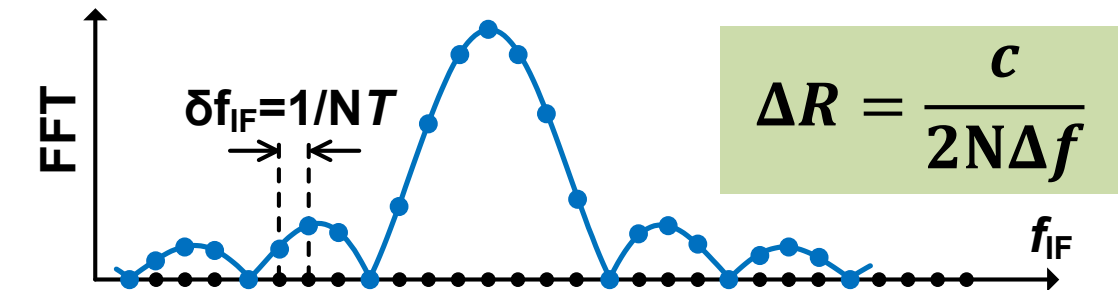
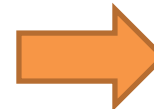
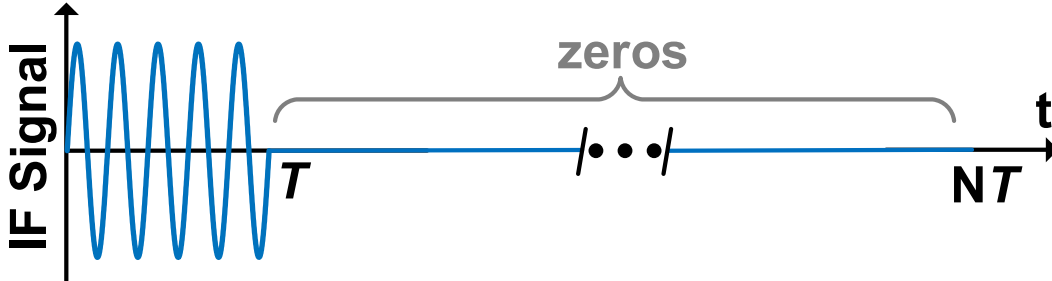
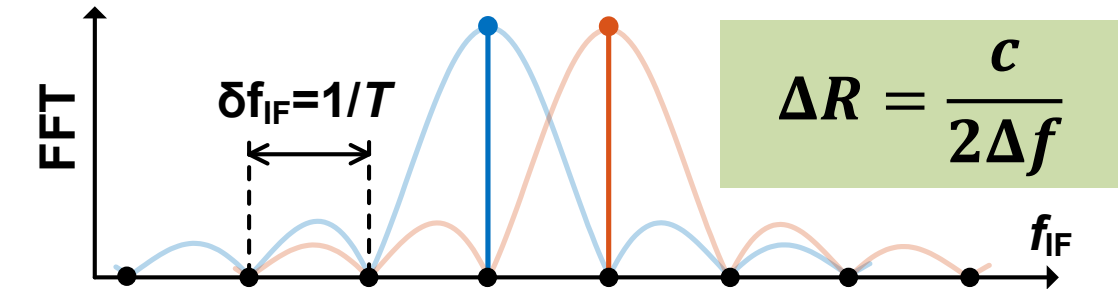
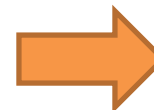
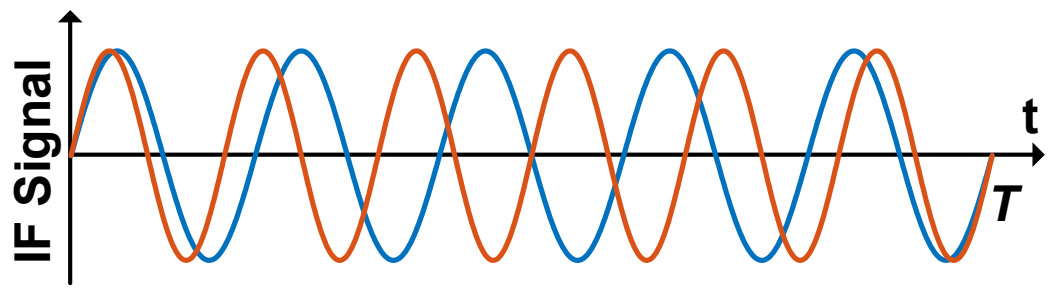
$$S_{\text{IF}}(t) \approx A_{\text{IF}} \exp(j(2\pi f_0 \tau + 2\pi \underbrace{\gamma \tau}_{= \phi(t)} t))$$

$f_{\text{IF}} = \frac{1}{2\pi} \frac{\partial \phi(t)}{\partial t} = \gamma \tau$

- Phase analysis (linear function of τ) 

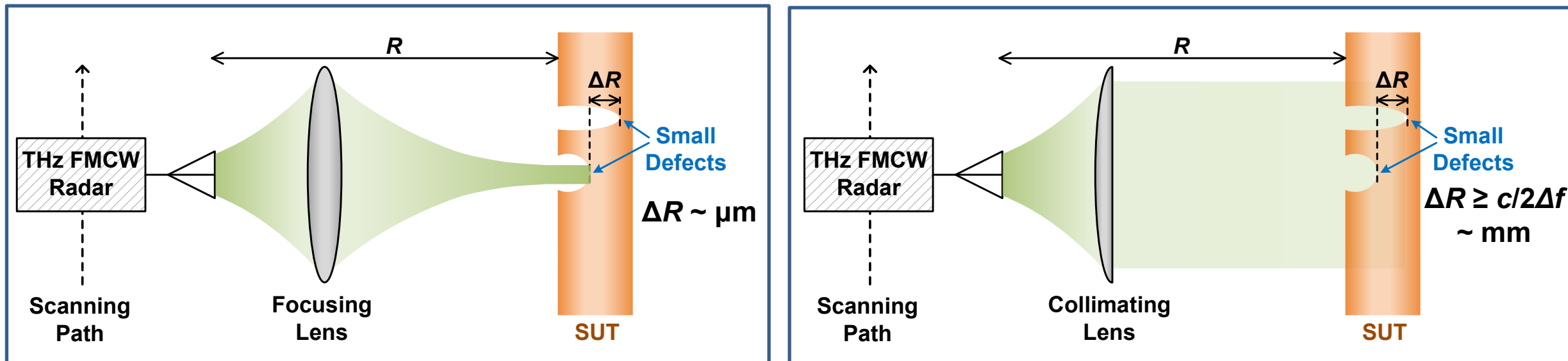
$$S_{\text{IF}}(t) \approx A_{\text{IF}} \exp(j(\underbrace{2\pi f_0 \tau}_{\phi_{\text{IF}}} + 2\pi \gamma \tau t))$$

High-Resolution FFT Processing



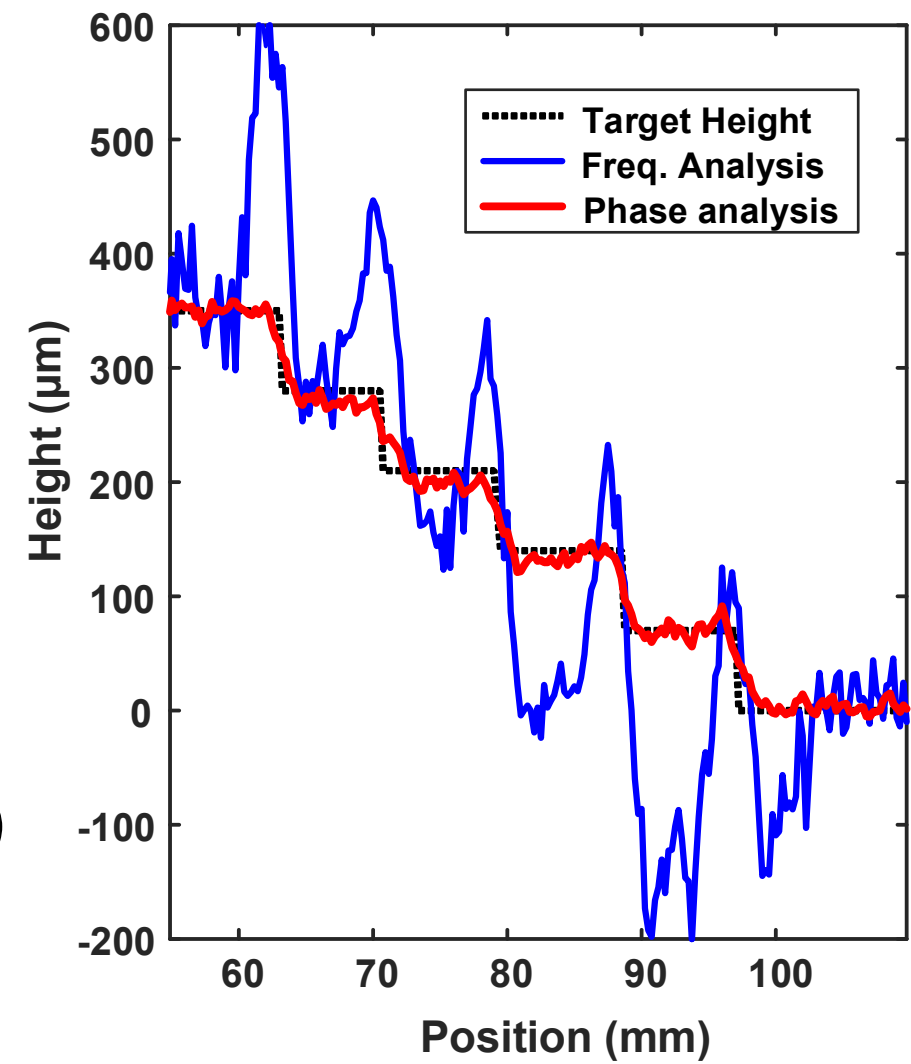
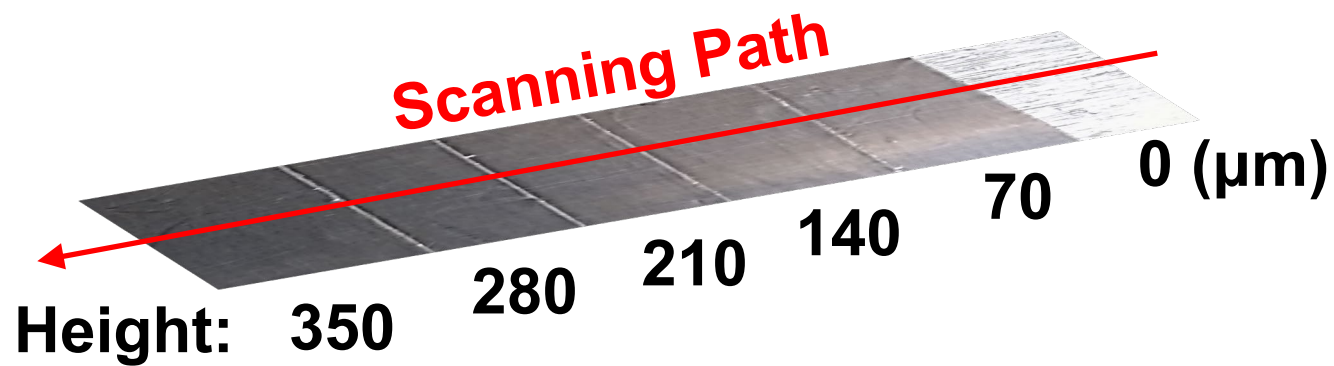
Single Target Requirement

- Focused beam can resolve objects in range with **54 μm resolution ($f_0=191\text{GHz}$, $\Delta f = 66.7\text{GHz}$).**
- Collimated beam can resolve objects in range with **54 μm resolution when $\Delta f = c/2\Delta R = 2.8\text{THz}$.**



Freq. and Phase Analysis Comparison

- Height measurement results for a staircase
- Frequency analysis has problem in edge transitions
- Phase analysis continuously follows the staircase



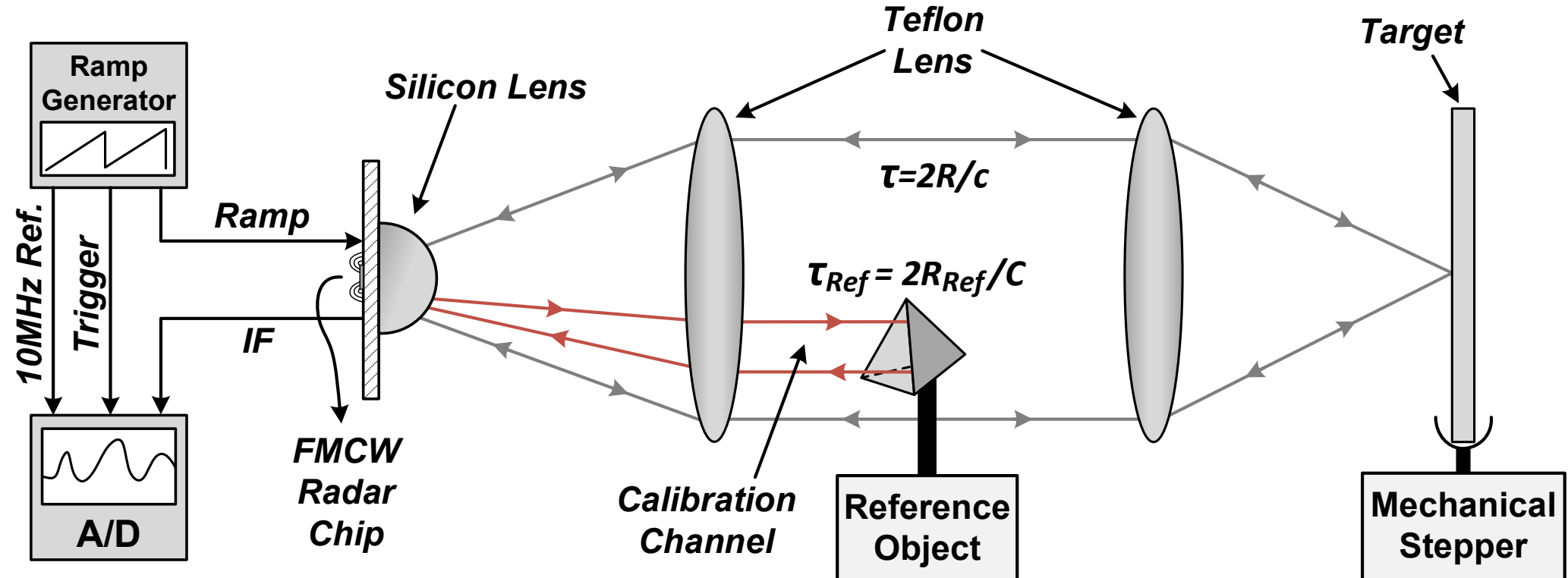
Freq. and Phase Analysis Comparison

Method	Pros & Cons	Precision	Edges
Freq. analysis ($\gamma\tau$)	1-to-1 relation between range & frequency 😊	Medium precision 😐	Inaccurate 😞
Phase analysis ($2\pi f_0 \tau$)	Phase wrapping 😞	High precision 😊	Accurate 😊

- Frequency analysis is good for coarse measurements, and phase analysis is good for fine measurements.
- A combination of frequency and phase analysis can provide a continuous high-precision range measurement.

Imaging Setup with Phase Processing Method

- Calibration channel to remove phase uncertainties
- τ_{Ref} and R_{Ref} are known values



Discrete-time Phase Processing

■ Discrete-time FMCW IF signal:

- k : integer number
- F_s : A/D sampling rate
- t_s : time delay between the start time of A/D sampling and the start time for the chirp signal

$$t = k/F_s + t_s \quad \phi_{\text{IF}} = 2\pi(f_0 + \gamma t_s)\tau = 2\pi\left(f_0 + \frac{\Delta f}{T} t_s\right)\tau$$

$$S_{\text{IF}}(k) \approx \exp(j(2\pi f_0 \tau + 2\pi \gamma t_s \tau + 2\pi \gamma \tau k / F_s))$$

Discrete-time phase

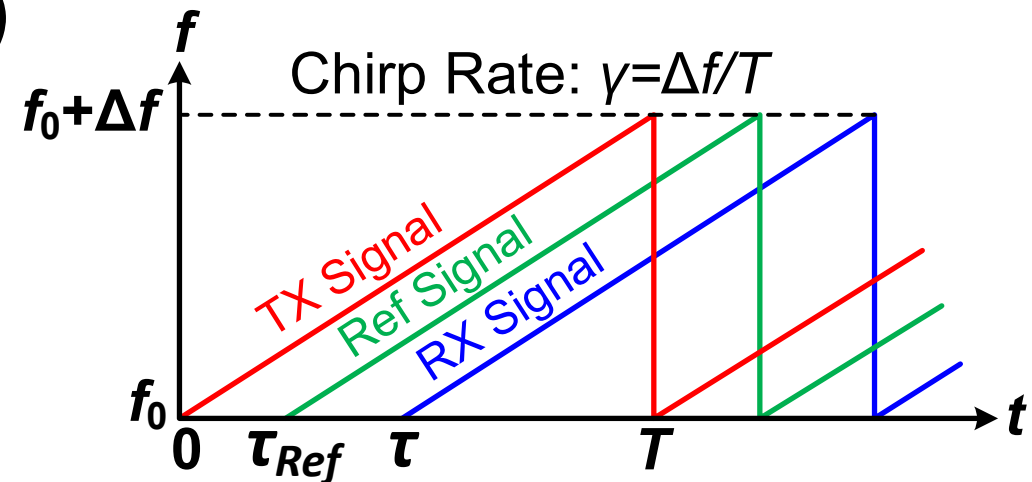
Phase Calibration

■ Uncertainties in the discrete IF signal phase:

- Chirp start frequency variation (f_0)
- Chirp bandwidth variation (Δf)
- Random t_s

$$\phi_{IF} = 2\pi \left(f_0 + \frac{\Delta f}{T} t_s \right) \tau$$

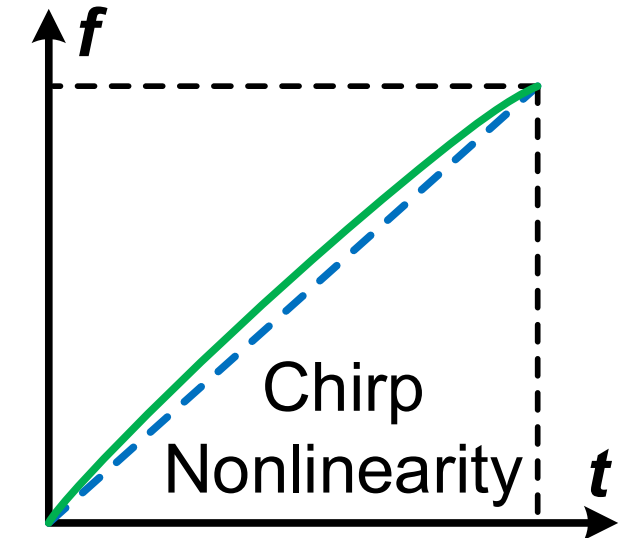
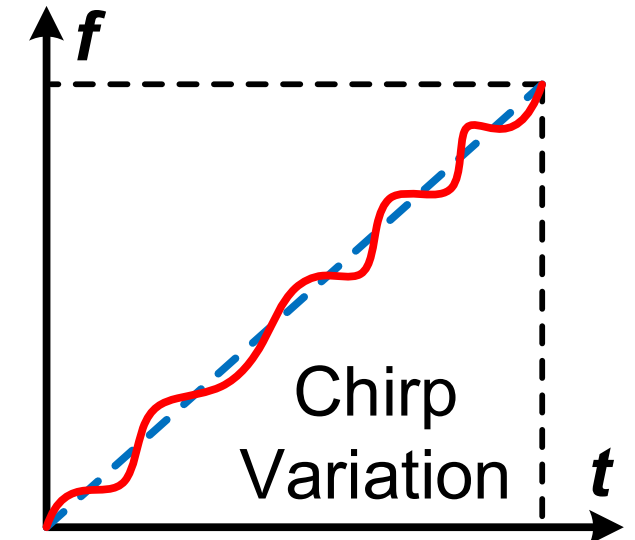
$$\phi_{Ref} = 2\pi \left(f_0 + \frac{\Delta f}{T} t_s \right) \tau_{Ref}$$



$$\tau = \frac{\phi_{IF}}{\phi_{Ref}} \tau_{Ref} \rightarrow R = \frac{\phi_{IF}}{\phi_{Ref}} R_{Ref}$$

Phase Calibration Limits

- Parameters that cannot be removed by calibration:
 - Phase noise
 - Random chirp variations during the sweep
 - Small chirp nonlinearity
 - Frequency quantization using FFT
- PLL can improve the phase stability



Outline

- Introduction
- Phase Processing Method
- **Circuit Implementation for Autodyne FMCW Radar**
- Measurement Results
- Conclusion

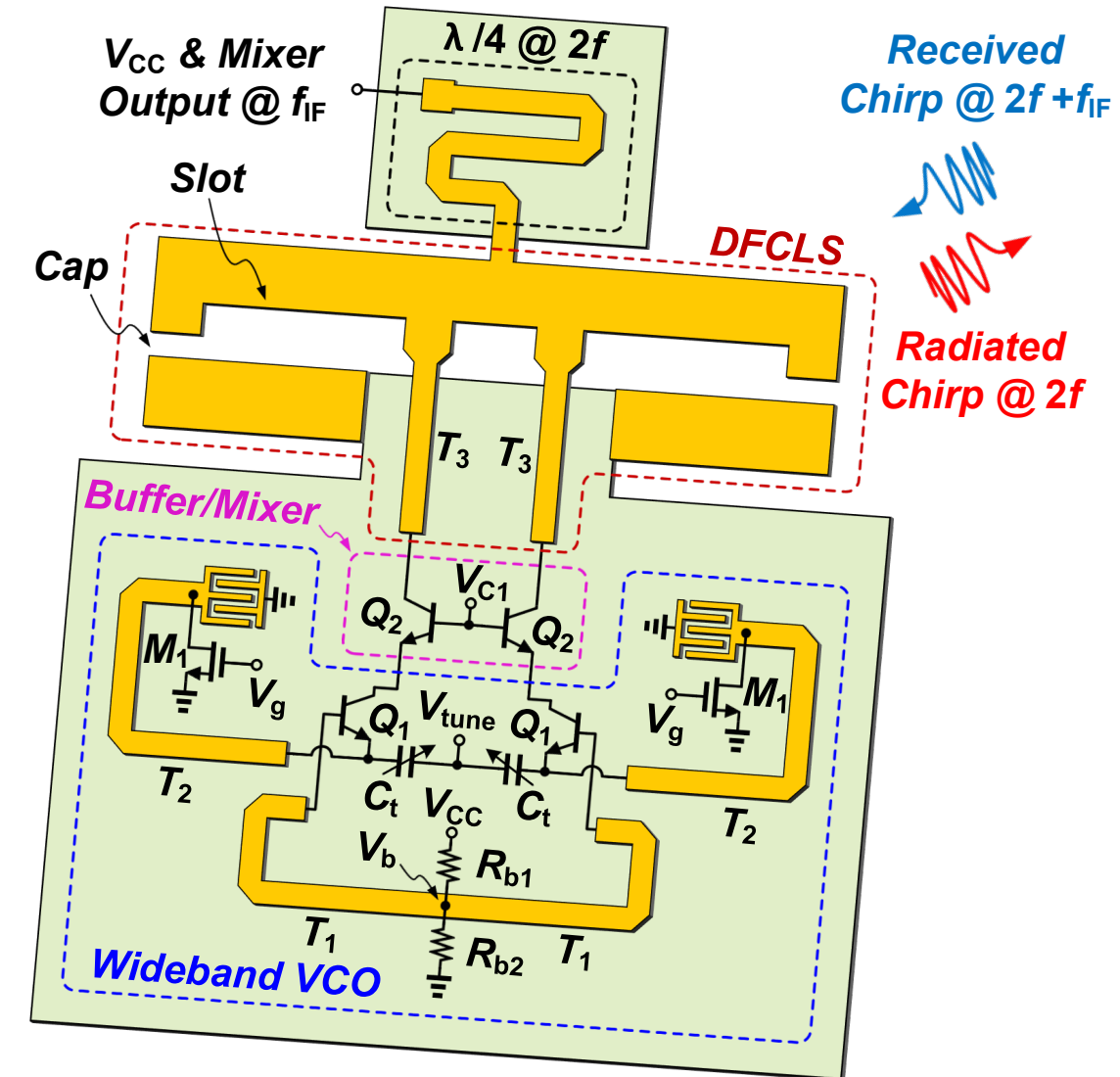
Autodyne FMCW Radar

■ What is Autodyne?

- Generating TX signal
- Mixing the TX and RX at the same path

■ Why Autodyne?

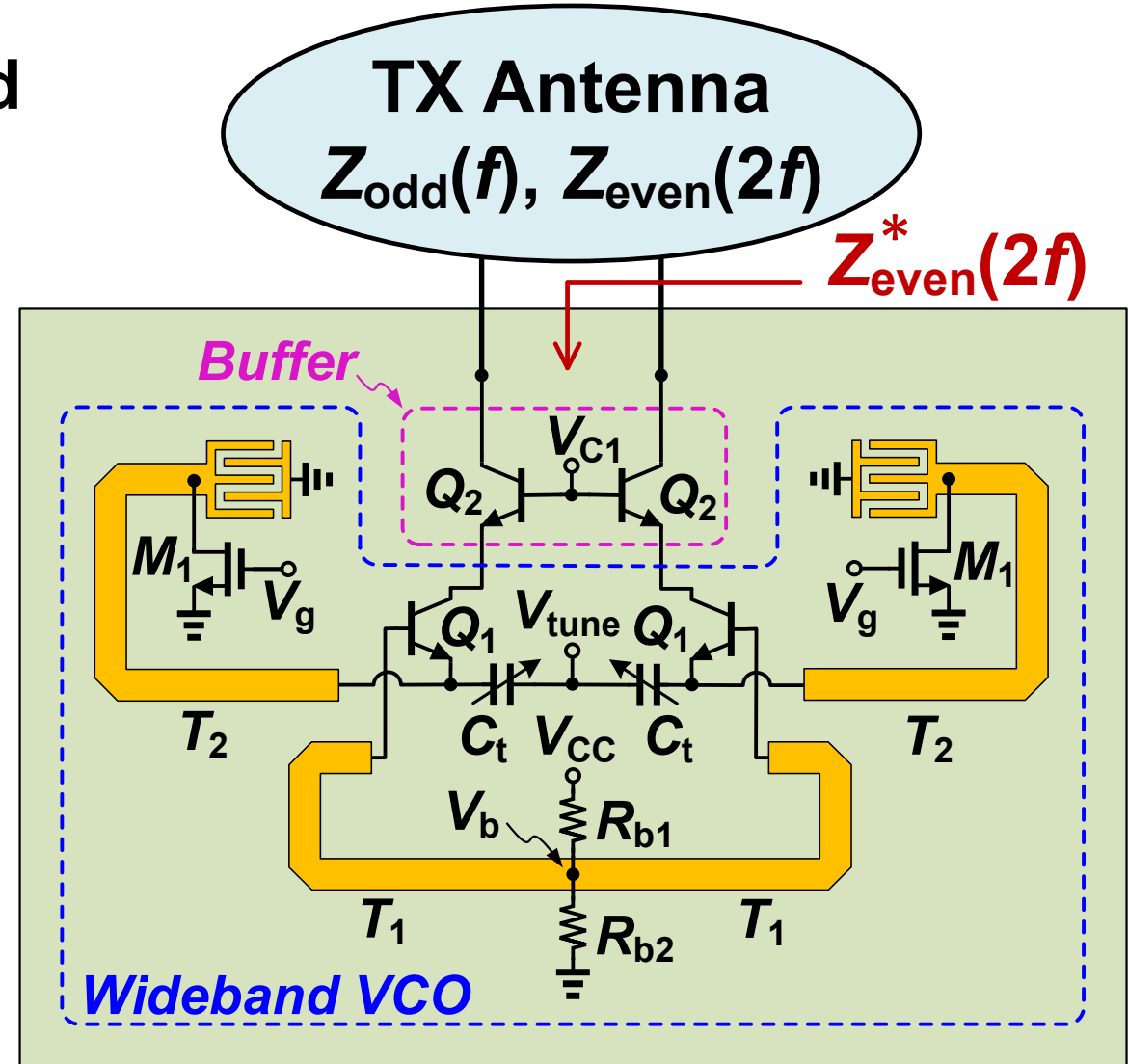
- Single antenna as TX/RX
- Consistent radiation pattern
- Compact → Making Array
- Low power



22.4: A 250GHz Autodyne FMCW Radar in 55nm BiCMOS with Micrometer Range Resolution

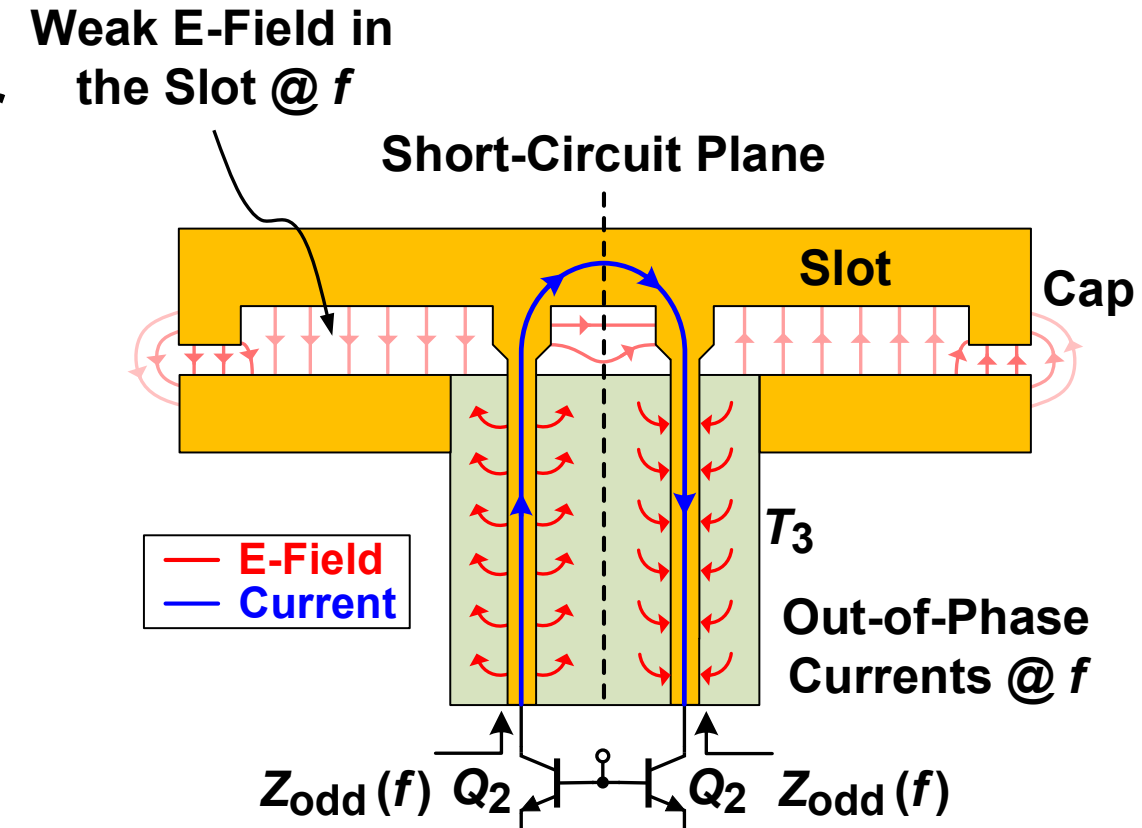
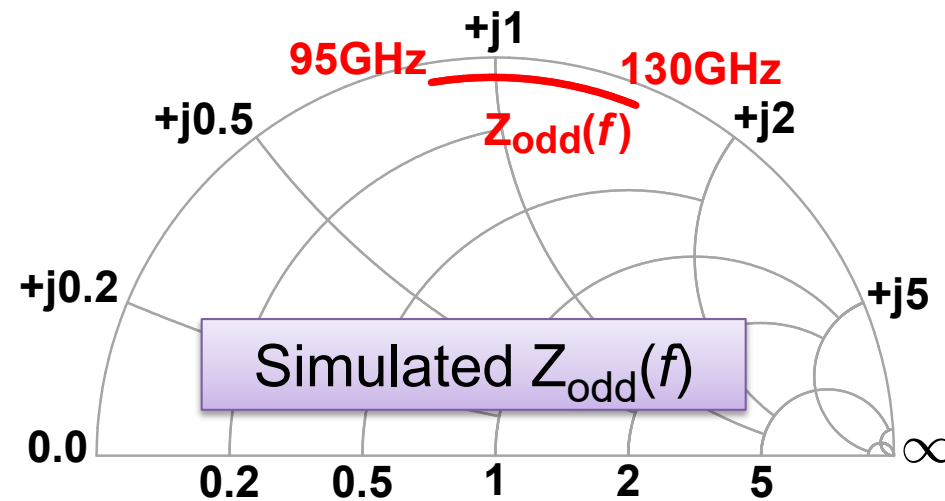
Transmitter: Wideband VCO

- Colpitts oscillator for wideband operation
- T_1 and C_t resonate
- R_{b1} and R_{b2} enforce differential oscillation
- T_2 : optimum loading for maximum activity of Q_1 , compensates parasitic caps
- Q_2 : boosts generated 2nd harmonic, isolates VCO tank from output network



Double-Fed Capacitive-Loaded Slot (DFCLS)

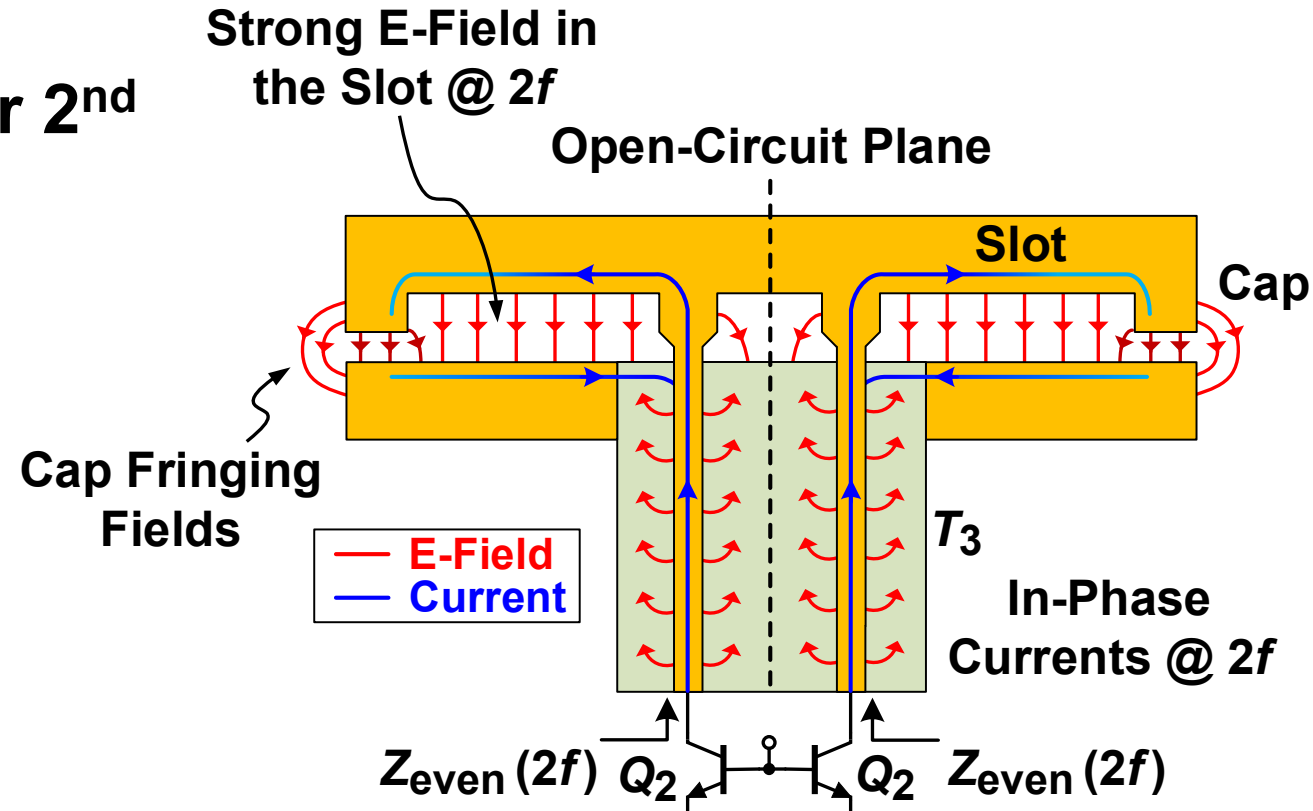
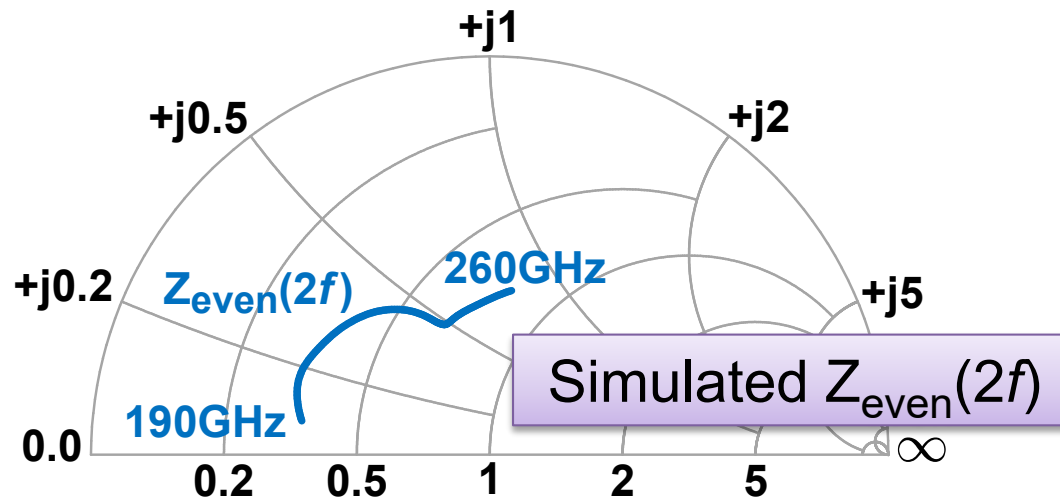
- Return current in T_3 provides a *wideband* optimum loading @ f for maximum activity of transistors.
- Weak E-field in the slots and capacitors @ f
- Out-of-phase E-field in slots



Current & E-Field Distribution @ f

Double-Fed Capacitive-Loaded Slot (DFCLS)

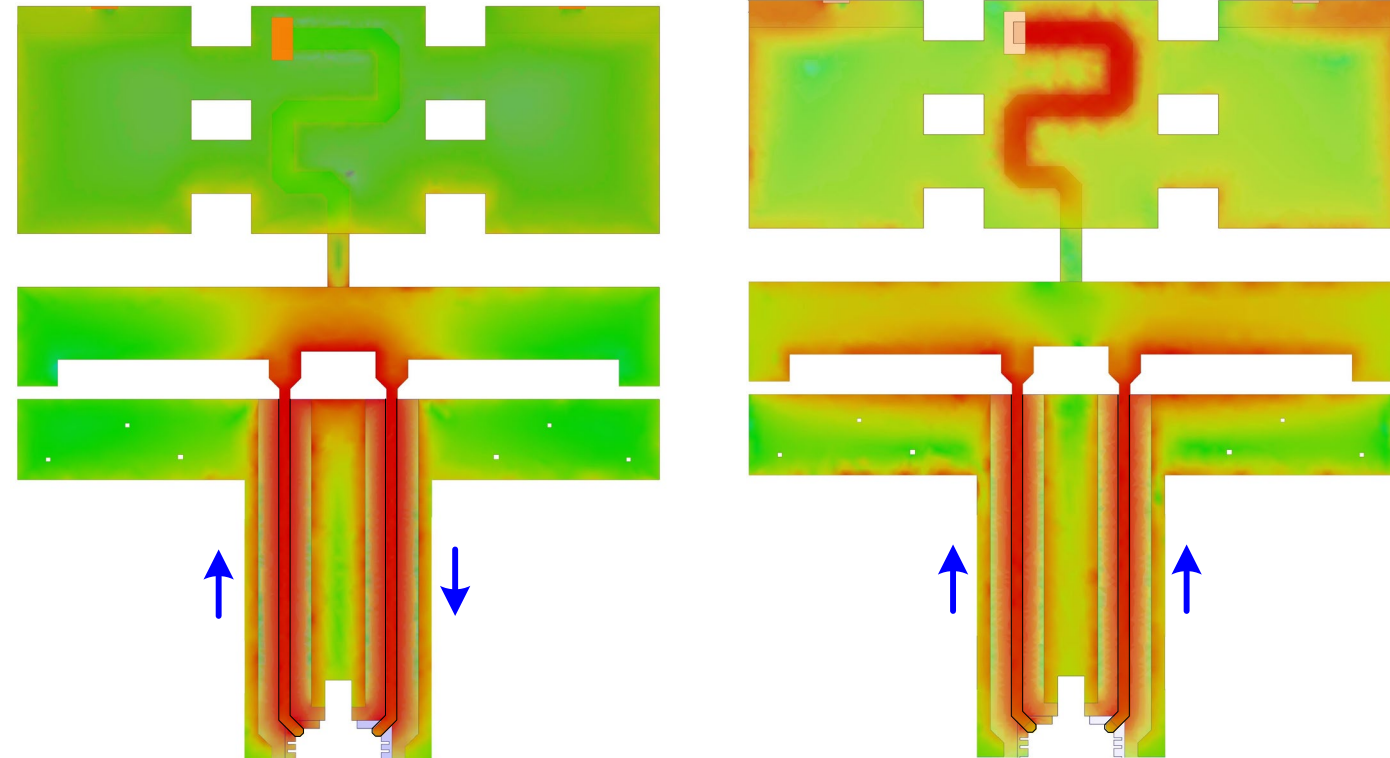
- Line T_3 , slot, and cap provide a **wideband** matching network for 2nd harmonic extraction.
- Strong E-field in the slots @ 2f
- In-phase E-field in the slots provides radiation resistance.



Current & E-Field Distribution @ 2f

Double-Fed Capacitive-Loaded Slot (DFCLS)

- Simulated density current results for in-phase and out-of-phase conditions
- $\lambda/4$ line prevents 2nd harmonic leakage to the V_{cc} port.

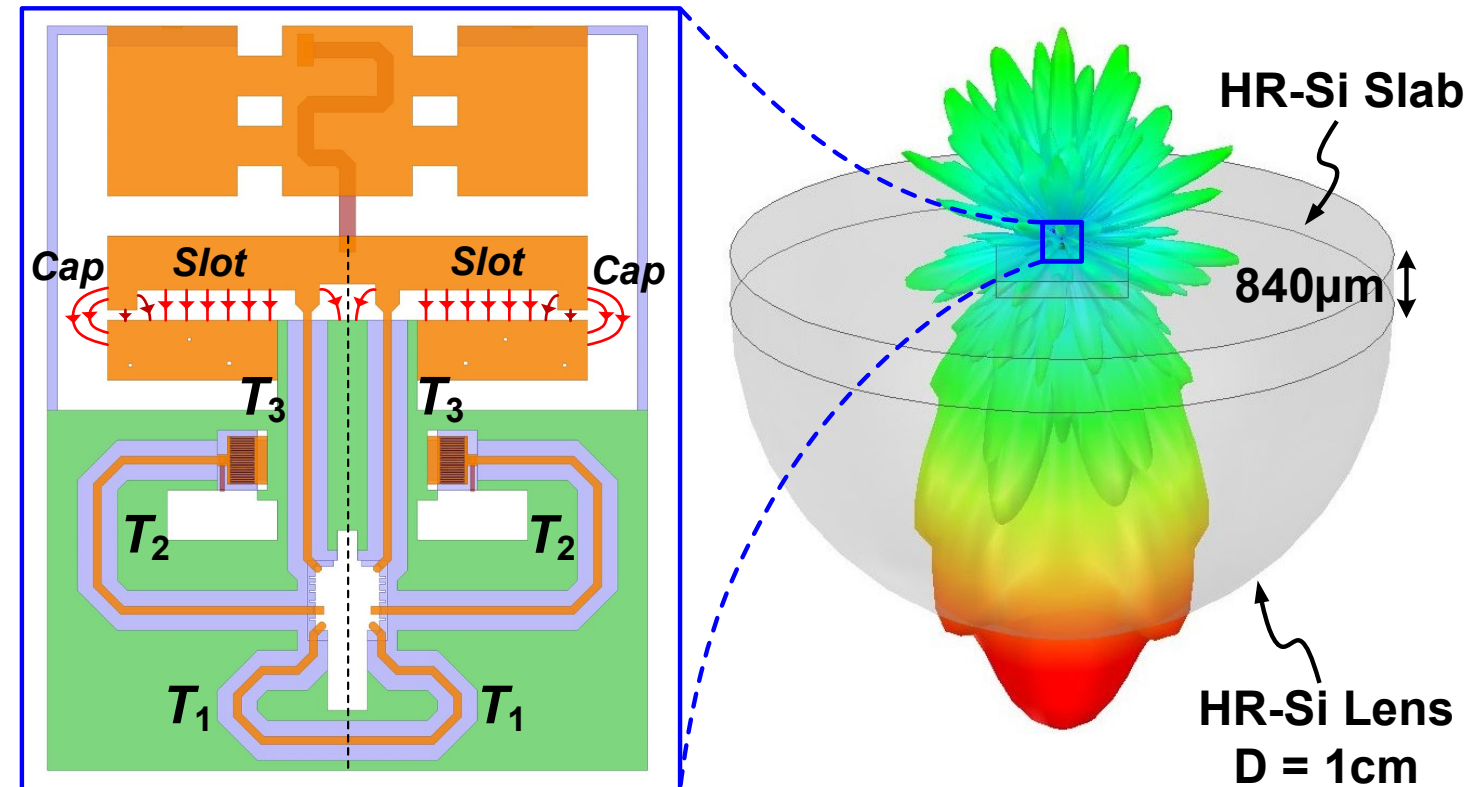


Simulated Current Density (110GHz)

Simulated Current Density (220GHz)

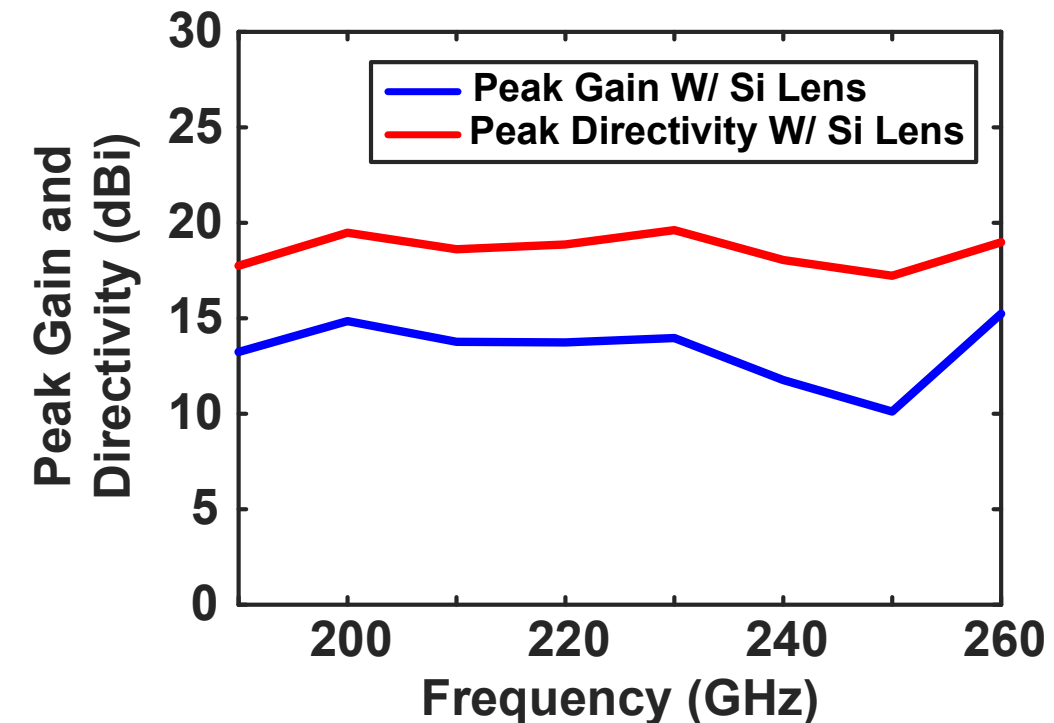
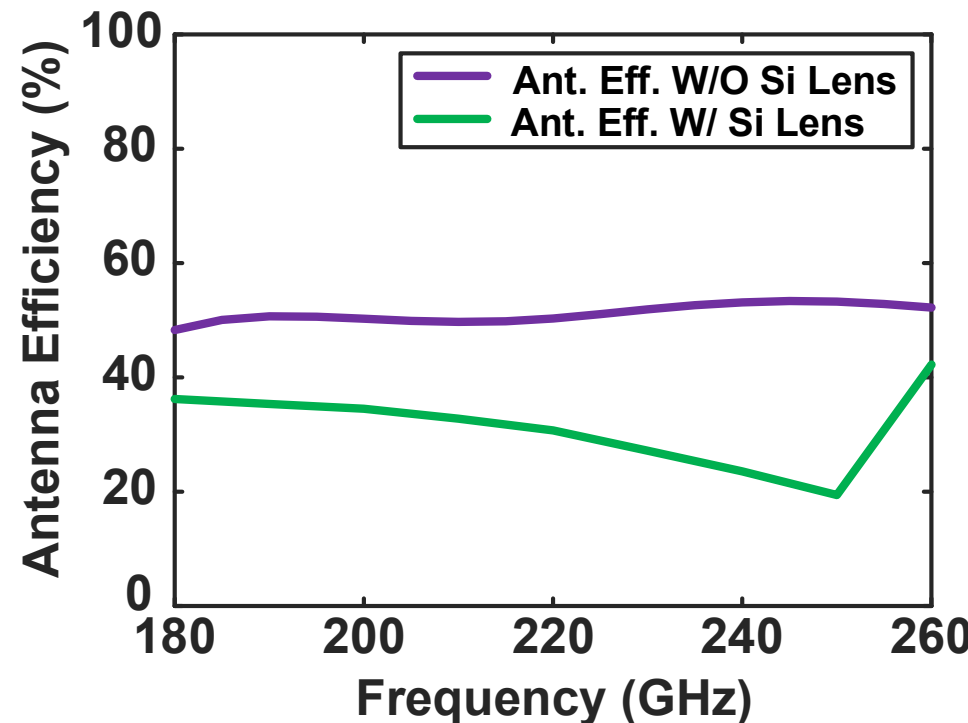
DFCLS as TX/RX Antenna

- Single slot as TX/RX antenna
- Antenna phase center is located at the Si lens center → Consistent radiation pattern at the entire frequency band
- $840\mu\text{m}$ Si slab and 1cm Si lens → low EIRP variation over the band



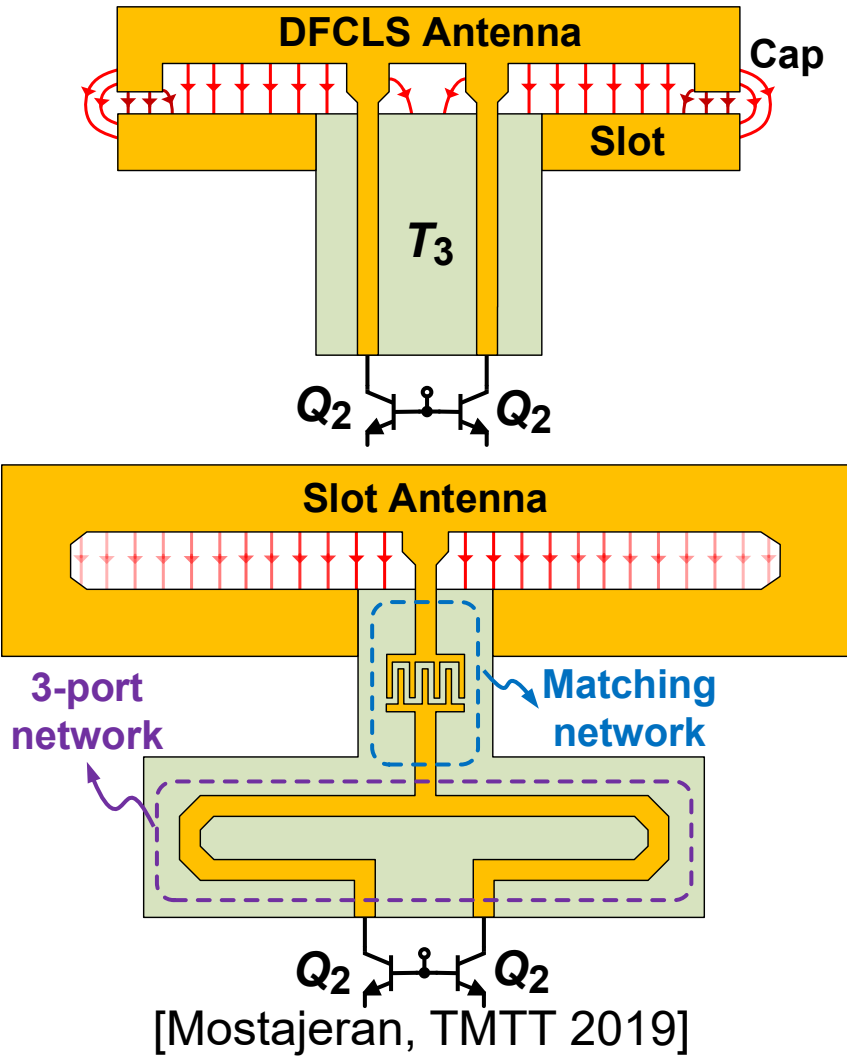
DFCLS as TX/RX Antenna

- Wide bandwidth: (>80GHz, 35%)
- Directivity fluctuation W/ Lens: 2.4dB
- Ant. Eff. W/O Lens: ~50%
- Ant. Eff. W/ Lens @ 220Gz: 31%



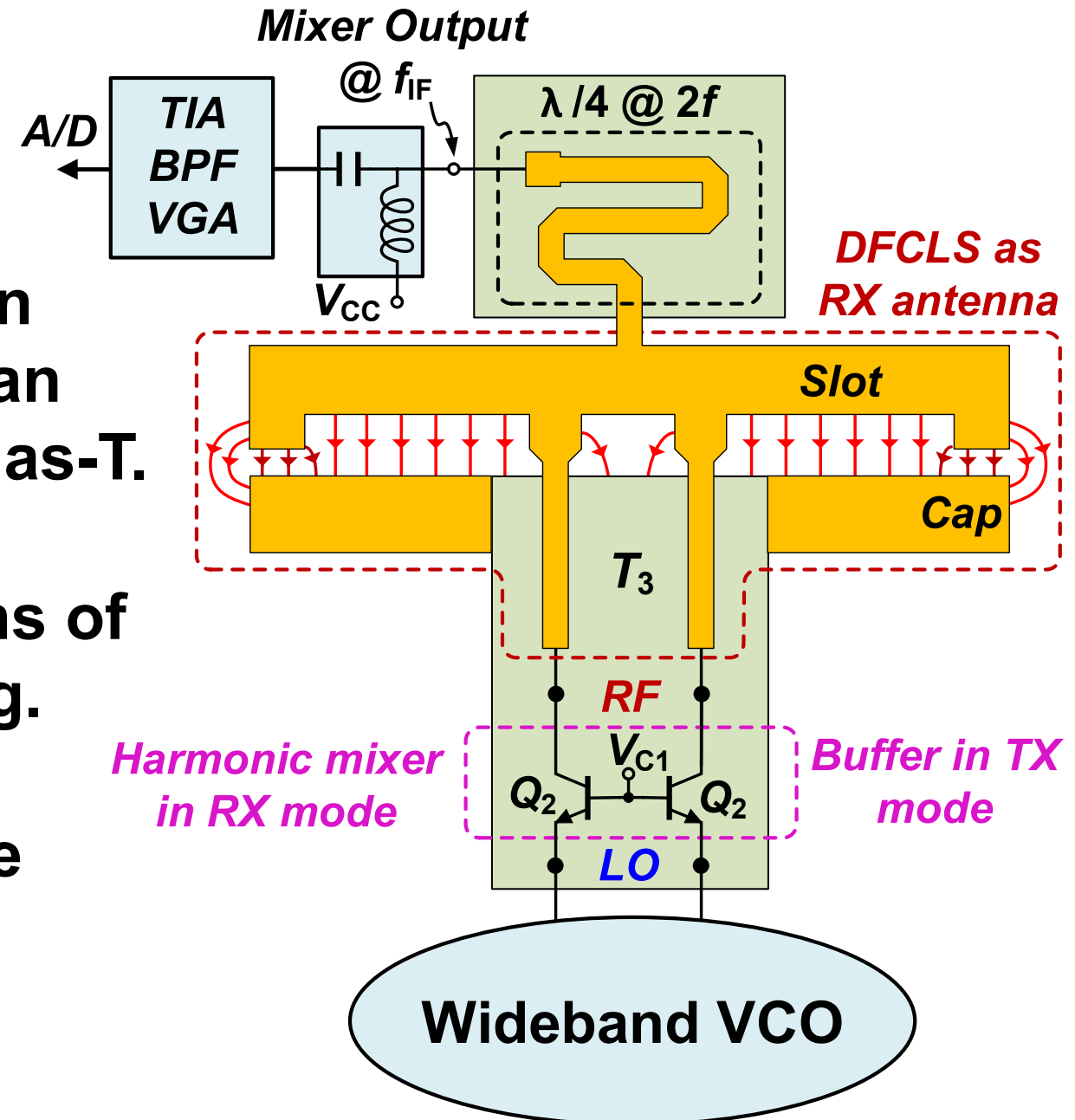
DFCLS vs. Slot Antenna

	Size	Matching network	3-port network
DFCLS antenna	Medium 😊	No need 😊	No need 😊
Slot antenna	Large 😥	Need 😥	Need 😥



Receiver

- RF and LO signals at $2f$ are in common mode; hence, we can extract f_{IF} from V_{cc} using a bias-T.
- Nonlinearities of CB junctions of Q_2 mainly perform the mixing.
- Mixer and oscillator parts are isolated → improved performance

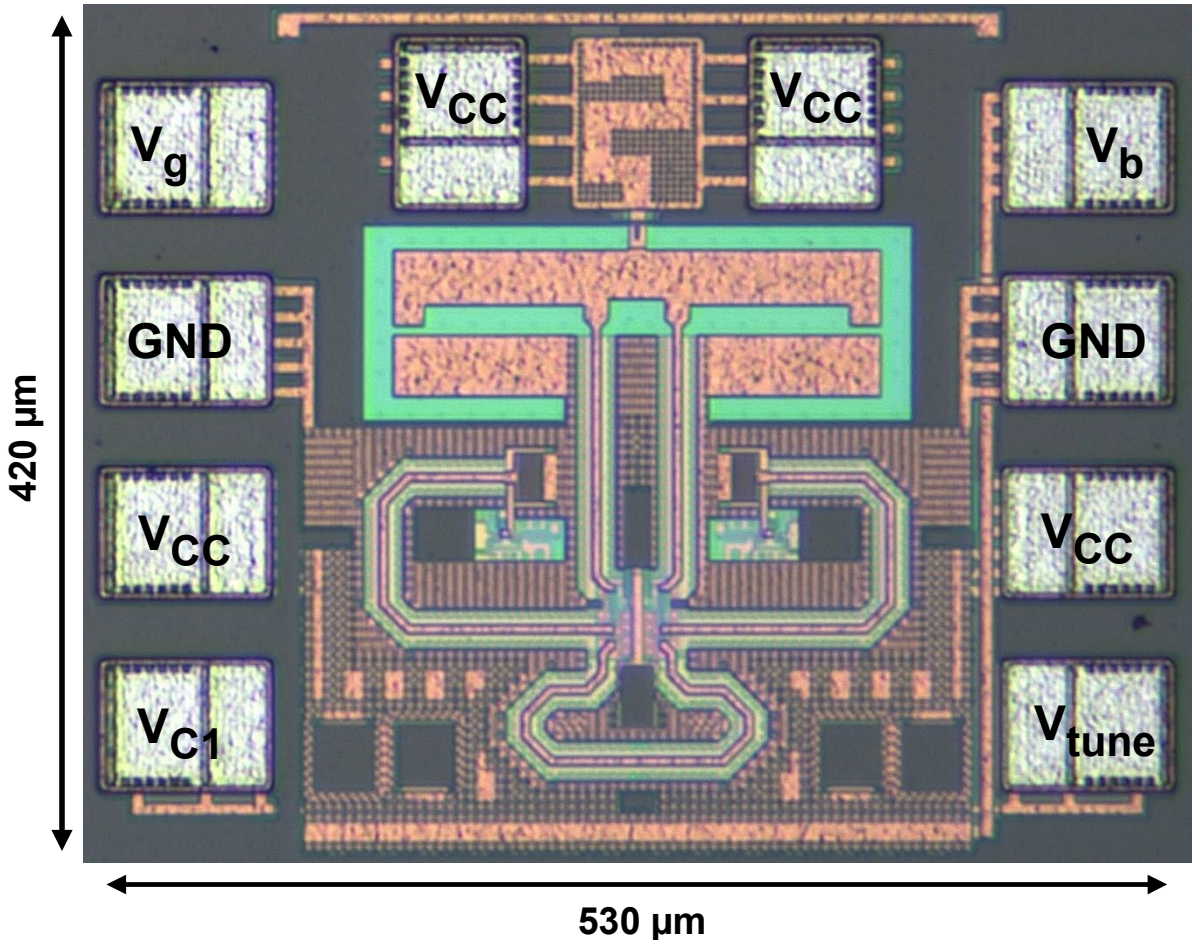


Outline

- Introduction
- Phase Processing Method
- Circuit Implementation for Autodyne FMCW Radar
- Measurement Results
- Conclusion

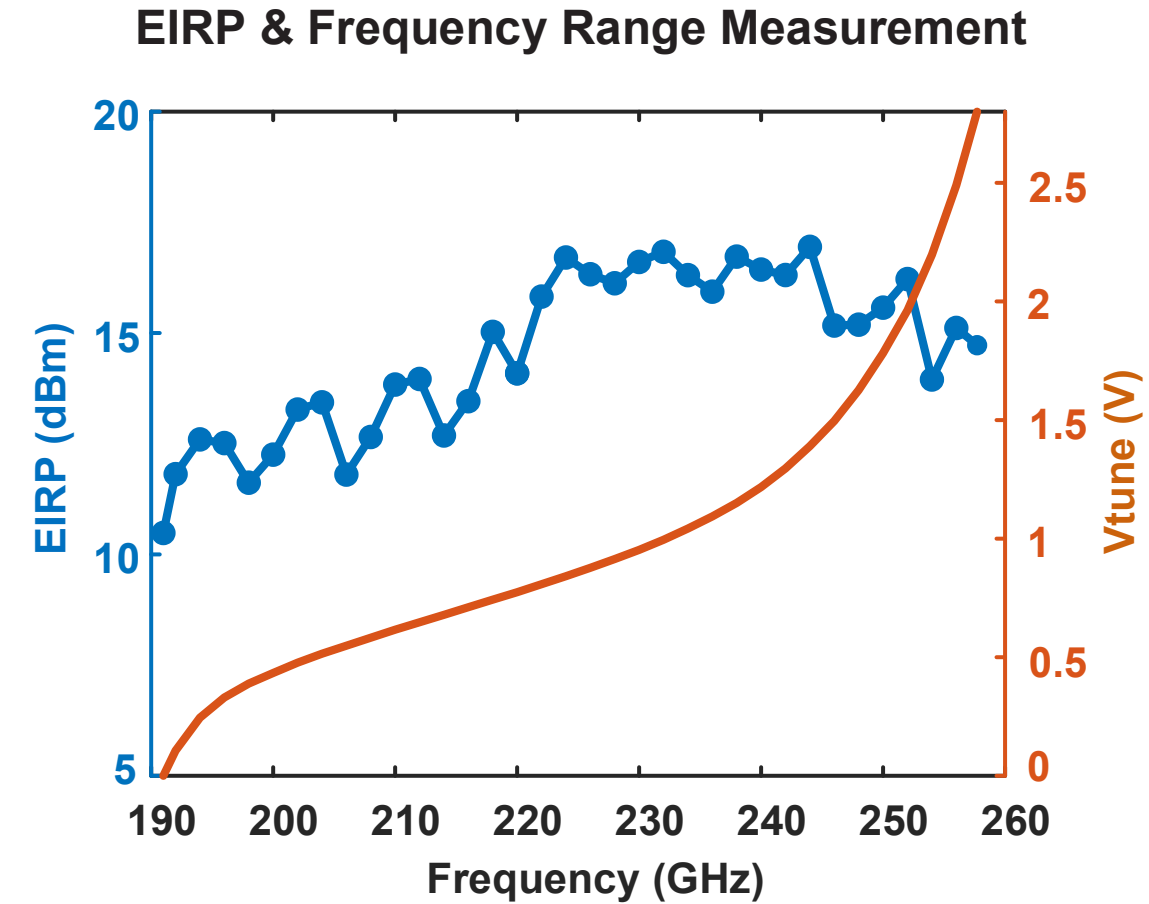
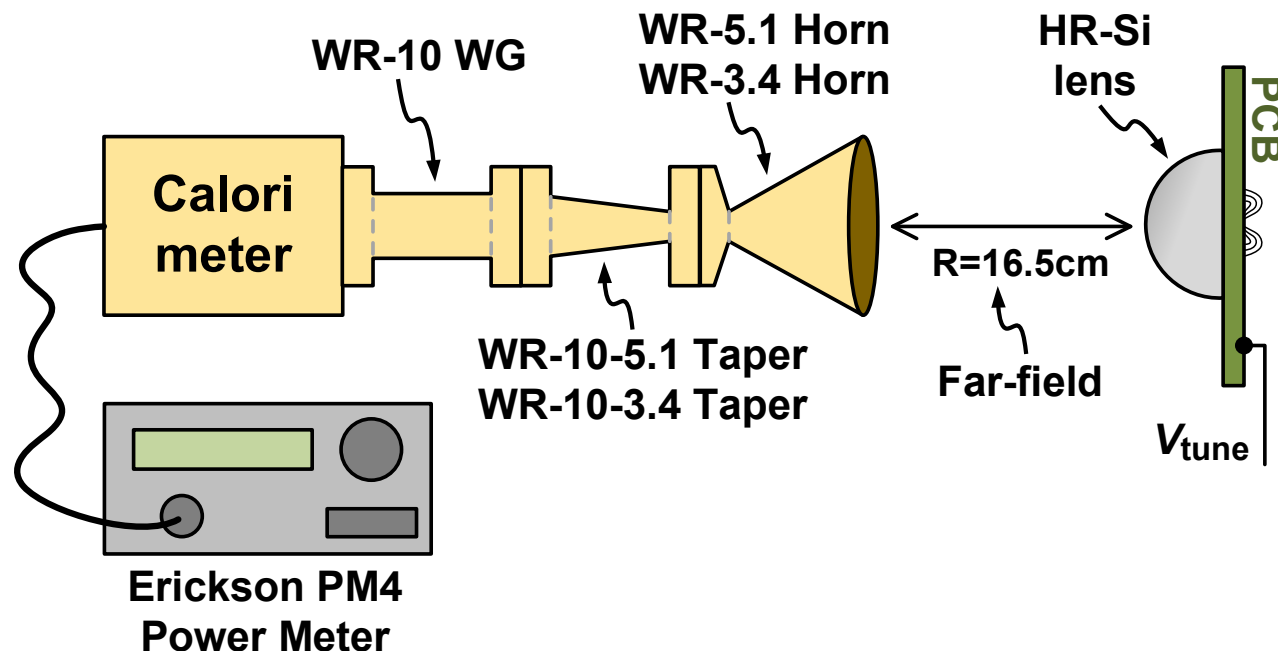
Chip Photograph

- STMicroelectronics 55nm BiCMOS technology
- Area: 0.22 mm²
- Total power consumption: 68mW



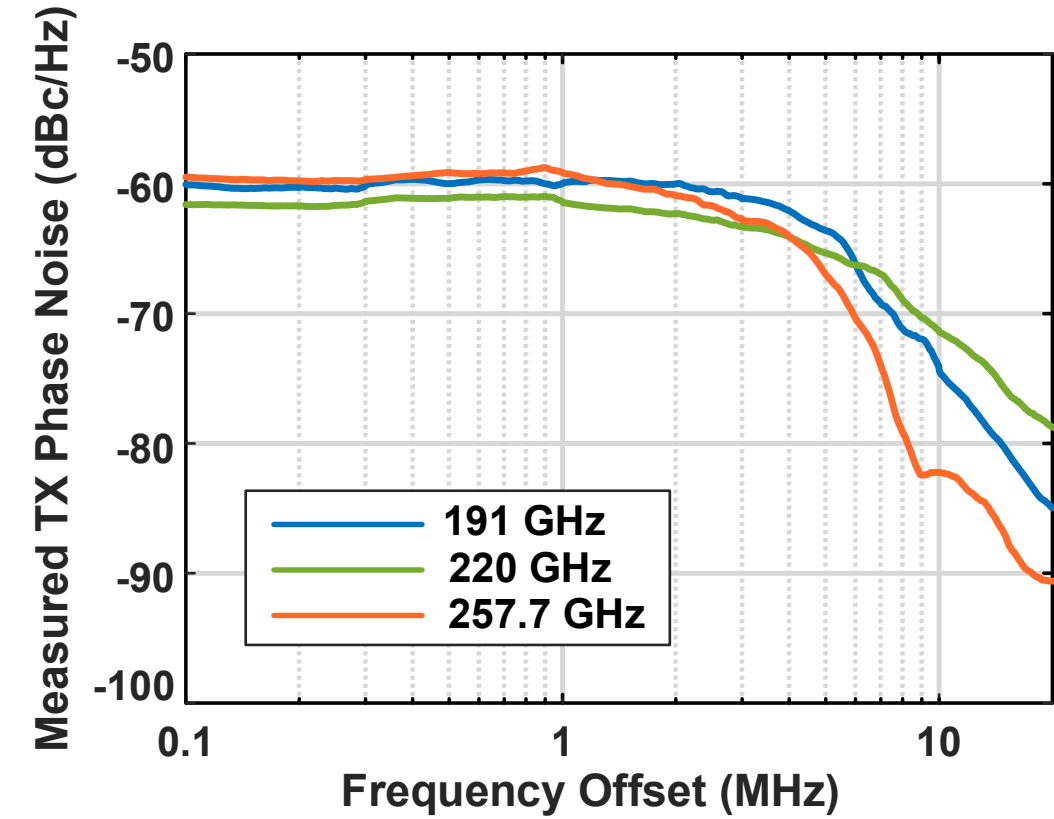
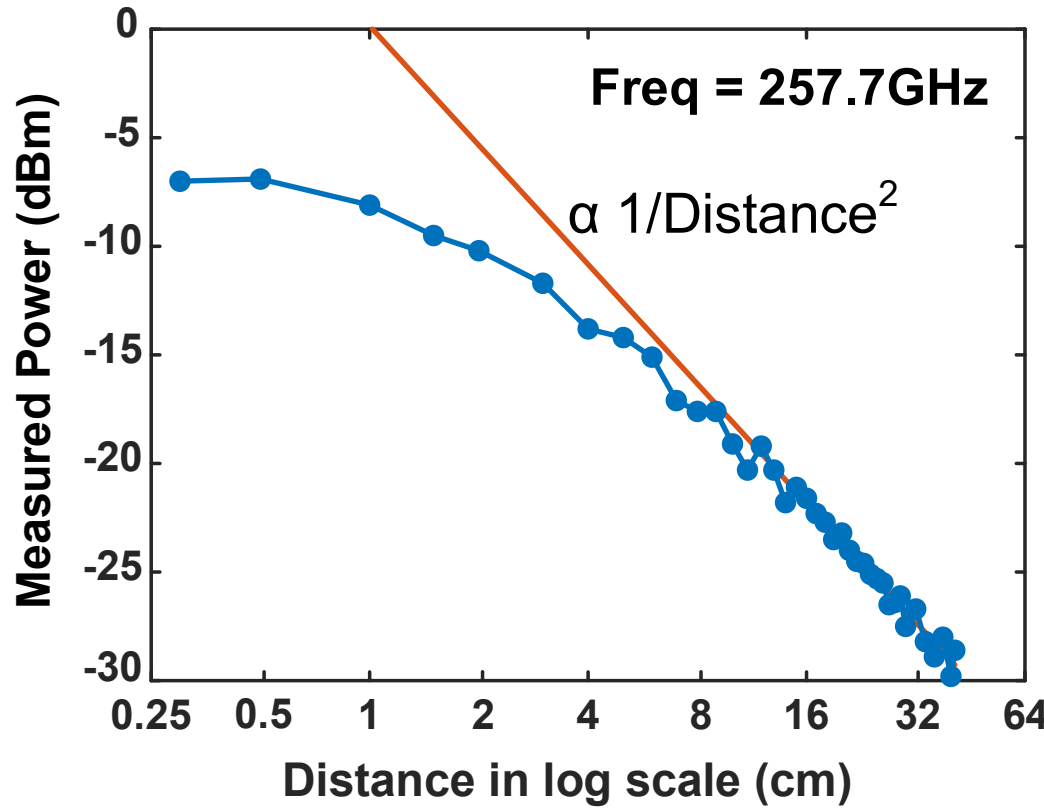
Transmitter Mode Measurements

- Frequency range: 191-257.7GHz
- Bandwidth: 66.7GHz, 29.7%
- Max EIRP: 17dBm
- EIRP fluctuation: 6.5dB



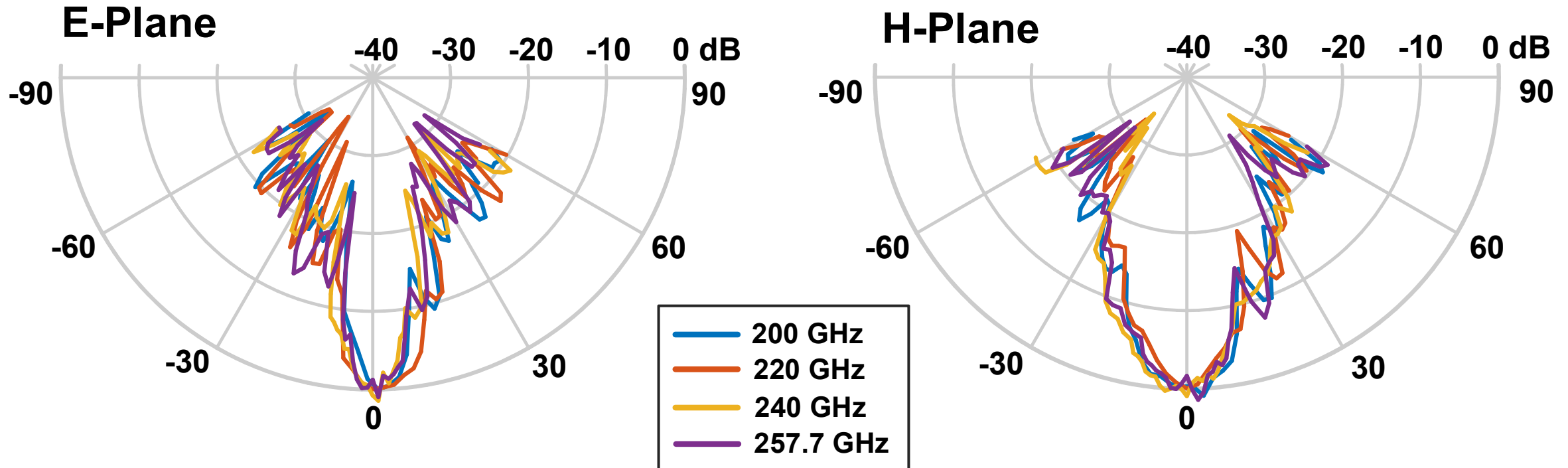
Transmitter Mode Measurements

- Friis equation is met at far-field.
- Self-referencing in FMCW radars diminishes the VCO's phase noise.



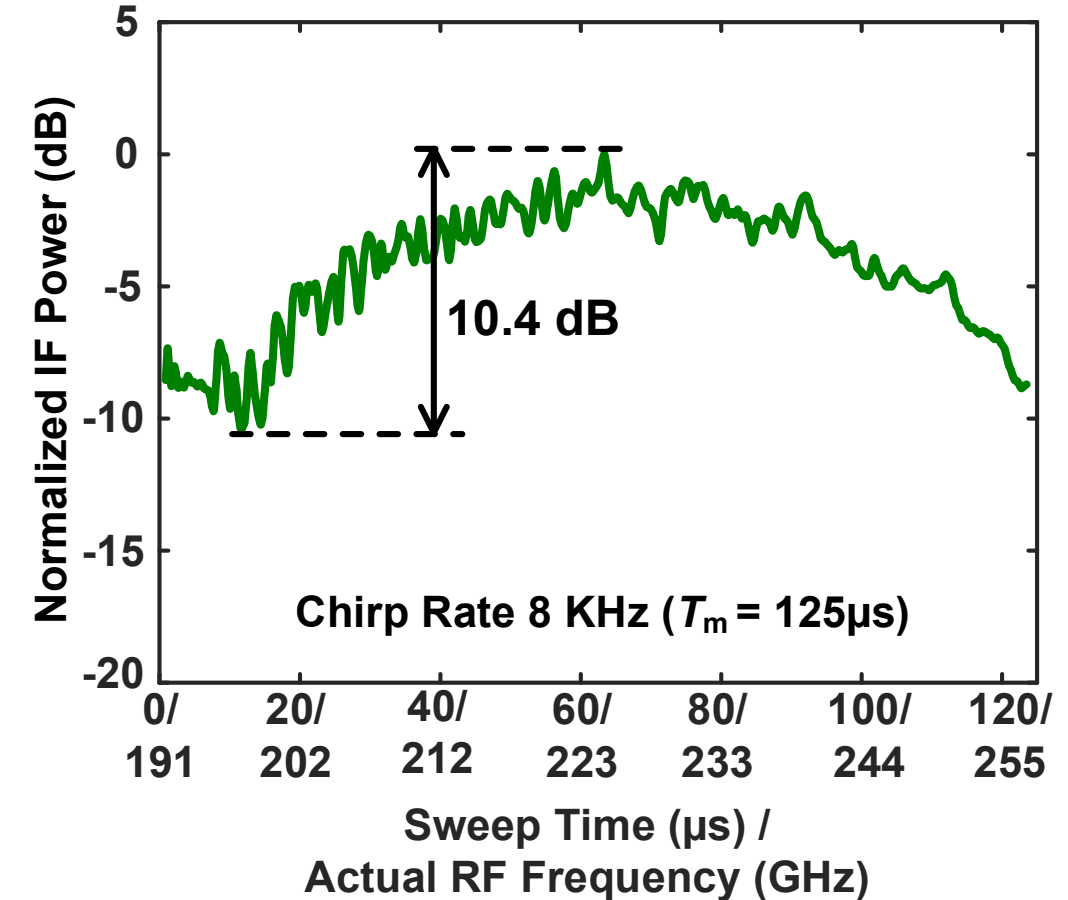
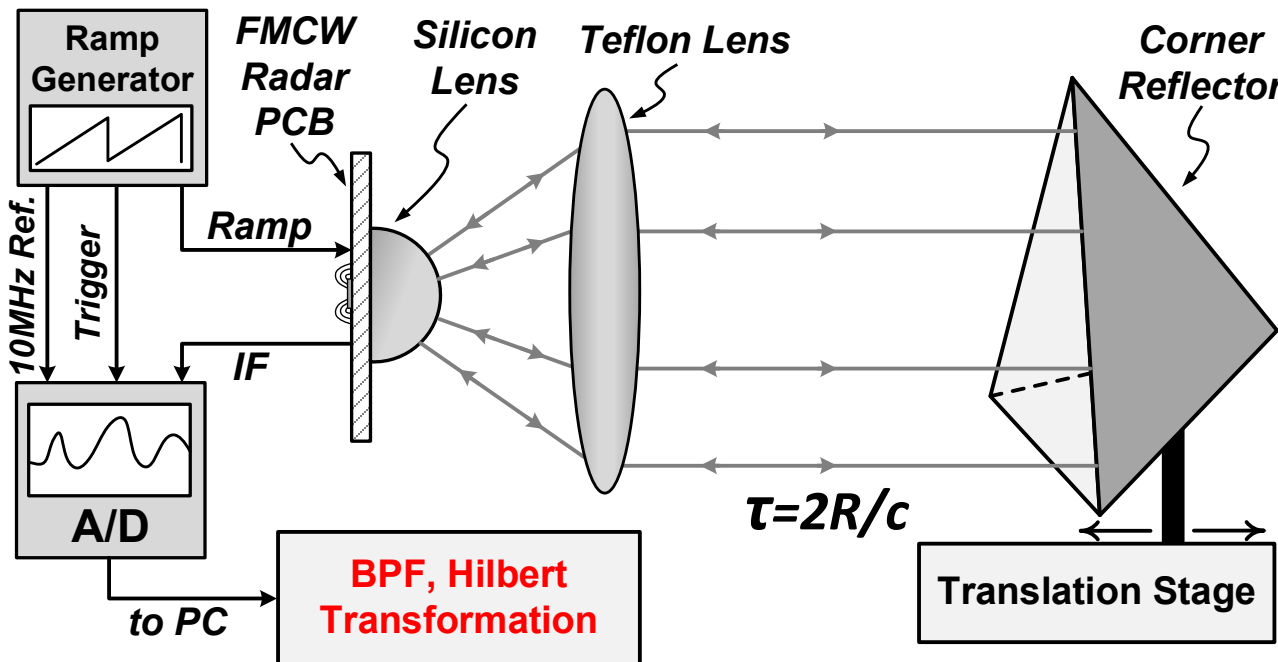
Radiation Pattern Measurements

- Radiation patterns are consistent over the frequency band.
- Antenna phase center remains at the center of Si Lens.
- TX and RX modes have the same radiation pattern.



Receiver Mode Measurements

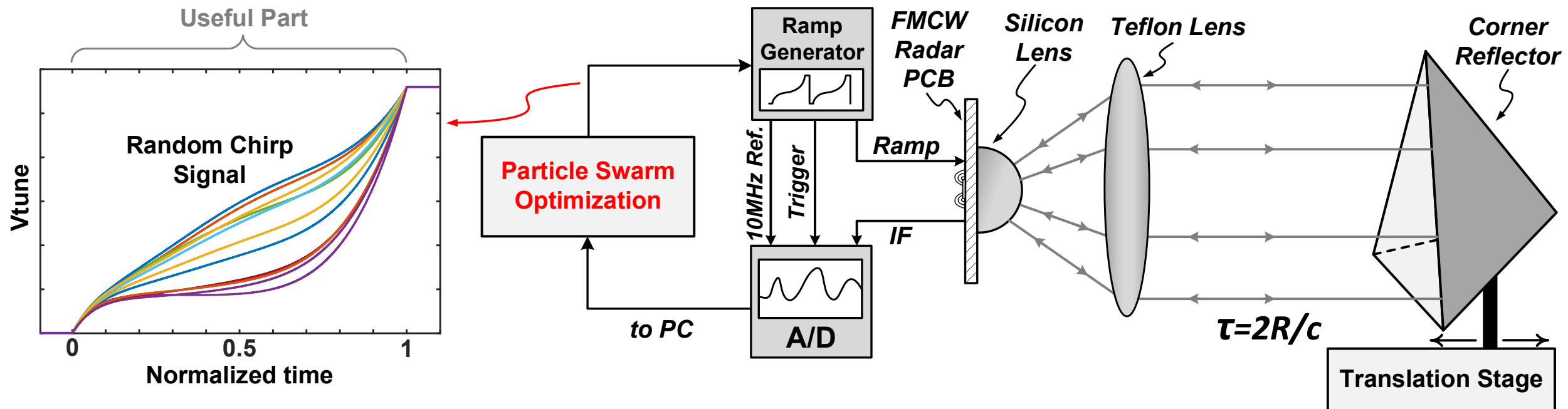
- Received power fluctuation includes: TX power variations, antenna pattern fluctuations, and RX conversion gain variations



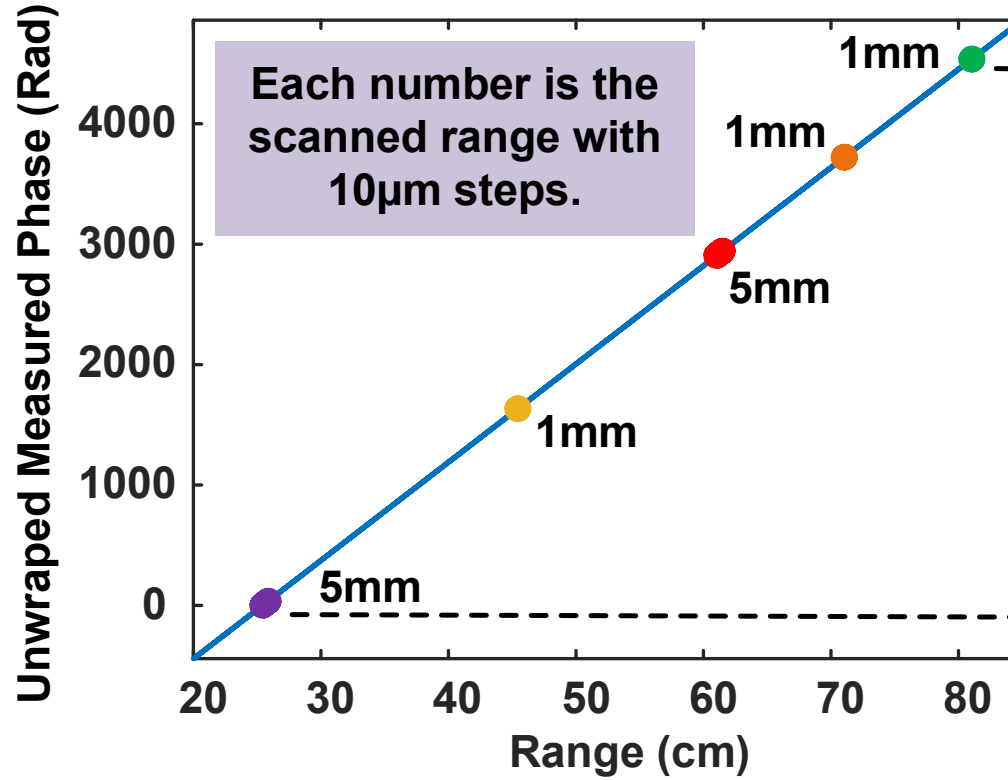
22.4: A 250GHz Autodyne FMCW Radar in 55nm BiCMOS with Micrometer Range Resolution

Chirp Linearization using PSO

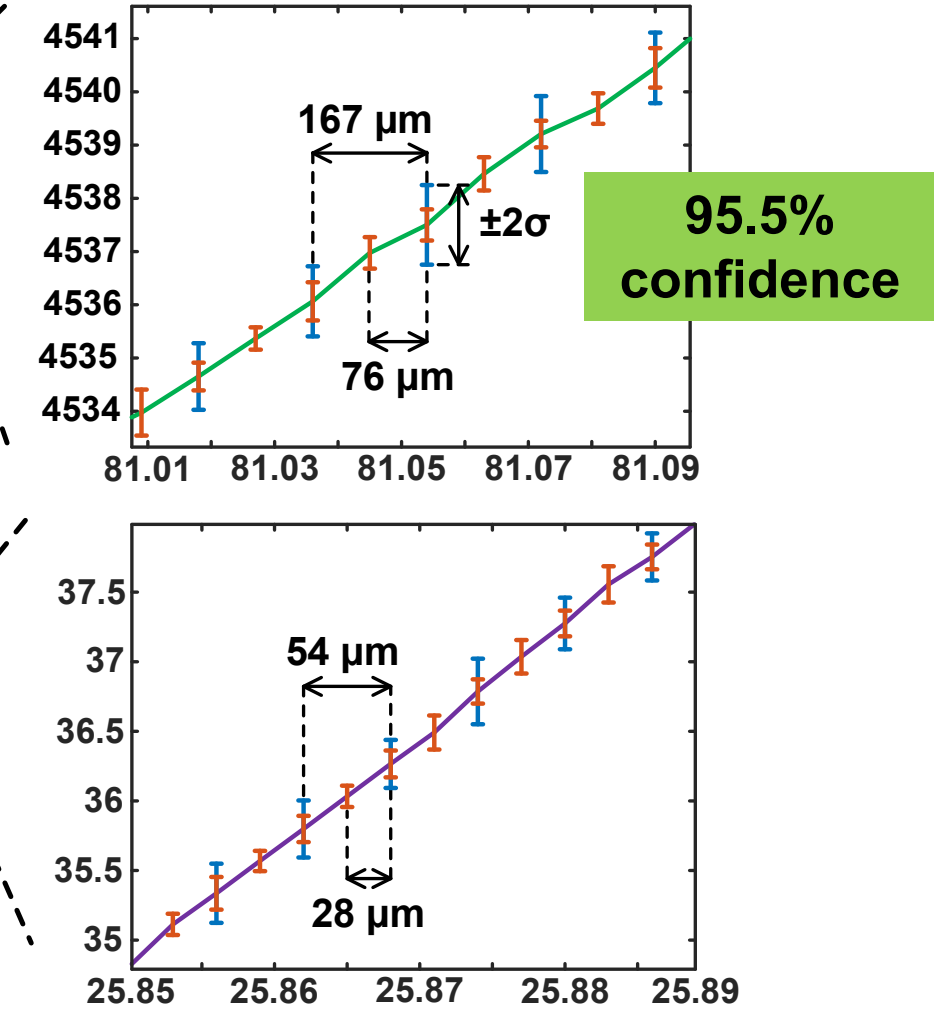
- The goal function in Particle Swarm Optimization (PSO):
 - Maximize the FFT
 - Make a single tone IF signal
 - Lower the FFT side-lobes of the IF signal



Micrometer Range Resolution using Phase Processing Method

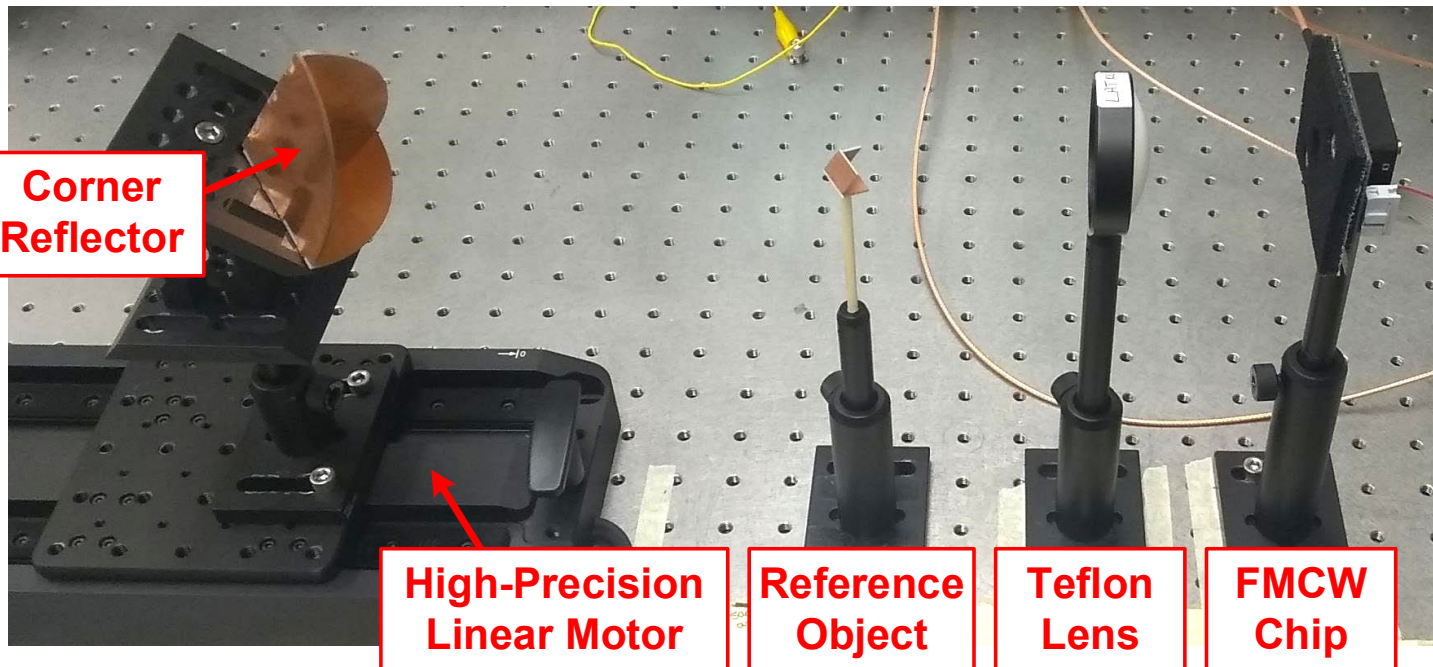


Blue error bars are without averaging, and orange error bars are with five times averaging. Averaging is performed after phase compensation of each measurement.



Micrometer Range Resolution using Phase Processing Method

- Measured range errors:
 - W/O averaging: < 0.025%
 - W/ five times averaging: < 0.015%

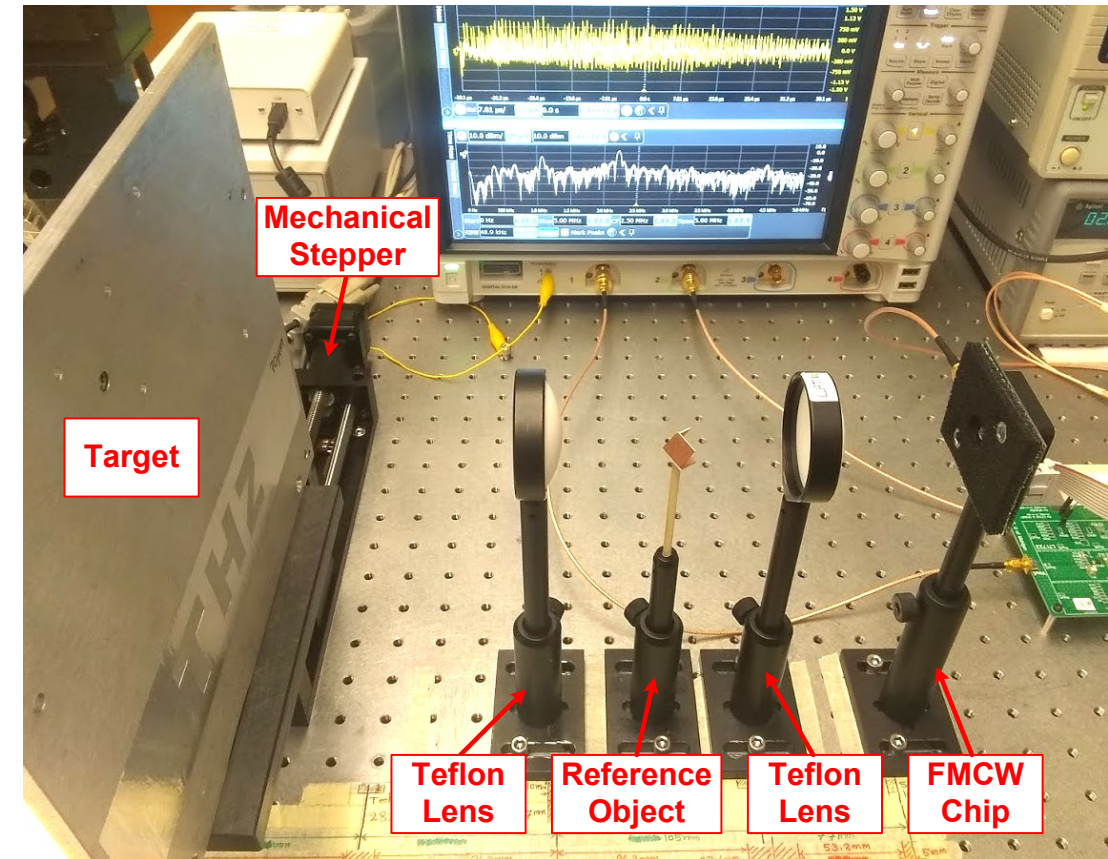
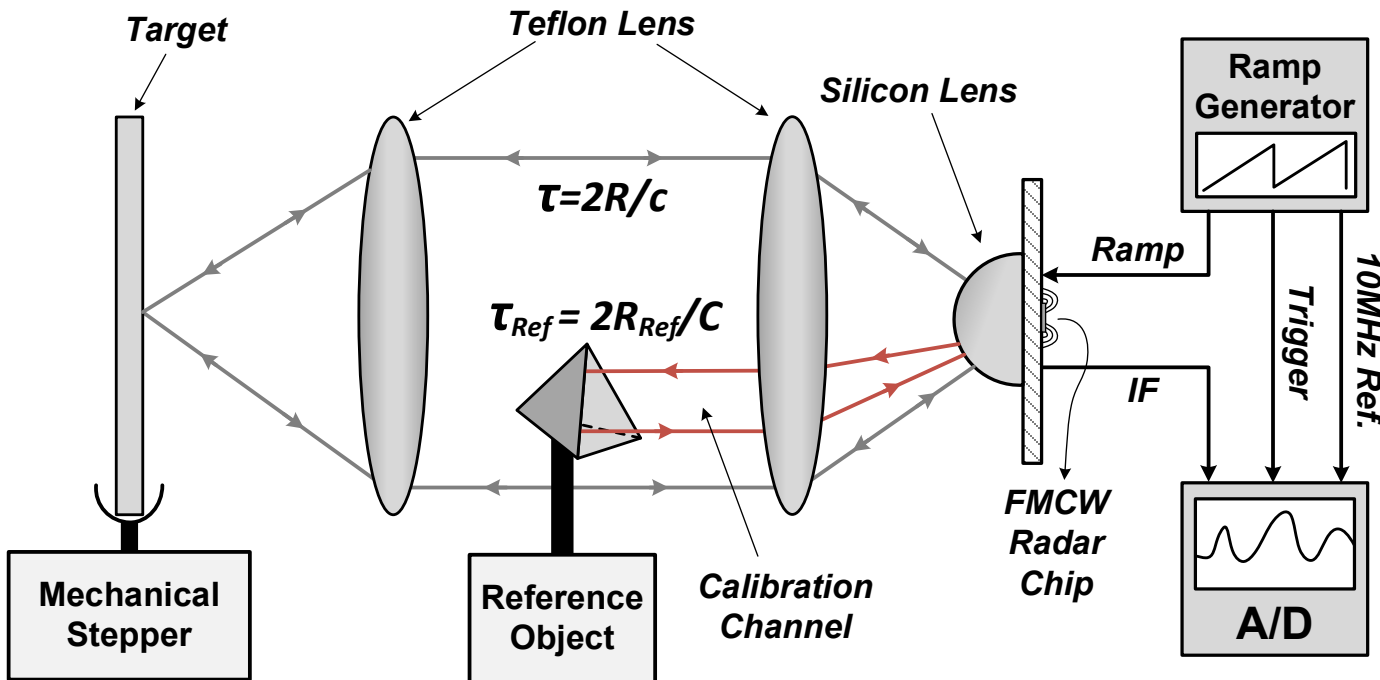


Range (cm)	Error W/O Avg. (μm)	Error W/ 5 Times Avg. (μm)
25.4	54	28
45.4	97	46
61	135	61
71	144	65
81	167	76

Measured Range Errors at Different Positions

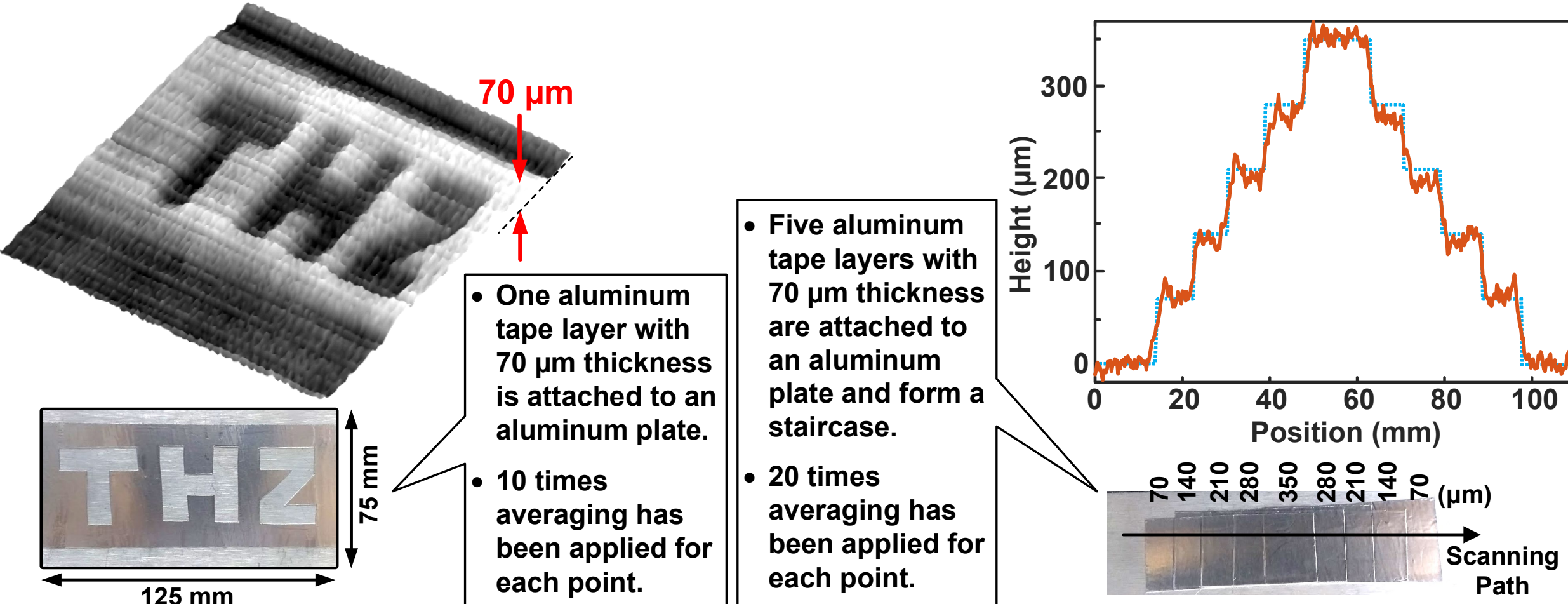
Imaging Setup using Phase Processing Method

- Schematic and implemented imaging setup using phase processing method



22.4: A 250GHz Autodyne FMCW Radar in 55nm BiCMOS with Micrometer Range Resolution

High-Resolution THz Images



Comparison Table

References	Technology	Frequency (GHz)	Bandwidth (GHz / %)	Resolution (μm)	EIRP (dBm)	EIRP Fluctuation (dB)	DC/RF ^(†) Efficiency (%)	IF Power Fluctuation (dB)	Chip Size (mm^2)	DC Power (mW)
This Work	55nm SiGe	191~257.7	66.7/29.7	54/167 ^(a)	17	6.5	1.03	10.4 ^(b)	0.22	68
ISSCC 2020 [1]	65nm CMOS	220~320	100/37 ^(c)	1500	20 ^(d)	8.8	0.04 ^(e)	N/A	5.0	840
Trans. THz 2016 [2]	130nm SiGe	210~270	60/25	2500	32.8	20	0.18	34	3.2	1800
TMTT 2019 [3]	55nm SiGe	189.9~252.3	62.4/28.2	2400	14	7.7	0.4	N/A	0.51	87
ISSCC 2019 [4]	28nm CMOS	138~151	13/9	11500	11.5	1.5	0.98	N/A	6.5	500
Trans. THz 2018 [5]	130nm SiGe	305~375	70/20.6	2100	18.4 ^(d)	10.5	0.06	36	2.85	1700

(†) Total DC power consumption / RF Radiated power

(a) In range of 25.4cm/81cm W/O averaging using phase processing method; (b) this chip has 74dB IF dynamic range with 1Hz-RBW; (c) achieved by five parallel FMCW radars each one with 20GHz bandwidth; (d) with TPX focusing lens; (e) multi-channel-aggregated power.

Outline

- Introduction
- Phase Processing Method
- Circuit Implementation for Autodyne FMCW Radar
- Measurement Results
- Conclusion

Conclusion

- **Phase Processing Method**
 - Micrometer range resolution in THz frequencies
- **Autodyne FMCW Radar**
 - Single wideband antenna in TX and RX paths
 - Radiation pattern consistency over a wide bandwidth
 - Compact and low power → Good for making array
- **An autodyne FMCW radar with micrometer range resolution was demonstrated in 55nm BiCMOS technology**

Acknowledgement

- **Chip fabrication: STMicroelectronics**
- **UNIC members (University of Michigan) for their help in the chip design and measurements**
- **Dr. Behzad Yektakhah (University of Michigan) for the help in PSO coding**